

## 5f Electrons in Transthorium Chemistry

By C. K. JØRGENSEN, Département de Chimie minérale, analytique et appliquée, Université de Genève,  
CH 1211 Geneva 4, Switzerland

(Received September 27, 1982)

*Electron configuration / Periodic Table / Transthorium elements / Unsaturated quarks / Uranyl ion*

### Abstract

The spectroscopic and chemical properties of 5f group compounds show several ramifications not exhibited by the lanthanides. When the oxidation state is M(III), they are indeed quite similar. Like M(IV) they vary their coordination number  $N$  rather indifferently, and available evidence from photo-electron spectra has modified our opinions on covalent bonding, weakening any idea of two electrons per bond. On the other hand, the uranyl ion and subsequent dioxo complexes have exceptional stereochemistry and electronic structure, of which all the details have not yet been clarified. Possible relations with unsaturated quarks and long-lived hypothetical "elementary" particles (such as technicolor hadrons) are discussed.

Half a century ago, quantum chemistry had started with the gaseous species  $H_2^+$  and gone on with the complicated  $H_2$  [1], and quarter a century ago, the controversy about the electronic structure of transthorium compounds was approaching its armistice. The two (equally absurd) extreme arguments had been that the presence of 5f electrons produces a propensity toward trivalency (like the 4f electrons in the lanthanides); and that the chemical stability of the oxidation states Pa(V), U(VI), Np(V) and Np(VI) shows the absence of 5f electrons, protactinium and uranium being 6d-homologs of the 5d-elements tantalum and tungsten. This whole discussion remains a clear-cut example of the much greater utility of induction from facts than of deduction in chemistry [2].

It is worthwhile to analyze what we mean by 5f elements. Whereas the individual  $nl$ -values go back to the energy levels of atomic alkaline-metals studied by RYDBERG in 1895, the explanation of the Periodic Table by an "Aufbau Princip" [3, 4] goes back to STONER in 1924 suggesting that each  $nl$ -shell is able to accommodate at most  $(4l + 2)$  electrons. It is useful to concentrate our attention [5–8] on gaseous ions  $M^{+z}$  with charges from +2 to +6. Indicating the closed shell systems isoelectronic with noble gas atoms by double inequality signs, the shells are filled in the order

$$1s \ll 2s < 2p \ll 3s < 3p \ll 3d < 4s < 4p \ll 4d < 5s < 5p \ll 4f < 5d < 6s < 6p \ll 5f < 6d < 7s \dots \quad (1)$$

to which only five exceptions are known, all for  $M^{+2}$  with  $M = La(5d)$ ,  $Gd(4f^7 5d)$ ,  $Lu(4f^{14} 6s)$ ,  $Ac(7s)$  and  $Th(5f 6d)$ , where the electrons not belonging to the previous noble-gas configuration with  $K = 54$  or 86 electrons are given in parentheses. Text-books frequently propose another sequence intended for neutral atoms, where the

shells 4s, 5s, 6s and 7s follow immediately after  $K = 18, 36, 54$  and 86. However, this sequence has 20 exceptions among the neutral atoms up to einsteinium ( $Z = 99$ ) and is of much less relevance to transition-group chemistry [5, 6] than (1).

It is by no means trivial to define what the sequence (1) is meant to convey. The discrete energy levels of a monatomic entity are always characterized by  $J$  and (odd or even) parity. In most cases, adjacent  $J$ -levels can be bunched together in Russell-Saunders coupling to terms having the quantum numbers  $S$  (total spin) and  $L$ . It is not generally recognized [9, 10] that electron configurations serve the same purpose of classification as Russell-Saunders coupling. In both these approximations, the numbers of levels showing a given value of  $J$  are correctly predicted, in spite of any deviations represented by intermixing of configurations and by intermediate coupling. It is an empirical fact that the first 20 to 400  $J$ -levels of a monatomic entity can be classified as belonging to definite configurations, and that there are no "superfluous" low-lying levels. The sequence (1) is intended to indicate the configuration to which the groundstate belongs, in this sense. The National Bureau of Standards tables [11–13] have not yet been extended beyond  $Z = 90$ , but reviews on uranium [14] and transuranium elements [15] provide some of the lacking material. This classificatory validity of electron configurations does not prevent that the total wave-function of a many-electron system is quite far removed [7, 16, 17] from being an anti-symmetrized Slater determinant. Whereas the squared amplitude of the preponderant configuration  $1s^2$  of the groundstate of the helium atom is 0.99, it is about 0.8 for  $1s^2 2s^2 2p^6$  of the neon atom, and likely to be below 0.5 for atoms heavier than krypton.

The relations between atomic spectroscopy and chemistry are also quite subtle. A major advance for the hypothesis that the 5f shell starts filling very soon after thorium was the assignment in 1946 of the groundstate of the uranium atom (this, of course, has only very remote relations to the electronic structure of metallic uranium) to the configuration [86]  $5f^3 6d 7s^2$ . Contrary to the ideas of HUND [3] this fact does not make U(III) the most frequent oxidation state (any more than [54]  $4f^4 6s^2$  of the neodymium groundstate [12] prevents Nd(II) from being far rarer than Nd(III), whereas atomic plutonium [86]  $5f^6 7s^2$  and samarium [54]  $4f^6 6s^2$  are now known to be isologous). Seen in hindsight, there have only been two significant arguments advanced before 1940 for the 5f group already starting among the known elements. GOLDSCHMIDT suggested from the stable fluorite-type

M(IV) oxides (now known of nine M up to CfO<sub>2</sub>) that thorium is followed by a series of predominantly quadrivalent thorides; and EPHRAIM [18] pointed out that the narrow absorption bands of green U(IV) salts indicate 5f<sup>2</sup> in analogy to 4f<sup>2</sup> of Pr(III). Recently [19], the twelve lowest *J*-levels of [86] 5f<sup>2</sup> were localized in gaseous U<sup>+4</sup> whereas the last level at much higher energy had been assigned 1955 to a narrow absorption band of U(IV) aqua ions [20]. Besides broad and intense electron transfer bands [21] due to one (or more) reducing ligands losing an electron to a low-lying, empty or partly filled, d or f shell of an oxidizing transition-group ion, the trivalent lanthanides from 4f<sup>2</sup>Pr(III) to 4f<sup>13</sup>Yb(III) have extremely characteristic narrow bands, essentially similar to transitions to excited *J*-levels of a monatomic entity [22] and with positions hardly dependent on the *N* = 6, 7, . . . , 12 ligating atoms [23]. This behaviour is quite different from the 3d(iron), 4d(palladium) and 5d(platinum) group compounds, where those excited states not due to electron transfer [21] are described by "ligand field" theory [5, 24, 25]. Before 1956, it was the general opinion that the energy differences between the five d-like orbitals are due to the (quite small) deviations of the Madelung potential from spherical symmetry, but it became clear that one, two (or three in tetrahedral complexes) of the d-like orbitals are strongly anti-bonding, and the rest approximately non-bonding (though slightly involved in  $\pi$  effects). Around 1970, it was believed that the 5f group in some way represents a case intermediate between the 4f and the 3d group. This seems also to be true, insofar the anti-bonding character of some of the 5f orbitals increases strongly with the oxidation state along the series M(IV) < M(V) < M(VI) [26–28]. On the other hand, the "ligand field" effects on 5f<sup>3</sup>U(III) in crystalline U<sub>x</sub>La<sub>1-x</sub>Cl<sub>3</sub> (with *N* = 9) are only twice as large as on the corresponding lanthanide 4f<sup>3</sup>Nd(III) [29, 30] joining the general picture all the way up to 5f<sup>8</sup>Bk(III) and beyond. The major difference in the distribution of the *J*-levels of the 4f and the 5f group M(III) is the much stronger deviations from Russell-Saunders coupling in the latter case, the Landé spin-orbit coupling parameter being twice as large, and at the same time the parameters of interelectronic repulsion about 40% smaller, under equal circumstances.

Such evidence, as well as calculated 4f and 5f radial functions, suggest that the electron affinity of the partly filled 4f shell is *much* smaller than the ionization energy. As first pointed out by CONNICK [31], this is the major reason [5, 32] why the lanthanides strongly prefer a constant oxidation state. There is no direct relation [2, 6] between the electron configuration of the monatomic entities containing 4f electrons, and the chemical fact that the preferred oxidation state is M(III). Going from the 3d to the 4d group [33, 34] there is the same tendency as going from the 4f to the 5f group. In the beginning of the 4d and 5f groups, the oxidation states are more varying and, on the average, higher, as known from Mo(VI), Tc(VII), Ru(VIII) or from Pa(V), U(VI) and (the strong-

ly oxidizing) Np(VII), whereas the last elements of the group are less readily oxidized. Much like Ag(II) is less stable than Cu(II), 5f<sup>13</sup>Md(II) is less reducing than 4f<sup>13</sup>Tm(II), and nobelium(II) is at least as difficult to oxidize to the ytterbium-homolog 5f<sup>13</sup>No(III) as cerium(III) to Ce(IV), making *Z* = 102 much more similar to radium than to actinium [35].

The smooth variation of oxidizing character of M(III) or M(IV) going from zero to 13 electrons in the 4f or 5f shell is modified by the position of the lowest *J*-level below the average energy of the partly filled shell. In the 4f group representing a good approximation to Russell-Saunders coupling for the lower levels [22] this additional effect is proportional to parameters of interelectronic repulsion and expressed in the refined spin-pairing energy description originally introduced [36–38] for rationalizing electron transfer spectra. However, the same treatment can be applied to standard oxidation potentials of aqua ions [5, 39] and to photo-electron spectra of metallic lanthanides and their solid compounds [32, 40]. Taking the deviations from Russell-Saunders coupling into account, the spin-pairing energy theory also works in the 5f group [41]. It remains true that the lanthanides have a few characteristics not possessed by the 5f group. Thus, 4f<sup>7</sup>europium(II) is more difficult to oxidize than 4f<sup>14</sup>ytterbium(II) whereas it is very well-known that 3d<sup>5</sup>Mn(II) is easier to oxidize than 3d<sup>10</sup>Zn(II), and 5f<sup>7</sup>Am(II) (now known in black but non-metallic AmI<sub>2</sub>) much easier to oxidize than 5f<sup>14</sup>No(II).

This explanation of varying standard oxidation potentials has renewed interest in the general question of hydration energies of gaseous ions [32, 33, 42, 43] allowing a certain understanding of which oxidation states are stable, at least in the form of aqua ions [44, 45]. A related problem is the photo-electron spectra providing ionization energies *I* of valence M.O. (molecular orbitals) and of inner shells [46–48]. It is highly instructive that such *I*-values have now become available by experiments, and it has turned out that they vary relatively much less in differing compounds of the same element than suggested by several M. O. calculations. A major reason is the large influence of the spherical part of the Madelung potential [4, 47]. The photo-electron signals of inner shells have a rather specific type of satellites [49] in mixed oxides of U(V).

With the various experimental techniques available today, we have obtained a relatively detailed and reliable picture of the importance of the 5f orbitals for chemical bonding in transthorium compounds, one important bit of the puzzle being the moderate nephelauxetic effect in uranium(IV) complexes [19, 20] evaluated by comparing the parameters of interelectronic repulsion with those of gaseous U<sup>+4</sup>. Much like the main part of the covalent bonding of lanthanide compounds must be due to the (experimentally rather inaccessible) empty 5d and 6s shells (in the L.C.A.O. model) at the same time as the weak nephelauxetic effect in M(III) provides severe higher limits for the extent of 4f participation in covalent bonding [5, 32] there occurs the same difficulty that empty

6d and 7s orbitals play the larger role in the 5f group.

A rather special category is the closed-shell systems containing no unpaired 5f electrons in the groundstate. It may be noted that many features of the analogous cerium(IV) are not too well understood. One of the chemical difficulties is that Ce(IV) aqua ions are too strong Brønsted acids to be compatible with aqueous solutions, and seem to transform to oligomeric hydroxo complexes, as is likely to be the case for  $5f^7$  Bk(IV) and  $5f^{14}$  104(IV) too. Actually, the only well-characterized M(IV) aqua ions are those of M=Th, Pa, U, Np and Pu. However, a far more enigmatic system is the uranyl ion, linear  $\text{OUO}^{+2}$  binding 6, 5 or 4 other atoms at much longer distances in the equatorial plane [50, 51] making a striking contrast to the indifference toward changing  $N$  and local symmetry in trivalent lanthanides [23] and in most of the 5f group.

The radioactivity was discovered [2, 52] by Henri Becquerel in 1896 following the somewhat far-fetched suggestion by the mathematician Poincaré that since the X-rays discovered by Röntgen make crystalline  $\text{BaPt}(\text{CN})_4 \cdot 4\text{H}_2\text{O}$  fluoresce, certain fluorescent materials may emit X-rays. The first excited state of the uranyl ion is both characterized by a rather violent photochemistry of hydrogen atom abstraction [50, 53, 54] and by a luminescent emission band having a vibrational structure indicating much longer equilibrium U–O distances in the excited state than in the electronic groundstate. This fluorescence in the yellow and green can be useful [55] for planar concentrators of solar energy, about 75% of the isotropic radiation being trapped inside a uranyl glass plate by a series of total reflections, until it arrives at the rim of the plate covered with much less photovoltaic silicon than would be needed to cover the entire plate. Contrary to tracking heliostats, such a device can use the major part of diffuse scattered sun-light.

There is general agreement today [56–59] that the quite weak absorption bands of  $\text{UO}_2^{+2}$  in the blue to near ultra-violet are strongly forbidden electron transfer bands, where an electron jumps from a M. O. with odd parity to the empty 5f shell. Because of the strong spin-orbit coupling, the appropriate quantum number of the excited levels is  $\Omega$  [25] whereas it has no meaning to ask whether these levels are triplet ( $S=1$ ) or singlet ( $S$  zero) [57]. There is at least 16 excited  $\Omega$  levels as recently reviewed [51], but it is more likely that the manifold contains 32 or 48  $\Omega$  levels. Comparison with electron transfer spectra of other complexes [21] and with photo-electron spectra of linear dihalides  $\text{XMX}$  [47] suggest the loosest bound M. O. to be  $\pi_u$  but DENNING *et al.* [60] measured  $^{18}\text{O}$  substituted  $\text{Cs}_2\text{UO}_2\text{Cl}_4$  at liquid helium temperature (to unravel the complicated vibrational structure) and located six  $\Omega$  values (the lowest excited level having  $\Omega = 1$ ) explained by transfer of one  $\sigma_u$  electron. This study has been continued [61] with the  $5f^1$  systems  $\text{NpO}_2\text{Cl}_4^{+2}$  and  $\text{NpO}_2(\text{O}_2\text{NO})_3^-$ .

One might have hoped that M. O. calculations could answer the question whether  $\pi_u$  or  $\sigma_u$  is most readily excited. However, the five most recent, quite sophisticated

$\text{UO}_2^{+2}$  calculations show a dispersion of results [51, 62] preventing any convincing conclusion. Another recent problem is that PYYKKÖ and LOHR [63] suggested the highest occupied M. O. to be  $\sigma_u$  but having the squared  $5f$  amplitude 0.86. Whereas the “ligand field” transitions in d-group complexes [5, 24, 25] are due to transitions between roughly non-bonding and strongly anti-bonding d-like orbitals, such a situation would mean that the ultra-weak absorption bands in the blue are not strictly speaking due to electron transfer, but to transitions from a bonding  $5f$ -like to roughly non-bonding  $5f$  orbitals. However, a closer analysis [64] indicates that this a strongly model-dependent result. It is still conceivable that the highest filled M. O. is  $\sigma_u$  but then, it is more likely to be due to “pushing from below” by the filled  $\text{U}6p$  shell, much like in  $\text{N}_2$  where photo-electron spectra [47] show the lowest  $I$ -value of an orbital  $\sigma_g$  which has to be orthogonal on the bonding combination of  $\text{N}2s$  orbitals.

One has to recognize that the occurrence of electron transfer bands at 4 eV ( $32000\text{ cm}^{-1}$ ) lower energy in the uranyl ion than in tungstate  $\text{WO}_4^{+2}$  is out of all proportion with the difference in oxidizing character of U(VI) and of W(VI). Much the same can be said [65] about gaseous  $\text{UF}_6$  and  $\text{WF}_6$ . Four M. O. calculations [51] of the octahedral molecule  $\text{UF}_6$  agree that the highest occupied orbital is the higher spin-orbit component of  $(\pi + \sigma)_{t_{1u}}$  whereas all other hexahalide complexes have electron transfer spectra [21] and photo-electron spectra showing that  $(\pi)_{t_{1g}}$  is most readily excited or ionized. The latter M. O. has four inter-ligand node-planes [25]. The exceptional behaviour of  $\text{UF}_6$  may be connected with “pushing from below” by  $\text{U}6p$  as discussed above [64] for  $\text{UO}_2^{+2}$ .

The extreme closed-shell characteristics of noble gases attenuate as a function of increasing  $Z$ . The first ionization energy (all given in eV) 15.759 of argon is already lower than 17.422 of fluorine; and there is not an enormous dispersion between 12.967 of chlorine, 12.130 of xenon, 10.437 of mercury and 10.748 of radon [43]. Seen from this point of view, it would not be too surprising [2] if strong oxidants may remove 6p electrons from francium(I) or radium(II). However, the absence of absorption bands of thorium(IV) aqua ions, at least below 6 eV, does not suggest a general easy excitation of the 6p shell. The specific behaviour of the uranyl ion must be connected with the high oxidation state and/or the unusually short inter-nuclear distances. A comparable stereochemical problem occurs in the beginning of the 3d group.  $3d^1$  titanium(III) forms purple  $\text{Ti}(\text{OH}_2)_6^{+3}$  but the isoelectronic vanadium(IV) the blue vanadyl ion  $\text{OV}(\text{OH}_2)_4^{+2}$  having a very short V–O distance, and (like CO,  $\text{CO}_2$  and the uranyl ion) lacking perceptible proton affinity in aqueous solution. As far goes  $\text{U}6p$ , strong spin-orbit coupling in linear symmetry provides three distinct  $I$ -values which have been studied [66] in photo-electron spectra of solid uranyl salts and agree with M. O. calculations [51] by surrounding the  $\text{O}2s$  signals and show a total spreading of some 14 eV.

Quantum chemistry has been far more successful in rationalizing spectra than chemical behaviour. This is main-

ly because of Franck and Condon's principle that photons excite or ionize many-electron systems without modifying the nuclear positions, whereas the potential surfaces of N nuclei (at least 3) take place in  $(3N-5)$ -dimensional spaces. The fact that the majority of stoichiometric compounds are organic molecules produces a traditional emphasis on multiple bond-orders, hybridization (which is not too stupid [67] in the elements from beryllium to oxygen having roughly similar 2s and 2p radial functions, but [24] has lost all credibility above neon) and additive bond dissociation energies. However, a much more radical problem is that the allocation of  $2N$  electrons to  $N$  "bonds" proposed by Lewis in 1916 has not been particularly valid in transition-group and many other areas of inorganic chemistry [47, 67]. Stereochemical behaviour can be quite specific for a given preponderant electron configuration [5] such as diamagnetic ( $S$  zero) quadratic  $p^2$  systems Br(III), Te(II), I(III) and Xe(IV) and  $d^8$  systems Ni(II), Cu(III), Rh(I), Pd(II), Ag(III), Ir(I), Pt(II) and Au(III) [25] or regular octahedral  $d^3$  ( $S = 3/2$ ) V(II), Cr(III), Mn(IV), Mo(III), Tc(IV), Ru(V), Re(IV), Os(V) and Ir(VI) as well as diamagnetic  $d^6$  V(-I), Cr(0), Mn(I), a few Fe(II), Co(III), Ni(IV), Mo(0), Ru(II), Rh(III), Pd(IV), W(0), Ir(III), Pt(IV) and Au(V). However, as soon  $N$  is above 6, there is hardly any rigid stereochemistry, and neither any specific preference for a given  $N$  value, as known for lanthanides [23] and for most transthorium compounds, excepting  $MO_2^{+2}$  and, to a slighter extent,  $MO_2^+$ .

It may be worthwhile finishing this paper with a more constructive vista in direction of the future, rather than describing the ruins of the paradigms of the past. GLASHOW [68] emphasized the utility of "passive experimentation" as a parallel alternative to high-energy physics. Thus, 1% of the unexpected element argon was found in the atmosphere in 1894; all data before 1932 of nuclear physics were obtained using radioactive isotopes extracted from uranium and thorium minerals; and the cosmic rays were worthy precursors of the huge accelerators. For instance, there may be a tiny concentration of technicolor hadrons  $X^-$  with atomic weight somewhere between 100 and a million, forming adducts with conventional  $Z$ -nuclei and behaving as superheavy isotopes of  $(Z-1)$ . Hence, the abundance (in weight)  $10^{-15}$  of actinium (to be compared with  $10^{-5}$  thorium in the Earth's crust) may serve as a carrier for  $^{232}\text{Th}X$  [69, 70]. Since  $^8\text{Be}X$  is not  $\alpha$ -radioactive (like  $^8\text{Be}$  is) there is no bottleneck toward nucleosynthesis [71] and  $X$ -containing heavy nuclei may have built up shortly after the Big Bang, not waiting for the collapse of the first-generation stars. The  $\alpha$ -half-life of  $^{244}\text{Pu}X$  and  $^{247}\text{Cm}X$  may be close to  $10^{10}$  years [70] allowing detection in minerals, when looking for traces of neptunium and americium.

For a few years, most theorists were convinced that quarks are dogmatically confined, 3 in each baryon. There is some evidence that concentrations of  $10^{-25}$  to  $10^{-20}$  unsaturated quarks per baryon may have survived from the Big Bang (when the temperature was sinking

below  $10^{13}$  K). Such amounts (60 to 6 million/kg) are on the limit of detectability. The geochemical behaviour [72] is expected to be quite different for mobile positive quarks bound to electronic systems and for negative quarks remaining very close to nuclei (like technicolor  $X^-$ ) but in both cases, fractional charges  $\pm e/3$  cannot be neutralized by electrons.

In 1869, thorium and uranium were outposts in the Periodic Table. When Maria Sklodowska and Pierre Curie discovered radium 1898, it was realized that the radioactivity of the (frequently short-lived) isotopes of elements with  $Z$  between 83 and 91 did not directly modify the chemistry of a given element. When genuine transuranium elements were made after 1940, the same experience was extended. However, elements with  $Z$  above 99 are only available in very small amounts, decreasing exponentially with  $Z$  and arriving at a few atoms of the last detected [73] with  $Z = 107$ . Though a major problem is a deficit of neutrons, inducing rapid spontaneous fission, and enhancing  $\beta$ -instability, all recent experiments [73] bombarding uranium or curium with  $^{48}\text{Ca}$ ,  $^{238}\text{U}$ , . . . have not yielded  $Z$ -values above 107 in spite of theoretical expectations [74] of certain isotopes with  $Z$  between 110 to 114, or close to 126 or 164, being relatively long-lived with respect to all decays. This is rather sad, because the experience with transthorium chemistry allows better predictions of chemical behaviour [6, 45] with special cases such as the thorium-like [34] system 126(IV) and the palladium-like  $7d^8 8s^2 8p^2$  164(II) strongly influenced by relativistic effects [44] which have been further reviewed [75, 76].

However, the trans-108 elements may come back via a hidden door. There is increasing expectation [77] that some systems containing unsaturated quarks have far lower rest-mass than an isolated free quark. Not only the diquark may be lighter than a single quark, but "quarklei" [78] containing  $(3A-1)$  quarks may have a rest-mass some 20 to 50 atomic weight units ( $1 \text{ amu} = 0.9315 \text{ GeV}$ ) higher than a conventional nucleus "containing"  $3A$  quarks, whereas systems with  $(3A-2)$  quarks may have an excess mass 100 to 1000 amu. Since the vacuum is an indefinite source of a pair of a nucleus and the corresponding anti-nucleus, at an energy cost of  $2A$  amu, a free quark can then form an adduct with an anti-nucleus, ejecting the nucleus, or what may be more appropriate for our purpose, a free anti-quark may react with the nucleus, ejecting the anti-nucleus [79]. Though spontaneous fission is expected to occur at a higher  $Z$  value than in conventional nuclei without unsaturated quarks, there will be a limit somewhere. The systems containing unsaturated quarks remaining in minerals may hence be relatively heavy fission products.

#### Acknowledgments

I am grateful to the late Professor MOÏSE HAISSINSKY for opening my eyes to the fascinating problems of trans-thorium elements.

I am also very grateful to Professor RENATA REISFELD, Hebrew University, Jerusalem, for continued fruitful collaboration on 4f and 5f group spectroscopy.

Much of the studies described here were made possible by grant no. 2.841-080 from the Swiss National Science Foundation.

#### References

1. RUEDENBERG, K.: *Rev. Mod. Phys.* **34** (1962) 326.
2. JØRGENSEN, C. K.: *J. Chim. Phys.* **76** (1979) 630.
3. HUND, F.: *Linienspektren und Periodisches System der Elemente*. Julius Springer, Berlin 1927.
4. RABINOWITCH, E., THILO, E.: *Periodisches System, Geschichte und Theorie*. Ferdinand Enke, Stuttgart 1930.
5. JØRGENSEN, C. K.: *Oxidation Numbers and Oxidation States*. Springer-Verlag, Berlin 1969.
6. JØRGENSEN, C. K.: *Angew. Chem.* **85** (1973) 1, *Int. Ed.* **12** (1973) 12.
7. JØRGENSEN, C. K.: *Adv. Quantum Chem.* **11** (1978) 51.
8. KATRIEL, J., JØRGENSEN, C. K.: *Chem. Phys. Lett.* **87** (1982) 315.
9. JØRGENSEN, C. K.: *Isr. J. Chem.* **19** (1980) 174.
10. JØRGENSEN, C. K.: *Int. Rev. Phys. Chem.* **1** (1981) 225.
11. MOORE, C. E.: *Atomic Energy Levels*. Vol. 1 (H to V), Vol. 2 (Cr to Nb), Vol. 3 (Mo to La, and Hf to Ac). National Bureau of Standards, Washington, D. C., 1949, 1952 and 1958.
12. MARTIN, W. C., ZALUBAS, R., HAGAN, L.: *Atomic Energy Levels, the Rare-Earth Elements*. NSRDS-NBS 34. National Bureau of Standards, Washington, D. C., 1978.
13. ZALUBAS, R.: *J. Res. Natl. Bur. Stand.* **80A** (1976) 221.
14. ENGLEMAN, R., PALMER, B. A.: *J. Opt. Soc. Am.* **70** (1980) 308.
15. *Gmelins Handbuch der anorganischen Chemie*. Ergänzungswerk Vol. 8, Transurane, Teil A2. Verlag Chemie, Weinheim/Bergstr. 1973.
16. JØRGENSEN, C. K.: *Orbitals in Atoms and Molecules*, Academic Press, London 1962.
17. JØRGENSEN, C. K.: *Solid State Phys.* **13** (1962) 375.
18. EPHRAIM, F., MEZENER, M.: *Helv. Chim. Acta* **16** (1933) 1257.
19. WYART, F., KAUFMAN, V., SUGAR, J.: *Physica Scripta* (Stockholm) **22** (1980) 389.
20. JØRGENSEN, C. K.: *Chem. Phys. Lett.* **87** (1982) 320.
21. JØRGENSEN, C. K.: *Prog. Inorg. Chem.* **12** (1970) 101.
22. REISFELD, R., JØRGENSEN, C. K.: *Lasers and Excited States of Rare Earths*. Springer-Verlag, Berlin 1977.
23. JØRGENSEN, C. K., REISFELD, R.: *Top. Curr. Chem.* **100** (1982) 127.
24. JØRGENSEN, C. K.: *Absorption Spectra and Chemical Bonding in Complexes*. Pergamon Press, Oxford 1962.
25. JØRGENSEN, C. K.: *Modern Aspects of Ligand Field Theory*. North-Holland Publ. Co., Amsterdam 1971.
26. BROWN, D., WHITTAKER, B., EDELSTEIN, N.: *Inorg. Chem.* **13** (1974) 1805.
27. WARREN, K. D.: *Inorg. Chem.* **19** (1980) 653.
28. THORNTON, G., ROESCH, N., EDELSTEIN, N.: *Inorg. Chem.* **19** (1980) 1304.
29. GRUBER, J. B., MORREY, J. R., CARTER, D. G.: *J. Chem. Phys.* **71** (1979) 3982.
30. CROSSWHITE, H. M., CROSSWHITE, H., CARNALL, W. T., PASZEK, A. P.: *J. Chem. Phys.* **72** (1980) 5103.
31. CONNICK, R. E.: *J. Chem. Soc. Suppl.* (London) 1949, p. 235.
32. JØRGENSEN, C. K.: *Handbook on the Physics and Chemistry of Rare Earths* (eds. K. G. SCHNEIDNER and LEROY EYRING) Vol. 3, p. 111. North-Holland Publ. Co., Amsterdam 1979.
33. JØRGENSEN, C. K.: *Chimia (Switz.)* **23** (1969) 292.
34. JØRGENSEN, C. K.: *Chem. Phys. Lett.* **2** (1968) 549.
35. SILVA, R. J., MCDOWELL, W. J., KELLER, O. L., TARRANT, J. R.: *Inorg. Chem.* **13** (1974) 2233.
36. JØRGENSEN, C. K.: *Mol. Phys.* **5** (1962) 271.
37. RYAN, J. L., JØRGENSEN, C. K.: *Mol. Phys.* **7** (1963) 17.
38. RYAN, J. L., JØRGENSEN, C. K.: *J. Phys. Chem.* **70** (1966) 2845.
39. JOHNSON, D. A.: *Adv. Inorg. Chem. Radiochem.* **20** (1977) 1.
40. COX, P. A., BAER, Y., JØRGENSEN, C. K.: *Chem. Phys. Lett.* **22** (1973) 433.
41. NUGENT, L. J., BAYBARZ, R. D., BURNETT, J. L., RYAN, J. L.: *J. Phys. Chem.* **77** (1973) 1528.
42. JØRGENSEN, C. K.: *Top. Curr. Chem.* **56** (1975) 1.
43. JØRGENSEN, C. K.: *Comments Inorg. Chem.* **1** (1981) 123.
44. PENNEMAN, R. A., MANN, J. B., JØRGENSEN, C. K.: *Chem. Phys. Lett.* **8** (1971) 321.
45. PENNEMAN, R. A., MANN, J. B.: *J. Inorg. Nucl. Chem. Suppl. about Proc. Moscow Symp. Transuranium Elements 1972* (eds. V. I. SPITSYN and J. J. KATZ) p. 257. Pergamon Press, Oxford 1976.
46. JØRGENSEN, C. K., BERTHOU, H.: *K. Dan. Vidensk. Selsk. Mat. - Fys. Medd.* **38** (1972) no. 15.
47. JØRGENSEN, C. K.: *Struct. Bonding* **22** (1975) 49, **24** (1975) 1 and **30** (1976) 141.
48. JØRGENSEN, C. K.: *Fresenius Z. Anal. Chem.* **288** (1977) 161.
49. KELLER, C., JØRGENSEN, C. K.: *Chem. Phys. Lett.* **32** (1975) 397.
50. JØRGENSEN, C. K.: *Rev. Chim. Minér. (Paris)* **14** (1977) 127.
51. JØRGENSEN, C. K., REISFELD, R.: *Struct. Bonding* **50** (1982) 121.
52. PAIS, A.: *Rev. Mod. Phys.* **49** (1977) 925.
53. RABINOWITCH, E., BELFORD, R. L.: *Spectroscopy and Photochemistry of Uranyl Compounds*. Pergamon Press, Oxford 1964.
54. BURROWS, H. D., KEMP, T. J.: *Chem. Soc. Rev. (London)* **3** (1974) 139.
55. REISFELD, R., JØRGENSEN, C. K.: *Struct. Bonding* **49** (1982) 1.
56. JØRGENSEN, C. K.: *Acta Chem. Scand.* **11** (1957) 166.
57. JØRGENSEN, C. K., REISFELD, R.: *Chem. Phys. Lett.* **35** (1975) 441.
58. LIEBLICH-SOFER, N., REISFELD, R., JØRGENSEN, C. K.: *Inorg. Chim. Acta* **30** (1978) 259.
59. JØRGENSEN, C. K.: *J. Lumin.* **18** (1979) 63.
60. DENNING, R. G., SNELLGROVE, T. R., WOODWARK, D. R.: *Mol. Phys.* **32** (1976) 419 and **37** (1979) 1109.
61. DENNING, R. G., NORRIS, J. O. W., BROWN, D.: *Mol. Phys.* **46** (1982) 287 and 325.
62. JØRGENSEN, C. K., REISFELD, R.: *J. Electrochem. Soc.* **130** (1983) 681.
63. PYYKKÖ, P., LOHR, L. L.: *Inorg. Chem.* **20** (1981) 1950.
64. JØRGENSEN, C. K.: *Chem. Phys. Lett.* **89** (1982) 455.
65. MCDIARMID, R.: *J. Chem. Phys.* **65** (1976) 168.
66. VEAL, B. W., LAM, D. J., CARNALL, W. T., HOEKSTRA, H. R.: *Phys. Rev. B* **12** (1975) 5651.
67. JØRGENSEN, C. K.: *Chimia (Switz.)* **25** (1971) 109 and **28** (1974) 605.
68. GLASHOW, S. L.: *Rev. Mod. Phys.* **52** (1980) 539.
69. JØRGENSEN, C. K.: *Nature* **292** (1981) 41.
70. CAHN, R. N., GLASHOW, S. L.: *Science* **213** (1981) 607.
71. TRIMBLE, V.: *Rev. Mod. Phys.* **47** (1975) 877.
72. JØRGENSEN, C. K.: *Struct. Bonding* **34** (1978) 19.
73. EDELSTEIN, N. M. (ed.): *Actinides in Perspective*. Pergamon Press, Oxford 1982.
74. JØRGENSEN, C. K.: *Struct. Bonding* **43** (1981) 1.
75. FRICKE, B.: *Struct. Bonding* **21** (1975) 89.
76. PYYKKÖ, P., DESCLAUX, J. P.: *Acc. Chem. Res.* **12** (1979) 276.
77. JØRGENSEN, C. K.: *Naturwissenschaften* **69** (1982) 420.
78. DE RUJULA, A., GILES, R. C., JAFFE, R. L.: *Phys. Rev. D* **17** (1978) 285.
79. JØRGENSEN, C. K.: *Nucl. Phys. B*, submitted.



## Chemistry of the Elements Einsteinium through Element-105

By E. K. HULET, University of California, Lawrence Livermore National Laboratory, P. O. Box 808, Livermore, California 94550

(Received December 23, 1982)

Review / Chemical properties / Atomic properties / Transplutonium elements / Transactinide elements

### Abstract

All known chemical properties of each of the elements 99 (Es) through 105 are reviewed and these properties are correlated with the electronic structure expected for  $5f$  and  $6d$  elements. A major feature of the heavier actinides, which differentiates them from the comparable lanthanides, is the increasing stability of the divalent oxidation state with increasing atomic number. The divalent oxidation state first becomes observable in the anhydrous halides of californium and increases in stability through the series to nobelium, where this valency becomes predominant in aqueous solution. In this range of elements, the II  $\rightarrow$  III oxidation potential decreases from  $\sim +1.5$  to  $-1.5$  volts. These observations lead to the conclusion that, in comparison with the analogous  $4f$  electrons, the  $5f$  electrons in the latter part of the series are more tightly bound. Thus, there is a lowering of the  $5f$  energy levels with respect to the Fermi level as the atomic number increases.

The metallic state of the heavier actinides has not been investigated except from the viewpoint of the relative volatility among members of the series. In aqueous solutions, ions of these elements behave as "normal" trivalent actinides and lanthanides (except for nobelium). Their ionic radii decrease with increasing nuclear charge which is moderated because of increased screening of the outer  $6p$  electrons by the  $5f$  electrons. These relative ionic radii have been obtained from comparisons of the elution position in chromatographic separations.

Lawrencium (Lr) completes the actinide series of elements with an electronic configuration of  $5f^{14}7s^27p$ . From Mendeleev's periodicity and Dirac-Fock calculations, the next group of elements is expected to be a  $d$ -transition series corresponding to the elements Hf through Hg. The chemical properties of elements 104 and 105 only have been studied and they indeed appear to show the properties expected of eka-Hf and eka-Ta. However, their nuclear lifetimes are so short and so few atoms can be produced that a rich variety of chemical information is probably unobtainable.

### Introduction

The detailed chemistry of the heavier actinides has only become discernable when berkelium, californium, and einsteinium first became available in appreciable quantities within the past 12–15 years. Microgram to milligram quantities of these elements were necessary for service as target isotopes in producing tracer amounts of even heavier actinides by charged particle bombardments. In addition, these quantities permitted progress in understanding the chemical properties of the transcurium elements (Bk–Es) beyond that gathered from tracer-scale experiments. However, with each step in atomic number above that of Es (element 99), we know less and less of each element's chemistry because of the increasingly shorter lifetimes of the nuclides and because of the difficulties in synthesizing sufficient numbers of atoms.

Because of the nuclear instabilities of these man-made elements, the range of atomic and chemical properties that are accessible to experimental study are indeed limited in comparison with the vastly wider spectrum of information obtainable from the naturally occurring elements. Among the basic chemical properties of the heavier actinides which have been investigated are the behavior of these ions in solution which includes separation chemistry, complex-ion formation, oxidation-reduction reactions, electro-chemistry, hydration, and absorption spectra. Our experimentally derived knowledge becomes scantier for other chemical forms and states of these elements as, for example, the organometallic compounds and the elemental and solid states. Atomic and physical-chemical properties are almost entirely unknown for the elements heavier than einsteinium, except where derived by theoretical extrapolations. Nevertheless, all of the bits of knowledge so far obtained allow us to piece together a rather clear picture of the basic chemistry of these elements.

A condensed scheme that summarizes the valence states and numbers of  $5f$  electrons in each state is shown for the actinides in Fig. 1. Elements within the first half of the series are stable in IV, V, and VI valence states, while the divalent state is almost unknown in this group. However, one of the major features uncovered in the investigations of the heavier actinides was a finding of increasing stability of the divalent state with progressive increases in atomic number. This trend, like the high and stable valences in the lighter members of the series, sets the actinides apart from the comparable lanthanide series and can be generally interpreted on the basis of subtle changes in electronic structure. The most important change occurring with increasing  $Z$  is a marked lowering of the  $5f$  energy levels with

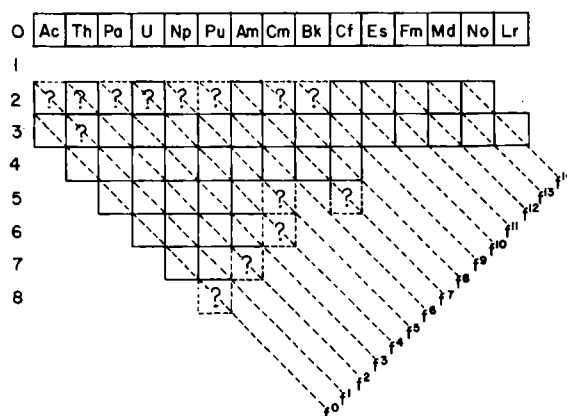


Fig. 1. Schematic of actinide oxidation states and associated  $5f$  electronic structure.

respect to the Fermi level and a widening separation between the  $5f$  ground states and the first excited states in the  $6d$  or  $7p$  levels. Thus, removing an outer  $5f$  valence electron becomes increasingly difficult until divalency predominates in the next to last actinide element in the series. These and other general features of the chemistry of the heavier actinides are summarized after the review of lawrencium.

## Einsteinium

### Production

The isotopes  $^{253}\text{Es}$  and  $^{254}\text{Es}$ , with half lives of 20.5 and 275.7 days, respectively, can be produced in high-flux nuclear reactors in sufficient quantities for chemical investigations. Starting with neutron capture by  $^{238}\text{U}$ , the production of  $^{253}\text{Es}$  proceeds through a long chain of further captures and beta decays by intermediate nuclides

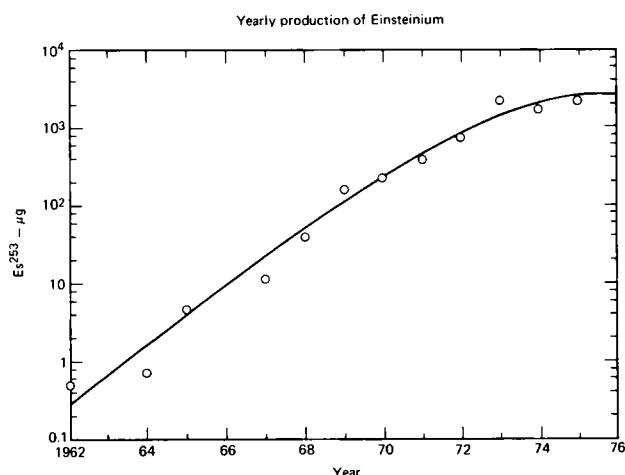


Fig. 2. Yearly production of  $^{253}\text{Es}$  in the United States.

during long neutron irradiations. The yearly production of  $^{253}\text{Es}$  from 1962 onward is shown in Fig. 2. The production of  $^{253}\text{Es}$  has by now leveled off at a rate of about two milligrams per year while the amounts of  $^{254}\text{Es}$  and  $^{255}\text{Es}$  are necessarily limited by the fission destruction of  $^{254}\text{Es}$  to about 0.3 and 0.06 percent of the  $^{253}\text{Es}$  quantities, respectively [1]. Prior to 1969, einsteinium and the other transplutonium elements were produced by the individual National Laboratories but an overall U.S. production program, maintained at the Oak Ridge National Laboratory by the U.S. Department of Energy, has since superseded those individual efforts.

### Atomic Properties

The electronic configurations of einsteinium in neutral and singly ionized gaseous atoms have been determined from emission spectra taken with electrodeless discharge lamps containing  $\text{EsI}_3$ . Although the first emission spectrum of einsteinium revealed only 9 lines [2], the most recent exposures using the 10-m spectrograph at the Argonne National Laboratory are expected to show some 20,000 lines [3]. Unfortunately, the measurements on these photographic plates are incomplete and the electronic configurations given in Table 3 are based on term assignments to a portion of the 290 lines observed earlier by WORDEN *et al.* [4]. It should be noted that not all of the lowest energy electronic configurations have been observed yet. BREWER has tabulated his estimated energies of the lowest level of the lowest spectroscopic term for each electron configuration [5, 6]. For the singly ionized free atom, it is apparent from his estimates that the  $f^{10}s^2$ ,  $f^{12}$  and  $f^{11}d$  levels should be lower in energy than the first excited level  $f^{11}p$  observed by WORDEN and others [4]. Other atomic properties from atomic beam and X-ray measurements are listed in Table 1.

Table 1. Atomic properties of einsteinium ( $^{253}\text{Es}$ )

	Ground level	Other levels	Energy ( $\text{cm}^{-1}$ )
Neutral, I	$5f^{11}7s^2, ^4I_{15/2}^0$	$5f^{11}7s7p, ^6I_{15/2}$ $5f^{10}6d7s^2, ^6I_{17/2}$ $5f^{11}7s8s, ^4I_{15/2}, ^3S_1$	17 802.89 19 367.93 33 829.35
Singly ionized, II	$5f^{11}7s, ^5I_8^0$	$5f^{11}7p, ^5I_7$ $5f^{10}6d7s$	27 751.12 32 897.77*
Property	Value		Reference
First ionization potential	6.42 ± 0.03 eV (calculated)		[7, 8]
Nuclear spin	7/2		[4]
Nuclear dipole moment	$\mu_I = 4.10 \pm 0.07 \mu_N$		[9]
Nuclear quadrupole moment	$Q_S = 6.7 \pm 0.8$ barns		[9]
K X-ray energies	$K\alpha_2$ 112.501 ± 0.01 keV		[10]
	$K\alpha_1$ 118.018 ± 0.01		
	$K\beta_3$ 131.848 ± 0.02		
	$K\beta_1$ 133.188 ± 0.02		

\* May not be the lowest level of this configuration.

## Metallic State

The high specific radioactivity of einsteinium has greatly limited the investigations of the metal. Of the two attempts to prepare the metal and determine its structure, the successful method employed electron diffraction rather than X-ray diffraction. The latter was largely inconclusive because of degradation of the metal's crystallinity caused by self-irradiation. The electron diffraction lines from eleven samples were indexed on the basis of a face-centered cubic structure with  $a_0 = 0.575 \pm 0.001$  nm [11]. This fcc form of einsteinium metal is believed to be divalent because it has the same lattice parameter as reported for the divalent form of californium metal.

A melting point for the metal was also noted while heating the samples in the electron microscope used for the diffraction measurements. Micro puddles of the metal formed during the heating and, after calibrating with metals of known melting points, a temperature of  $860 \pm 50^\circ\text{C}$  was established as the melting point of einsteinium metal.

Further evidence for divalency in Es metal has come from studies comparing the condensation temperatures of elemental lanthanides and actinides in thermochromatographic columns [12]. The trivalent metals Sc, La, and Bk were not volatilized at the initial temperature of  $1425^\circ\text{K}$ , whereas the metals of Yb, Es, Fm, and Md were vaporized and later condensed at the same temperature ( $\sim 700^\circ\text{K}$ ). The behavior of divalent Eu, Sm, and Ca metals was intermediate between those extremes. Since volatilities are correlated with promotional energies and the number and energy of the valence bonds, the more volatile actinides are associated with the divalent metals. The estimates of NUGENT *et al.* [13] for the enthalpy of sublimation of lanthanide and actinide metals closely agree with the relative volatilities found in the thermochromatographic study reported above. Furthermore, WARD and colleagues [14] have recently completed detailed analyses of the cohesive energy of the actinide metals (entropies and heats

of sublimation), in which they also indicate that einsteinium is a divalent metal.

The thermal conductivity of einsteinium has been estimated to be  $10 \text{ W m}^{-1} \text{ K}^{-1}$  at  $300^\circ\text{K}$  [15].

## Compounds

Only a few simple compounds of einsteinium have been prepared and structurally identified because of problems associated with self irradiation. Aside from self-destruction of the crystal structures, there is a rapid in-growth of the  $\alpha$ -daughter  $^{249}\text{Bk}$ ; the L, M, and N X-rays, emitted following  $\alpha$ -decay, blacken the X-ray film used in Debye-Scherrer cameras within 10 to 20 minutes with microgram samples of  $^{253}\text{Es}$  or  $^{254}\text{Es}$ . A synchrotron radiation source may be the only way of overwhelming this sample background source of radiation with sufficient intensity of monochromatic radiation to permit diffraction measurements.

The known compounds of einsteinium are listed in Table 2 together with the rather sparse information detailing their properties. Divalent compounds were not identified by their crystal structure, but by adsorption spectra of their halides, taken with crystallites, of samples first melted and then quenched. These spectra show a sharp difference in the  $f$ - $f$  absorption bands when compared to the corresponding spectra of the trivalent halides (Fig. 3). We emphasize that the apparent stability of the divalent oxidation state in einsteinium was not realized until a decade ago and that this feature in the heavier actinides clearly sets this series of elements apart from the later elements in the  $4f$  series.

Electron paramagnetic-resonance spectra of divalent einsteinium have been recorded in single-crystal hosts of  $\text{CaF}_2$  [16],  $\text{BaF}_2$ , and  $\text{SrF}_2$  [17]. Reduction of  $\text{Es}^{3+}$  to  $\text{Es}^{2+}$  was spontaneous from electron displacement caused by the  $\alpha$ -radiation. A  $5f^{11}$  configuration with a ground

Table 2. Simple compounds of di- and trivalent einsteinium characterized by either structural or spectroscopic analysis

Compound	Structural type*	Lattice parameters ( $a_0, b_0, c_0$ in nm; $\beta$ in $^\circ$ )				Major absorption bands ( $10^5 \text{ m}^{-1}$ )	Reference
		$a_0$	$b_0$	$c_0$	$\beta$		
$\text{Es}_2\text{O}_3$	$\text{Mn}_2\text{O}_3$ -bcc	$1.0766 \pm 0.0006$				—	22
$\text{EsCl}_3$	$\text{UCl}_3$ -hex	$0.740 \pm 0.002$		$0.407 \pm 0.002$		(see Ref. 23)	23, 24
$\text{EsCl}_2$	—					11.1, 18.5, 24.5	25, 26
$\text{EsOCl}$	$\text{PbFCl}$ -tetra	$0.3948 \pm 0.0004$		$0.6702 \pm 0.0019$		—	23, 24
$\text{EsBr}_3$	$\text{AlCl}_3$ -mono	$0.727 \pm 0.002$	$1.259 \pm 0.003$	$0.681 \pm 0.002$	$110.8 \pm 0.2$	12.6, 19.8	27
$\text{EsBr}_2$	—					11.2, 18.3	25
$\text{EsOBr}$	—					(no published data)	23
$\text{EsI}_3$	$\text{BiI}_3$ -hex	0.753		2.084		(see Ref. 23)	23, 28
$\text{EsI}_2$	—					11.2, 18.5	25
$\text{EsOI}$	—					(no published data)	23
$\text{EsF}_3$	—					13.2, 20.3	23

\* bcc = body-centered cubic  
hex = hexagonal  
tetra = tetragonal  
mono = monoclinic

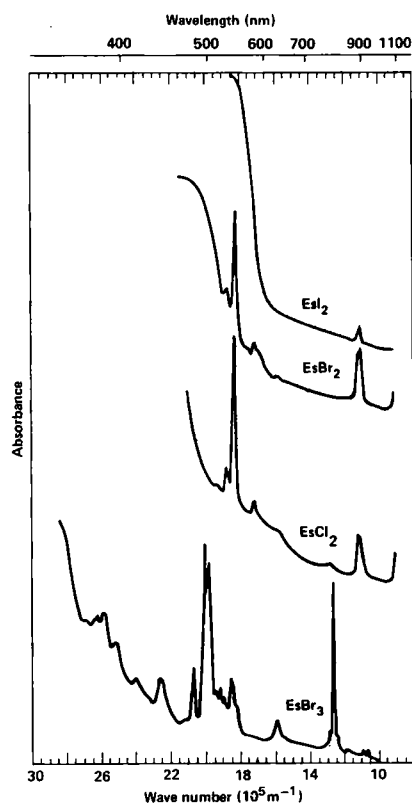


Fig. 3. Absorption spectra of the divalent einsteinium halides and trivalent  $\text{EsBr}_3$ . Reprinted with the permission of the J. Phys. Collo. (Ref. 25).

state close to the  $4^1\text{I}_{15/2}$  level, but with a small admixture of the  $2^2\text{K}_{15/2}$ , was found, which indicated the cubic crystal-field only slightly perturbs the inner  $5f$  orbitals.

A possible tetravalent compound  $\text{EsF}_4$  may also exist, as judged by comparing the volatility of an einsteinium fluoride with  $\text{PuF}_4$ ,  $\text{AmF}_4$ ,  $\text{CmF}_4$ ,  $\text{BkF}_4$ , and  $\text{CfF}_4$  [18]. The  $f-f$  electronic spectrum of the  $\text{Es}^{4+}$  free ion has been calculated by VARGA and coworkers [19]. NUGENT *et al.* [20] and LEBEDEV [21] estimated a III  $\rightarrow$  IV oxidation potential of  $-4.6$  V which NUGENT thought might allow the synthesis of the compound  $\text{Cs}_3\text{EsF}_7$ .

### Separation and Purification

The chemical recovery of einsteinium (and Bk, Cf, and Fm) after irradiation is performed remotely in large shielded cells. Details of the chemical separation processes used in the United States and by the Soviets at the Kurchatov Institute of Atomic Energy have been reviewed by HULET and BODÉ [29] and by KOSYAKOV and coworkers [30], respectively. Nearly all of the separation steps used in these large-scale processes were developed earlier for applications in laboratory separations, but extensive modifications were required to adapt them to the special and nearly always adverse conditions encountered in remote operations with very high levels of radioactivity present. These separation processes are unlikely to be scaled up further as, for instance, for the recovery of transplutonium elements during the reprocessing of fuel from power reactors.

This is largely because they were born in the laboratory where corrosive chemicals could be easily contained in glass apparatus and where the chemist could oversee the difficult chromatographic separations.

Purification of einsteinium requires two difficult separations: 1) from lanthanide fission products and 2) from adjacent actinides. The main difficulty arises from the great similarity in the chemical properties of their trivalent ions. Fortunately, the contraction in size of the aqueous ions with increasing atomic number can be exploited with complexing ligands to offer slight variations in complex strengths between members of either series of  $f$  elements. Chromatographic methods then exploit these small chemical differences many times over to give useful separation factors for the tri-positive elements.

Separation of einsteinium from the lanthanides is usually accomplished by elution with either  $13M$  HCl or 20 vol % ethanol saturated with HCl from an ion-exchange column containing a strongly acidic cation exchange resin [31]. Einsteinium and the other actinides are rapidly eluted in a band while the trivalent lanthanides are retained and eluted somewhat later. The purification of einsteinium from many milligrams of lanthanides necessitates an anion-exchange procedure using  $10M$  LiCl as an eluant [32]. With this elution method, Cf, Es, and Fm are separated from all lanthanides, Pu, Am, and Cm with separation factors ranging from 4 to 23.

The intragroup separation of einsteinium from adjacent actinides can be performed by either of two chromatographic methods. In the ion-exchange method the trivalent actinides are eluted with a complexing agent such as 2-hydroxy-2-methylpropanoic acid ( $\alpha$ -hydroxyisobutyric acid or  $\alpha$ HIB) from a heated column of cation exchange resin containing a strongly acidic, highly cross-linked resin [33]. Such columns are often run at pressures up to 17.2 MPa to force the eluant through the very fine particles of ion-exchange resin [34]. The second method employs extraction chromatography in which the extractants, either bis(2-ethylhexyl) phosphoric acid (HDEHP) or 2-ethyl-hexylphenyl phosphonic acid (HEH $\Phi$ P), are absorbed on an inert support material [29]. An eluant of approximately 0.3 to 0.4  $M$  HCl or  $\text{HNO}_3$  provides distribution coefficients appropriate for Es-Fm separations. Table 3 summarizes the separation factors (ratio of distribution coefficients) obtainable by each of these methods. Clearly, the purification of Cf from Es is the poorest;

Table 3. Separation factors ( $S = K_d(Z)/K_d(Z+1)$ ) for Es/Fm and Cf/Es obtained with acidic extractants and by cation-exchange. Average values from Ref. 29, p. 11, and Ref. 35 are listed.

Elements	$\alpha$ HIB (87°C)	HDEHP (60°C)		HEH $\Phi$ P (25°C)
	S	(HCl) S	( $\text{HNO}_3$ ) S	HCl S
Cf	1.5	0.99	1.02	1.3
Es	1.7	2.04	2.20	2.5
Fm				

hence, the cation exchange method is preferred because of the larger separation factor. The significant difference between the two methods of chromatographic separation lies in a reversal of the elution sequence with atomic number.

## Solution Chemistry

### Trivalent ions

Across the actinide series from Pu to Lr, the solution properties of the  $An^{3+}$  ion vary only slowly and in a regular manner. Thus, much of the behavior described for trivalent actinide ions can be safely extrapolated to estimate that of  $Es^{3+}$ . Bonding with ligands is almost entirely attributed to electrostatic forces, but with some second-order contribution from covalent sharing of electrons due to the relatively large radial extension of the  $5f$  orbitals. The ionic radius of  $Es^{3+}$  has been calculated from the six-coordinated sesquioxide to give a value of 0.0928 nm [22], or about 1 pm smaller than the radius of  $Cf^{3+}$ . Einsteinium is stable only as the trivalent ion in aqueous solution.

A number of measurements of the absorption spectrum of  $^{253}Es^{3+}$  have been made over the energy range of 9430 to 34,000  $cm^{-1}$  [36–39]. The band structure (12 peaks) observed could be reasonably well fitted in both energy and intensity by assuming  $Es^{3+}$  behaved as a free ion and that the  $f-f$  transition arose from eigenstates which were strongly mixed because of coupling that is intermediate between L-S and j-j [37–40]. These assumptions follow closely those used in fitting calculated levels to identified absorption bands in preceding members of the actinide (and lanthanide) series.

Studies of the complex-ion chemistry of  $Es^{3+}$  have been made in conjunction with measurements of the stability constants of other trivalent actinides. A summary of the known stability constants for einsteinium complexes is shown in Table 4. Fig. 4 is illustrative of the trend of greater complex formation with increasing atomic number for the trivalent actinides. The step-wise increase in  $\beta_3$  between Cm and Bk, often seen as part of the tetrad effect, is related to the first pairing of a  $5f$  electron at Bk after half filling the  $5f$  shell in Cm. With the possible exception of the two lower thiocyanate complexes, the chloride is the only outer-sphere complex, in which waters of hydration lie between the ligand and einsteinium ion. The remaining complexes are believed to be inner-sphere as inferred from the increase of a given stability constant with an increase in atomic number and from the enthalpy and entropy of formation of the complex.

Hydrated radii and hydration numbers for the  $An^{3+}$  ions have recently been derived from migration rates in an electric field and from STOKES' LAW [48]. The hydrated ions of einsteinium and fermium are the largest in the series  $Am^{3+}$  to  $Md^{3+}$ ; the hydrated radius of einsteinium is 0.492 nm which would allow 16.6 molecules of water in the total hydration sphere. Several parameters of thermodynamic interest have been measured or estimated; e.g.

Table 4. The stability constants of  $Es^{3+}$  complexes

Complex	Stability constant			Reference
	$\log \beta_1$	$\log \beta_2$	$\log \beta_3$	
$EsCl^{2+}$	-0.18			[41]
$EsOH^{2+}$	8.86			[42]
$Es(SO_4)_n^{3-2n}$	-2.19	-4.3	-4.93	[43]
$Es(SCN)_n^{3-n}$	0.559	-1.4	0.468	[44]
$EsHCit^{2-}$	10.6			[45]
$Es(Cit)_2^{3-}$	12.1			
$Es(HIB)^{2+}$	4.29			
$Es(tartrate)^+$	5.86			[46]
$Es(malate)^+$	7.06			
$EsDETPA^{2-}$	22.62			
$EsDACTA^-$	19.43			[47]
$EsEDTA$	19.11			

Cit = citrate ion  
 $\alpha$ HIB = 2-hydroxy-2-methylpropanoate ion  
 DEPTA = diethylenetriaminepentaacetate ion  
 DACTA = 1,2-diaminocyclohexanetetraacetate ion  
 EDTA = ethylenediaminetetraacetate ion

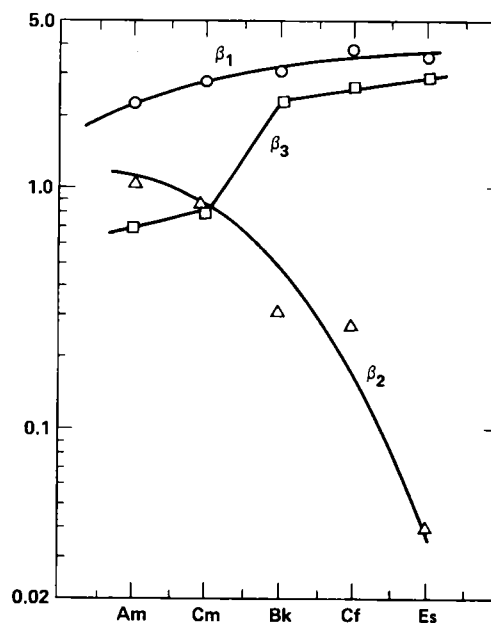


Fig. 4. First three stability constants of the actinide(III) thiocyanate complexes as a function of atomic number. Redrawn from the data of HARMON and PETERSON [44].

the molar activity coefficient of  $Es^{3+}$  in  $NaNO_3$  solution [49] and the free energy, enthalpy, and entropy of formation of  $Es^{3+}$  in aqueous solution [21, 50, 52]. The values  $\Delta H_f^0 = 595.8 \pm 21$  kJ mole $^{-1}$ ,  $\Delta S_f^0 = 76.1$  J mole $^{-1}$  K $^{-1}$ , and  $\Delta F_f^0 = 573 \pm 17$  kJ mole $^{-1}$  given by DAVID and colleagues [50] were obtained from an entropy prescription and the standard reduction potential,  $III \rightarrow 0$ , described in the following paragraph.

For the purpose of measuring the electropotential, reduction of the trivalent einsteinium ion to the metal (Hg amalgam) has been performed by polarographic methods. A single half-wave representing the  $III \rightarrow 0$  reduction potential was observed [53]. The potential found for the combined reactions of reduction and amalgamation was

$-1.460 \pm 0.005$  V. After correcting for the amalgamation energy by an empirical method suggested by NUGENT [52], the standard potential derived was  $-1.98$  V relative to the standard hydrogen potential. Because the amalgamation energy represents a large correction, caution should be exercised in using the standard potential in thermodynamic calculations.

### Divalent ions

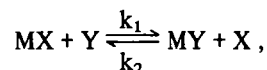
The divalent state is of major importance and has attracted the interest of many experimenters since 1967 when the appreciable stability of this state was first recognized in the actinides. The III  $\rightarrow$  II reduction potential of einsteinium was first estimated to be  $-1.6$  V from the lowest energy electron-transfer band [55]. A later estimate of  $-1.21$  V was obtained for chloroaluminate melts [56] as well as another estimate of the standard potential of  $-1.18$  V [21]. MIKHEEV and coworkers identified Es(II) from the cocrystallization of einsteinium tracer with  $\text{SmCl}_2$  in an ethanol solution [57]. Einsteinium was only partially reduced to the (II) state by  $\text{SmCl}_2$  which allowed them to conclude that the standard reduction potential of  $\text{Es}^{3+}$  was close to that of  $\text{Sm}^{3+}$ , or  $-1.55 \pm 0.06$  V [58]. An ionic radius of  $0.105$  nm was estimated from the radius of maximum electron density obtained in Hartree-Fock calculations, which was then corrected to obtain the crystal-line radius by an empirical proportionality constant [59].

### Few atom chemistry

Beginning with fermium and with each advancement in atomic number beyond, the amounts of these rare elements that can be made available for chemical research are measured in atoms rather than fractions of a gram. Weighable quantities cannot be synthesized and we speak of "atom chemistry" and even "one-atom-at-a-time chemistry" for the heaviest actinide and transactinides. These realities are illustrated in Table 5, which also points to a second grave obstacle to chemical research with the elements listed, namely, the sharply decreasing nuclear half-lives. Clearly, with these limitations on the time in which to complete an experiment and the few atoms available, many fundamental and important physical and chemical properties are outside the domain of experimental measurement.

If we observe the chemical behavior of fewer than a hundred atoms, can we be reasonably certain that our ob-

servations represent the "true" chemistry of an element? This troublesome question has only recently been addressed and a rational response is now available. BORG and DIENES [60] considered the rate of approach to a thermodynamic equilibrium in an ensemble where only a few atoms of an element are present. Taking a single-step exchange reaction,



as one commonly encountered, they assume a displacement mechanism illustrated in the simple activation energy diagram of Fig. 5. If  $\Delta G^\ddagger$  was less than  $\sim 15$  to  $17$  kcal, the residence time in each state MX or MY was calculated to be very short and an equilibrium would be rapidly (1 s) reached. This assumes a collision frequency of the same magnitude as vibration frequencies, or about  $10^{14} \text{ s}^{-1}$ . Once equilibrium is reached, the fractional average time an atom spends as MY or MX is proportional to the equilibrium value of  $(\text{MY})/(\text{MX})$ . Thus, an experimental measurement of  $(\text{MY})$  and  $(\text{MX})$  with very few atoms of M present will yield an equilibrium constant statistically close to the "true" value provided both states are rapidly sampled. They calculated from the binomial law that with as few as 10 atoms of M, the probability of obtaining twice the most probable value in an experimental measurement was 10% or less when the fraction of either species was greater than 1%.

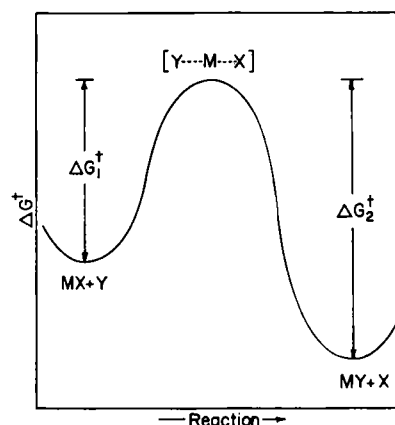


Fig. 5. Activation energy diagram for a single-step exchange reaction.

### Fermium

Several Fm isotopes with half lives of nearly a day to 100 days are available in amounts of  $10^9$  atoms or more. The nuclides  $^{255}\text{Fm}$  and  $^{257}\text{Fm}$  are conveniently used for chemical investigation of Fm; they are obtainable as products from long neutron irradiations of  $^{242}\text{Pu}$  and  $^{244}\text{Cm}$ . The 20-h  $^{255}\text{Fm}$  is generated by the beta decay of 40-d  $^{255}\text{Es}$  produced in the neutron irradiations. By chemically isolating the Es and periodically re-separating Fm from its parent, one can secure a fairly long-term source of  $^{255}\text{Fm}$  adequate for all tracer experiments.

Table 5. Half-lives and numbers of atoms available for the chemical investigations of the heaviest actinides

Isotope	Half-life	Average atoms per experiment
$^{255}\text{Fm}$	20.1 h	$10^{11}$
$^{256}\text{Md}$	77 min	$10^6$
$^{255}\text{No}$	3.1 min	$10^3$
$^{256}\text{Lr}$	31 s	10

The ground-state electronic configuration of Fm is  $5f^{12}7s^2$  or an  ${}^3H_6$  level [61]. This was established by an atomic-beam measurement of the magnetic moment  $g_J$  of  $3.24\text{-h } {}^{254}\text{Fm}$ . In this elegant measurement,  $\text{FmF}_3$  was reduced with  $\text{ZrC}_2$  in an atomic-beam apparatus to produce a beam of neutral Fm atoms. Three magnetic resonances were detected and the best value for  $g_J$  was calculated. To obtain the level term, it was necessary to extrapolate the mixing due to intermediate coupling in the electron spin-orbit interactions ( $j-j$  and  $L-S$ ). These extrapolations were made from lower actinides and supplemented by Hartree-Fock calculations for free atoms. From similar calculations, the next higher level is predicted to be  ${}^5G_7$ , starting about  $20,000\text{ cm}^{-1}$  above the ground state and having the configuration  $5f^{11}6d7s^2$ . However, the  $f^{12}sp$  and  $f^{11}s^2p$  configurations are very close in energy [5] to the  $f^{11}ds^2$  so that it is impossible to unambiguously estimate the next level above the ground state.

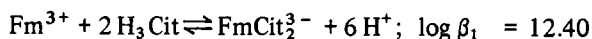
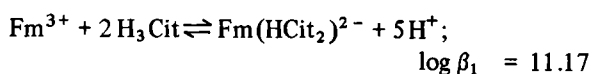
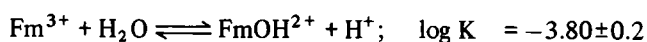
The electron binding energies of Fm have been measured for the  $K$ ,  $L_{1-3}$ ,  $N_{1-5}$ ,  $N_{6,7}$ ,  $O_{1-3}$ ,  $O_{4,5}$ , and  $P_{2,3}$  shells [62, 63]. These were determined to an accuracy of 10 eV by conversion-electron spectroscopy in the beta decay of  ${}^{254m}\text{Es}$  to  ${}^{254}\text{Fm}$ . A surprisingly low binding energy for the  $P_{2,3}$  ( $6p_{1/2,3/2}$ ) shell of  $24 \pm 9$  eV was found. Predicted values derived either from extrapolations of those measured in lower actinides or calculated by Hartree-Fock and relativistic local-density methods are about 20 to 60 eV higher in energy. However, relativistic Dirac-Fock calculations with the addition of a Lamb shift correction gave binding energies in excellent agreement with the experimental ones [64]. As the authors suggested, a binding energy of 24 eV might provide a possibility for  $6p$  involvement in chemical and spectroscopic interactions.

The properties of Fm metal and of its solid compounds are for the most part unknown because there are insufficient quantities to prepare even micro-samples. In the numerous thermochromatographic studies by ZVARA and coworkers, the evaporation of Fm and Md tracer from molten La at  $1150^\circ\text{C}$  was compared with the behavior of other selected lanthanides and actinides [65]. The volatility of Md and Fm was found to be greater than that of Cf, and Cf was about equivalent to Yb and Eu. All were much more volatile than Am and Ce. A later study at this Laboratory by HÜBENER [12] extended these studies by comparing the adsorption of elemental Cf, Es, Fm, and Md in the gaseous state on the Ti surface of a thermochromatographic column. Since they had established that for the  $s$  and  $f$  elements there was a correspondence between the metallic valence and the deposition temperature, their purpose was to characterize the metallic state properties of the heavy actinides which are available only in trace amounts. On the basis of virtually equal deposition temperatures, HÜBENER concluded that Cf, Es, Fm, and Md were divalent metals, although Cf condensed at a slightly higher temperature than the other actinides. Ytterbium behaved the same as the Es, Fm, and Md, but Eu and Sm condensed at a temperature  $300^\circ$  higher. The evaporation rates of Cf and Fm from molten U have also been found to be

equal [66] which again shows that if Cf is to be considered a divalent metal, then so should Fm metal.

The separation methods for Fm are the same as those used for separating other trivalent lanthanides and actinides. Additional methods for separating trivalent actinides from lanthanides are given in the Separation and Purification section on einsteinium. For separating the adjacent elements, Es and Md, a high-resolution chromatographic method is necessary. Either ion exchange, using strongly acidic resins [67], or extraction chromatography employing alkylphosphoric acids [68] is strongly preferred. A complexing agent ( $\alpha$ -hydroxyisobutyric acid) is required to selectively elute the actinides from cation-exchange resins. The separation factors, defined as the ratio of the distribution coefficients of two metal ions, are small for both cation exchange and extraction chromatography. These factors range from 1.7 to 2.04 for Es-Fm separations using a Dowex-50 cation exchanger [67] or extraction chromatography with HCl as the eluant and bis(2-ethylhexyl)phosphoric acid diluted with heptane as the extractant [69]. The Fm-Md separation factors obtained by these two methods were 1.4 and 4.0, respectively [67, 69].

The solution chemistry of Fm deals largely with the highly-stable tripositive oxidation state, although the dipositive state is also known. Formation constants for citrate complexes [70] and the first hydrolysis constant have been accurately determined for  $\text{Fm}^{3+}$  [71, 72]. Since the formation and hydrolysis constants for Am, Cm, Cf, and Es were measured simultaneously with those for Fm, the complex strengths of many of the trivalent actinides can be compared [72]. All constants were determined at an ionic strength of  $\mu = 0.1$  in a perchlorate medium by measuring the partitioning of the radioactive tracers between a thenoyltrifluoroacetate-benzene phase and the aqueous phase. The results for Fm may be expressed as follows:



Compared to the other actinide ions investigated, Fm formed stronger complexes with citrate and hydroxyl ions because of its smaller ionic radius. The smaller radius is a direct consequence of the increased nuclear charge with partial shielding of the outermost  $6p$  electrons by the inner  $f$  electrons.

The reduction of  $\text{Fm}^{3+}$  to  $\text{Fm}^{2+}$  was first reported in 1972 by N. B. MIKHEEV and coworkers [73]. The reduction was accomplished with Mg metal in the presence of  $\text{Sm}^{3+}$  which was coreduced in an aqueous-ethanol solution. Identification of the divalent state of Fm was established by determining the extent of its cocrystallization with  $\text{SmCl}_2$  and this was compared to the amount of tracer  $\text{Sr}^{2+}$  also carried with  $\text{SmCl}_2$ . A milder reductant,  $\text{Eu}^{2+}$ , failed to reduce  $\text{Fm}^{3+}$ , which placed the standard reduction potential of  $\text{Fm}^{3+}$  between  $\text{Eu}^{2+}$  and  $\text{Sm}^{2+}$  or  $-0.43$

to  $-1.55$  V relative to the standard Pt,  $H_2 | H^+$  electrode. Later work [74] by these scientists narrowed the range to between  $-0.64$  and  $-1.15$  V and, most recently, they were able to estimate the potential was the same as the  $Yb^{3+} \rightarrow Yb^{2+}$  couple within  $0.02$  V, or  $-1.15$  V [75, 76]. This estimate was based on measuring the ratio of Fm(III) to Fm(II) during the cocrystallization of Fm(II) with  $SrCl_2$  while changing the ratio of Yb(II)/Yb(III) in each experiment. The difference between the standard potentials of Fm and Yb is then easily determined from the Nernst equation. The reduction of Fm to a divalent ion with  $SmCl_2$  has also been observed recently by HULET *et al.* [77].

In further work related to the divalent state, the electrode potential for the reduction of  $Fm^{2+}$  to  $Fm^0$  has been measured by SAMHOUN and DAVID [78]. Over a period of years, they developed and refined a radiopolarographic technique for determining half-wave potentials at a dropping-Hg cathode. In addition to Fm, they have measured either the  $III \rightarrow 0$  or  $II \rightarrow 0$  potential for all transplutonium actinides except Lr [53, 78, 79]. The polarograph for Fm is shown in Fig. 6. The electrochemical reaction taking place at a reversible electrode can be deduced from the slope of the polarographic wave. Specifically, the number of electrons exchanged at the electrode, based on the Nernst equation, is obtained from this slope. From their analysis of the polarograms, there were three electrons involved in the electro-chemical reduction of the trivalent ions of the elements Am through Es and only two electrons for the reduction of Fm, Md and No. This implies that  $Fm^{3+}$  was first reduced to  $Fm^{2+}$  before being further reduced to metal. The  $III \rightarrow II$  reduction step is not detected by this radiopolarographic technique because both III and

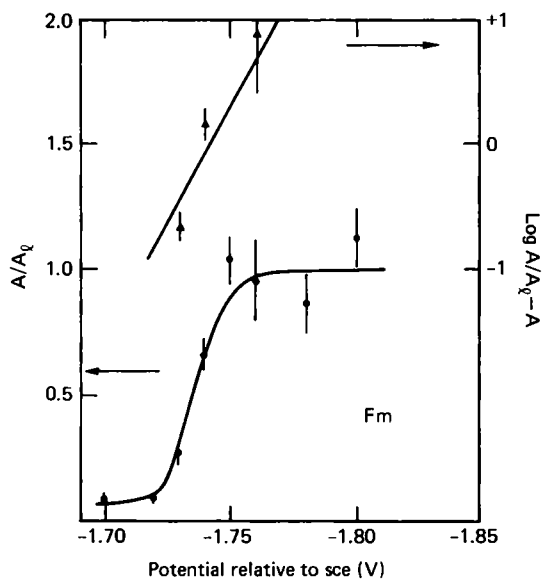


Fig. 6. Distribution of Fm as a function of applied voltage between mercury in a dropping Hg cathode and  $0.1 M$  tetramethyl ammonium perchlorate at  $pH = 2.4$ . The slope of the logarithmically-transformed line indicates two electrons were exchanged in the electrolysis reaction (Ref. 79).

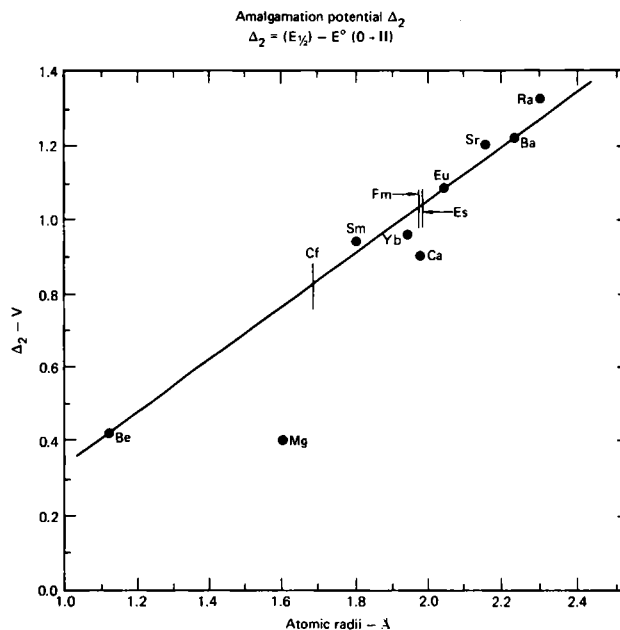


Fig. 7. Amalgamation potentials,  $\Delta_2$ , derived from experimental data are plotted as a function of the atomic (metallic) radii. The amalgamation potential for Fm is obtained by using an estimated radius. Partially redrawn from Ref. [52].

II ions are in the solution phase, whereas the measured parameter is the distribution of the tracer between the aqueous and Hg phase. The half-wave potentials measured by this method include the amalgamation potential of the metal-mercury reaction. The potential for the overall process for Fm, *i.e.*



was found to be  $-1.474$  V with reference to the standard hydrogen electrode. The amalgamation potential was estimated to be  $0.90$  V by using the metallic radius as a correlating parameter and interpolating within a series of divalent elements with known amalgamation potentials [52]. This correlation is shown in Fig. 7. The standard electrode potential is then given as  $-2.37$  V for the  $Fm^{2+} + 2e^- = Fm^0$  reaction. The authors' estimated  $5$  mV accuracy for the measured half-wave potential seems reasonable, but there is a much larger uncertainty in the estimated amalgamation potential.

### Mendelevium

The isotope  $^{256}Md$  is nearly always employed for chemical studies of this element. Besides having a convenient half-life of  $77$  min, this nuclide can be made with millibarn cross sections by a number of nuclear reactions using light or heavy ions with actinide target nuclei. We have found that the bombardment of fractions of a microgram of  $^{254}Es$  with intense alpha-particle beams will produce  $\sim 10^6$  atoms of  $^{256}Md$  in one to two hours of irradiation time.

Table 6. Comparison of the extraction behavior of tracer einsteinium, fermium, and mendelevium after treatment with various reducing agents. The column-elution method of extraction chromatography was used with the extractant HDEHP adsorbed on a column bed of a fluoroplastic powder. Ref. 80

Conditions for reduction	Standard potential of reducing agent (volts)	% Non-extracted by HDEHP column	
		Md	Es-Fm
Zn (Hg) amalgam in upper half of extraction column	-0.763	77	0.10
0.01 M Eu <sup>2+</sup> , 0.1 M HCl, ~ 2-3 min, 80°C; Zn (Hg) amalgam in upper half of extraction column	-0.43	75	0.10
0.6 M Cr <sup>2+</sup> , 0.1 M HCl, ~ 2 min, 25°C; extraction column prewashed with 0.6 M Cr <sup>2+</sup> in 0.1 M HCl	-0.41	99	0.56

The <sup>256</sup>Md is most easily detected through spontaneous fission arising from the ingrowth of its electron-capture daughter, <sup>256</sup>Fm. A difficulty with using spontaneous-fission counting to determine the Md content of samples is that the growth and decay of fission radioactivity in each sample must be followed with time in order to resolve the amounts of Md and Fm initially present. However, alpha-particles of a distinctive energy coming from a 10% alpha-decay branch can also be used to identify <sup>256</sup>Md in a mixture of actinide tracers.

The volatility of mendelevium metal has been compared with that of other actinide metals [12, 65]; these results were described in the fermium section. Because of the high volatility found, mendelevium was believed to be a divalent metal.

There are no experimental verifications of the electronic structure of Md, but this has been calculated by several methods to be  $5f^{13}7s^2$  in which the ground state level is  $^2F_{7/2}$  [5].

The separation of Md from the other actinides can be accomplished either by reduction of Md<sup>3+</sup> to the divalent state [80] or by chromatographic separations with Md remaining in the tripositive state. Historically, Md<sup>3+</sup> has been separated in columns of cation-exchange resin by elution with  $\alpha$ -hydroxy isobutyric acid solutions [67]. This method is still widely used even though extraction chromatography requires less effort and attention to technique. HORWITZ and coworkers [69] developed a highly-efficient and rapid separation of Md<sup>3+</sup> by employing HNO<sub>3</sub> elutions from columns of silica powder saturated with an organic extractant, bis(2-ethylhexyl)phosphoric acid. The separation of Md from Es and Fm could be completed in under 20 minutes and had the advantage of providing final solutions of Md free of complexing agents that might be an interference in subsequent experiments.

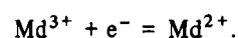
When the divalent state of Md was first discovered, extraction chromatography was used to prove that the behavior of Md<sup>2+</sup> was dissimilar to that of Es<sup>3+</sup> and Fm<sup>3+</sup> [80]. The extractant, bis(2-ethylhexyl)phosphoric acid (HDEHP), has a much lower affinity for divalent ions than

it does for the tri- and tetravalent ones. Thus, the extraction of Md<sup>2+</sup> is much poorer than the extraction of the neighboring tripositive actinides as indicated by the results shown in Table 6. This became the basis for a separation method in which tracer Md in 0.1 M HCl is reduced by fresh Jones Reductor in the upper half of an extraction column containing HDEHP adsorbed on a fluorocarbon powder in the lower half. Mendelevium, in the dipositive state, is rapidly eluted with 0.1 M HCl whereas the other actinides are retained by the extractant. The separation is quickly performed, but the Md contains small amounts of Zn<sup>2+</sup> from the Jones Reductor and also Eu<sup>2+</sup>, which is usually added prior to the elution to prevent reoxidation of Md<sup>2+</sup> by the extractant.

The solution chemistry of the trivalent oxidation state has not been investigated beyond its behavior in the separation procedures described above. All observations indicate that Md<sup>3+</sup> is a "normal" actinide with an ionic radius slightly less than that of Fm. As might be expected, attempts to oxidize Md<sup>3+</sup> with sodium bismuthate failed to show any evidence for Md<sup>4+</sup> [80].

The divalent oxidation state was the first found for any member of the actinide series [80, 81] and, therefore, stirred a strong theoretical and experimental effort to establish the reasons for the unexpected stability of this state in Md and, subsequently, in the adjacent actinides. We shall summarize the interpretations for divalency in the heaviest actinides in a later section of this review, but in this section, only the known properties of Md<sup>2+</sup> will be presented.

In the earliest experiments with Md<sup>2+</sup>, rough measurements were made of the reduction potential for the half-reaction



The first measurement gave a reduction potential of -0.2 V with respect to the standard hydrogen electrode [80]. This value was obtained from determining the equilibrium

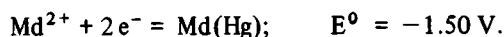
concentration of each metal ion in the reaction



and then calculating the equilibrium constant. After entering the equilibrium constant into the Nernst equation, it was found that  $\text{V}^{3+}$  was a better reducing agent than  $\text{Md}^{2+}$  by about 0.07 V. In other experiments, Mály observed the complete reduction of  $\text{Md}^{3+}$  with  $\text{V}^{2+}$  but the reduction was incomplete when  $\text{Ti}^{3+}$  was used [81]. From these observations, he concluded the standard reduction potential of  $\text{Md}^{3+}$  was close to  $-0.1$  volt. The standard potentials obtained by both groups are in reasonable agreement and, most importantly, they conclusively show that the stability of  $\text{Md}^{2+}$  is greater than that of any lanthanide(II) ion. This finding was surprising since divalency in the lanthanides is mainly associated with the special stability given by the half-filled and fully-filled  $f$ -electron shell. Divalent Md ions are at least one electron short of the stable  $5f^{14}$  configuration.

Additional experiments, which may not be clearly relevant to the divalent oxidation state, include the reduction of  $\text{Md}^{3+}$  to  $\text{Md}(\text{Hg})$  by sodium amalgams and by electrolysis [82]. Both the extraction experiments with Na amalgams and the electrolysis at a Hg cathode indicated a large enrichment of Md in the Hg phase relative to that of Np, Pu, Am, Cm, and Cf. The percentages of Es and Fm in the sodium amalgam were not greatly different from the percentage of Md. But a clear enrichment of Md was obtained in the electrolysis experiments because the initial rate of amalgamation was much larger for Md than for Es and Fm.

Recently, new electrochemical experiments were carried out with Md in which controlled-potential electrolysis was used to study the reduction of  $\text{Md}^{3+}$  to the metallic state in a Hg amalgam [79, 83]. Half-wave potentials were measured by radiocoulometry and radiopolarography in the presence of noncomplexing and weak and strong complexing agents. The radiopolarogram obtained for Md in a noncomplexing medium is presented in Fig. 8. The half-wave potential for Fm was remeasured at the same time as that of Md because of its presence as a decay product of  $^{256}\text{Md}$ . The results showed that the reduction potential of Md was about 10 mV more negative than Fm and that no significant difference was observed upon changing the medium from  $\text{ClO}_4^-$  to  $\text{Cl}^-$ . In citrate solutions, a shift of 90 mV was obtained for Md which is about the same shift seen with Fm and Ba ions in a citrate medium. The slope of the logarithmically transformed wave was 30 mV for Md and Fm and, for the reasons noted in the section on Fm, this slope corresponds to a two-electron exchange at the electrode. These results demonstrate that the electrochemical behavior of Md is very similar to that of Fm and can be summarized in the equation



If a 0.90 V amalgamation potential is assumed, then a

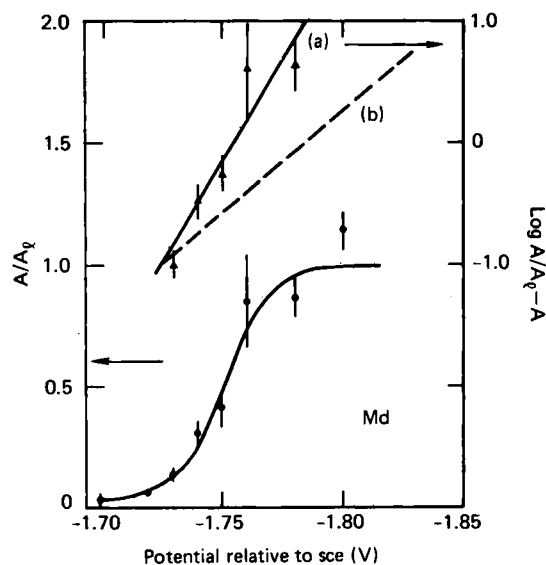


Fig. 8. Distribution of Md as a function of applied voltage between mercury in a dropping Hg cathode and 0.1 M tetramethyl ammonium perchlorate at pH = 2.4. The slope of the logarithmically-transformed line indicates the number of electrons exchanged in the electrolysis reaction. The slope of line (a), showing a two electron reduction, is 30 mV, and (b) is 60 mV, which corresponds to a one-electron reduction (Ref. 79).

standard reduction potential of  $-2.40$  V is obtained.

In addition to the di- and trivalent ions of Md, a stable monovalent ion was reported by MIKHEEV *et al.* in 1972 [84]. This oxidation state was indicated in the cocrystallization of Md with CsCl and RbCl after the coreduction of  $\text{Md}^{3+}$  and  $\text{Sm}^{3+}$  with Mg in an ethanol-7 M HCl solution. Mendelevium was also found enriched in  $\text{Rb}_2\text{PtCl}_6$  precipitates, a specific carrier for the larger ions of the alkali metals. These results were explained by a stabilization of the monovalent ion due to completing the  $f$  shell which would give the  $5f^{14}$  electronic configuration.

In response to the negative findings from others' studies [77, 83], MIKHEEV and his colleagues [85] carried out new cocrystallizations of Md with NaCl and KCl after reducing with  $\text{Eu}^{2+}$  or  $\text{Yb}^{2+}$ . The NaCl or KCl salts were forced to crystallize by heavily salting the nearly neutral  $\text{H}_2\text{O}$ -ethanol solutions, containing tracer Md, with 4 M LiCl. Because anomalous mixed crystals were not formed, they again claimed the cocrystallization of Md with NaCl or KCl demonstrated the presence of  $\text{Md}^+$ .

The RbCl cocrystallizations and  $\text{Rb}_2\text{PtCl}_6$  coprecipitations of Ref. 84 were recently repeated and an extensive series of new experiments were performed in which attempts were made to prepare  $\text{Md}^+$  by reduction with  $\text{SmCl}_2$  in an ethanolic or fused KCl medium [77]. After the reductions, the coprecipitation behavior of Md was compared with the behavior of tracer amounts of Es, Fm, Eu, Sr, Y, and Cs, also present in the same solution. A large number of experiments showed that Md consistently followed the behavior of  $\text{Fm}^{2+}$ ,  $\text{Eu}^{2+}$ , and  $\text{Sr}^{2+}$  rather than the behavior of  $\text{Cs}^+$ . The most telling experiment was the precipitation of  $\text{Rb}_2\text{PtCl}_6$  after reduction of  $\text{Md}^{3+}$  with  $\text{Sm}^{2+}$ . The distribution of the tracer elements between the precipitate and an 85% ethanol solution is given

Table 7. Distribution of tracer elements after reduction with  $\text{Sm}^{2+}$  and coprecipitation with  $\text{Rb}_2\text{PtCl}_6$  in 85% ethanol. Ref. 77

Fm	Md	Distribution ratio for			Es	Cs
		Eu	Sr	Y		
0.004	0.005	0.006	0.012	0.017	0.033	110

in the form of a ratio in Table 7. These results clearly demonstrate that Md did not coprecipitate with  $\text{Rb}_2\text{PtCl}_6$ , whereas virtually all of the Cs did so. The overall conclusion of this work was that Md cannot be reduced to a monovalent ion with  $\text{Sm}^{2+}$  and, therefore, the earlier claim for  $\text{Md}^+$  was unsubstantiated.

This same conclusion was reached also by SAMHOUN *et al.* [83] and DAVID and coworkers [79] on the basis of their electrochemical investigations of Md, which we described earlier. If the potential for the reaction  $\text{Md}^+ + e^- = \text{Md}$  was more positive than  $-1.5$  V, it would have been observed in the electrochemical reductions. Furthermore, the logarithmic slope of the Md reduction waves could not be fitted to a slope of 60 mV expected for a one-electron change. And lastly, the shifts in potential caused by complexing Md with either citrate or chloride ions were consistent with it being a divalent ion and not with it being either a cesium-like or silver-like ion.

Because of the large number and variety of negative results, the weight of evidence is heavily against  $\text{Md}^+$ , but the attempts to produce a monovalent state have the positive effect of setting limits on its stability. From the limits obtained, we can then make an estimate on the stability of the  $5f^{14}$  configuration relative to the  $5f^{13}7s$ . Presumably, the  $f^{13}s$  configuration lies lower in energy than the  $f^{14}$  because there is no obvious stabilization of a monovalent state due to a possible closing of the  $5f$  shell. The divalent ion is then at least 1.3 V more stable than the monovalent ion.

## Nobelium

The principle isotope of nobelium produced for investigations of its chemical properties is 3.1-min  $^{255}\text{No}$ . In the earliest studies [86], this nuclide was synthesized by irradiating  $^{244}\text{Pu}$  with 97-MeV  $^{16}\text{O}$  ions, but larger yields were later obtained in bombardments of  $^{249}\text{Cf}$  targets with 73-MeV  $^{12}\text{C}$  ions [87]. From the latter nuclear reaction, about 1200 atoms of  $^{255}\text{No}$  were collected every ten minutes. Of these 1200 atoms, only 3 to 20% were detected after the chemical experiments because of losses by radioactive decay, losses in the experiments, and a 30% geometry for counting alpha particles emitted in the decay of this isotope. To obtain results that were statistically significant, the experiments were repeated until the required accuracy was attained.

Future work with No may require techniques or procedures of greater complexity than the one-step chemical methods used in past studies. The author believes that  $^{259}\text{No}$ , because of its 1-h half-life, would permit these

more extensive investigations of No chemistry. Approximately 1100 atoms can be made in a two-hour irradiation of  $^{248}\text{Cm}$  with 96-MeV  $^{18}\text{O}$  ions. In combination with the long half-life, this number of atoms is sufficient to permit a broader range of experiments to be performed.

A central feature in the chemistry of No is the dominance of the divalent oxidation state [86]. In this respect, No is unique within the lanthanide and actinide series, since none of the other twenty-seven members possesses a highly-stable divalent ion. The electronic configuration of the neutral atom obtained from relativistic Hartree-Fock calculations is  $5f^{14}7s^2$  [5]. Clearly the special stability of  $\text{No}^{2+}$  must arise from the difficulty in ionizing an  $f$  valence electron from the completed  $5f$  shell. Thus, pairing of the last electron to close the shell results in the  $f$  electron levels taking a rather abrupt drop in energy below the Fermi surface.

The separation of No from other actinide elements is based entirely on the dissimilar behavior of  $\text{No}^{2+}$  in comparison with the tripositive actinide ions. Without the addition of strong oxidants, No will be present as  $\text{No}^{2+}$  in acidic solutions and will have the general chemical properties of Group IIA elements in the Periodic Table. We have found that the extraction chromatographic method described in the section on Md provides an effective separation from all other actinides and lanthanides. In contrast to Md, reducing agents are unnecessary in separating No by this extraction chemistry.

The solution chemistry of No was explored shortly after the discovery of divalent Md [86]. Subsequent studies include an estimation of the III  $\rightarrow$  II reduction potential [88], aqueous complexing with carboxylate ions [89], and a determination of  $\text{No}^{2+}$  extraction and ion-exchange behavior in comparison with the alkaline earths [87]. The first studies [86] indicated that the normal state of No in aqueous solution was that of a divalent ion. Nobelium was coprecipitated with  $\text{BaSO}_4$  but not with  $\text{LaF}_3$ . After oxidation with  $\text{Ce}^{4+}$ , a large fraction of the No coprecipitated with  $\text{LaF}_3$ . This behavior is consistent with a change in oxidation state from (II) to (III). An elution position of No relative to tracer quantities of Es, Y, Sr, Ba, and Ra (Fig. 9)

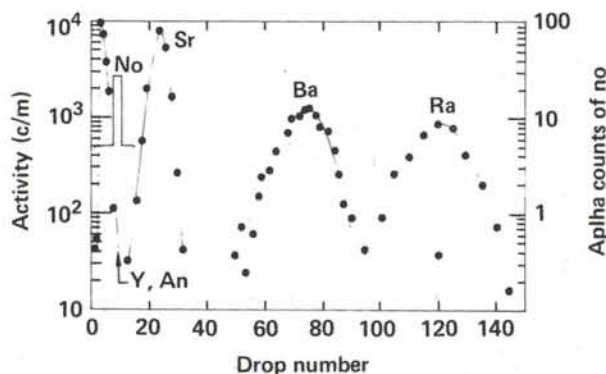


Fig. 9. Elution of nobelium from a heated ( $80^\circ\text{C}$ ) Dowex 50  $\times$  12 cation-exchange column with 1.9 M ammonium  $\alpha$ -hydroxyisobutyrate (pH 4.8). (Reprinted with the permission of Science (Ref. 86): Copyright 1968 by the American Association for Advancement of Science).

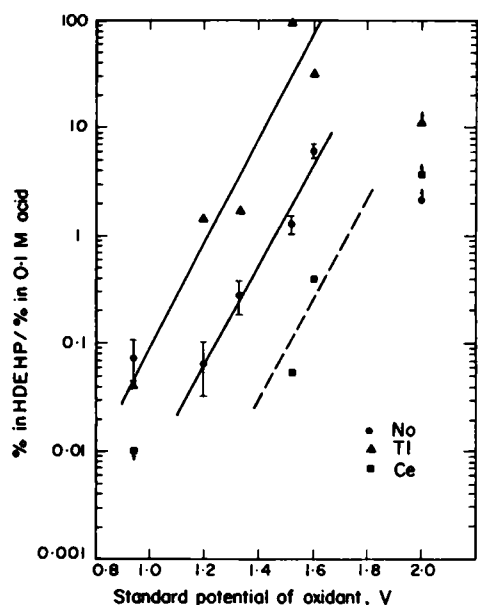


Fig. 10. Ratio of the percent of nobelium, thallium, and cerium extracted into the organic phase (HDEHP) to the percent left in the  $\sim 0.1 M$  acid phase versus the standard potential of the oxidant used. Reprinted with the permission of Pergamon Press (Ref. 88).

showed that No did not elute before Es as would be expected of a tripositive actinide ion.

The standard reduction potential of the  $\text{No}^{3+}/\text{No}^{2+}$  couple in aqueous solution was estimated by SILVA and coworkers [88] from the extractability of No after treatment with a variety of oxidants. The distinction between  $\text{No}^{2+}$  and  $\text{No}^{3+}$  was made on the basis of the affinity of the extractant, bis(2-ethylhexyl) phosphoric acid, for highly-charged cations. In  $0.1 M$  acid, mono- and dipositive ions are poorly extracted, whereas the tri- and tetrapositive ions are strongly absorbed in the extractant. In comparison with the behavior of the tracer ions of Ra, Tl, Ce, Cm, and Cf (see Fig. 10) it was shown that No was not fully extracted until  $\text{H}_5\text{IO}_6$  (standard potential = 1.6 V) was used as an oxidant. Chromate and  $\text{HBrO}_3$  partially oxidized  $\text{No}^{2+}$  to  $\text{No}^{3+}$ . From these observations, a potential of 1.4 to 1.5 V was estimated for the couple.

The extraction behavior of  $\text{No}^{2+}$  in a tri-*n*-octylamine-HCl system was compared with that of divalent Hg, Cd, Cu, Co, and Ba [87]. This experiment provided a test of the chloride complex strength of  $\text{No}^{2+}$  because the amine anion-exchanger will only extract anionic species. It was found that  $\text{Ba}^{2+}$  and  $\text{No}^{2+}$  were not extractable over a range of 0.2 to  $10 M$  HCl, while the other divalent ions of Hg, Cd, Cu, and Co were strongly extracted. This implies noncomplexing of No in the chloride medium which is a characteristic of the alkaline earths.

The elution position of  $\text{No}^{2+}$  from a cation-exchange resin with  $4 M$  HCl eluant was compared with the elution positions of  $\text{Be}^{2+}$ ,  $\text{Mg}^{2+}$ ,  $\text{Ca}^{2+}$ ,  $\text{Sr}^{2+}$ ,  $\text{Ba}^{2+}$ , and  $\text{Ra}^{2+}$  [87]. The  $\text{No}^{2+}$  ions eluted at exactly the  $\text{Ca}^{2+}$  position. Similar column elution experiments, using bis(2-ethylhexyl) phosphoric acid (HDEHP) adsorbed on an inert support

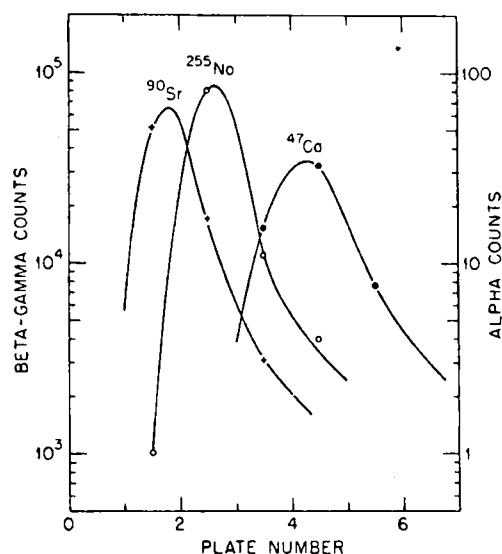


Fig. 11. Elution of  $\text{No}^{2+}$ ,  $\text{Ca}^{2+}$ , and  $\text{Sr}^{2+}$  with  $0.025 M$  HCl from a column of bis(2-ethylhexyl) phosphoric acid on an inert support. Reprinted with the permission of Inorganic Chemistry (Ref. 87).

material and  $0.025 M$  HCl as the eluting acid, showed  $\text{No}^{2+}$  eluting between  $\text{Ca}^{2+}$  and  $\text{Sr}^{2+}$ . These elution curves are illustrated in Fig. 11. With the same extractant, the distribution coefficient for  $\text{No}^{2+}$  was measured as a function of hydrogen-ion concentration. From the mass-action expression for the ion exchange, a slope of +2 was obtained from the line describing the log of the distribution coefficients vs. pH. The extraction of  $\text{No}^{2+}$  is second power with respect to the  $\text{H}^+$  concentration, thus indicating a charge state of two for No because of the cation-exchange mechanism for extraction in this system.

SILVA and coworkers [87] noted that other investigators had shown a linear correlation between the log of the distribution coefficients of the alkaline earths and their ionic radii. This appeared to be the case wherever a pure cation-exchange mechanism governed the distributions between phases and, hence, was applicable to distributions obtained with either cation-exchange resins or extractants. In Fig. 12,  $\log D$  is plotted as a function of ionic radius for the extraction of various dipositive cations into  $0.1 M$  HDEHP from aqueous solutions. The measured distribution coefficient for  $\text{No}^{2+}$ , when placed on the correlation line, gave an ionic radius of 0.11 nm. If the distribution coefficients from their ion-exchange elutions were used, the ionic radius of  $\text{No}^{2+}$  would be the same as that of  $\text{Ca}^{2+}$  (0.10 nm), since both ions have the same elution position. An ionic radius of 0.11 nm was also obtained by applying Pauling's correction to the radius of the outermost,  $6p_{3/2}$  shell, which was calculated from a relativistic radial wave function (Hartree-Fock-Slater). The calculated ionic radius is in agreement with the radii derived from their solvent-extraction and ion-exchange results. A radius of 0.11 nm for  $\text{No}^{2+}$  can be compared with 0.103 nm found for  $\text{Yb}^{2+}$  [90], the lanthanide homolog of No. Insertion of the  $\text{No}^{2+}$  ionic radius into an empirical form

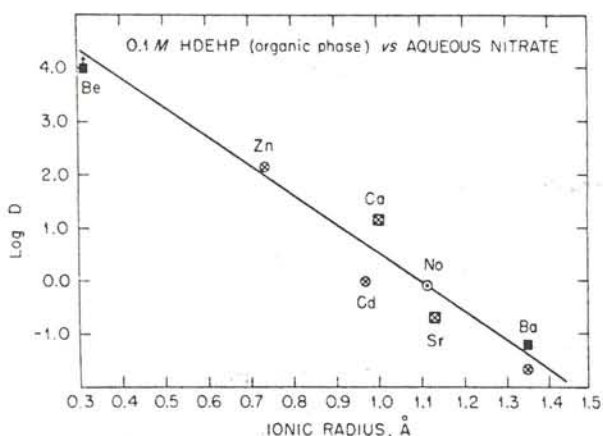


Fig. 12. Log D vs. ionic radii for typical divalent cations in the bis(2-ethylhexyl) phosphoric acid-aqueous nitrate system. Reprinted with the permission of Inorganic Chemistry (Ref. 87).

of the Born equation gave a single-ion heat of hydration of  $-1490 \text{ kJ mole}^{-1}$ .

The ability of  $\text{No}^{2+}$  to form complexes with citrate, oxalate, and acetate ions in an aqueous solution of  $0.5 \text{ M NH}_4\text{NO}_3$  was investigated by MCDOWELL and coworkers [89]. The complex strengths of  $\text{Ca}^{2+}$  and  $\text{Sr}^{2+}$  with these carboxylate ions were measured under the same conditions for comparison with the No results. The formation constants they obtained are given in Table 8 and indicate for each anion, the complexing tendency of  $\text{No}^{2+}$  is between that of  $\text{Ca}^{2+}$  and  $\text{Sr}^{2+}$  with  $\text{Sr}^{2+}$  being slightly more favored.

Table 8. Complex formation constants for  $\text{No}^{2+}$ ,  $\text{Ca}^{2+}$ , and  $\text{Sr}^{2+}$  from distribution data. Ref. 89

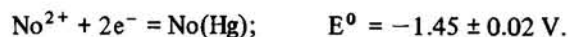
System		Formation constants	
Cation	Ligand	$\beta_1$	$\sigma^a$
$\text{No}^{2+}$	Cit	151.9	18.5
	Ox	48	5.6
	Ac	-5	5
$\text{Ca}^{2+}$	Cit	333	11.2
	Ox	88.9	2.1
	Ac	5.5	0.7
$\text{Sr}^{2+}$	Cit	96.7	1.7
	Ox	25.3	0.5
	Ac	0.58	0.12

<sup>a</sup> Standard deviation of fitting of  $\beta_1$

The standard potential for the reduction of  $\text{No}^{2+}$  to  $\text{No}(\text{Hg})$  was measured by a modified radiopolarographic technique [91]. Usually, the half-wave potential is determined by measuring the distribution of an element between the mercury and aqueous phase as a function of applied voltage. The half-life of  $^{255}\text{No}$  is too short to allow time for the recovery of No from the Hg phase for assay, therefore MEYER *et al.* measured the depletion of No in the aqueous phase as a function of a controlled potential. They assumed that equilibrium was reached in 3 minutes of electrolysis and that the electrode reaction was reversible. A sharp drop in No concentration in the aqueous

phase occurred between  $-1.8$  and  $-1.9 \text{ V}$  vs. the saturated calomel electrode or  $1.6 \text{ V}$  vs. the standard hydrogen electrode.

This potential was recently remeasured [91 a] using  $1\text{-h } ^{259}\text{No}$  and, thereby, allowing sufficient time to determine the amounts of No in both phases. In a  $0.05 \text{ M}$  acetate buffer, a potential of  $-1.72 \text{ V}$  vs. the saturated calomel electrode was obtained. Thus, the best standard value (vs. hydrogen electrode) for the potential of the reaction shown is



If this potential is reduced by about the  $0.9 \text{ V}$  estimated for the amalgamation potential, then a value of about  $-2.35 \text{ V}$  would be given for the  $\text{II} \rightarrow 0$  couple.

### Lawrencium

Element 103, lawrencium, is the last member of the actinide series and its chemical nature should be similar to its counterpart in the lanthanide series, Lu. However, confirming experimental information is nearly nonexistent because of the 35-s half-life of  $^{256}\text{Lr}$  and the great difficulty in producing a useful quantity for experiments. The bombardment of  $^{249}\text{Cf}$  with  $^{11}\text{B}$  ions is probably the most favorable nuclear reaction for producing  $^{256}\text{Lr}$ . Even so, only about ten atoms have been made in each short irradiation and of these, only one or two were detected after completion of the chemical experiments [92].

Lawrencium was expected to have a  $5f^{14}6d7s^2$  electronic configuration [93] although BREWER computed a  $5f^{14}7s^27p$  configuration [5]. BREWER'S estimates have now been confirmed by multiconfigurational (relativistic) Dirac-Fock calculations in which the ground state of lawrencium was found to be a  $2p_{1/2}$  or  $7s^27p$  electronic configuration [94]. This deviation from the  $6d7s^2$  configuration expected from extrapolation of the Periodic Table is due entirely to strong relativistic effects on the outermost  $7p_{1/2}$  orbital. The energy difference between the two possible ground states is no more than a few thousand wave numbers.

The ionization of Lr would be expected to stop with the  $f^{14}$  core intact because of the enhanced binding energy of possible valence electrons in the filled  $f$  shell. The stable valence state of Lr would then be the (III) state. Experiments to confirm this oxidation state of Lr were undertaken by SILVA and co-workers [92]. They compared the extraction behavior of Lr with several tri- and tetravalent actinides and with  $\text{Ba}^{2+}$ ,  $\text{Ra}^{2+}$ , and  $\text{No}^{2+}$ . A chelating extractant, thenoyltrifluoroacetone dissolved in methyl isobutyl ketone, was employed to extract the tracer ions from aqueous solutions that had been buffered with acetate anions. Their results, shown in Fig. 13, demonstrate that Lr is extracted within the same pH range as the trivalent actinides and, therefore, prove that Lr is trivalent.

Further studies of Lr have not been attempted.

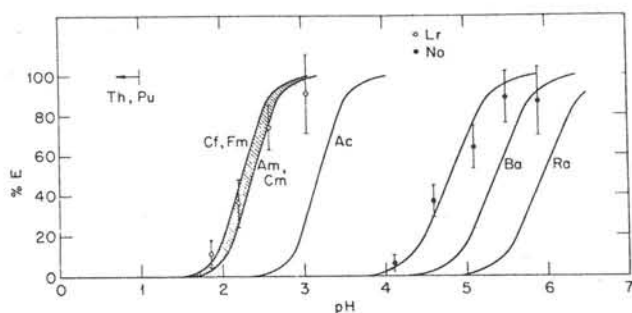


Fig. 13. Percent extracted into the organic phase as a function of the pH of the aqueous phase. Solid lines are a summary of earlier data by the same authors. Reprinted with the permission of Pergamon Press (Ref. 92).

### Actinide summary

The main result ensuing from about 15 years of intensive study of the heavier actinides is the finding of an unexpected stability of the divalent state. Table 9, summarizing the redox properties of these elements, most clearly shows the increasing stability of this state with increasing atomic number. The sinking of the  $5f$  levels with respect to the Fermi level provides the explanation for this behavior. Thus, we see, as is also the case in the light actinides, another major differentiation between the  $5f$  actinide and  $4f$  lanthanide series of elements.

Table 9. Reduction potentials of the heavier actinides. Reported as  $-E^{\circ}$  vs standard  $H^{+}$  electrode

Half reaction	Es	Fm	Md	No	Lr
III $\rightarrow$ II	1.55	1.15	0.2	-1.4	-
II $\rightarrow$ 0	2.20	2.37	2.4	2.35	-
III $\rightarrow$ 0	1.98	1.95	1.7	1.1	2.06

### Transactinides

Four elements are known with atomic numbers greater than that of lawrencium. Because none of the names proposed for these elements have received official acceptance from the International Union of Pure and Applied Chemistry, they are referred to as elements 104, 105, 106, and 107, or E-104, *etc.* This lack of authorized names is very likely to continue for many more years because of difficulties in resolving conflicting claims for their discovery. A dimension of these conflicts, namely, the certitude of the atomic number assigned to a particular nuclide used in several of the chemical investigations, is not examined in this review.

The chemistry of these elements, as estimated from extrapolation of the Periodic Table and verified by quantum mechanical calculations, should follow that of another  $d$  transition series, comparable with the  $5d$  series begin-

ning with Hf. Therefore, the chemical properties of E-104 should be quite similar to those of Hf, and E-105 to those of Ta, and so forth. In aqueous solutions, E-104 would be expected to possess a stable tetravalent state while E-105 would be pentavalent. It is the verification of these predicted chemical properties that has been the main thrust of the experimental work with these elements.

### Element 104

The chemistry of E-104 has been investigated in the gas phase as the tetrachloride [95–98] and in aqueous solution as complexes of chloride [99] and  $\alpha$ -hydroxyisobutyrate anions [100]. It has been very much of an uphill struggle to produce and identify the few atoms used in these experiments and to perform the experiments many times over with very short-lived isotopes. In the thermochromatography research carried out at the Joint Institute for Nuclear Research, Dubna, USSR, a 3-s isotope,  $^{259}(104)$ , was produced by  $^{22}\text{Ne}$  bombardment of  $^{242}\text{Pu}$  targets. The aqueous chemistry was carried out with 1-min  $^{261}(104)$  formed in the reaction of  $^{248}\text{Cm}$  with  $^{18}\text{O}$  ions. Very few atoms were produced and identified in any of the E-104 chemical investigations.

The goal of the gas-phase experiments was to show the sharp difference in volatility of the higher halides of eka-Hf relative to the volatility of the preceding Group IIIB series of actinides [95–97]. The Group IVB tetrachlorides sublime at temperatures slightly over  $300^{\circ}\text{C}$ , whereas the actinide trichlorides would require temperatures several times greater before they became volatile at an atmosphere of pressure. Therefore, the volatility of  $\text{E-104Cl}_4$  would be a distinctive measure of whether or not this element was eka-Hf. All such experiments were performed on-line at the Dubna accelerator. Atoms of E-104 recoiling from the target were stopped in a heated stream of inert carrier gas of  $\text{N}_2$  and then chlorinated downstream with  $\text{TiCl}_4$  or mixtures of  $\text{SOCl}_2$ ,  $\text{NbCl}_5$ ,  $\text{ZrCl}_4$ , and  $\text{TiCl}_4$ . The molecules of  $\text{E-104Cl}_4$  passed through a chromatographic column heated to  $300\text{--}350^{\circ}\text{C}$  and eventually deposited on mica detectors located inside and along the length of a section of the column held at  $280^{\circ}\text{C}$ . Hundreds of hours of accelerator beam time resulted in the detection of 79 spontaneous fission events, at first attributed to the decay of 0.3-s  $^{260}(104)$  [97]. However, current work supports a half-life of only 20 ms for this isotope [101].

In the last vapour-phase experiments performed by ZVARA's group [98], frontal chromatography of the chlorides was used to separate 3-s  $^{259}(104)$  and coproduced  $^{170,171}\text{Hf}$  from Sc,  $^{242}\text{Cm}$ ,  $^{246}\text{Cf}$ , and  $^{242}\text{Pu}$  also swept into the gas stream from the target region. The apparatus employed in this work was essentially unchanged from earlier experiments except that a thermal gradient was maintained beginning with  $400^{\circ}\text{C}$  at the entrance and decreasing to  $50^{\circ}\text{C}$  at the exit of the 70-cm long thermochromatographic section. The Hf isotopes and 15 spon-

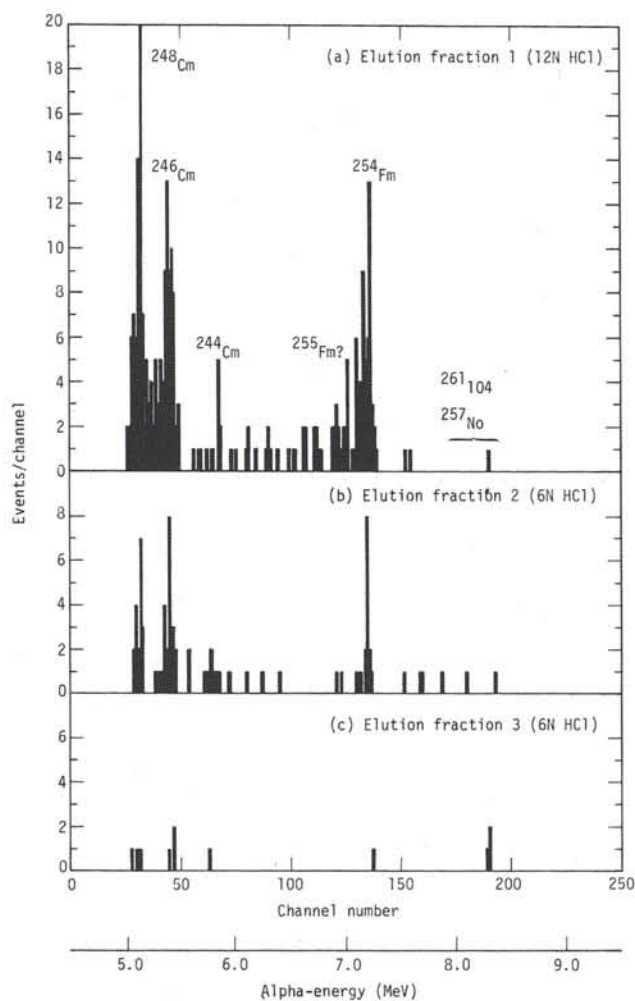


Fig. 14. Alpha spectra showing the decay of  $^{261}(104)$  and daughter atoms in three, sequential elution fractions from a column containing an anionic extractant (see text). Reprinted with the permission of Pergamon Press (Ref. 99).

taneous-fission events were found deposited in this section of the thermal-gradient column at a position corresponding to a condensation temperature of  $220^{\circ}\text{C}$ . Scandium and various actinide nuclides produced by other nuclear reactions with the target were found 100 to 125 cm upstream in an initial section of a separate  $400^{\circ}\text{C}$  tube. The volatility of  $\text{E-104Cl}_4$  clearly corresponded to that of  $\text{HfCl}_4$  and established E-104 as being eka-Hf.

During several hundred experiments, SILVA and co-workers [100] investigated the complexing and cation-exchange behavior of 1-min  $^{261}(104)$ . Recoil atoms of E-104 were trapped in an  $\text{NH}_4\text{Cl}$  layer sublimed onto Pt discs, dissolved with ammonium  $\alpha$ -hydroxyisobutyrate and passed onto a column of heated cation resin. Because of the strong formation of neutral and anionic complexes by the tetravalent IVB elements, one would expect very little adsorption and retention by the cation resin in the column. Indeed, this was the outcome of the many experiments, although the decay of only 17 atoms was observed in the eluant from the resin column. The elution position was the same as that of Hf and Zr, which were separately tested. Nobelium and other actinides were re-

tained on the resin until over 100 column-volumes of eluant had passed through the column.

In later experiments which tested the chloride complexation of E-104 [99], computer automation was used to perform all chemical manipulations rapidly, to prepare  $\alpha$  sources, and to do  $\alpha$ -spectroscopy. An extraction chromatographic method was chosen to investigate chloride complexing in high concentrations of HCl which thereby avoided the hydrolysis reaction possible at lower acidities. The extraction columns were loaded with 0.25 *F* trioctylmethylammonium chloride, since anionic-chloride complexes formed in the aqueous phase are strongly extracted by this ammonium compound. Such complexes are formed in 12 *M* HCl by the Group IVB elements and are extracted, whereas Group IA, IIA, and IIIB elements, including the actinides, form weaker complexes and are not appreciably extracted. Thus, the actinide recoil products were eluted with 12 *M* HCl while Zr, Hf, and E-104 were extracted and subsequently eluted with 6 *M* HCl, in which anionic chloride complexation is less favored. Fig. 14 shows the atoms of  $^{261}(104)$  observed by  $\alpha$ -decay in three sequential elution fractions. Only six events were observed in over one hundred experiments; one in fraction (a), two in fraction (b), and three in fraction (c). The percentage of Hf corresponding to these same fractions was 12%, 59%, and 29%. These results showed the chloride complexation of E-104 is considerably stronger than that of the trivalent actinides and is similar to that of Hf.

## Element 105

Our chemical knowledge of the heavy elements ends with E-105 although the nuclear properties are known for several isotopes of elements 106 and 107. Element 105, with a  $6d^3$  electronic configuration, is expected to have the general chemical properties of its  $5d^3$  homolog, Ta. ZVARA *et al.*, using much of the same thermochromatographic techniques employed earlier in their studies of element 104, have extended the method to determining the volatilities of the chloride and bromide compounds of E-105 [102, 103]. The chloride of E-105 was deposited on the walls of the chromatography tube at  $\sim 150^{\circ}\text{C}$ , but because of the short 2-s half-life of  $^{261}(105)$ , a distribution slewed  $50^{\circ}\text{C}$  lower in temperature was suggested by the authors. This correction was based on the appreciable decay of the  $^{261}(105)$  nuclei during their travel through the tube. The corrected distribution of the 18 observed spontaneous fission events indicated that the chlorides of E-105 are more volatile than Hf and less volatile than Nb, a  $4d^3$  homolog of E-105.

The bromides of E-105 were also found to be very volatile as shown by the location of the circles in relation to the thermal gradient in the upper part of Fig. 15. Niobium, which in separate experiments was shown to have the same deposition temperature as Ta, is obviously more volatile than E-105. From this work, the boiling point of  $\text{E-105Br}_5$  was estimated to be  $430^{\circ}\text{C}$ . An analysis of the

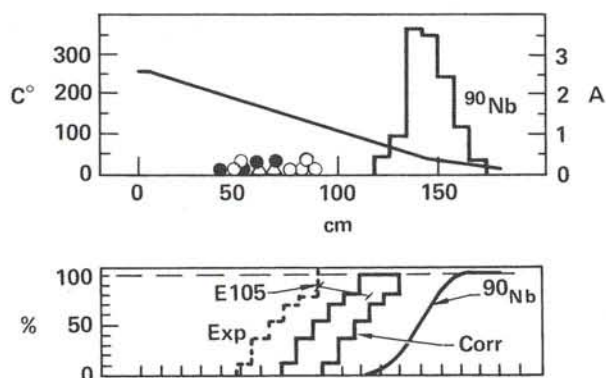


Fig. 15. Upper: Thermal gradient and deposition positions of E-105 (circles) and Nb (histogram) bromides. Lower: Integral distributions of experimental (dashed lines), and corrected (solid area) of E-105 and of Nb (solid curve) bromides. Redrawn from Ref. 103.

boiling points of pentabromides of the same structure allowed an estimate of  $\sim 0.09$  nm for the metallic radius, or  $\sim 0.02$  nm larger than that of Nb and Ta. In sum, all of the experimental observations are consistent with E-105 being a homolog of Nb and Ta.

#### Acknowledgement

This review was prepared under the auspices of the U.S. Department of Energy by the Lawrence Livermore National Laboratory under contract number W-7405-ENG-48. Portions of this review were adapted with permission from E. K. HULET in "Lanthanide and Actinide Chemistry and Spectroscopy," Norman M. EDELSTEIN, Ed., ACS Symposium Series No. 131, 1980, p. 239. Copyright 1980 American Chemical Society.

#### References

- FERGUSON, D. E.: *Proceedings Commemorating the 25th Anniversary of Elements 99 and 100*, SEABORG, G. T., ed., LBL Report 7701, National Technical Information Service, Springfield, Virginia, p. 35 (1978).
- GUTMACHER, R. G., EVANS, J. E., HULET, E. K.: *J. Opt. Soc. Am.* **57**, 1389 (1967).
- CONWAY, J. G.: In Ref. 1, p. 69 (1978).
- WORDEN, E. F., LOUGHEED, R. W., GUTMACHER, R. G., CONWAY, J. G.: *J. Opt. Soc. Am.* **64**, 77 (1974).
- BREWER, L.: *J. Opt. Soc. Am.* **61**, 1101 (1971).
- BREWER, L.: *J. Opt. Soc. Am.* **61**, 1666 (1971).
- SUGAR, J.: *J. Chem. Phys.* **60**, 4103 (1974).
- RAJNAK, K., SHORE, B. W.: *J. Opt. Soc. Am.* **68**, 360 (1978).
- GOODMAN, L. S., DIAMOND, H., STANTON, H. E.: *Phys. Rev. A* **11**, 499 (1975).
- DITTNER, P. F., BEMIS, C. E., JR.: *Phys. Rev. A* **5**, 481 (1972).
- HAIRE, R. G., BAYBARZ, R. D.: *J. Phys. Collo. (Orsay)* **49**, C4-101 (1979).
- HÜBENER, S.: *Radiochem. Radioanal. Lett.* **44**, 79 (1980).
- NUGENT, L. J., BURNETT, J. L., MORSS, L. R.: *J. Chem. Thermody.* **5**, 665 (1973).
- WARD, J. W., KLEINSCHMIDT, P. D., HAIRE, R. G., BROWN, D.: In *Lanthanide and Actinide Chemistry and Spectroscopy*, EDELSTEIN, N., ed., American Chemical Society Symposium Series 131, Washington, DC, p. 199 (1980).
- HO, POWELL, LILLY: *J. Phys. Chem. Ref. Data* **1**, 418 (1972).
- EDELSTEIN, N.: *J. Chem. Phys.* **54**, 2488 (1971).
- BOATNER, L. A., REYNOLDS, R. W., FINCH, C. B., ABRAHAM, M. M.: *Phys. Rev. B* **13**, 953 (1975).
- BOUISSIÈRES, G., JOUNIAUX, B., LEGOUX, Y., MERINIS, J., DAVID, F., SAMHOUN, K.: *Radiochem. Radioanal. Lett.* **45**, 121 (1980).
- VARGA, L. P., BAYBARZ, R. D., REISFELD, M. J., ASPREY, L. B.: *J. Inorg. Nucl. Chem.* **35**, 2775 (1973).
- NUGENT, L. J., BAYBARZ, R. D., BURNETT, J. L., RYAN, J. L.: *J. Inorg. Nucl. Chem.* **33**, 2503 (1971).
- LEBEDEV, I. A.: *Soviet Radiochemistry* **20**, 556 (1978).
- HAIRE, R. G., BAYBARZ, R. D.: *J. Inorg. Nucl. Chem.* **35**, 489 (1973).
- PETERSON, J. R.: In Ref. 1, p. 55 (1978).
- FUJITA, D. K., CUNNINGHAM, B. B., PARSONS, T. C.: *Inorg. Nucl. Chem. Lett.* **5**, 307 (1969).
- PETERSON, J. R., ENSOR, D. D., FELLOWS, R. L., HAIRE, R. G., YOUNG, J. P.: *J. Phys. Collo. (Orsay)* **49**, C4-111 (1979).
- FELLOWS, R. L., PETERSON, J. R., YOUNG, J. P., HAIRE, R. G.: *The Rare Earths in Modern Science and Technology*, MCCARTHY, G. J. and RYNE, J. J., ed., Plenum Press, New York, p. 493 (1977).
- FELLOWS, R. L., PETERSON, J. R., NOE, M., YOUNG, J. P., HAIRE, R. G.: *Inorg. Nucl. Chem. Lett.* **11**, 737 (1975).
- FELLOWS, R. L., YOUNG, J. P., HAIRE, R. G., PETERSON, J. R.: In Ref. 1 and private communication (1978).
- HULET, E. K., BODÉ, D. D.: *MTP International Review of Science, Series I, Vol. 7, Lanthanides and Actinides*, BAGNALL, K. W., ed., Butterworths, London, p. 1 (1972).
- KOSYAKOV, V. N., CHUDINOV, É. G., SHVETSOV, I. K.: *Soviet Radiochemistry* **16**, 722 (1974).
- STREET, K., JR., SEABORG, G. T.: *J. Am. Chem. Soc.* **72**, 2790 (1950).
- HULET, E. K., GUTMACHER, R. G., COOPS, M. S.: *J. Inorg. Nucl. Chem.* **17**, 350 (1961).
- CHOPPIN, G. R., SILVA, R. J.: *J. Inorg. Nucl. Chem.* **3**, 153 (1956).
- CAMPBELL, D. O.: *Ind. Eng. Chem. Process Des. Develop.* **9**, 95 (1970).
- HARBOUR, R. M.: *J. Inorg. Nucl. Chem.* **34**, 2680 (1972).
- FUJITA, D. K., CUNNINGHAM, B. B., PARSONS, T. C., PETERSON, J. R.: *Inorg. Nucl. Chem. Lett.* **5**, 245 (1969).
- NUGENT, L. J., BAYBARZ, R. D., WERNER, G. K., FRIEDMAN, H. A.: *Chem. Phys. Lett.* **7**, 179 (1970).
- VARGA, L. P., BAYBARZ, R. D., REISFELD, M. J., MANN, J. B.: *J. Inorg. Nucl. Chem.* **35**, 2303 (1973).
- CARNALL, W. T., COHEN, D., FIELDS, P. R., SJOBLUM, R. K., BARNES, R. F.: *J. Chem. Phys.* **59**, 1785 (1973).
- NUGENT, L. J., BURNETT, J. L., BAYBARZ, R. D., WERNER, G. K., TANNER, S. R., TARRANT, J. B., KELLER, O. L., JR.: *J. Phys. Chem.* **73**, 1540 (1969).
- HARMON, H. D., PETERSON, J. R.: *Inorg. Nucl. Chem. Lett.* **8**, 57 (1972).
- HUSSONNOIS, M., HUBERT, S., BRILLARD, L., GUILLAUMONT, R.: *Radiochem. Radioanal. Lett.* **15**, 47 (1973).
- MCDOWELL, W. J., COLEMAN, C. F.: *J. Inorg. Nucl. Chem.* **34**, 2837 (1972).
- HARMON, H. D., PETERSON, J. R.: *J. Inorg. Nucl. Chem.* **34**, 1381 (1972).
- HUBERT, S., HUSSONNOIS, M., BRILLARD, L., GOBY, G., GUILLAUMONT, R.: *J. Inorg. Nucl. Chem.* **36**, 2366 (1974).
- ALY, H. F., LATIMER, R. M.: *Radiochim. Acta* **14**, 27 (1970).
- MYASOEDOV, B. F., GUSEVA, L. I., MILYUKOVA, M. S., CHMUTOVA, M. K.: *Analytical Chemistry of the Transplutonium Elements*, Kester Publishing House, Jerusalem, p. 358 (1974).
- LUNDQVIST, R. D., HULET, E. K., BAISDEN, P. A.: *Acta Chem. Scand.* **A35**, 653 (1981).
- CHUDINOV, E. G., PIROZKHOV, S. V.: *Soviet Radiochemistry* **15**, 200 (1973).
- DAVID, F., SAMHOUN, K., GUILLAUMONT, R., EDELSTEIN, N.: *J. Inorg. Nucl. Chem.* **40**, 69 (1978).
- NUGENT, L. J.: *J. Inorg. Nucl. Chem.* **37**, 1767 (1975).
- SAMHOUN, K., DAVID, F.: *J. Inorg. Nucl. Chem.* **41**, 357 (1979).

55. NUGENT, L. J.: *J. Phys. Chem.* **73**, 1177 (1969).
56. DUYKAERTS, G., GILBERT, B.: *Inorg. Nucl. Chem. Lett.* **13**, 537 (1977).
57. MIKHEEV, N. B., SPITSYN, V. I., KAMENSKAYA, A. N., ROZENKEVICH, N. A., RUMER, I. A., AUÉRMAN, L. N.: *Soviet Radiochemistry* **14**, 494 (1972).
58. MIKHEEV, N. B., RUMER, I. A.: *Soviet Radiochemistry* **14**, 502 (1972).
59. IONOVA, G. V., MIKHEEV, N. B., SPITSYN, V. I.: *Soviet Radiochemistry* **20**, 89 (1978).
60. BORG, R. J., DIENES, G. J.: *J. Inorg. Nucl. Chem.* **43**, 1129 (1981).
61. GOODMAN, L. S., DIAMOND, H., STANTON, H. E., FRED, M. S.: *Phys. Rev.* **A4**, 473 (1971).
62. PORTER, F. T., FREEDMAN, M. S.: *Phys. Rev. Lett.* **27**, 293 (1971).
63. PORTER, F. T., FREEDMAN, M. S.: *J. Phys. Chem. Ref. Data* **7**, 1267 (1978).
64. FRICKE, B., DESCLAUX, J.-P., WABER, J. T.: *Phys. Rev. Lett.* **28**, 714 (1972).
65. ZVÁRA, I., BELOV, V. Z., DOMANOV, V. P., ZHOKOV, B. L., RYOTTS, T., CHUBENER, Z., SHALAEVSKI, M. R.: Joint Institute for Nuclear Research, Dubna, USSR, Preprint P6-10334 (in Russian) (1976).
66. MERINIS, J., LEGOUX, Y., BOUISSIÈRES, G.: *Radiochem. Radioanal. Lett.* **13**, 221 (1973).
67. CHOPPIN, G. R., HARVEY, B. G., THOMPSON, S. G.: *J. Inorg. Nucl. Chem.* **2**, 66 (1955).
68. HORWITZ, E. P., BLOOMQUIST, C. A. A.: *J. Inorg. Nucl. Chem.* **35**, 271 (1973).
69. HORWITZ, E. P., BLOOMQUIST, C. A. A.: *Inorg. Nucl. Chem. Lett.* **5**, 753 (1969).
70. HUBERT, S., HUSSONNOIS, M., BRILLARD, L., GODY, G., GUILLAUMONT, R.: *J. Inorg. Nucl. Chem.* **36**, 2361 (1974).
71. HUBERT, S., HUSSONNOIS, M., BRILLARD, L., GUILLAUMONT, R.: *Transplutonium Elements*, W. MÜLLER and R. LINDNER, eds., North-Holland, Amsterdam, p. 109 (1976).
72. HUSSONNOIS, M., HUBERT, S., AUBIN, L., GUILLAUMONT, R., BOUISSIÈRES, G.: *Radiochem. Radioanal. Lett.* **10**, 231 (1972).
73. MIKHEEV, N. B., SPITSYN, V. I., KAMENSKAYA, A. N., GVOZDEV, B. A., DRUIN, V. A., RUMER, I. A., DYACHKOVA, R. A., ROZENKEVITCH, N. A., AUERMAN, L. N.: *Inorg. Nucl. Chem. Lett.* **8**, 929 (1972).
74. ROZENKEVITCH, N. A., MIKHEEV, N. B., RUMER, I. A., AUÉRMAN, L. N., GVOZDEV, B. A., KAMENSKAYA, A. N.: *Radiokhimiya* **17**, 441 (1975).
75. MIKHEEV, N. B., SPITSYN, V. I., KAMENSKAYA, A. N., KONOVALOVA, N. A., RUMER, I. A., AUÉRMAN, L. N., PODOROZHNYI, A. M.: *Inorg. Nucl. Chem. Lett.* **13**, 651 (1977).
76. RUMER, I. A., MIKHEEV, N. B., KAMENSKAYA, A. N., KONOVALOVA, N. A., AUÉRMAN, L. N., PODOROZHNYI, A. M.: *Soviet Radiochemistry* **21**, 232 (1979).
77. HULET, E. K., LOUGHEED, R. W., BAISDEN, P. A., LANDRUM, J. H., WILD, J. F., LUNDQVIST, R. F. D.: *J. Inorg. Nucl. Chem.* **41**, 1743 (1979).
78. SAMHOUN, K., DAVID, F.: *Transplutonium Elements*, MÜLLER, W. and LINDNER, R., eds., North-Holland, Amsterdam, p. 297 (1976).
79. DAVID, F., SAMHOUN, K., HULET, E. K., BAISDEN, P. A., DOUGAN, R., LANDRUM, J. H., LOUGHEED, R. W., WILD, J. F., O'KELLEY, G. D.: *J. Inorg. Nucl. Chem.* **43**, 2941 (1981).
80. HULET, E. K., LOUGHEED, R. W., BRADY, J. D., STONE, R. E., COOPS, M. S.: *Science* **158**, 486 (1967).
81. MÁLY, J., CUNNINGHAM, B. B.: *J. Inorg. Nucl. Chem. Lett.* **3**, 445 (1967).
82. MÁLY, J.: *J. Inorg. Nucl. Chem.* **31**, 741 (1969).
83. SAMHOUN, K., DAVID, F., HAHN, R. L., O'KELLEY, G. D., TARRANT, J. R., HOBART, D. E.: *J. Inorg. Nucl. Chem.* **41**, 1749 (1979).
84. MIKHEEV, N. B., SPITSYN, V. I., KAMENSKAYA, A. N., RUMER, I. A., GVOZDEV, B. A., ROSENKEVICH, N. A., AUÉRMAN, L. N.: *Dokl. Akad. Nauk SSSR* **208**, 1146 (1973).
85. MIKHEEV, N. B., SPITSYN, V. I., KAMENSKAYA, A. N., MIKULSKI, J., PETRYNA, T.: *Radiochem. Radioanal. Lett.* **43**, 85 (1980).
86. MÁLY, J., SIKKELAND, T., SILVA, R., GHIORSO, A.: *Science* **160**, 1114 (1968).
87. SILVA, R. J., MCDOWELL, W. J., KELLER, O. L., JR., TARRANT, J. R.: *Inorg. Chem.* **13**, 2233 (1974).
88. SILVA, R. J., SIKKELAND, T., NURMIA, M., GHIORSO, A., HULET, E. K.: *J. Inorg. Nucl. Chem.* **31**, 3405 (1969).
89. MCDOWELL, W. J., KELLER, O. L., JR., DITTNER, P. E., TARRANT, J. R., CASE, G. N.: *J. Inorg. Nucl. Chem.* **38**, 1207 (1976).
90. BECK, H. P., BÄRNIGHAUSEN, H.: *Z. Anorg. Allg. Chem.* **386**, 221 (1971).
91. MEYER, R. E., MCDOWELL, W. J., DITTNER, P. F., SILVA, R. J., TARRANT, J. R.: *J. Inorg. Nucl. Chem.* **38**, 1171 (1976).
- 91a. SAMHOUN, K., LOUGHEED, R. W., LANDRUM, J. H., DOUGAN, R. J., HOOVER, A. D., WILD, J. F., HULET, E. K., DAVID, F.: Unpublished work (1982).
92. SILVA, R., SIKKELAND, T., NURMIA, M., GHIORSO, A.: *Inorg. Nucl. Chem. Lett.* **6**, 733 (1970).
93. NUGENT, L. J., VANDER SLUIS, K. L., FRICKE, B., MANN, J. B.: *Phys. Rev. A* **9**, 2270 (1974).
94. DESCLAUX, J.-P., FRICKE, B.: *J. Phys.* **41**, 943 (1980).
95. ZVÁRA, I., CHUBURKOV, YU. T., TSALETKA, R., SHALAEVSKII, M. R.: *Soviet Radiochemistry* **11**, 153 (1969).
96. ZVÁRA, I., CHUBURKOV, YU. T., TSALETKA, R., SHALAEVSKII, M. R.: *Soviet Radiochemistry* **11**, 161 (1969).
97. ZVÁRA, I., CHUBURKOV, YU. T., BELOV, V. Z., BUKLANOV, G. V., ZAKHVATAEV, B. B., ZVÁROVA, T. S., MASLOV, O. D., CALETKA, R., SHALAEVSKII, M. R.: *J. Inorg. Nucl. Chem.* **32**, 1885 (1970).
98. ZVÁRA, I., BELOV, V. Z., CHELNOKOV, L. P., DOMANOV, V. P., HUSSONNOIS, M., KOROTKIN, YU. S., SCHEGOLEV, V. A., SHALAEVSKII, M. R.: *Inorg. Nucl. Chem. Lett.* **7**, 1109 (1971).
99. HULET, E. K., LOUGHEED, R. W., WILD, J. F., LANDRUM, J. H., NITSCHKE, J. M., GHIORSO, A.: *J. Inorg. Nucl. Chem.* **42**, 79 (1980).
100. SILVA, R., HARRIS, J., NURMIA, M., ESKOLA, K., GHIORSO, A.: *Inorg. Nucl. Chem. Lett.* **6**, 871 (1970).
101. NITSCHKE, J. M., FOWLER, M., GHIORSO, A., LEBER, R. E., NURMIA, M., SOMERVILLE, L. P., WILLIAMS, K. E., HULET, E. K., LANDRUM, J. H., LOUGHEED, R. W., WILD, J. F., BEMIS, C. E., SILVA, R. J., ESKOLA, P.: *Nucl. Phys.* **A 352**, 138 (1981).
102. ZVÁRA, I.: *XXIV International Congress of Pure and Applied Chemistry*, Butterworths, London, vol. 6, p. 73 (1974).
103. ZVÁRA, I., BELOV, V. Z., DOMANOV, V. P., SHALAEVSKII, M. R.: *Soviet Radiochemistry* **18**, 328 (1976).



## The Search for Superheavy Elements

By J. V. KRATZ\*, Gesellschaft für Schwerionenforschung, D-61 Darmstadt, Germany

(Received February 17, 1982)

*Superheavy elements/Predicted properties/Search for superheavy elements in nature/Attempted syntheses by heavy-ion reactions*

### Summary

Extensive experimental efforts have been made during the past 12 years to detect superheavy elements in nature and to produce them in heavy-ion collisions. The search in nature remained inconclusive. Attempts to synthesize superheavy elements in the laboratory produced negative results. The concurrent study of heavy-ion reaction mechanisms has suggest new synthetic routes and modifications of old ones for future experiments.

### 1. Introduction

For many years nuclear scientists believed that the periodic table of elements had been extended nearly to its limit, defined as the point where the Coulomb repulsion between the protons in the nucleus becomes so large that the cohesive nuclear forces cannot hold the nucleus together and the nucleus undergoes rapid spontaneous fission. This was based both on the liquid drop theory and on the observation of shorter and shorter spontaneous fission half-lives as the atomic number of the nucleus increased. However, in the period from 1966 to 1972 a number of detailed theoretical studies [1–5] showed that in the region of proton number  $Z = 114$  and neutron number  $N = 184$  the ground states of nuclei were again stabilized against spontaneous fission decay. The renewed stabilization was due to predicted shell closures at  $Z = 114$ ,  $N = 184$  and estimates of total half-lives involving all major modes of decay resulted in values for the most stable nuclei on the order of the age of the solar system. This was the reason for many nuclear chemists and physicists during the past 12 years to devote a considerable fraction of their scientific efforts and resources to attempts to detect these “superheavy elements” (SHE’s), i.e. elements with atomic number  $Z \geq 110$ , either in natural samples or among the nuclear reaction products of heavy-ion collisions.

Today, the early optimistic view that a massive extension of the periodic table of the elements was possible through the production and identification of SHE’s, has to be seen with scepticism. The present article will comment on current views of these expectations, summarize the results of attempts to synthesize SHE’s at accelerators and briefly comment on recent searches for SHE’s in nature. Reports on earlier work can be found in a number of review articles (e.g. Refs. [6] and [7] and conference proceedings [8, 9]).

### 2. Predicted properties of superheavy elements

#### 2.1. Nuclear properties

In order to predict the stability of a superheavy nucleus one must rely on calculations of single-particle levels in nuclear potentials that have been extrapolated from the region of known nuclei. Most theoretical studies, e.g. those by NILSSON [10] and NIX [11], agree that the next major shell closures beyond  $Z = 82$  and  $N = 126$  occur at  $Z = 114$  and  $N = 184$ , thus providing maximum stability against spontaneous fission for the doubly magic nucleus  ${}_{114}^{298}\text{X}^{184}$ . Besides spontaneous fission other decay modes, notably  $\alpha$ -decay, beta decay, and electron capture, have to be considered for the calculation of the total half-life. In Fig. 1 two sets of predicted overall half-lives of superheavy nuclei are presented. In Fig. 1a, calculations by FISET and NIX [12] are indicated. The maximum half-life of  $10^9$  y is predicted for  ${}_{110}^{294}\text{X}^{184}$ . The shift of the longest half-life from  $Z = 114$  to  $Z = 110$  is due to the competition of  $\alpha$ -decay with spontaneous fission which decreases the half-lives for the higher atomic numbers. For the synthesis of SHE’s by fusion reactions the shape of the shore of the “island of stability” in the west is extremely important because all possible landing places for this type of reaction are on the neutron-deficient side of the island. More recent calculations by SOBICZEWSKI [13] reproduce this shape of the island but the half-lives are several orders of magnitude shorter with a maximum value of  $10^3$  y for  ${}_{112}^{296}\text{X}^{184}$ . A quite different shape of the island as predicted by RAN-

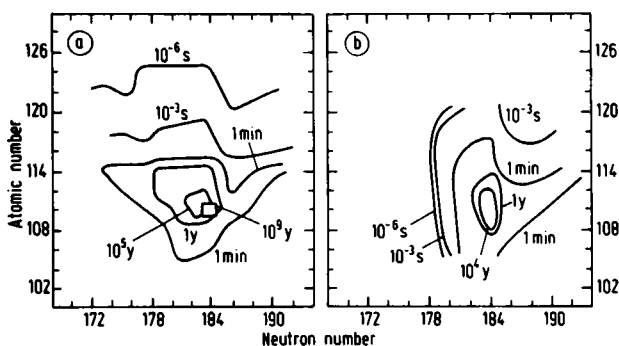


Fig. 1. Predicted half-lives of SHE’s indicated as isopleths of constant overall half-life as a function of proton and neutron number. (a) according to FISET and NIX [12] and (b) according to RANDRUP *et al.* [14, 15]

\* Present address: Institut für Kernchemie, Universität Mainz, D-65 Mainz, Germany



versially. In the most recent studies the production of SHE's in the  $r$ -process is considered unlikely [30–32], the results depend, however, on a delicate balance between extrapolated fission barriers and neutron binding energies.

Despite these uncertainties hundreds of natural samples were examined for superheavy elements. The most sensitive method used in these searches was the detection of spontaneous fission events [33]. For untreated samples detection limits of  $10^{-12}$  to  $10^{-15}$  grams of SHE's per gram sample were achieved if the spontaneous fission half-life was assumed to be  $10^9$  years. These limits have been improved in some cases by chemical enrichment and mass separation. Most of these efforts gave no conclusive evidence for the presence of SHE's but there have been a number of observations that do not definitely rule out the existence of SHE's. One of these spontaneous fission activities was detected in the hot spring waters on the Cheleken peninsula (USSR) by FLEROV *et al.* [34]. This water is enriched with heavy volatile elements and is assumed to originate from a large depth. About 2000 m<sup>3</sup> of this water were passed through a barrel containing 850 kg of anion exchange resin. Some 170 kg of the resin were eluted with water and different acids, and hydroxides were precipitated in the effluent. The resulting samples were measured by high-efficiency neutron multiplicity counters. The spontaneous fission count rate was 0,5 per day per 9 kg of saturated resin, a rate which is much higher than background. The hydroxide precipitate contained an activity of 5 counts per day and had thus enriched about 50% of the original activity of the resin. The neutron multiplicity distribution obtained with the saturated resin and with the hydroxides is shown in Fig. 3 together with known multiplicity distributions occurring in the spontaneous fission decay of <sup>238</sup>U, <sup>246</sup>Cm, and <sup>252</sup>Cf, as well as distributions for some hypothetical emitters. The experimental neutron multiplicity distribution is compatible with that of <sup>252</sup>Cf, whereas <sup>246</sup>Cm and <sup>238</sup>U can be ruled out. In order to check for a possible contamination by fallout from nuclear weapons tests or by actinides present in the laboratory the authors isolated an Am through Cf fraction from a representative portion of the hydroxides. From the measured ratio of  $\alpha$ -particle-to-spontaneous fission activity in this Am-Cf fraction the authors concluded that the activity cannot be due to a contamination by actinides with the exception of pure <sup>252</sup>Cf. The latter possibility was considered unlikely and it was suggested that the spontaneously fissioning nuclide detected in the Cheleken waters may be a SHE. Attempts to further concentrate this activity by chemical procedures which are more specific for the expected chemical behaviour of SHE's failed because of increased losses of the activity at each stage of processing [35]. No evidence for spontaneous fission decay has been found in solid deposits from hot springs at the bottom of the Red Sea which are assumed to be of a similar geological origin as the Cheleken samples [36, 37], even though their chemical composition is different.

The Dubna group [38–40] also examined several meteorites for spontaneous fission activity, among them

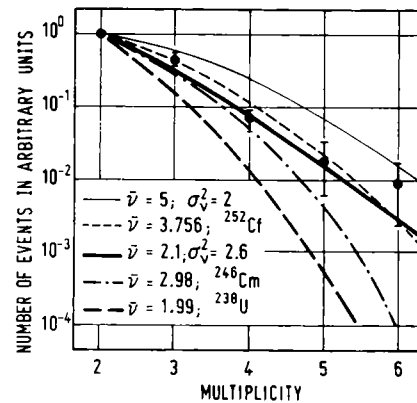


Fig. 3. Neutron multiplicity distribution of the fission events in hot-spring water from the Cheleken peninsula detected in experiments with saturated resin and hydroxides (black dots). The multiplicity distribution for various actinides and two hypothetical spontaneous fission activities are also shown. From FLEROV *et al.* [34]

the meteorite Allende, a carbonaceous chondrite, in which ANDERS *et al.* [41–44] had previously found evidence for anomalous isotopic ratios for xenon isotopes which were interpreted as the result of spontaneous fission decay of a now-extinct, volatile SHE. The latter hypothesis was met with criticism, see e.g. Ref. [45]. The meteorites examined with neutron multiplicity counters at Dubna showed, on the average, one event per five days in 10 kg of sample, which is 10–30 times higher than the counting rate expected from the uranium content of the meteorites and from other sources of background. Chemical separations based on the volatility of SHE's in the elementary or in an oxidized state were also applied by ZVARA *et al.* [46] and it was suggested that the meteoritic samples contained a long-lived spontaneously fissioning nuclide of a SHE. However, in attempts to further concentrate the activity chemically the yield dropped down to a level close to the detection sensitivity [47].

Another possible indication for the natural occurrence of SHE's arose from studies of the heavy component of galactic cosmic rays by Dubna Scientists [48]. Meteorites are exposed to the flux of cosmic rays during an average of  $1 \times 10^7$  years; as a result of this exposure they accumulate an enormous amount of information on the charge spectrum of cosmic rays. By etching suitable minerals such as olivines located not too far from the surface of the meteorite one can obtain visible tracks the length of which is directly related to the atomic number of the nuclei producing the tracks. About 1 cm<sup>3</sup> of olivine crystals were microscopically scanned and about 2500 tracks produced by heavy nuclei with  $Z \geq 70$  were registered. The distribution of track lengths after annealing shows a peak at 180–230  $\mu\text{m}$  which belongs to the uranium-thorium group. In addition, two tracks of 320 and 370  $\mu\text{m}$  length were found indicating nuclei with  $Z \sim 110$ . The annealing procedure reduces considerably the tremendous background associated with the abundant iron group in the galactic cosmic rays. Calibrations of track lengths were achieved by heavy-ion bombardments using Ti

through Xe projectiles. Most recently, more olivine crystals were scanned and two more tracks of about  $300\ \mu\text{m}$  length were found [38]. An important test of the method will be carried out in the near future when high-energy  $^{238}\text{U}$  beams will be available from the Berkeley Bevalac accelerator.

#### 4. Attempts to synthesize superheavy elements in heavy-ion collisions

During the period following the initial optimistic predictions concerning the production cross sections [49] for SHE's efforts began at the heavy-ion accelerators at Berkeley, Orsay and Dubna to "jump the gap" between the region of known nuclei and the predicted magic island by fusing two heavy nuclei together. Somewhat later, at Darmstadt, through the availability of projectiles as heavy as  $^{238}\text{U}$  new prospects for the synthesis of SHE's showed up with the observation of a massive transfer of nucleons from one heavy nucleus to another at relatively low excitation energies. Both approaches are schematically illustrated in Fig. 4 which also gives some characteristic times (in units of  $10^{-21}$  s). In a complete fusion reaction (see the upper branch) projectile and target amalgamate to a nearly spherical compound nucleus. The compound nucleus, even if formed with the minimum kinetic energy possible (i. e. at the barrier) carries several tens of MeV of excitation energy because, in general, more kinetic energy is required to overcome the Coulomb barrier than energy is consumed in the subsequent (endothermic) fusion process. The excitation energy can be carried away by the subsequent evaporation of light particles, mostly neutrons, which is followed by the emission of  $\gamma$ -rays before the ground state of the final evaporation residues is reached. For heavy nuclei the number of evaporation residues is a minuscule fraction of the number of compound nuclei that are primarily produced because at each step of the de-excitation chain fission into two fragments of comparable size competes heavily with particle evaporation. Thus the probability of producing a detectable superheavy nucleus is the product of two factors: i) the probability to fuse the reacting heavy ions to form an equilibrated superheavy compound nucleus, and ii) the cumulative probability of the excited superheavy compound nucleus to survive its de-excitation process.

The lower branch in Fig. 4 illustrates the alternative process termed deep-inelastic collision, in which the interacting nuclei stick together for a short time forming an excited, rotating double-nuclear system which then separates again into two heavy nuclei. During the life-time of the double-nuclear system kinetic energy of the relative motion is partially or completely transformed through friction into internal excitation energy, orbital angular momentum is dissipated into intrinsic spin of the fragments, and a substantial number of protons and neutrons can be transferred between the interacting nuclei. Ultimate-

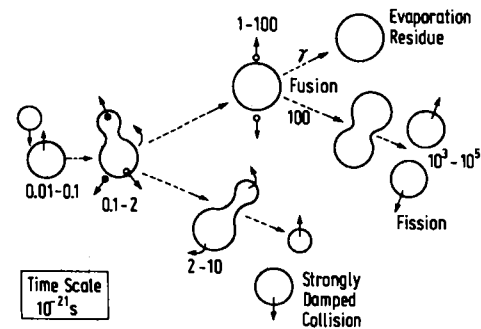


Fig. 4. Schematic representation of interactions between heavy nuclei leading to fusion into an equilibrated compound nucleus (upper branch) and to a deep-inelastic-collision (lower branch) with characteristic times in units of  $10^{-21}$  s. After BRIX [50]

ly, the separated fragments de-excite by particle emission and the competing fission as discussed above. In contrast to complete fusion where the fused product is characterized by discrete mass and charge numbers, by a discrete excitation energy and a narrow bin of angular momenta, deep-inelastic collisions produce broad distributions of product mass and charge numbers, and broad distributions of excitation energies and angular momenta. In the following sections we shall summarize the results of attempts to synthesize SHE's using these alternative approaches and comment on the reasons why these attempts have failed. This is followed by a brief discussion of new insights into heavy-ion reaction mechanisms which might serve as guidance for future research.

##### 4.1. Complete fusion reactions

Since complete fusion was so successful in the synthesis of the heaviest known elements it was natural to use this type of reaction in the first attempt to synthesize SHE's by bombarding  $^{248}_{96}\text{Cm}$  with  $^{40}_{18}\text{Ar}$ -ions to form  $^{288}_{114}\text{X}^{174}$  compound nuclei [51, 52]. The dilemma of this reaction and of many similar other ones lies in the fact that the possible compound nuclei have neutron numbers far below  $N = 184$  where fission barriers are predicted to be vanishingly small [14] or zero so that the cumulative survival probability is zero. Table 1 lists the fusion reactions tried so far together with the upper limit for the production cross section and the ranges of half-lives that were covered by the experiments. As suggested by SEABORG *et al.* [53] the reactions are ordered in three classes. Class 1 comprises those reactions where compound nuclei in the close vicinity of element 114 were produced. Unfortunately, this is only possible in projectile-target combinations with much less than the optimum number of neutrons resulting in very low survival probabilities precluding production and observation of SHE's. The magic neutron-number  $N = 184$  can be reached if compound nuclei with proton numbers as high as  $Z = 122$  are produced. These so-called "overshoot"-reactions (class 2 in Table 1) are expected to produce compound nuclei for which very good overall survival rates are predicted [53]. After de-excitation, decays by  $\alpha$ -

Table 1. Reported attempts to synthesize superheavy elements by heavy-ion fusion reactions

Reaction studied	Compound nucleus	Upper-limit cross section for SHE production (cm <sup>2</sup> )	Range of half-lives covered	Reference
Class 1: Compound nuclei with vanishing survivability				
$^{48}_{20}\text{Ca} + ^{232}_{90}\text{Th}$	$^{280}_{110}170$	$3 \times 10^{-35}$	$> 3 \times 10^{-3}$ s	54
$^{48}_{20}\text{Ca} + ^{231}_{91}\text{Pa}$	$^{279}_{111}168$	$4 \times 10^{-35}$	$> 3 \times 10^{-3}$ s	54
$^{48}_{20}\text{Ca} + ^{233}_{92}\text{U}$	$^{281}_{112}169$	$7 \times 10^{-35}$	$> 2$ h	54
$^{40}_{18}\text{Ar} + ^{248}_{96}\text{Cm}$	$^{288}_{114}174$	$2 \times 10^{-32}$	$10^{-3}$ s – 1 d	51, 52
$^{48}_{20}\text{Ca} + ^{242}_{94}\text{Pu}$	$^{290}_{114}176$	$1 \times 10^{-35}$	2 h – 1 y	55
$^{48}_{20}\text{Ca} + ^{243}_{95}\text{Am}$	$^{291}_{115}176$	$2 \times 10^{-35}$	2 h – 1 y	55
Class 2: Dynamical hindrance for fusion				
$^{84}_{36}\text{Kr} + ^{208}_{82}\text{Pb}$	$^{292}_{118}174$	$1 \times 10^{-30}$	$> 6 \times 10^{-7}$ s	56
$^{86}_{36}\text{Kr} + ^{208}_{82}\text{Pb}$	$^{294}_{118}176$	$6 \times 10^{-35}$	$3 \times 10^{-3}$ s – 100 d	57
		$1.5 \times 10^{-30}$	$2 \times 10^{-9}$ s – 5 h	58
$^{59}_{27}\text{Co} + ^{238}_{92}\text{U}$	$^{297}_{119}178$	$4 \times 10^{-33}$	1 s – 30 h	59
$^{60}_{28}\text{Ni} + ^{238}_{92}\text{U}$	$^{298}_{120}178$	$2 \times 10^{-33}$	1 s – 30 h	59
$^{65}_{29}\text{Cu} + ^{238}_{92}\text{U}$	$^{303}_{121}182$	$8 \times 10^{-33}$	1 s – 30 h	59
$^{65}_{29}\text{Cu} + ^{238}_{92}\text{U}$	$^{303}_{121}182$	$2 \times 10^{-33}$	2 h – 1 y	60
$^{65}_{29}\text{Cu} + ^{238}_{92}\text{U}$	$^{303}_{121}182$	$4 \times 10^{-34}$	$2 \times 10^{-6}$ s – 10 h	61
$^{76}_{32}\text{Ge} + ^{232}_{90}\text{Th}$	$^{308}_{122}186$	$1 \times 10^{-34}$	$5 \times 10^{-3}$ s – 1 y	63
$^{136}_{54}\text{Xe} + ^{170}_{68}\text{Er}$	$^{306}_{122}184$	$1.5 \times 10^{-33}$	$2 \times 10^{-6}$ s – 10 h	61
$^{76}_{32}\text{Ge} + ^{238}_{92}\text{U}$	$^{314}_{124}190$	$1 \times 10^{-34}$	$5 \times 10^{-3}$ s – 1 y	63
$^{68}_{30}\text{Zn} + ^{243}_{95}\text{Am}$	$^{311}_{125}186$	$5 \times 10^{-32}$	$10^{-9}$ s – 5 d	64
$^{84}_{36}\text{Kr} + ^{232}_{90}\text{Th}$	$^{316}_{126}190$	$5 \times 10^{-30}$	$> 6 \times 10^{-7}$ s	56
$^{84}_{36}\text{Kr} + ^{238}_{92}\text{U}$	$^{322}_{128}194$	$8 \times 10^{-29}$	$> 6 \times 10^{-7}$ s	58
$^{84}_{36}\text{Kr} + ^{238}_{92}\text{U}$	$^{322}_{128}194$	$9 \times 10^{-36}$	2 h – 100 d	65
Class 3: Compound nuclei with possible survival				
$^{48}_{20}\text{Ca} + ^{246}_{96}\text{Cm}$	$^{294}_{116}178$	$2 \times 10^{-35}$	2 h – 1 y	55
$^{48}_{20}\text{Ca} + ^{248}_{96}\text{Cm}$	$^{296}_{116}180$	see Fig. 6		55, 28, 66–68

and beta-decay toward the center of the island of stability are predicted [12, 14, 15]. This is illustrated in Fig. 5 for the  $^{136}_{54}\text{Xe} + ^{170}_{68}\text{Er}$  reaction used by MÜNZENBERG *et al.* [61] in an attempt to produce evaporation residues of the magic compound nucleus  $^{306}_{122}\text{X}^{184}$ .

This reaction was selected because the energetics is such that the compound nucleus is formed with very little excitation energy, so that only one neutron was expected to be evaporated in its de-excitation. The experiment was performed with the velocity separator SHIP at the UNILAC accelerator at Darmstadt. SHIP separated the fast projectiles ( $10^{11}$  /s) and transfer products by electrical and magnetic fields from eventual fusion products which would have been ejected from the target with much lower velocity. The slow fusion products would have been focussed onto a position-sensitive surface barrier detector which would i) register the implantation of a heavy nucleus and measure its velocity, ii) register the position of the implanted product inside the detector, and iii) register any  $\alpha$ -particles or fission fragments that are emitted from this position inside the detector as a result of subsequent decay of the implanted evaporation residue. These decay events would be further characterized by the measurement of the

associated energies and the correlation time elapsed between the implantation and the decay event. A significant signal for the production and subsequent decay of a SHE would then consist of an implantation signal indicating the proper product velocity followed by a correlated sequence of rapid  $\alpha$ -decays ending by a spontaneous fission decay. Through combination of the velocity separation from the primary beam particles and transfer products with the requirement of such a unique sequence of signals a signal-to-noise ratio of  $10^{18} : 1$  was achieved. No single event was observed, defining an upper limit for the production cross section of about 1 nanobarn. The same technique was successfully applied in the recent discovery of element 107 in the  $^{54}_{24}\text{Cr} + ^{209}_{83}\text{Bi}$  reaction by MÜNZENBERG *et al.* [62].

Despite extensive searches using class 2 reactions over a wide range of bombarding energies, projectile-target combinations, and product half-lives, there were no successful SHE syntheses and rather low upper limits were set on SHE production. There is now, see subsection 4.4.2., solid evidence for the fact that the probability for fusion at the coulomb barrier has vanished for the class 2 reactions in Table 1. Thus, no SHE's appear to be formed for dynamical reasons by these overshoot reactions even though the sur-

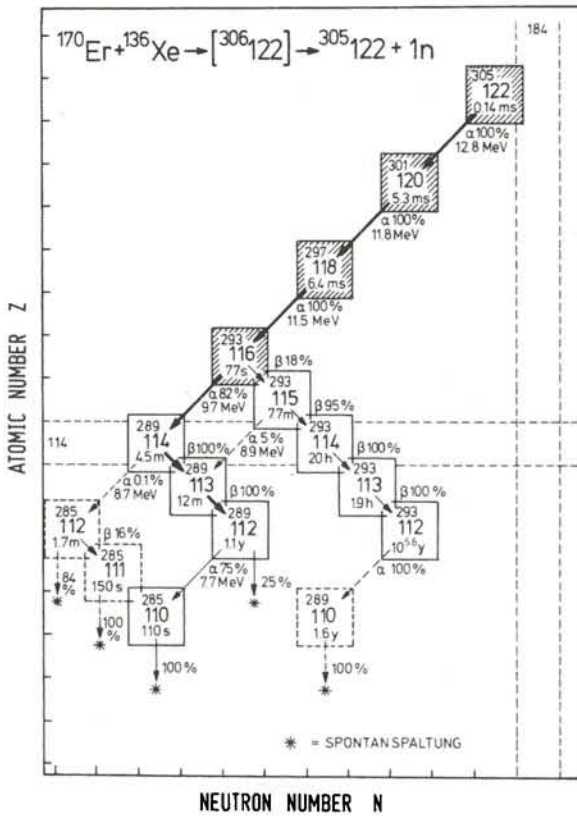
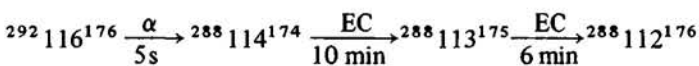


Fig. 5. Predicted decay chain for the evaporation residues of the  $^{136}_{54}\text{Xe} + ^{170}_{68}\text{Er}$  reaction tried by MÜNZENBERG *et al.* [61]. The experiment was optimized for the detection of a rapid sequence of high-energy  $\alpha$ -particles followed by a spontaneous fission event, see text

vivability of the respective compound nuclei would have been rather promising.

Among the reactions listed in Table 1 the class 3 reaction of  $^{48}_{20}\text{Ca}$  projectiles with a  $^{248}_{96}\text{Cm}$  target has been studied most extensively both at Berkeley and at Dubna. This reaction represents the intriguing case in which both the fusion probability and the survivability have been considered favourable. Projectile and target nucleus were brought together [55, 28, 66–68] with an energy exceeding the barrier by about 20 MeV. The extra energy was thought to be necessary to induce complete fusion to produce a compound nucleus with some 40 MeV of excitation energy which is expected to de-excite by the evaporation of 4 neutrons. The resulting evaporation residue  $^{292}_{116}\text{X}^{176}$ , according to FISET and NIX [12], decays in the following major decay chain



with the final nucleus  $^{288}_{112}\text{X}^{176}$  having a calculated spontaneous fission half-life of about 1 h. In the more recent studies by RANDRUP, ÅBERG and collaborators [14, 15] the life-times and decay modes are much less favourable, i.e.  $^{292}_{116}\text{X}^{176}$  decays with a half-life of  $1.6 \times 10^{-15}$  s by spontaneous fission, thus precluding its observation in any of the experiments performed.

The  $^{48}_{20}\text{Ca} + ^{248}_{96}\text{Cm}$  experiments were quite difficult and expensive because not only the target material (a high-

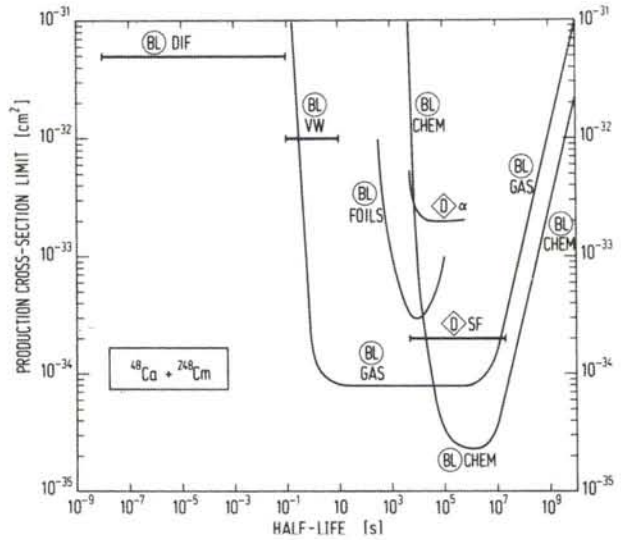


Fig. 6. Upper limits for the production cross section for super-heavy elements produced in the  $^{48}\text{Ca} + ^{248}\text{Cm}$  reaction vs. half-life. Labeling of the curves is explained in the text. The data are from experiments of the Dubna group [55] and of the Berkeley-Livermore collaboration [28, 66–68]

ly radioactive isotope) but also the projectile  $^{48}\text{Ca}$  with only 0.19% natural abundance are available (only in the USA and the USSR) in very limited amounts. The negative results produced in the course of many carefully planned and executed experiments both at Berkeley and at Dubna are summarized in Fig. 6 where upper limits for the production cross sections are plotted as a function of the lifetimes covered by a given experimental technique. The Dubna group [55] used two different chemical separation schemes followed by spontaneous fission (SF) and  $\alpha$ -particle counting ( $\alpha$ ), denoted by D in Fig. 6. At Berkeley (BL in Fig. 6) a variety of techniques was applied: a) chemical separations [66, 28] with two alternative procedures followed by  $\alpha$ -particle and spontaneous fission counting (CHEM); b) examination [67] of condensed noble gases and extremely volatile species for  $\alpha$ -particle decay and fission (GAS); c) direct fission fragment counting of stopped recoils [28] (FOILS); d) gas-jet transport to a rotating wheel counting system [68] (VW), and e) spontaneous fission decay in flight [68], labeled DIF in Fig. 6.

SEABORG *et al.* [53] have analyzed reasons why SHE's were not seen in the  $^{48}\text{Ca} + ^{248}\text{Cm}$  reaction by calculating the relative neutron decay widths  $\Gamma_n/\Gamma_f$  at each step of the 4n-evaporation chain using the formalism outlined by VANDENBOSCH *et al.* [69] and two different sets [12, 14] of fission barrier heights. The estimates of the latter quantities are either typical for most theoretical calculations done in the period from 1966 to 1972 [12], or represent a more pessimistic recent approach [14]. The resulting fraction of the compound nuclei surviving fission are then 96% or  $< 4 \times 10^{-9}$ %, respectively [53]. With an estimated fusion cross section of  $\geq 10^{-27}$  cm<sup>2</sup> and the experimental upper limit on the production cross section of SHE's one can estimate an "experimental" upper limit for the survival rate in this reaction as  $5 \times 10^{-35} / 10^{-27} = 5 \times 10^{-8}$ . Clearly, this figure is dramatically smaller than the 96% resulting from the barriers of FISET and NIX [12]. According

to SEABORG *et al.* [53] the “experimental” survival rate requires the assumption of fission barrier heights that are 4 to 5 MeV lower than those originally predicted which are, thus, more in line with the barrier heights of RANDRUP *et al.* [14]. This conclusion is not unique, because reduced barrier heights are associated with largely reduced half-lives (recall the  $1.6 \times 10^{-15}$  s for  ${}_{116}^{292}\text{X}^{176}$  predicted by ÅBERG *et al.* [15]) where the experimental sensitivity was much less than optimum or where no experimental technique was available at all, see Fig. 6. Also, the calculations [53] were performed with barrier heights corresponding to the full shell strength of a spherical SHE thus ignoring the reduction in barrier heights by excitation energy and the extremely delicate dependence of the stability of a SHE on deformation. We shall come back to a discussion of these problems in section 4.4.3.

#### 4.2. Deep-inelastic transfer reactions

The failure of the complete fusion approach to produce SHE’s may be associated in some direct or indirect way with the failure of even the best projectile-target combination to produce compound nuclei in the center of the island of stability where fission barriers are highest and the losses of yield to prompt fission are the least. Therefore, it was natural to look for alternative approaches allowing production of more neutron-rich superheavy nuclei.

In 1977 studies of the interactions of two colliding uranium nuclei at the Darmstadt UNILAC accelerator [70, 71, 72] showed that the distributions in mass- and charge numbers of excited primary transfer products from deep-inelastic collisions extend into the region of SHE’s. The evidence is based on the observation of the complementary light products. If the doubly magic  ${}_{114}^{298}\text{X}^{184}$  would be formed through transfer of nucleons from one  ${}_{92}^{238}\text{U}$  nucleus to another one, the complementary light product would be an ytterbium isotope:



Fig. 7 shows the element distribution in the reaction of 7.5 MeV/u  ${}^{238}\text{U}$ -ions with a thick  ${}^{238}\text{U}$  target obtained in radiochemical studies by SCHÄDEL *et al.* [72]. The distribution is interpreted as a super-imposition of four components: (i) products in the closest vicinity of  ${}^{238}\text{U}$  from quasi-elastic few-nucleon-transfer reactions (890 mb), (ii) products with atomic numbers from  $Z = 73$  through 100 arising from an originally symmetric distribution around  $Z = 92$  produced by deep-inelastic transfer processes (290 mb), (iii) a nearly symmetric fission product distribution originating from highly excited deep-inelastic fragments (1040 mb), and (iv) a double-humped distribution of neutron-rich fission products from the sequential fission of quasi-elastic transfer products (860 mb). Because the total cross section for deep-inelastic collisions has been measured (the sum of components (ii) and (iii))

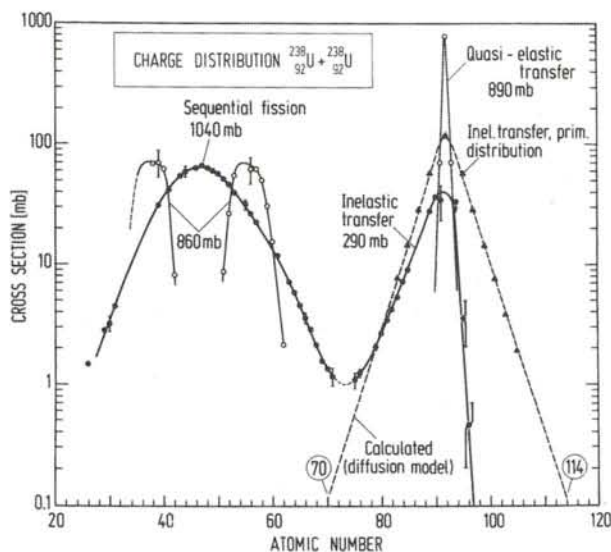


Fig. 7. Charge distribution of reaction products from quasi-elastic transfer and sequential fission at low excitation energies (open circles), and for deep-inelastic collisions with the associated mass-symmetric sequential fission product distribution (full circles) in the  ${}^{238}\text{U} + {}^{238}\text{U}$  reaction at  $\leq 7.5$  MeV/u [72]. Triangles represent the reconstructed primary distribution of deep-inelastic transfer processes prior to sequential fission. The dashed curve is the result of a diffusion model calculation [73]

the original pre-fission distribution can be reconstructed [72] as indicated by the triangles in Fig. 7. The resulting distribution is well reproduced by a semi-phenomenological theory by RIEDEL and NÖRENBERG in which the nucleon transfer is treated as a diffusion process [73]. The latter calculation predicts that the complementary elements  $Z = 70$  and  $Z = 114$  are formed with a cross section of  $10^{-28}$  cm<sup>2</sup>. If one applies the rules [74] that describe the distribution of neutrons and protons between both complementary fragments on the basis of the phase space available above the potential energy as a function of  $N$  and  $Z$ , one predicts a relatively broad distribution in neutron numbers for  $Z = 114$  close to  $N = 184$ . Thus, deep-inelastic transfer reactions lead to a much closer access to the center of the island of stability than any fusion reaction, as is demonstrated by Fig. 8. The important question to be asked is whether there is a chance for these heavy fragments around  $Z = 114$  to survive their de-excitation.

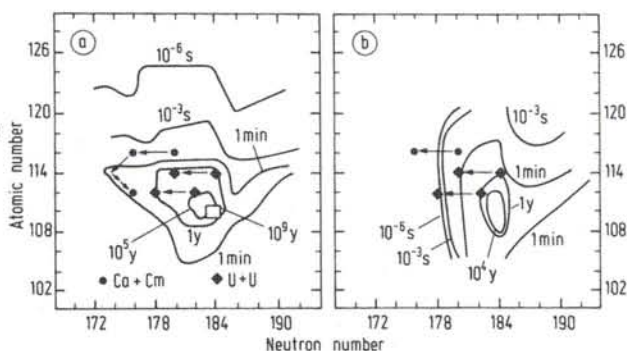


Fig. 8. Landing places for the fusion of  ${}^{44}\text{Ca}$  with  ${}^{248}\text{Cm}$  (dots) and for deep-inelastic transfer processes between two  ${}^{238}\text{U}$  nuclei (diamonds) in the contour maps of Fig. 1a, b

Counter experiments [70, 71] revealed that more nucleons are transferred per MeV of excitation energy in the  $^{238}\text{U} + ^{238}\text{U}$  reaction than in other deep-inelastic collisions involving heavy targets and lighter projectiles, indicating the production of "colder" products in the  $^{238}\text{U} + ^{238}\text{U}$  system. In radiochemical studies the production cross sections of surviving transuranium nuclides were followed over eight orders of magnitude up to fermium [72], and it was found that the production rates for the heaviest actinides in the  $^{238}\text{U} + ^{238}\text{U}$  reaction exceeded considerably those in the  $^{136}\text{Xe} + ^{238}\text{U}$ ,  $^{84}\text{Kr} + ^{238}\text{U}$ , or  $^{40}\text{Ar} + ^{238}\text{U}$  reactions. This result was not necessarily expected: In a deep-inelastic collision the amount of excitation energy showing up in the final fragments depends i) on the amount of kinetic energy that is dissipated into internal excitation energy during the collision, and ii) on the difference in the binding energies of the projectile and target and the emerging fragments in the exit channel. The latter is called the ground state  $Q$ -value,  $Q_{\text{gg}}$ , and resumes negative values for endothermic transfer reactions. It appears now, that formation of  $_{98}\text{Cf}$  in the bombardment of  $^{238}\text{U}$  with the lighter projectiles  $^{40}\text{Ar}$ ,  $^{84}\text{Kr}$  or  $^{136}\text{Xe}$  is associated with strongly negative values of  $Q_{\text{gg}}$  of  $-43$  MeV,  $-40$  MeV, and  $-33$  MeV, respectively. In the  $^{238}\text{U} + ^{238}\text{U}$  reaction the same product is formed with  $Q_{\text{gg}} = -2$  MeV. Since a negative value of  $Q_{\text{gg}}$  reduces the excitation energy showing up in the final fragments and thus increases their survivability, one might expect, contrary to the experimental observation, increased actinide yields with the lighter projectiles if the primary yield before fission at the same amount of dissipated kinetic energy is the same in all reactions. In turn, the experimental observation of increased actinide yields in  $^{238}\text{U} + ^{238}\text{U}$  collisions is evidence for a much higher primary yield at a given dissipated energy than in the other reactions.

Additional studies and analyses [75, 76], see also subsect. 4.4.4., demonstrated that the survival rates of these actinides are compatible with neutron evaporation-fission competition of fully equilibrated compound nuclei, i.e. can be calculated in the same way as for compound nuclei produced in fusion reactions. If we assume that this is also true for formation of  $Z = 114$  in deep-inelastic collisions we can fold the predicted production cross section for  $Z = 114$  with less than 30 MeV of excitation energy [73] with an energy-dependent survival rate [17] and obtain a cross section of about  $10^{-35}\text{cm}^2$  for surviving residues, a value which corresponds, with the accessible beam intensities, to production rates of a few atoms per week of beam time, a rate just exceeding the detection limit of the most sensitive methods available at present.

In view of these not completely hopeless estimates direct searches for surviving SHE's in the  $^{238}\text{U} + ^{238}\text{U}$  reaction were performed by a Darmstadt-Mainz collaboration. In these experiments thick  $^{238}\text{U}$  metal targets were bombarded with 8.6 MeV/u  $^{238}\text{U}$  beams. The thickness of the targets assured that the whole (unknown) excitation function for SHE production was physically integrat-

ed inside the target. Integral particle numbers of up to  $5 \times 10^{16}$  were accumulated within typical beam times of five days [77]. After bombardment the targets were processed with two chemical separation procedures [78] based on different predictions of the chemical behaviour of SHE's. In the gas phase chemistry the predicted volatility and ease of reduction of elements 112 through 117 [24] was utilized. The solution chemistry was based on the predicted ion exchange behaviour of bromide complexes [26] and on the predicted affinity to sulfur [29] for elements 108 through 116. In both procedures provisions were made to condense noble gases and other species that are volatile at room temperature. In one experiment the solution chemistry was extended in order to search also for members of the superactinide series. Experimental details can be found in Ref. [78]. Superheavy element fractions were assayed for  $\alpha$ -particle and spontaneous fission events between two large-area surface barrier detectors with an efficiency of 60% for recording both fission fragments in coincidence. More recently these counter pairs were positioned inside a neutron multiplicity counter so that neutrons could be registered in coincidence with fission fragments. Upper limits for the production cross sections of SHE's vs. the assumed half-life are summarized in Fig. 9. The limits obtained with chemical techniques [77] are labeled CHEM. The variation of these limits with half-life is the result of decay during the chemical separations for short-lived species, and incomplete saturation and decay for life-times comparable to or longer than the total counting time (usually about 200 d). The limits denoted WHEEL are the result of fission track detection with a rotating wheel system [77] where the sensitivity for spontaneously fissioning SHE's is limited by a background produced by the spontaneously fissioning actinide nuclei  $^{244\text{f}}\text{Am}$ ,  $^{242\text{f}}\text{Am}$ ,  $^{256}\text{Fm}$ ,  $^{254}\text{Cf}$ , and  $^{252}\text{Cf}$  in the unseparated reaction product mixture collected in the rotating catcher foils. Also included in Fig. 9 are upper limits from gas-jet experiments labeled JET [59, 79] and from the implantation of recoil atoms [70] in a surface barrier detector (REC).

All experiments have produced negative results. As in the case of the  $^{48}\text{Ca} + ^{248}\text{Cm}$  reaction one notes a lack of sensitive measurements for very short-lived nuclei which would have to involve an efficient separation from actinide nuclei. Because the predicted cross sections for surviving SHE's in the  $^{238}\text{U} + ^{238}\text{U}$  reaction were so close to the detection limits it was natural to think about ways to increase the production rates. Since no gain in the production rates for heavy actinides was observed in bombardments at higher projectile energies [75] it was not considered reasonable to use higher energies. More promising was the use of a heavier target material. Calculations with the diffusion model predict an increase in the production cross section for  $Z = 114$  at 30 MeV of excitation energy by two orders of magnitude if a thick  $^{248}\text{Cm}$  target is used instead of a  $^{238}\text{U}$  target [73]. After extensive development efforts at Berkeley, Darmstadt, Livermore and Mainz the first bombardments of thick  $^{248}\text{Cm}$  targets with  $^{238}\text{U}$  beams were performed at the UNILAC accelerator in

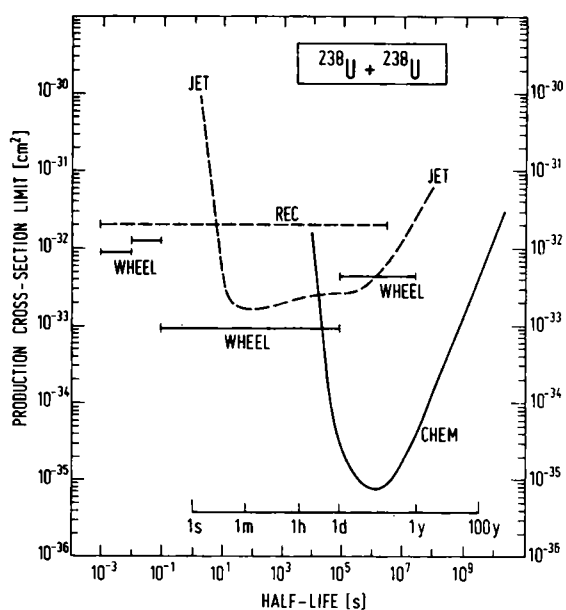


Fig. 9. Upper limits for the production cross section of superheavy elements in collisions of two uranium nuclei as a function of the assumed half-life. For labeling and References, see text

october 1979.  $^{248}\text{Cm}$  targets of 3.5 to 7 mg/cm<sup>2</sup> areal density were prepared by evaporation of  $^{248}\text{Cm}$  metal onto Mo-foils of 4.5 mg/cm<sup>2</sup> thickness. These targets contain a spontaneous fission activity of about  $10^9$  events per day, whereas a rate of a few fission events per year occurring in one of the SHE fractions would be considered a significant signal for SHE production. This shows that extreme care had to be taken in order to prevent an uncontrolled destruction of the target and subsequent contamination of the beam line, the accelerator and the laboratory. Details on the target cooling, temperature monitoring, beam wobbling, on the use of an interlock system, fast-acting valves, and glove boxes are given in Ref. [75]. The target thicknesses were sufficient to degrade the beam energy from 7.4 MeV/u to or below the interaction barrier. In the first experiment, in which a beam integral of  $3 \times 10^{15}$  particles was accumulated, the heavy reaction products were stopped in a water-cooled stack of copper catchers. After the end of bombardment these catchers were heated to 1020°C in the presence of hydrogen in order to separate volatile elements. The catchers were then dissolved in order to perform also the solution chemistry. These fractions mounted on thin foils were counted between opposed surface barrier detectors inside a neutron multiplicity counter. Elements that are volatile at room temperature like Rn were condensed on a cryostat faced by a single surface barrier detector. Preliminary upper limits resulting from these experiments were of the order of  $2\text{--}3 \times 10^{-34}$  cm<sup>2</sup> for half-lives between several hours and about 100 d [78]. Simultaneously, various actinide fractions up to nobelium were separated in order to measure actinide production cross section, see section 4.4.4. A second experiment to detect gaseous SHE's ended after 4 hours of beam time ( $2 \times 10^{14}$  particles) when the  $^{248}\text{Cm}$  target developed a hole. Here, Krypton gas was used to stop the reaction

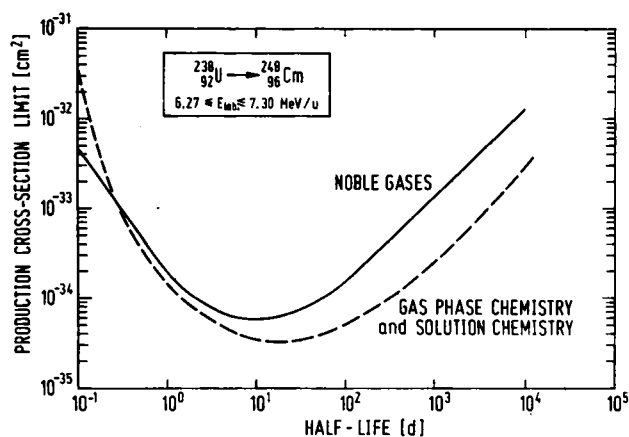


Fig. 10. Preliminary upper limits for the production cross section of superheavy elements in the  $^{238}\text{U} + ^{248}\text{Cm}$  reaction [81]

products and to sweep gaseous products through a filter system (removal of non-volatile actinides) to a copper cryostat cooled to  $-150^\circ\text{C}$  where they were continuously counted for fission events and high-energy  $\alpha$ -particles. No such events were observed resulting in an upper limit of  $10^{-33}$  cm<sup>2</sup> for volatile SHE's with half-lives between two minutes and several hours [80]. Both experiments were hampered by the unexpected early failure of the  $^{248}\text{Cm}$  metal targets in the  $^{238}\text{U}$  beam thus reducing the beam integrals to far below the integrals reached in the  $^{238}\text{U} + ^{238}\text{U}$  experiments. Inspections of the  $^{248}\text{Cm}$  targets, of irradiated targets of its homologue gadolinium, extensive bombardments of similar targets with pulsed electron beams, low-energy heavy-ion beams and additional 7.5 MeV/u  $^{238}\text{U}$  bombardments led to the conclusion that there was a problem in transferring heat from the target through the Cm/Mo interface to the gas-cooled Mo substrate during heavy-ion bombardment causing rapid temperature cycling and tensile stresses that ultimately led to a mechanical failure of the targets along the rolling lines of the Mo substrate. An acceptable, partial solution to these heat transfer problems was achieved by modifications of the target apparatus which allows now to cool the target on both sides by 1.5 l/s nitrogen gas. In July 1981, with this improvement, about  $2 \times 10^{16}$   $^{238}\text{U}$  particles could be accumulated on target. The reaction products were again stopped in a stack of copper catchers and chemically processed as before. Counting of the isolated fractions is still being continued. Upper limits [81] for the production cross sections of SHE's after 180 d of counting are presented in Fig. 10. Even though there is the prediction of a hundred-fold increase in yield of SHE's in the  $^{238}\text{U} + ^{248}\text{Cm}$  reaction relative to the  $^{238}\text{U} + ^{238}\text{U}$  reaction [73], no detectable amounts of SHE's have been found in the bombardments of  $^{248}\text{Cm}$  with  $^{238}\text{U}$  ions in the half-life region of a few hours to some years with a sensitivity close to the edge of current technological limits.

#### 4.3. The "fusion-after-instantaneous-fission" approach

A third series of experiments is based on the theoretical

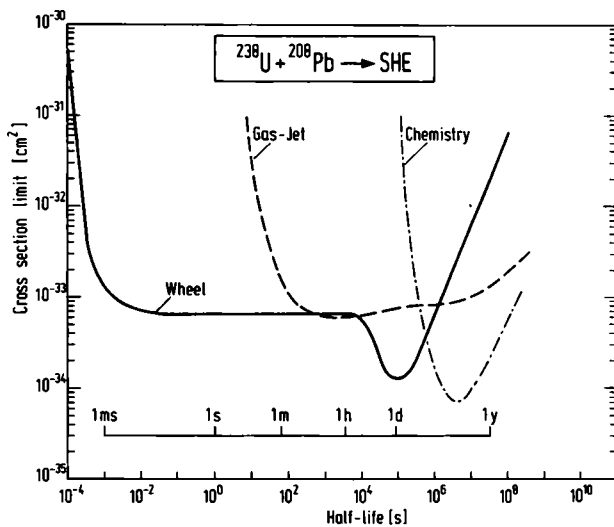


Fig. 11. Upper cross section limits for spontaneously fissioning SHE's in the reaction  $^{238}\text{U} + ^{208}\text{Pb} \rightarrow \text{SHE}$  vs. half-life from Ref. [84]

suggestion of instantaneous fission of a heavy nucleus during the close contact with another heavy nucleus followed by fusion of one of the fission fragments with the nucleus causing the fast fission process [82]. This suggestion has been shown [83] to produce negative results in the reaction of  $^{208}\text{Pb}$  with  $^{136}\text{Xe}$  where an upper cross section limit of  $1.2 \times 10^{-30} \text{ cm}^2$  was obtained for half-lives between  $10^{-12}$  and  $10^4 \text{ s}$ , and in the reaction of  $^{208}\text{Pb}$  with  $^{238}\text{U}$  using a rotating wheel system (Wheel), the gas-jet method (Gas-Jet) and off-line chemistry (Chemistry) [84], see Fig. 11. The continuation of experiments along this line appears to be the least promising because i) there is no evidence for production of known nuclei through this mechanism [85], ii) "fast fission" does not seem to occur at near barrier energies [86], and iii) fusion of an uranium fission product with a  $^{208}\text{Pb}$  nucleus is dynamically hindered at near-barrier energies, see section 4.4.2.

#### 4.4. New results on heavy-ion reaction mechanisms

Many of the above mentioned investigations, while failing to synthesize SHE's, have provided as a by-product valuable data on heavy-ion reaction mechanisms. Also, there is a growing body of relevant data emerging from concurrent studies of reaction mechanisms concerned with the limitations of complete fusion by the barrier and by entrance channel effects, with the production of cold heavy nuclei in transfer reactions, and with the survivability of excited heavy nuclei. These new results seem to provide highly significant guidance for future attempts to synthesize SHE.

##### 4.4.1. Cold fusion through barrier penetration

Fusion above the classical barrier is reasonably well described by conventional one-dimensional fusion models using conservative nucleus-nucleus potentials [87]. However, from recent experiments [88–91] it follows that

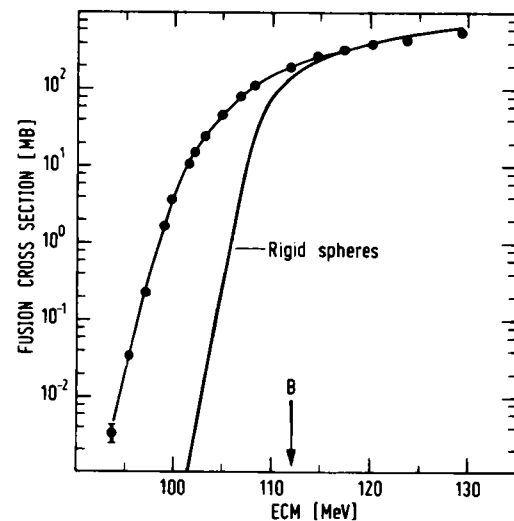


Fig. 12. Experimental fusion cross sections for  $^{40}\text{Ar} + ^{122}\text{Sn}$  from REISDORF *et al.* [91]. The solid curve is a transmission calculation (WKB) using a proximity potential and assuming rigid sphericity for both target and projectile. The conventional fusion barrier is indicated by the arrow

fusion well below the barrier (involving the quantum-mechanical penetration of the fusion barrier) cannot be described with such one-dimensional models of colliding rigid spheres involving WKB theory or the Hill-Wheeler expression for the transmission through a potential barrier. As a general rule one observes unexpectedly large cross sections below the barrier. More specifically, there is evidence that the cross section enhancement is dependent on the nature of the amalgamating nuclei. In a comparative study [88, 89] it was shown, first, that the cross section enhancement was larger for deformed target nuclei ( $^{154}\text{Sm}$ ) than for spherical nuclei, and, second, that the global effect was much stronger if a heavier projectile ( $^{40}\text{Ar}$ ) was used instead of a light one ( $^{16}\text{O}$ ). As shown in a particularly clear way by REISDORF *et al.* [91] in the fusion of  $^{40}\text{Ar}$  with  $^{112, 116, 122}\text{Sn}$  there is a striking gain in cross sections relative to the fusion cross sections calculated for rigid spheres *even for spherical target nuclei*, see Fig. 12. For statically deformed and "soft" nuclei the gain is larger. For even heavier projectiles than  $^{40}\text{Ar}$  this trend is further accentuated [92]. Similar trends are likely to hold for superheavy target-projectile combinations. Thus, Fig. 12 tells us that lowering of the centre-of-mass bombarding energy below the barrier by 10 MeV reduces the fusion cross section by a factor of  $\sim 13$  or less, whereas conventional fusion models predict a decrease by about 5 orders of magnitude. Since lowering of the entrance channel kinetic energy decreases the compound nucleus excitation energy by the same amount of MeV and since the survivability of a heavy, highly fissile compound nucleus depends so dramatically on its excitation energy the net result of choosing a bombarding energy  $\sim 10 \text{ MeV}$  below the one-dimensional barrier will be a gain in the cross section for surviving superheavy evaporation residues by several orders of magnitude. Quantitative estimates of these gain factors are difficult to obtain because the sur-

vivability of a SHE (section 4.4.3.) depends also on the rate of weakening of the shell effects near  $Z = 114$  and  $N = 184$  by excitation energy and compound nucleus deformation, both factors being poorly known at present.

The cross section enhancements for fusion below the barrier is far from being theoretically understood. Qualitatively, as the size of the projectile becomes comparable to that of the target, dimensions other than the separation of the centers of two rigid nuclei are expected to become important. Among the additional degrees of freedom that have to be considered we mention deformations, both static or momentary as a result of the zero-point motion of low-lying surface vibrations and the rapid formation of a neck between target and projectile which make the barrier penetration problem multidimensional.

#### 4.4.2. Dynamical limitations of fusion near the barrier

The above statement on the time scale for the necking degree of freedom comes from low-energy fission studies [93] where fully paired even-even fragmentations into the ground states of the fission fragments have not been detected. The finding of pair breaking even for the coldest fragmentations allows to estimate a time for the necking-in process of at most  $3 \times 10^{-22}$  s. This time is short compared to the equilibration time for the mass asymmetry degree of freedom which is known from deep-inelastic heavy-ion collisions to be about  $4 \times 10^{-21}$  s. The time for formation of a neck in a fusion reaction, i.e. the transition time from a binary system to an elongated saddle point shape (the barrier crossing time) is, therefore, believed to be also much smaller than the time required for the disappearance of the mass asymmetry of the entrance channel. Therefore, it makes sense to study the dynamics of fusion at frozen mass asymmetry as a function of the separation of the colliding nuclei and as a function of the neck-size as proposed by SWIATECKI [94]. Then, in analogy to fission where the fissility of the system is governed by the ratio between repulsive Coulomb forces and attractive nuclear forces, the fusibility of two touching nuclei will be governed by an effective value of  $Z^2/A$  defined as the ratio of forces in the entrance channel as

$$(Z^2/A)_{\text{eff}} = \frac{4Z_1Z_2}{A_1^{1/3} \cdot A_2^{1/3}(A_1^{1/3} + A_2^{1/3})},$$

if centrifugal forces are ignored. The latter is justified for the formation of very heavy fusion-evaporation-residues where only the lowest partial waves contribute.  $(Z^2/A)_{\text{eff}}$  is a measure for the depth of the potential pocket which is required for fusion. Using a proximity potential and a Coulomb potential one can calculate that the pocket disappears for  $(Z^2/A)_{\text{eff}} \simeq 46$ . Unfortunately, however, there is a geometrical limitation of fusion in the entrance channel which is given by the elongation of the "conditional" saddle point shape with respect to the elongation associated with the touching point of projectile and target, as schematically illustrated in Fig. 13. In the upper part

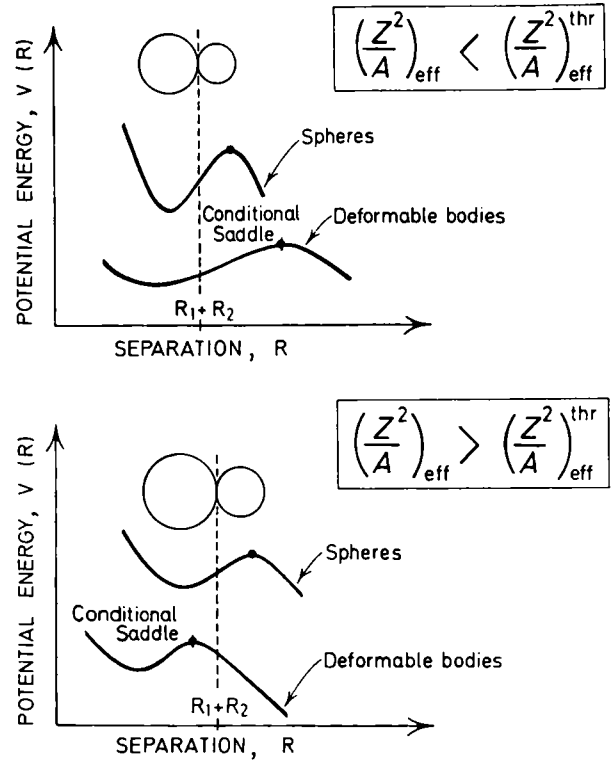


Fig. 13. Schematic representation of one-dimensional two-center potentials,  $V(R)$ , showing a reaction barrier and a pocket behind it. These quantities are defined in the one-dimensional space of two spheres separated by a variable distance  $R$ . Also shown are potential curves appropriate to two deformable bodies with fixed masses connected by a neck. Such curves represent cuts in a multidimensional deformation space, but there is in general a well-defined saddle point, named the "conditional" saddle to emphasize the condition of fixed mass asymmetry at variable neck size and variable separation  $R$ . The top figure illustrates the cases where the conditional saddle is more elongated than two spheres in contact. In the lower figure the conditional saddle point is more compact than two spheres in contact. Here the existence of a pocket in the one-dimensional potential is not sufficient for the system to get trapped. An extra inward push of kinetic energy is required to bring the system inside the conditional saddle [94]

of the Figure the touching point lies within the separation  $R$  appropriate for the conditional saddle point, thus allowing the system to fall into the pocket and to fuse. For a system with  $(Z^2/A)_{\text{eff}}$  being larger than a threshold value  $(Z^2/A)_{\text{eff}}^{\text{thr}}$  the system is not trapped unless an extra amount of kinetic energy is provided which brings the system inside the conditional saddle point. This "extra push", if supplied, results in additional excitation of the compound nucleus which, in turn, reduces its survivability. The extra push for systems with  $(Z^2/A)_{\text{eff}} > (Z^2/A)_{\text{eff}}^{\text{thr}}$  increases quadratically as

$$\Delta E_{\text{push}} = a^2 \eta_0 [(Z^2/A)_{\text{eff}} - (Z^2/A)_{\text{eff}}^{\text{thr}}]^2$$

where the parameter  $a$  is the rate at which the extra push increases and  $\eta_0$  is a dimensional constant. An important task for the experimenters was now to find out the value of  $(Z^2/A)_{\text{eff}}^{\text{thr}}$  and to check whether this value is independent of the fissility of the compound system. SANN *et al.* [95] and SWIATECKI [94] asserted on the basis of

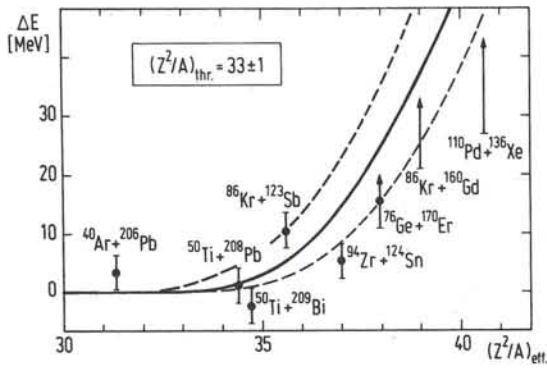


Fig. 14. Extra push of kinetic energy required to fuse given target-projectile combinations [96]. The “fusability” of a given system is characterized by the entrance channel model parameter  $(Z^2/A)_{\text{eff}}$  for angular momentum  $l = 0 \hbar$ . Systems that have been shown to fuse and to produce detectable amounts of evaporation residues are  $^{40}\text{Ar} + ^{206}\text{Pb}$  [97],  $^{50}\text{Ti} + ^{208}\text{Pb}$  and  $^{50}\text{Ti} + ^{209}\text{Bi}$  [98],  $^{86}\text{Kr} + ^{123}\text{Sb}$  and  $^{94}\text{Zr} + ^{124}\text{Sn}$  [99], and  $^{76}\text{Ge} + ^{170}\text{Er}$  [96]. No evaporation residues could be detected for  $^{86}\text{Kr} + ^{160}\text{Gd}$  and  $^{110}\text{Pd} + ^{136}\text{Xe}$  [96] indicating the existence of a “thud wall” for fusion beyond  $(Z^2/A)_{\text{eff}} \approx 38$ . The solid line and the dashed lines are the result of a fit of SWIATECKI’s model to symmetric fission cross sections [94, 95] using angular momentum dependent values of  $(Z^2/A)_{\text{eff}}$  with  $(Z^2/A)_{\text{eff}}^{\text{thr}} (l = 0) = 33 \pm 1$  and  $a \approx 12$ . The latter model [94] assumes that barrier crossing is a highly viscous process involving one-body friction

measurements of the cross sections for symmetric fission in a large number of target-projectile combinations [95] that the threshold is located at  $(Z^2/A)_{\text{eff}}^{\text{thr}} \approx 33 \pm 1$  and the slope is a  $\approx 12$ . One may argue that the observation of symmetric fragmentation does not prove that a compound nucleus was existing. Therefore, measurements of compound nucleus evaporation residue cross sections are a more stringent test of the location of the dynamical threshold for fusion. Fig. 14 shows the experimentally determined extra push  $\Delta E_{\text{push}}$  relative to the one-dimensional barrier for touching spheres as a function of  $(Z^2/A)_{\text{eff}}$  [96]. Several important conclusions can be drawn from the data shown in Fig. 14: i) The concept of a conditional saddle point allowing scaling of the fusability of different target-projectile combinations with the entrance channel parameter  $(Z^2/A)_{\text{eff}}$  has been confirmed for systems with very different fissility  $(Z_0^2/A_0)$ . This confirms that the barrier crossing time (the time for formation of a neck) is short compared to the equilibration time for the mass asymmetry. ii) Up to  $(Z^2/A)_{\text{eff}} \sim 38$  fusion has been observed unhindered with compound nucleus excitation energies as low as 15–20 MeV. iii) Below  $(Z^2/A)_{\text{eff}} \sim 38$  fusion of two nuclei which are very gently brought together with zero relative velocity and negligible angular momentum seems to be possible without the release of intrinsic energy due to friction, whereas one-body dissipation [94] already predicts “extra push” energies of up to 20 MeV. For  $(Z^2/A)_{\text{eff}} < 38$  at the lowest possible bombarding energies the neck formation or barrier crossing is a friction-less transition. iv) Beyond  $(Z^2/A)_{\text{eff}} \sim 38$  there seems to be a “thud wall” preventing heavy target-projectile combinations from being fused at low excitation energies.

The messages concerning the production of SHE’s in fusion reactions that we get from these conclusions are as follows: Among the reactions listed in Table 1 that were hoped to form compound nuclei with possible survival all class 2 reactions are characterized by values of  $(Z^2/A)_{\text{eff}} > 38$  so that compound nucleus formation did not take place at the near-barrier energies used in the experiments. Inasmuch as the class 1 reactions did not seriously test the existence of SHE’s because of too unstable, neutron-deficient landing places, none of the many class 2 reactions can be seen as a serious test of the existence of the predicted island of stability because the synthetic route that was chosen does not exist.

The only access to the SHE island in fusion reactions is possible by combining heavy targets with  $Z \approx 88-98$  with medium size projectiles with  $Z < 27$  (“class 3” reactions). When considering the required availability of weighable amounts of both projectile and target material with  $(Z^2/A)_{\text{eff}} < 38$  we find only a few combinations using  $^{48}\text{Ca}$  and  $^{50}\text{Ti}$  beams with  $^{244}\text{Pu}$ ,  $^{248}\text{Cm}$  and  $^{252}\text{Cf}$  targets that fulfill the requirement of unhindered fusion into compound nuclei with possible survival.

But why did the extensive attempts with the  $^{48}\text{Ca} + ^{248}\text{Cm}$  reaction fail? Both in Berkeley [28, 66–68] and at Dubna [55] on the basis of some indirect hints for entrance channel limitations in heavy-ion fusion reactions [53] it was decided that some tens of MeV of extra push had to be provided to fuse  $^{48}\text{Ca}$  with  $^{248}\text{Cm}$  so that the compound system was formed with excitation energies between 34 and 54 MeV, which probably reduced their overall survival rates to hopelessly small values [53]. Today, in view of the results of the recent high-precision and high-sensitivity fusion studies mentioned above, we conclude that this decision was wrong. The reasons for this conclusion are summarized in Table 2 which compares some of the reactions investigated with the three most promising combinations reaching the island of stability. The excitation energies at the fusion barrier,  $E_B^x$ , are calculated from the experimentally determined barrier heights which are, for  $(Z^2/A) < 38$ , in agreement with calculated barriers using the proximity theory and reducing the resulting barrier heights by 4% [94]. The same recipe was used to predict fusion barriers for the three most promising superheavy target-projectile combinations and to estimate the respective compound nucleus excitation energies at the barrier,  $E_B^x$ . The column  $E_{\text{min}}^x$  lists the lowest excitation energies at which evaporation residues were observed or are expected due to barrier penetration. Thus, it should be possible to form the superheavy compound systems at about 15 MeV of excitation energy. Their entrance channel parameters are very similar to those, e.g., of the  $^{94}\text{Zr} + ^{124}\text{Sn}$  reaction. However, there exists an important difference.  $^{218}\text{Th}$  has a liquid drop barrier of 4–5 MeV at rather large deformations while the superheavy nucleus  $^{296}114$  owes its stability entirely to shell stabilization with a fission barrier at much smaller deformations. The important question to be asked is how shell-stabilized narrow fission barriers of spherical nuclei are preserved at higher excitation energy.

Table 2. Entrance and exit channel parameters for several heavy-ion fusion reactions with  $(Z^2/A)_{\text{eff}} < 38$ . The height of the fission barrier at zero excitation energy is given as  $E_f = B_f - \delta U$ , if an additional (small) shell effect at the barrier is ignored

Reaction	Compound nucleus	Fission barrier $B_f^a)$	Fusability $\delta U^b)$	Fusability $(Z^2/A)_{\text{eff}}$	Fissility $(Z_0^2/A_0)$	Fusion barrier $B$ (MeV)	Excitation energy (MeV)		lowest xn channel observed	Reference
							$E_B^x$	$E_{\text{min}}^x$		
$^{40}_{18}\text{Ar} + ^{206}_{82}\text{Pb}$	$^{246}_{100}\text{Fm}$	1.5	-2.3	31.3	40.7	$162 \pm 3$	33	19	2 n	97
$^{50}_{22}\text{Ti} + ^{208}_{82}\text{Pb}$	$^{258}_{104}$	0.8	-2.9	34.4	41.9	$191 \pm 3$	22	18	1 n	98
$^{50}_{22}\text{Ti} + ^{209}_{83}\text{Bi}$	$^{259}_{105}$	0.6	-3.0	34.7	42.6	$190 \pm 3$	15	12	1 n	98
$^{54}_{24}\text{Cr} + ^{209}_{83}\text{Bi}$	$^{263}_{107}$	0.4	-2.9	36.6	43.5	$\sim 209$	20	15	1 n	62, 98
$^{86}_{36}\text{Kr} + ^{123}_{51}\text{Sb}$	$^{209}_{87}\text{Fr}$	7.2	-4.6	35.6	36.2	$209 \pm 3$	40	28	3 n	99
$^{94}_{40}\text{Zr} + ^{124}_{50}\text{Sn}$	$^{218}_{90}\text{Th}$	5.3	-4.3	37.0	37.2	$219 \pm 3$	31	20	1 n	99
$^{48}_{20}\text{Ca} + ^{248}_{96}\text{Cm}$	$^{296}_{116}$	0	-4.9	33.9	45.5	196 <sup>c)</sup>	25 <sup>d)</sup>	< 15		
$^{50}_{22}\text{Ti} + ^{244}_{94}\text{Pu}$	$^{294}_{116}$	0	-3.6	36.2	45.8	212 <sup>c)</sup>	28 <sup>d)</sup>	< 18		
$^{50}_{22}\text{Ti} + ^{248}_{96}\text{Cm}$	$^{298}_{118}$	0	-5.7	36.6	46.7	216 <sup>c)</sup>	28 <sup>d)</sup>	< 18		

- a) empirical liquid drop fission barriers, from Ref. [104]
- b) ground state shell correction, from Ref. [105]
- c) calculated using the proximity theory and reducing the barrier height by 4%
- d) relative to the droplet model ground state in the absence of shell effects, Ref. [105]

#### 4.4.3. A comment on the survivability of shell-stabilized compound nuclei

SAHM *et al.* [100–102] have studied the deexcitation by neutron emission of  $^{214-220}\text{Th}$  produced by fusion of  $^{40}\text{Ar}$  with  $^{178-180}\text{Hf}$  and of  $^{90-96}\text{Zr}$  with  $^{124}\text{Sn}$ . The deduced relative neutron decay widths  $\langle \Gamma_n/\Gamma_f \rangle$ , i.e. the average values of  $\Gamma_n/\Gamma_f$  over the neutron cascade, or the cross sections, show no increase at the magic neutron number  $N = 126$  for 4n or 3n channels. For 2n and 1n channels being observed at much lower excitation energies there is a small increase. As already pointed out by SCHMIDT *et al.* [102] these results are consistent with a reduction of the spherical ground state shell effect to 1/e of its full strength by an excitation energy of less than 10 MeV. On the other hand many actinide and transactinide isotopes with  $Z < 106$  have been produced [103] in 4n reactions at 35 to 45 MeV of excitation energy. These nuclei are deformed in their ground state and their shell effects seem to be much more stable against intrinsic excitation than those of spherical nuclei. This is dramatically illustrated by Fig. 15 showing the ratio of measured to calculated 2n–5n cross sections for a large number of deformed and spherical compound nuclei [101]. The upper part, where the calculations included the ground state shell effect, shows that for nuclei with deformed ground states the measured cross sections are fairly well reproduced by the calculations. In contrast, for nuclei with spherical or almost spherical ground states, the measured cross sections are much lower than predicted and are reproduced much better by calculations (middle part of Fig. 15) where the shell effects are completely neglected. This is to say that the stabilizing effect of spherical shells on the survival probability of compound nuclei is, if existing at all, extremely weak. One can appreciate the consequences of this result

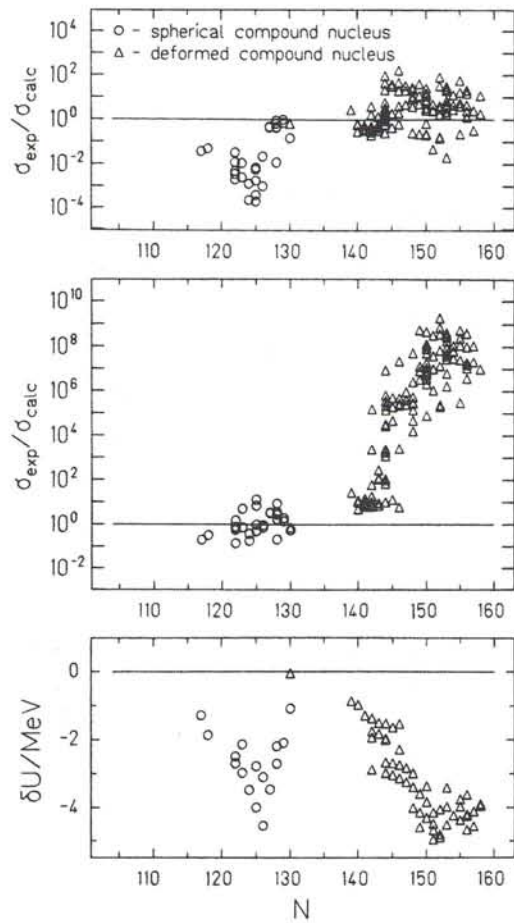


Fig. 15. Ratio of measured and calculated xn cross section for  $2 < x < 5$  as a function of the residual neutron number from Ref. [101]. Upper part:  $\sigma_{\text{calc}}$  includes ground state shell effects. Middle part:  $\sigma_{\text{calc}}$  calculated by neglecting ground state shell effects. Lower part: Ground state shell effects for spherical nuclei near  $N = 126$  and for deformed nuclei near  $N = 152$

if one realizes that our test cases, i.e. the spherical compound nuclei near  $N = 126$  have solid (liquid drop) barriers of several MeV even in the complete absence of stabilizing shell effects. Nevertheless, their cross sections in fusion reactions are reduced by up to four orders of magnitude by the damping-out of their shell effects. Superheavy elements near  $N = 184$ , on the other hand, have no stability at all from the liquid drop. Thus, their survival rates will depend entirely on the residual shell strength at the minimum excitation energy possible and at the unavoidable deformation introduced by the entrance channel of the fusion reaction. It is clear that future attempts to synthesize SHE's in the fusion reactions listed in Table 2 will have to be performed at energies 10 to 15 MeV below the calculated fusion barrier energies. The expected excitation energies are then similar to those in the  $^{54}\text{Cr} + ^{209}\text{Bi}$  reaction so that there is some hope for the formation of a superheavy evaporation residue by the evaporation of one neutron.

#### 4.4.4. New results on deep-inelastic transfer reactions

After the original optimistic extrapolations [70–73] of production rates of SHE's in deep-inelastic collisions the question has been raised [86, 75] whether the heavy fragments produced in these collisions are formed in statistical equilibrium and, thus, decay by a neutron evaporation cascade typical for an equilibrated compound nucleus, or, whether they are deformed (under the influence of the large angular momenta involved) to or beyond the fission saddle point. The latter situation would result in a fast non-equilibrium fission process which might be detectable experimentally.

Two very different types of experiments have addressed themselves to this important question. By using  $1\text{ m}^2$  large position-sensitive counters GLÄSSEL *et al.* [86] performed kinematically complete investigations of deep-inelastic collisions followed by sequential fission of the heavy reaction product in  $^{238}\text{U} + ^{238}\text{U}$  and  $^{238}\text{U} + ^{248}\text{Cm}$  collisions. These experiments provided no evidence for a fast sequential break-up of the heavy fragments. Even for the largest mass transfers leading to heavy fragments with  $Z > 110$ , the data are still compatible with a two-step reaction mechanism where fission of the heavy fragment follows the deep-inelastic collisions with minimum scission-to-scission times of  $\geq 10^{-20}$  sec. However, the observed fission fragment angular distributions were found [86] to be incompatible with the usual statistical distribution of states at the liquid drop saddle point. Also, in the region of the heaviest elements, GLÄSSEL *et al.* observed a considerable broadening of the fission fragment mass distribution. A possibly related broadening in the mass distribution has also been observed in fusion-fission reactions of lighter elements when the fission barriers reach zero because of very high angular momenta. Irrespective of the apparent two-step nature of the observed fission phenomena, GLÄSSEL *et al.* concluded [86] that non-equilibrated systems may be involved. It is important to note here, that

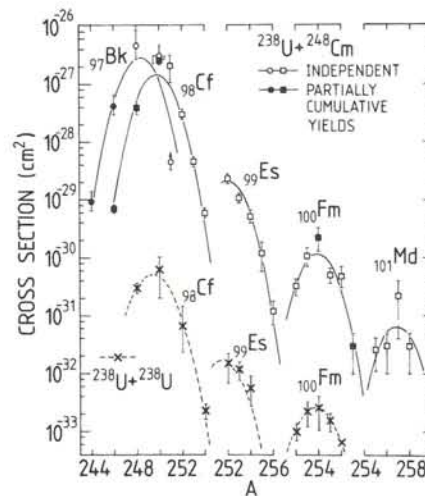


Fig. 16. Cross section for the formation of transcurium isotopes in the  $^{238}\text{U} + ^{248}\text{Cm}$  reaction at 7.4 MeV/nucleon incident energy, from Ref. [106]. Also plotted for comparison are data for the  $^{238}\text{U} + ^{238}\text{U}$  reaction from Ref. [72]

their results refer to values of total kinetic energy loss (TKEL) of  $> 150$  MeV in the first reaction step. Similar investigations of the fission phenomena of  $Z > 110$  fragments at much lower values of TKEL are highly desirable.

The second type of experiments related to the basic question of a statistical equilibrium of the heavy fragments in deep-inelastic collisions was performed by SCHÄDEL *et al.* [72, 76, 106] by using the extreme sensitivity of radiochemical techniques. In the  $^{238}\text{U} + ^{238}\text{U}$  reaction the steep decrease in the element yields beyond uranium, see Fig. 7, was followed over eight orders of magnitude up to fermium ( $Z = 100$ ) [72]. Analyses of these actinide cross sections indicated that the surviving transuranium isotopes were produced in the low-energy tails of the broad excitation energy distributions at average excitation energies on the order of 35 MeV. In order to reproduce the residual Cf- through Fm-yields relative neutron decay widths  $\Gamma_n/\Gamma_f$  a factor of two smaller than the empirical values by SIKKELAND [107] have to be used [76]. This reduction is in agreement with semi-quantitative estimates of the influence of the angular momenta on  $\Gamma_n/\Gamma_f$ , however, alternatively, a loss of yield due to non-equilibrium fission could not absolutely be excluded. Here, the formation cross sections for transuranium isotopes in the  $^{238}\text{U} + ^{248}\text{Cm}$  reaction have helped to exclude the latter possibility. These data are shown in Fig. 16, where they are compared to the cross sections observed in the  $^{238}\text{U} + ^{238}\text{U}$  reaction. The cross sections for Fm, Es, and Cf in the  $^{238}\text{U} + ^{248}\text{Cm}$  reaction are three to four orders of magnitude higher than in the  $^{238}\text{U} + ^{238}\text{U}$  reaction. These increases are qualitatively expected because fewer nucleons have to be transferred to the target nucleus  $^{248}\text{Cm}$  to make Cf, Es, Fm or Md isotopes than need to be transferred to  $^{238}\text{U}$  in order to produce the same product nuclei. Because the number of transferred nucleons and the intrinsic excitation of the product are correlated it is expected that Cf-, Es- and Fm-fragments produced in  $^{238}\text{U} + ^{238}\text{U}$  collisions have on the average much higher

excitation energies than the same fragments originating from  $^{238}\text{U} + ^{248}\text{Cm}$  collisions. The resulting larger loss of yield to sequential fission explains the reduced yields of surviving actinides in the  $^{238}\text{U} + ^{238}\text{U}$  reaction relative to the  $^{238}\text{U} + ^{248}\text{Cm}$  reaction, see Fig. 16. A quantitative analysis of the observed yield ratios [106] revealed that on the average 3 to 4 neutrons were evaporated in the de-excitation chains leading to surviving heavy actinides in the  $^{238}\text{U} + ^{248}\text{Cm}$  reaction implying average excitation energies of about 30 MeV. This is entirely consistent with the earlier findings for the  $^{238}\text{U} + ^{238}\text{U}$  reaction [72] and largely excludes losses of yield to fast non-equilibrium fission processes. Based on these results and on the great similarities that exist in the reaction mechanisms of  $^{238}\text{U} + ^{238}\text{U}$  and  $^{238}\text{U} + ^{248}\text{Cm}$  collisions SCHÄDEL *et al.* [106] have asserted that a cross section of  $10^{-32}$  cm<sup>2</sup> at excitation energies of 25–30 MeV is expected for  $Z = 114$  in the  $^{238}\text{U} + ^{248}\text{Cm}$  reaction. This is a factor of 30 higher than the estimate for the  $^{238}\text{U} + ^{238}\text{U}$  reaction.

If excited SHE's can be formed with < 15 MeV of excitation energy and with millibarn cross sections in fusion reactions such as  $^{48}\text{Ca} + ^{248}\text{Cm}$  the deep-inelastic transfer approach appears to be clearly inferior. However, we should keep in mind that with deep-inelastic  $^{238}\text{U} + ^{248}\text{Cm}$  collisions we are capable of reaching neutron-rich areas in the island of stability inaccessible to fusion reactions, see again Fig. 8. If these neutron-rich species can be formed with little deformation, the chances of surviving their formation may be much better than those of any superheavy compound nucleus produced in a fusion reaction. Thus, at present, continued efforts along both alternative synthetic routes are necessary as well as continued studies of both reaction mechanisms which are of great interest in themselves.

## 5. Outlook

After more than a decade of extensive experimental efforts to search for SHE's in nature and to synthesize SHE's in heavy-ion reactions the anticipated massive extension of the periodic table of the elements has not been achieved. Still, the original reasons for this attempt are valid and motivate for further effort. There is the opportunity to test the predictive power of modern theories describing the stability of atomic nuclei. And there is still hope to test the predictions of chemical properties of the SHE's, predictions based on relativistic rules whose consequences are just becoming apparent in the atomic properties of the heaviest known elements. Experimental tests of these physical and chemical predictions would greatly expand our understanding of the periodic table of the elements.

The failure to observe SHE's has been interpreted [53] as an indication for considerably lower fission barriers of these elements than those predicted in the early "optimistic" calculations. This would preclude their observation in nature and diminish our expectations for the possible production of SHE's in the laboratory. However, as we have

discussed in this review, recent insight into heavy-ion reaction mechanisms behooves us to believe that perhaps none of the heavy-ion experiments performed to date has provided a real test for the existence of the predicted island of stability. This is connected i) with a general lack of ultra-sensitive detection techniques for very short-lived species, ii) with the threshold for fusion reactions at  $(Z^2/A)_{\text{eff}} > 38$  which precludes formation of superheavy compound nuclei in all "class 2" reactions and which leaves only very few target-projectile combinations for meaningful future experiments, and iii) with the extreme sensitivity of the ground state shell effect of spherical nuclei towards intrinsic excitation which may have reduced the overall production rates of any residual SHE formed either in complete fusion reactions or in deep-inelastic transfer reactions to undetectable values.

For the near future we anticipate

- 1) Further studies on the de-excitation of spherical nuclei.
- 2) Further studies on energy- and system-dependences of heavy actinide production in deep-inelastic heavy-ion collisions
- 3) Developments of new methods for the detection of very short-lived SHE's and their application in future  $^{238}\text{U} + ^{248}\text{Cm}$  bombardments.
- 4) A repetition of the  $^{48}\text{Ca} + ^{248}\text{Cm}$  fusion experiments at substantially lower bombarding energies (4.5–4.9 MeV/nucleon) as well as attempts with the  $^{48}\text{Ca} + ^{244}\text{Pu}$  and  $^{50}\text{Ti} + ^{248}\text{Cm}$  reactions at comparably low energies.

None of these experiments will be simple because we need tens of milligrams of exotic target materials such as highly enriched  $^{244}\text{Pu}$  and  $^{248}\text{Cm}$ , large quantities of isotopically separated  $^{48}\text{Ca}$  and  $^{50}\text{Ti}$ , for which the worldwide supply is very limited, powerful heavy-ion accelerators producing intense beams of these exotic projectiles, highly sophisticated experimental techniques, and a considerable amount of man power. In none of the competing laboratories all these prerequisites are simultaneously fulfilled. This clearly calls for international collaboration.

If the new experiments fail we should keep in mind that in a fusion reaction there is a long way from the deformed configuration at the barrier showing no shell stabilization to the spherical ground state which is shell stabilized. Also deep-inelastic collisions are likely to produce SHE's in deformed shapes. How to bridge this gap is a question for which an answer is not at hand.

## Acknowledgements

It is a pleasure for the author to thank G. HERRMANN and N. TRAUTMANN from the University of Mainz and the nuclear chemistry group at GSI for many years of enjoyable collaboration. Discussions with S. BJØRNHOLM, A. GOBBI, G. MÜNZENBERG, W. NÖRENBERG, W. REISDORF, C. RIEDEL, and H. J. SPECHT are gratefully acknowledged.

## References

1. MELDNER, H.: Ark. Fysik 36, 593–598 (1967).
2. MYERS, W. D., SWIATECKI, W. J.: Nucl. Phys. 81, 1–60 (1966).
3. MOSEL, U., GREINER, W.: Z. Physik 222, 261–282 (1969).
4. NILSSON, S. G., NIX, J. R., SOBICZEWSKI, A., SZYMANSKI, Z., WYCECH, S., GUSTAFSON, C., MÖLLER, P.: Nucl. Phys. A 115, 545–562 (1968).
5. NILSSON, S. G., TSANG, C. F., SOBICZEWSKI, A., SZYMANSKI, Z., WYCECH, S., GUSTAFSON, C., LAMM, I. L., MÖLLER, P., NILSSON, B.: Nucl. Phys. A 131, 1–66 (1969).
6. HERRMANN, G., in: MADDOCK, A. G. (Ed.), *Int. Rev. of Science, Inorg. Chem. Ser. 2, Vol. 8, Radiochemistry*. Butterworth, London, p. 221–272 (1975).
7. HERRMANN, G.: Nature 280, 543–549 (1979).
8. NILSSON, S. G., NILSSON, N. R. (Ed.): Superheavy Elements – Theoretical Prediction and Experimental Generation, Proc. of the Nobel Sympos., Rønneby 1974, Phys. Scr. 10A (1974).
9. LODHI, M. A. K. (Ed.): Superheavy Elements, Proc. of the Int. Sympos., Lubbock 1978, Pergamon Press, New York (1978).
10. NILSSON, S. G., in: LODHI, M.A.K., (Ed.), Superheavy Elements, Proc. of the Int. Sympos., Lubbock 1978, Pergamon Press, New York (1978), p. 237–273.
11. NIX, J. R.: Ann. Rev. Nucl. Sci. 22, 65–120 (1972).
12. FISET, E. O., NIX, J. R.: Nucl. Phys. A 193, 647–671 (1972).
13. SOBICZEWSKI, A., in: LODHI, M.A.K. (Ed.), Superheavy Elements Proc. of the Int. Sympos., Lubbock 1978, Pergamon Press, New York (1978), p. 274–283.
14. RANDRUP, J., LARSSON, S. E., MÖLLER, P., SOBICZEWSKI, A., LUKASIAK, A.: Phys. Scr. 10A, 60–64 (1974).
15. ÅBERG, S.: private communication to G. HERRMANN.
16. BEMIS, C. E., NIX, J. R.: Comments Nucl. Part. Phys. 7, 65–78 (1977).
17. MORETTO, L. G.: Nucl. Phys. A 180, 337–362 (1972).
18. MUSTAFA, M. G., in: LODHI, M.A.K., (Ed.), Superheavy Elements, Proc. of the Int. Sympos., Lubbock 1978, Pergamon Press, New York (1978), p. 284–295.
19. SCHMITT, H. W., MOSEL, U.: Nucl. Phys. A 186, 1–14 (1972).
20. HOFFMAN, D. C., in: LODHI, M.A.K., (Ed.), Superheavy Elements, Proc. Int. Sympos., Lubbock 1978, Pergamon Press, New York (1978), p. 24–33.
21. FRICKE, B.: Struct. Bonding 21, 89–144 (1975).
22. PITZER, K. S.: J. Chem. Phys. 63, 1032–1033 (1975).
23. KELLER, O. L., SEABORG, G. T.: Ann. Rev. Nucl. Sci. 27, 139–166 (1977).
24. EICHLER, B.: Kernenergie 19, 307–311 (1976).
25. KRATZ, J. V., LILJENZIN, J. O., SILVA, R. J., SEABORG, G. T.: Lawrence Berkeley Lab. Report LBL-1666 (1973), pp. 308–310.
26. KRATZ, J. V., LILJENZIN, J. O., SEABORG, G. T.: Inorg. Nucl. Chem. Lett. 10, 951–957 (1974).
27. FLEROV, G. N., in: ROBINSON, R. L., MCGOWAN, F. K., BALL, J. B., HAMILTON, J. H. (Ed.), Proc. of the Int. Conf. on Reactions between Complex Nuclei, Nashville 1974, North-Holland, Amsterdam (1974), vol. 2, pp. 459–481.
28. OTTO, R. J., MORRISSEY, D. J., LEE, D., GHIORSO, A., NITSCHKE, J. M., SEABORG, G. T., FOWLER, M. M., SILVA, R. J.: J. Inorg. Nucl. Chem. 40, 589–595 (1978).
29. BRÜCHLE, W., TITTEL, G., TRAUTMANN, N., ZENDEL, M., in: W. MÜLLER and R. LINDNER (Ed.), *Transplutonium Elements*, North-Holland, Amsterdam (1976), p. 29–36.
30. HOWARD, W. M., NIX, J. R.: Nature 247, 17–20 (1974).
31. MATHEWS, G. R., VIOLA, V. E.: Nature 261, 382–385 (1976).
32. SCHRAMM, D. N., FISET, E. O.: Astrophys. J. 180, 551–570 (1973).
33. HERRMANN, G.: Phys. Scr. 10A, 71–76 (1974).
34. FLEROV, G. N., KOROTKIN, YU. S., TER-AKOPYAN, G. M., ZVARA, I., OGANESSIAN, YU. TS., POPEKO, A. G., CHURBUKOV, YU. T., CHELNOKOV, L. P., MASLOV, O. P., SMIRNOV, V. I., GERSTENBERGER, R.: Z. Physik A 292, 43–48 (1979).
35. FLEROV, G. N.: Contribution to the 4th Int. Conf. on Nuclei far from Stability, Helsingør (1981).
36. HALPERIN, J., STOUGHTON, R. W., KETTELE, B. H., LUND, T., BRANDT, R.: Z. Physik A 300, 281–284 (1981).
37. LUND, T., BRANDT, R., MOLZAHN, D., TRESS, G., VATER, P., MARINOV, A.: Z. Physik A 300, 285–288 (1981).
38. FLEROV, G. N., TER-AKOPYAN, G. M., POPEKO, A. G., FEFILOV, B. V., SUBBOTIN, V. G.: Yad. Fiz. 26, 449–454 (1977). Sov. J. Nucl. Phys. 26, 237–240 (1977).
39. POPEKO, A. G., SKOBOLEV, N. K., TER-AKOPYAN, G. M., GONCHAROV, G. N.: Phys. Lett. 52B, 417–420 (1974).
40. POPEKO, A. G., TER-AKOPYAN, G. M.: Yad. Fiz. 29, 604–607 (1979). Sov. J. Nucl. Phys. 29, 310–312 (1979).
41. ANDERS, E., HEYMANN, D.: Science 164, 821–823 (1969).
42. ANDERS, E., LARIMER, J. W.: Science 175, 981–983 (1972).
43. ANDERS, E., HIGUCHI, J., GROS, H., TAKAHASHI, H., MORGAN, J. W.: Science 190, 1262–1271 (1975).
44. ANDERS, E.: Proc. R. Soc. London A 374, 207–238 (1981).
45. MANUEL, O. K., SABU, D. D.: Science 195, 208–209 (1977).
46. ZVÁRA, I., FLEROV, G. N., ZHUIKOV, B. L., REETZ, T., SHALAEVSKII, M. R., SKOBELEV, N. K.: Yad. Fiz. 26, 455–460 (1977). Sov. J. Nucl. Phys. 26, 240–243 (1977).
47. ZHUIKOV, B. L., ZVÁRA, I.: Radiochem. Radioanal. Lett. 44, 47–60 (1980).
48. FLEROV, G. N., TER-AKOPYAN, G. M.: Pure Appl. Chem. 53, 909–923 (1981).
49. See for example SIKKELAND, T.: Ark. Fysik 36, 539–552 (1967).
50. BRIX, P.: Max-Planck-Inst. für Kernphysik, Heidelberg, Report MPI H-1977-V41 (1977).
51. NILSSON, S. G., THOMPSON, S. G., TSANG, C. F.: Phys. Lett. 28B, 458–461 (1969).
52. THOMPSON, S. G., SWIATECKI, W. J., GATTI, R. C., BOWMAN, H. R., MORETTO, L. G., JARED, R. C., LATIMER, R. M.: Univ. of California Radiat. Lab. Berkeley Report UCRL 18667 (1969), p. 283.
53. SEABORG, G. T., LOVELAND, W., MORRISSEY, D. J.: Science 203, 711–717 (1979).
54. TER-AKOPYAN, G. M., BRUCHERTSEIFER, H., BUKLANOV, G. V., ORLOVA, O. A., PLEVE, A. A., CHERPIGIN, V. I., CHOY VAL SEK: Yad. Fiz. 29, 608–614 (1979). Sov. J. Nucl. Phys. 29, 312–316 (1979).
55. OGANESSIAN, YU. TS., BRUCHERTSEIFER, H., BUKLANOV, G. V., CHERPIGIN, V. I., CHOY VAL SEK, EICHLER, B., GAVRILOV, K. A., GÄGGELER, H., KOROTKIN, YU. S., ORLOVA, O. A., REETZ, T., SEIDEL, W., TER-AKOPYAN, G. M., TRETYAKOVA, S. P., ZVÁRA, I.: Nucl. Phys. A 294, 213–224 (1978).
56. COLOMBANI, P., GATTY, B., JACMART, J. C., LEFORT, M., PÉTER, J., RIOU, M., STÉPHAN, C., TARRAGO, X.: Phys. Lett. 42B, 208–210 (1972).
57. WIRTH, G., AHRENS, H., BÖGL, W., FRANZ, G., KRATZ, J. V., MARX, D., NICKEL, F., WARNECKE, I., WEBER, W.: GSI Ann. Rep. 1976, GSI-J-1-77, p. 72.
58. BUTLER, P. A., GRODZINS, L., VIDEBAEK, F., YOUNG, G. R., DIAMOND, R. M., LEE, I. Y., STEPHENS, F. S.: Phys. Lett. 74B, 222–224 (1978).
59. AUMANN, D. C., FALESCHINI, W., FRIEDMANN, L., WEISMANN, D.: Phys. Lett. 82B, 361–364 (1979).
60. ESTERLUND, R. A., MOLZAHN, D., BRANDT, R., PATZELT, P., VATER, P., BOOS, H. A., CHANDRATILLAKE, M. R., GRANT, I. S., HEMINGWAY, J. D., NEWTON, G. W. A.: Phys. Rev. C 15, 319–324 (1977).
61. MÜNZENBERG, G., ARMBRUSTER, P., FAUST, W., HOFMANN, S., REISDORF, W., SCHMIDT, K.-H., VALLI, K., EWALD, H., GÜTTNER, K., CLERC, H. G., LANG, W.: GSI Ann. Rep. 1977, GSI-J-1-78, p. 75.
62. MÜNZENBERG, G., HOFMANN, S., HESSBERGER, F. P., REISDORF, W., SCHMIDT, K. H., SCHNEIDER, J. R. H., ARMBRUSTER, P., SAHM, C. C., THUMA, B.: Z. Physik A 300, 107–108 (1981).
63. FLEROV, G. N., OGANESSIAN, YU. TS., LOBANOV, YU. V., PLEVE, A. A., TER-AKOPYAN, G. M., DEMIN, A. G., TRETYAKOVA, S. P., CHERPIGIN, V. I., TRETYAKOV, YU. P.: Yad. Fiz. 19, 492–498 (1974). Sov. J. Nucl. Phys. 19, 247–250 (1974).
64. PLEVE, A. A., DEMIN, A. G., KUSH, V., MILLER, M. B., DANILOV, N. A.: Yad. Fiz. 19, 252–258 (1974). Sov. J. Nucl. Phys. 19, 123–126 (1974).
65. KRATZ, J. V., LILJENZIN, J. O., NORRIS, A. E., BINDER, I., SEABORG, G. T., in: ROBINSON, R. L., MCGOWAN,

- F. K., BALL, J. B., HAMILTON, J. H. (Ed.), Proc. Int. Conf. on Reactions between Complex Nuclei, Nashville 1974, North-Holland, Amsterdam (1974), vol. 1, p. 88.
66. HULET, E. K., LOUGHEED, R. W., WILD, J. F., LANDRUM, J. H., STEVENSON, P. C., GHIORSO, A., NITSCHKE, J. M., OTTO, R. J., MORRISSEY, D. J., BAISDEN, P. A., GAVIN, B. F., LEE, D., SILVA, R. J., FOWLER, M. M., SEABORG, G. T.: Phys. Rev. Lett. 39, 385–389 (1977).
  67. ILLIGE, J. D., HULET, E. K., NITSCHKE, J. M., DOUGAN, R. J., LOUGHEED, R. W., GHIORSO, A., LANDRUM, J. H.: Phys. Lett. 78B, 209–212 (1978).
  68. GHIORSO, A., NITSCHKE, J. M., NURMIA, M. J., LEBER, R. E., SOMERVILLE, L. P., YASHITA, S.: Lawrence Berkeley Lab. Report LBL 6575 (1977), pp. 242–244.
  69. VANDENBOSCH, R., HUIZENGA, J. R.: *Nuclear Fission*, Academic Press, New York (1973), pp. 233–250.
  70. HILDENBRAND, K. D., FREIESLEBEN, H., PÜHLHOFER, F., SCHNEIDER, W. F. W., BOCK, R., v. HARRACH, D., SPECHT, H. J.: Phys. Rev. Lett. 39, 1065–1068 (1977).
  71. FREIESLEBEN, H., HILDENBRAND, K. D., PÜHLHOFER, F., SCHNEIDER, W. F. W., BOCK, R., v. HARRACH, D., SPECHT, H. J.: Z. Physik A292, 171–189 (1979).
  72. SCHÄDEL, M., KRATZ, J. V., AHRENS, H., BRÜCHLE, W., FRANZ, G., GÄGGELER, H., WARNECKE, I., WIRTH, G., HERRMANN, G., TRAUTMANN, N., WEIS, M.: Phys. Rev. Lett. 41, 469–472 (1978).
  73. RIEDEL, C., NÖRENBERG, W.: Z. Physik A290, 385–391 (1979).
  74. KRATZ, J. V., BRÜCHLE, W., FRANZ, G., SCHÄDEL, M., WARNECKE, I., WIRTH, G., WEIS, M.: Nucl. Phys. A332, 477–500 (1979).
  75. KRATZ, J. V., in: PRADE, H., TESCH, S. (Ed.), Proc. Int. Conf. on Extreme States in Nuclear Systems, Dresden 1980, Report ZfK-430 (1980), Vol. 1, pp. 48–59 and Report GSI 80-1 (1980).
  76. GÄGGELER, H., SCHÄDEL, M., BRÜCHLE, W., KRATZ, J. V., SÜMMERER, K., WIRTH, G., TRAUTMANN, N., PEUSER, P., TITTEL, G., STAKEMANN, R., HERRMANN, G., HULET, E. K., LOUGHEED, R. W., NITSCHKE, J. M., HAHN, R. L., FERGUSON, R. L.: Proc. of the 4th Int. Conf. on Nuclei far from Stability, Helsingør, June 1981, CERN 81-09 (1981), pp. 763–771.
  77. GÄGGELER, H., TRAUTMANN, N., BRÜCHLE, W., HERRMANN, G., KRATZ, J. V., PEUSER, P., SCHÄDEL, M., TITTEL, G., WIRTH, G., AHRENS, H., FOLGER, H., FRANZ, G., SÜMMERER, K., ZENDEL, M.: Phys. Rev. Lett. 45, 1824–1827 (1980).
  78. HERRMANN, G.: Pure Appl. Chem. 53, 949–964 (1981).
  79. JUNGCLAS, H., HIRDES, D., BRANDT, R., LEMMERTZ, P., GEORG, E., WOLLNIK, H.: Phys. Lett. 79B, 58–60 (1978) and HIRDES, D., JUNGCLAS, H., BRANDT, R., LEMMERTZ, P., FASS, R., WOLLNIK, H.: GSI Ann. Rep. 1978, GSI 79-11 (1979), p. 71.
  80. HULET, E. K., LOUGHEED, R. W., NITSCHKE, J. M., HAHN, R. L., FERGUSON, R. L., BRÜCHLE, W., GÄGGELER, H., KRATZ, J. V., SCHÄDEL, M., WIRTH, G., HERRMANN, G., TITTEL, G., TRAUTMANN, N.: Pure Appl. Chem. 53, 965–972 (1981).
  81. SCHÄDEL, M., BRÜCHLE, W., GÄGGELER, H., KRATZ, J. V., SÜMMERER, K., WIRTH, G., GREULICH, N., HICKMANN, U., PEUSER, P., TRAUTMANN, N., HERRMANN, G., NITSCHKE, J. M., HULET, E. K., LOUGHEED, R. W.: unpublished results (1981).
  82. DEUBLER, H. H., DIETRICH, K.: Phys. Lett. 62B, 369–373 (1976) and DEUBLER, H. H., LEKKAS, K., SPERR, P., DIETRICH, K.: Z. Physik A284, 237–244 (1978).
  83. SPERR, P., WAGNER, W., ESSEL, H., HARTEL, K., HENNING, W., KIENLE, P., KÖRNER, H. J., REHM, K. E., WEBER, J.: Z. Physik A287, 57–60 (1978).
  84. LUND, T., HIRDES, D., JUNGCLAS, H., MOLZAHN, D., VATER, P., BRANDT, R., LEMMERTZ, P., FASS, R., WOLLNIK, H., GÄGGELER, H.: Z. Physik A303, 115–121 (1981).
  85. LUCAS, R., POITOU, J., KRATZ, J. V., WIRTH, G.: Z. Physik A290, 327–334 (1979).
  86. GLÄSSEL, P., v. HARRACH, D., MÄNNER, R., SPECHT, H. J., WILHELMI, J. B., FREIESLEBEN, H., HILDENBRAND, K. D.: Phys. Rev. Lett. 43, 1483–1486 (1979).
  87. BIRKELUND, J. R., TUBBS, L. E., HUIZENGA, J. R., DE, J. N., SPERBER, D.: Phys. Rep. 56, 107–166 (1979).
  88. STOKSTAD, R. G., EISEN, Y., KAPLANIS, S., PELTE, D., SMILANSKY, U., TSERRUYA, I.: Phys. Rev. Lett. 47, 465–469 (1978).
  89. STOKSTAD, R. G., REISDORF, W., HILDENBRAND, K., KRATZ, J. V., WIRTH, G., LUCAS, R., POITOU, J.: Z. Physik A295, 269–286 (1980).
  90. SIKORA, B., BISPLINGHOFF, J., SCOBEL, W., BECKERMAN, M., BLANN, M.: Phys. Rev. C20, 2219–2226 (1979).
  91. REISDORF, W., HESSBERGER, F., HILDENBRAND, K. D., HOFMANN, S., KRATZ, J. V., MÜNZENBERG, G., SCHMIDT, K. H., SCHNEIDER, W. F. W., SÜMMERER, K., WIRTH, G.: Scientific Report 1980, GSI 81-2 (1981), p. 2.
  92. REISDORF, W., HESSBERGER, F., HILDENBRAND, K. D., HOFMANN, S., KRATZ, J. V., MÜNZENBERG, G., SCHMIDT, K. H., SCHNEIDER, W. F. W., SÜMMERER, K., WIRTH, G.: Unpublished results (1982).
  93. ARMBRUSTER, P., QUADE, U., RUDOLPH, K., CLERC, H.-G., MUTTERER, M., PANNICKE, J., SCHMITT, C., THEOBALD, J. P., ENGELHARDT, W., GÖNNEWINE, F., SCHRADER, H.: Proc. of the 4th Int. Conf. on Nuclei far from Stability, Helsingør, June 1981, CERN 81-09 (1981), pp. 675–679.
  94. SWIATECKI, W. J.: Phys. Scr. 24, 113–141 (1981) and Nucl. Phys. A376, 275–291 (1982).
  95. SANN, H., BOCK, R., CHU, Y. T., GOBBI, A., OLMI, A., H.: Phys. Rev. Lett. 47, 1248–1251 (1981).
  96. GÄGGELER, H., BRÜCHLE, W., KRATZ, J. V., SCHÄDEL, M., SÜMMERER, K., WIRTH, G., SIKKELAND, T.: Proc. Int. Workshop X on Gross Properties of Nuclei and Nuclear Excitations, Hirschegg, Austria, January 18–22, 1982.
  97. GÄGGELER, H., ILJINOV, A. S., POPEKO, G. S., SEIDEL, W., TER-AKOPYAN, G. M., TRETYAKOVA, S. P.: Z. Physik A289, 415–420 (1979).
  98. MÜNZENBERG, G., HOFMANN, S., HESSBERGER, F. P., REISDORF, W., SCHMIDT, K.-H., FAUST, W., ARMBRUSTER, P., GÜTTNER, K., THUMA, B., VERMEULEN, D., SAHM, C. C.: Proc. 4th Int. Conf. on Nuclei far from Stability, Helsingør, June 1981, CERN 81-09 (1981), pp. 755–762.
  99. SCHMIDT, K.-H., ARMBRUSTER, P., HESSBERGER, F. P., MÜNZENBERG, G., REISDORF, W., SAHM, C. C., VERMEULEN, D., CLERC, H.-G., KELLER, J., SCHULTE, H.: Z. Physik A301, 21–28 (1981).
  100. SAHM, C. C., CLERC, H.-G., VERMEULEN, D., SCHMIDT, K.-H., ARMBRUSTER, P., HESSBERGER, F. P., MÜNZENBERG, G., KELLER, J. G., REISDORF, W.: Proc. Int. Workshop X on Gross Properties of Nuclei and Nuclear Excitations, Hirschegg, Austria, January 18–22, 1982.
  101. CLERC, H.-J.: Contribution to the Int. Sympos. on Nuclear Fission and Related Collective Phenomena and Properties of Heavy Nuclei, Bad Honnef, October 1981, and KELLER, J. G., CLERC, H.-J., VERMEULEN, D., SCHMIDT, K.-H.: The Influence of Shell Effects on the Survival Probability of Heavy Nuclei Produced in Fusion Reactions, Report IKDA 81-7 (1981).
  102. SCHMIDT, K.-H., FAUST, W., MÜNZENBERG, G., REISDORF, W., CLERC, H.-G., VERMEULEN, D., LANG, W.: Proc. Int. Sympos. on Physics and Chemistry of Fission, Jülich 1979, I.A.E.A. Vienna (1979), Vol. 1, pp. 409–419.
  103. GHIORSO, A.: In EDELSTEIN, N. M. (Ed.), Actinides in Perspective, Pergamon Press, New York (1982), pp. 23–56.
  104. DAHLINGER, M., VERMEULEN, D., SCHMIDT, K.-H.: Nucl. Phys. A376, 94–130 (1982).
  105. MYERS, W. D.: Droplet Model of Atomic Nuclei, Plenum, New York 1977.
  106. SCHÄDEL, M., BRÜCHLE, W., GÄGGELER, H., KRATZ, J. V., SÜMMERER, K., WIRTH, G., HERRMANN, G., STAKEMANN, R., TITTEL, G., TRAUTMANN, N., NITSCHKE, J. M., HULET, E. K., LOUGHEED, R. W., HAHN, R. L., FERGUSON, R. L.: Phys. Rev. Lett. 48, 852–855 (1982).
  107. SIKKELAND, T., GHIORSO, A., NURMIA, M. J.: Phys. Rev. 172, 1232–1238 (1968).



## Solution Chemistry of the Actinides

By GREGORY R. CHOPPIN, Department of Chemistry, Florida State University, Tallahassee, Florida 32306, U.S.A.

(Received June 21, 1982)

*Actinide elements / Actinide complexation / Actinide hydration / Actinide kinetics / Actinide radii*

### Abstract

The redox and complexation behavior of the actinide ions in aqueous solution is reviewed. An equation is offered to calculate the ionic radii of actinide cations in different oxidation states and coordination numbers. The models for hydration are reviewed with emphasis on one involving long range ordering of a solvent sheath. Some selected values for hydrolysis constants reflect the problems of studying actinide ions in near-neutral or basic solutions.

A simple modified BORN equation is shown to provide values of the complexation constants in very good agreement with experimental values. Interpretation of the entropy and enthalpy changes for complexation is discussed in terms of a model of desolvation plus cation-anion combination. Some general observations on redox and complexation kinetics are offered to indicate possible directions for further studies.

### I. Introduction

Since the earliest days of the Manhattan Project, much of the interest in the solution chemistry of the actinide elements has been directly associated with the separation science of these elements. Whether dealing with a few kilograms of plutonium or a few atoms of mendelevium, the primary motive in most studies of actinide solutions was the isolation and purification of these elements rather than expansion of our knowledge about their fundamental chemical behavior. International interest in nuclear fuel reprocessing methods, which typically involves acid solutions, is a continuing motivation for actinide research. Lately, studies of actinide behavior in neutral and basic solutions have attempted to provide answers on the fate of these elements in potential nuclear waste disposal sites and in the environment. Even beyond these applied concerns, the actinides have a richly diverse chemistry in solution which provides sufficient justification to the solution chemist for their continuing study. In this review, the focus is on the fundamental aspects of actinide solution chemistry; if well understood, these can serve as the basis for direction of the studies of a more applied nature.

### II. Oxidation states in solution

The actinide ions exhibit an unusually broad range of oxidation states in aqueous solution – from II to VII. Following the normal pattern for polyvalent cations, lower oxidation states are stabilized by more acidic conditions while high oxidation states are more stable in basic solutions. Of course, this generalization can be negated by other factors, such as complexing, and these trends in the relative stability of different oxidation states can be reversed. For example, the greater strength of complexing of M(IV) cations relative to that of M(III) can significant-

ly increase the apparent redox stability of the M(VI) species compared to M(III). Pu(III) is stable to air and water in acid solutions but in the presence of acetate or EDTA (pH 3.5), it partially oxidizes to Pu(IV) [1]. Similarly, the greater tendency to hydrolysis of Pu(IV) causes Pu(III) in aqueous solution to be oxidized to Pu(IV) in neutral media [ $E^0$  (III)  $\rightarrow$  (IV) =  $-0.98$  v in 1 M HClO<sub>4</sub> vs.  $+0.63$  v at pH 7] [2]. Methods of preparation of the different oxidation states have been discussed recently by AHRLAND *et al.* [3] and MYASOEDOV [4].

Disproportionation reactions, leading to several oxidation states simultaneously in solution is a significant aspect of actinide chemistry, particularly for some IV and V species. Such reactions have been discussed also in ref. [3, 4, and 5]. In the following section, the various oxidation states found in aqueous solution for the different actinides are briefly reviewed.

#### M(I)

The existence of Md(I) has been reported by MIKHEEV and coworkers [6] but studies by other groups [7] have failed to provide confirmation.

#### M(II)

Both Md(II) and No(II) form readily in aqueous solution and No(II) is the most stable species of that element. Cf(II), Es(II) and Fm(II) have been shown to have much lower stability than the III state [4]. Am(II), Cm(II) and Cf(II) were produced in acid solution for periods of 10–100 msec by pulse radiolysis [8, 9].

#### M(III)

This is the most stable oxidation state in aqueous solutions for the actinides Am-Md and Lw. However, as noted previously, other states can be made predominant in basic or in strongly complexing solutions. Pu(III) and Np(III) are rather easily obtained although U(III) is such a strong reducing agent that it is difficult to maintain in solution.

#### M(IV)

Th(IV) is the common and stable state for that element. Pa(IV), U(IV) and Np(IV) do not react with water but are oxidized by O<sub>2</sub>. Pu(IV) is stable only in concentrated acids and at low concentrations of Pu(IV). The IV state of Am, Cm, Bk and Cf can be produced in alkaline solutions by persulfate oxidation. The presence of potassium phosphotungstate, K<sub>10</sub>P<sub>2</sub>W<sub>17</sub>O<sub>61</sub>, stabilizes these species by complexation [4]. Am(IV) and Bk(IV) are relatively stable and can be produced by a variety of oxidation techniques. Am(IV), Cm(IV) and Cf(IV) have also been produced in aqueous solution by pulse radiolysis.

**M(V)**

The  $\text{MO}_2^+$  ion can be formed in solution by the actinides Pa through Am. This is the most stable state for Pa although it is uncertain whether the better formulation of the aqueous species is  $\text{PaO}_2^+$  or  $\text{PaO}(\text{OH})_2^+$  [10].  $\text{NpO}_2^+$  is stable except at high acidities and high concentrations under which conditions it disproportionates.  $\text{UO}_2^+$  and  $\text{PuO}_2^+$  increase in stability as the pH is increased but have a strong tendency to disproportionate.  $\text{AmO}_2^+$  is a strong oxidant; it also disproportionates in highly acid solutions. There is evidence that  $\text{PuO}_2^+$  may be the predominant plutonium species in solution in natural waters [11].

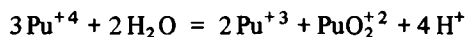
**M(VI)**

U, Np, Pu and Am form  $\text{MO}_2^{+2}$  ions in solution with the stability decreasing in the order  $\text{U} > \text{Pu} > \text{Np} > \text{Am}$ .  $\text{UO}_2^{+2}$  is the most stable uranium species while  $\text{AmO}_2^{+2}$  is a strong oxidizing agent although it can be formed quantitatively in basic solutions of phosphotungstates.

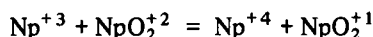
**M(VII)**

In acid solutions, Np(VII) and Pu(VII) are reduced rapidly by water but the reduction is considerably slower in basic solution. Am(VII) is reported to form but is so unstable even in alkaline solution that it oxidizes Np(VI) and Pu(VI) to their VII state in 1–2 M NaOH [12]. However, research at Argonne and Los Alamos have failed to produce Am(VII) under the conditions reported earlier [12]. The M(VII) species seems to be trinegative, corresponding most simply to  $\text{MO}_3^-$  but the more likely correct formulation is  $\text{MO}_2(\text{OH})_6^{3-}$  [14].

The rates of the disproportionation reactions as well as the rates of many of the redox reactions of the actinides can be markedly influenced by the chemical nature of the reactants and the products. For example, the reduction of M(VI) to M(IV) requires extensive rearrangement of the primary coordination sphere of  $\text{MO}_2^{+2}$  (i. e. change of the linear dioxo structure) prior to electron transfer. This results in an activation barrier such that a disproportionation reaction such as

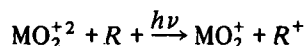


requires about 200 hours in 0.5 M HCl to attain equilibrium. By contrast, the reaction:



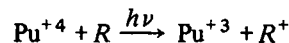
is very fast, presumably because it occurs via rapid electron exchange in two half reactions:  $\text{Np}^{+3} \rightarrow \text{Np}^{+4}$  and  $\text{NpO}_2^{+2} \rightarrow \text{NpO}_2^{+1}$ .

Photochemically induced redox reactions of U, Np and Pu were reviewed recently by TOTH *et al.* [15]. For U(VI) and Pu(VI) the general reaction:



has been found to take place when R is an alcohol, an aldehyde, hydrazine or hydroxylamine. The  $\text{MO}_2^+$  species disproportionates to  $\text{M}^{+4}$  and  $\text{MO}_2^{+2}$  with a rate which is dependent on acidity and  $\text{MO}_2^+$  concentration. The quan-

tum efficiency in 1 M acid with  $\text{C}_2\text{H}_5\text{OH}$  present is 50 times greater for  $\text{UO}_2^{+2}$  (250–600 nm) than for  $\text{PuO}_2^{+2}$  (< 350 nm). Direct photochemical reduction occurs in this same system:



Neptunium in the III, IV and V states is oxidized in sequential one electron transfer reactions to Np(VI) by absorption of 300 nm radiation in perchloric acid solutions. However, photochemical reduction can occur also in acid solutions when ethanol is present whereby Np(VI) is reduced in steps to Np(III). In  $\text{HNO}_3$  solutions, these photochemical redox reactions are complicated by the photolytic reduction of  $\text{NO}_3^-$ . As a result, Np(VI) and Np(IV) solutions can be converted completely to Np(V). The redox photochemistry of the actinides would seem to be a promising research field for both basic and applied interest.

Fig. 1 gives the oxidation potentials for U, Np and Pu at pH 0 [3] and, as estimated by ALLARD *et al.* [16], at pH 8 and 14.

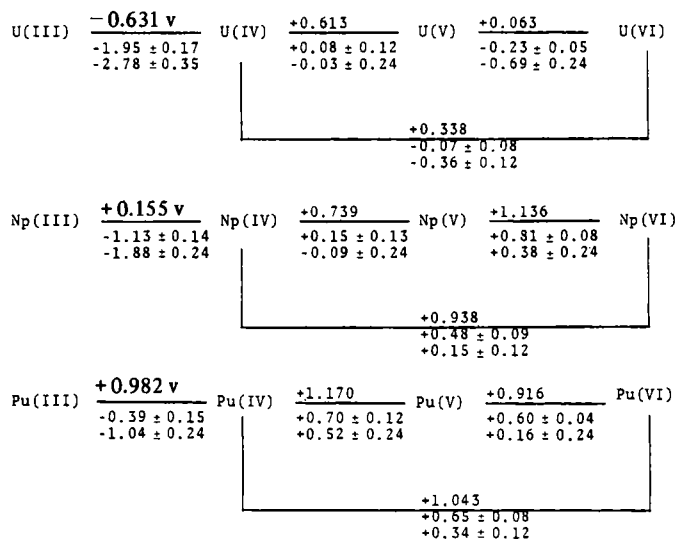


Fig. 1. Redox potential diagram for U, Np and Pu. The reduction potentials as listed are for the pH values: pH = 0; pH = 8; pH = 14.

**III. Coordination number and radii**

The actinide cations are "hard acids" — that is, their bonding in complexes is rather well described by an electrostatic model and they show strong preference for oxygen donor atoms. There is evidence for some greater degree of covalency in actinide-ligand bonds than in analogous lanthanide-ligand bonds, but, for both groups of metals, the ionic character of the bonding is predominant. This is true for the metal-oxygen and metal-nitrogen donor bonds prevalent in complexes in aqueous solution [17] as well as for the metal-carbon bonds in organometallic compounds [18].

As a result of the ionic nature of the bonding, actinide cations do not display the restricted stereochemistry typical of the d transition elements. The coordination number and

the geometry of the coordination sphere in the d elements are strongly influenced by the overlap of the metal and ligand orbitals. By contrast, in the ionic interactions of actinide complexes, the number and arrangement of the ligands are determined primarily by steric and electrostatic factors. This leads to a range of coordination numbers from 6 to 12 observed for complexes with simple actinide cations while for the oxygenated cations, such as  $\text{UO}_2^{+2}$ , coordination numbers of 2 to 8 are reported.

Little direct evidence can be found on the coordination number of actinides in aqueous solutions. However, coordination numbers of 8 and 9 are the most likely for trivalent lanthanide systems [17], and it is reasonable that this is also true for trivalent actinides. Even in polydentate complexes such as  $\text{AmEDTA}_{(\text{aq})}^{-1}$ , the coordination sphere of the actinide cation probably includes 3 or 4 water molecules. For tetravalent species, the smaller cation size may result in smaller values – 7 and 8.

Directly tied to the question of coordination number is that of the proper radius to assign the actinide cations. Solid state structural determinations have been concerned, for the most part, with CN = 6 compounds, although other systems such as Th(IV) of CN = 6–12 and U(VI) of CN = 2, 4, 6–8 have been studied. SHANNON [19] has published the most comprehensive list of such data and used them to calculate the “effective ionic radii” which include consideration of coordination number, electronic spin, covalency, repulsive forces and polyhedral distortion. These radii are assumed to be independent of the coordination sphere symmetry and are directly additive (to the donor atom radius) for ionic bonds. The values of the effective radii of SHANNON for CN = 6 are listed in Table 1.

Table 1. *Effective ionic radii*  
Coordination number = 6

Actinide	Oxidation state			
	III	IV	V	VI
Th	–	0.94	–	–
Pa	1.04	0.90	0.78	–
U	1.025	0.89	0.76	0.73
Np	1.01	0.87	0.75	0.72
Pu	1.00	0.86	0.74	0.71
Am	0.975	0.85	–	–
Cm	0.97	0.85	–	–
Bk	0.96	0.83	–	–
Cf	0.95	0.82	–	–

These CN = 6 radii,  $r_6$ , can be converted to radii for other coordination numbers,  $r_i$ , by using the following relationships:

$$r_4 = r_6 - 0.21$$

$$r_7 = r_6 + 0.06$$

$$r_8 = r_6 + 0.12$$

$$r_9 = r_6 + 0.17$$

$$r_{10} = r_6 + 0.22$$

$$r_{12} = r_6 + 0.27$$

Comparison of the radii derived by SHANNON with those calculated by these equations show that  $r_4$ ,  $r_7$ , and  $r_8$  agree to  $\pm 0.01$  Å while  $r_9$ ,  $r_{10}$  and  $r_{12}$  to  $\pm 0.02$  Å.

#### IV. Hydration and hydrolysis

Several authors have proposed hydration numbers for trivalent actinides. LEBEDEV [20] estimated values of  $S_{\text{aq}}^0$  for the An(III) ions, obtaining values in reasonable agreement with those reported by FUGER and OETTING from a critical evaluation of the literature values [21]. The values were used to obtain an estimate of the hydration number of  $7.0 \pm 0.1$ . GOLDMAN and MORSS [22] reported a value of 5.1 from a semiempirical calculation based on an electrostatic hydration model. Experimental measurements of the ionic migration velocities in an electric potential gradient were used with STOKES' Law equation [23] to calculate values from 13.6 (Am) to 16.9 (Fm). These values agree with the net hydration numbers (first + second sphere) of trivalent lanthanide cations obtained by various techniques [24]. These numbers are related to a first sphere hydration of 8 to 10 [25, 26] for the trivalent cations.

The values of the hydration numbers in the preceding paragraph are based on calculations which assume that the experimental data are related to a cation species with a definite, small number of waters attached in one (or, at most, two) layers. An alternate model of hydration is based on the orienting effect of the cation on a larger volume of water molecules. The structuring imposed by this cationic orientation competes with that of the normal 3-dimensional hydrogen-bonded order of water [27] to produce a net hydration effect.

Support for a model of this longer range cationic ordering effect has been offered for trivalent lanthanides based on the crystal field splitting of  $\text{Gd(III)}_{\text{aq}}$  [28]. These splittings are attributed to second order crystal field operators whose coefficients converge slowly with distance. The conclusion is that the hydration effect on the water structure extends over a volume as large as 50 Å around each cation. Moreover, the symmetry at the rare earth cation site is very low and  $C_{2v}$  at maximum.

Further support for a model of a long range, more general structuring effect in hydration of cations is found in Fig. 2. The correlation of  $S_{\text{aq}}^0$  with the ionic charge density is consistent with a regularly increasing hydration structuring as the cationic orienting effect, proportional to  $Z^2/r$ , increases. Such a model is not inconsistent with data such as the cationic electromigration velocities but is not consistent with interpretation of such data in terms of definite “hydration numbers”.

If the model of large hydrate “icebergs” is accepted, the correlation in Fig. 2 suggests that the tetravalent actinides have even larger solvated structures – perhaps twice as large as the trivalent cations. Also, for  $\text{MO}_2^{+2}$  species, Fig. 2 suggests that the hydration structure is smaller than for the M(III) species and the low charge

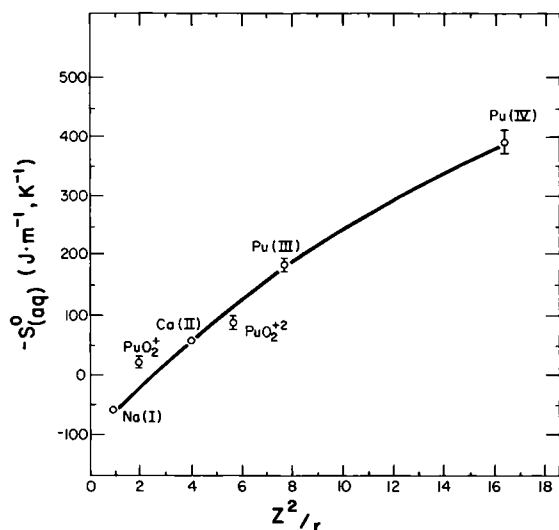
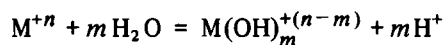


Fig. 2. The correlation between  $-S_{aq}^0$  and  $Z^2/r$ ; for the radius,  $r$ , the C.N. = 6 values are used for Na(I), Ca(II) and  $\text{PuO}_2^{+2}$ , that of C.N. = 8 for Pu(IV), that of C.N. = 9 for Pu(III) and that of C.N. = 4 for  $\text{PuO}_2^{+1}$ .

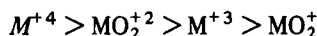
density of  $\text{MO}_2^{+1}$  cations has relatively little structuring effect on the solvent.

The importance of the extensive hydration of the III, IV and VI species is seen in the values of the thermodynamic parameters of complexation reactions. For many complexation reactions, the entropy and enthalpy changes are both positive, but since  $|\Delta S| > |\Delta H|$  in most cases, the result is a favorable (negative) free energy change. The positive values for  $\Delta S$  and  $\Delta H$  are interpreted to be a result of the dehydration which accompanies complexation. Thus, the thermodynamic driving force for many actinide complexation reactions is the increased entropy resulting from the disruption of the hydrate structure associated with the metal cation when it interacts with a ligand [17, 29]. These thermodynamic parameters are discussed more extensively in a later section.

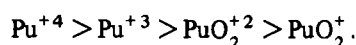
A significant aspect of actinide hydration is the importance, as the pH increases, of hydrolysis reactions such as:



The strength of hydrolysis follows the pattern:



which differs from that in Fig. 2 for the hydration entropies, i.e.,



The hydrate entropies are related simply to the net positive charge on the cationic species. However, the hydrolysis reaction is the result of interaction of a water molecule with the metal atom itself — i.e., Pu in  $\text{PuO}_2^{+2}$ . The hydrolysis order indicates that the charge on Pu in  $\text{PuO}_2^{+2}$  is actually between +3 and +4 and probably about +3.3.

The variation of the concentration of free (non-hydrolyzed) cation with pH is shown for plutonium in Fig. 3. These curves are based on estimated values of the hydrolysis constants [16] but are of sufficient accuracy to indicate the pH values at which hydrolysis becomes significant (e.g.,  $\sim 6-8$  for  $\text{Pu}^{+3}$ ,  $< 0$  for  $\text{Pu}^{+4}$ ,  $9-10$  for  $\text{PuO}_2^+$  and  $4-5$  for  $\text{PuO}_2^{+2}$ ).

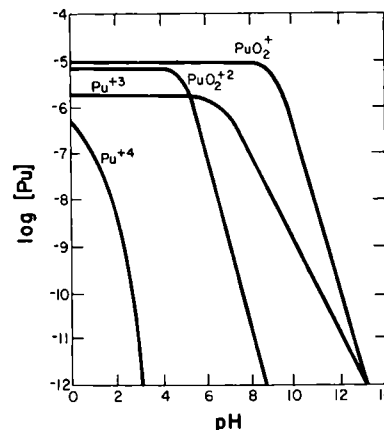


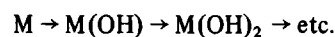
Fig. 3. The effect of hydrolysis, as a function of pH, on the concentration of hydrated Pu cationic species. The initial ( $\log [\text{Pu}]$  at  $\text{pH} = 0$ ) concentrations are those at  $\text{pH} \geq 8$  which correspond to the  $K_{sp}$  values of the hydroxide precipitate of each species.

Hydrolysis constants of the actinides reported by different authors are rarely in agreement. Some values which seem to be the most reliable are listed in Table 2. SULLIVAN and coworkers [30] used a technique involving pulse radiolysis + transient conductivity to obtain their data in Table 2 while the M(III) values were measured by a solvent extraction technique which minimizes the experimental problems encountered in hydrolysis studies [31]. Other estimated and experimental values can be found in ref. [3, 16, 32 and 33].

Table 2. Hydrolysis constants  
 $\text{An} + \text{H}_2\text{O} = \text{An}(\text{OH}) + \text{H}; K_i$

An	pK <sub>i</sub>	Concentration of An	Ref.
$\text{UO}_2^{+2}$	$5.2 \pm 0.1$	$2-5 \times 10^{-4}$ M (I = 0)	30
$\text{NpO}_2^{+2}$	$5.4 \pm 0.1$	$2-5 \times 10^{-4}$ M (I = 0)	30
$\text{PuO}_2^{+2}$	$6.3 \pm 0.1$	$2-5 \times 10^{-4}$ M (I = 0)	30
$\text{NpO}_2^+$	8.75	$5 \times 10^{-4}$ M (I = 0)	30
$\text{Np}^{+4}$	$2.3 \pm 0.1$	$2 \times 10^{-3}$ M (I = 2.0 M)	32
$\text{NpOH}^{+3}$	4.5	$2-5 \times 10^{-4}$ M (I = 0)	30
$\text{Am}^{+3}$	$7.84 \pm 0.05$	Tracer (I = 0.7 M)	31

The hydrolysis of  $\text{M}^{+4}$  and  $\text{MO}_2^{+2}$  species follows a stepwise pattern



However, the  $\text{M}^{+4}$  and  $\text{MO}_2^{+2}$  species are reported also to form oligomers (i.e.,  $[\text{M}(\text{OH})_i]_n$ ). The competition be-

tween monomer and oligomer is dependent on the actinide concentration. For example, using the hydrolysis values of ref. [16], at pH 5 and  $(\text{UO}_2)_{\text{Total}} \sim 0.05 \text{ M}$ , the ratio of U in  $(\text{UO}_2)_2(\text{OH})_2^{+2}$  to that in  $\text{UO}_2(\text{OH})^{+1}$  is ca. 4 while at pH 5 and  $(\text{UO}_2)_{\text{Total}} \sim 10^{-8} \text{ M}$ , the ratio is ca. 0.004.

The hydrolysis of  $\text{Pu}^{+4}$  can result in the formation of polymers which are rather intractable to reversal to simpler species. As a result of this irreversible polymerization, the validity of  $K_{sp}$  values for  $\text{Pu}(\text{OH})_{4(s)}$  should be questioned. For  $[\text{Pu}(\text{IV})]_{\text{T}} > 10^{-6} \text{ M}$ , hydrolytic polymers of a wide range of molecular weights can be formed even in moderately acid solutions. Initially, such polymers can be readily decomposed to simple species in solution by acidification or by oxidation to Pu(VI). However, as the polymers age, the decomposition process requires increasingly rigorous treatment. The rate of such irreversible aging varies with temperature, Pu(IV) concentration, the nature of the anions present in solution, etc. A reasonable model would involve initial formation of aggregates with hydroxy bridging (Fig. 4a) which age to structures with oxygen bridging (4b). The relative percentage of oxygen bridges presumably determines the relative inertness of the polymer. These polymers are sorbed on vessel walls, ion exchange resins, etc. Their depolymerization depends on the conditions of formation as well as on their age and is best accomplished for aged solutions by treatment first with a strong oxidant [to form Pu(VI)] followed by a strong reductant [to form Pu(III)].

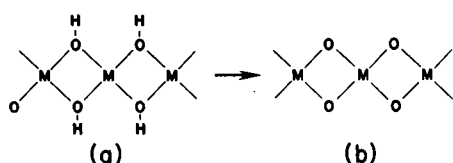


Fig. 4. Possible model for the 'irreversible' aging of hydrolyzed polymers wherein hydroxy bridges (a) are replaced by oxo bridges (b).

## V. Complexation

The limitations on this review present any attempt to survey in depth the rather extensive literature on complexation reactions of the actinides. Instead, the general principles involved in the formation of actinide complexes are discussed with consideration of a few ligand systems as examples.

Perhaps the most basic aspect of actinide cations is their "hard acid" property. This means that their bonding to ligands is well described as electrostatic interaction with covalency playing a quite minor role. As hard acids, these cations interact preferentially with hard bases such as oxygen or fluoride atoms rather than softer bases such as nitrogen, sulfur or phosphorous donors. The actinides do interact with these soft bases in organic solvents of low solvating power but, except for nitrogen, do not do so in aqueous solution where the soft base would have to re-

place water, which is a hard base. Interaction of actinide cations with nitrogen donors in aqueous systems usually occurs when one or more oxygen donor sites are also present, as in the aminocarboxylates. In these systems, it is likely that the oxygen donors have produced sufficient desolvation that the nitrogen donor can interact without further displacement of  $\text{H}_2\text{O}$ .

There is strong evidence that the entropy of complexation of actinide cations primarily reflects the desolvation of the cation [34]. Fig. 5 shows the relationship between the measured entropy for Am(III) chelation and the number of carboxylate groups in the ligand. Although the data for Am(III) is limited, the fact that the trend for Am(III) parallels that of the more extensive data for Sm(III) supports the same interpretation for both, i.e., the same degree of dehydration of the cation by each of the carboxylate groups of the ligands. The nitrogen in the aminocarboxylate ligands seems to play no role in the  $\Delta S$  value [35]. However, the enthalpy values show no such correlation for the aminocarboxylate complexation and are more exothermic than expected from carboxylate complexation alone, indicating the effect of actinide-nitrogen interaction. Further evidence for Ln-N bonding in aminocarboxylate complexes is provided by NMR spectra [36] which, by implication, also argues for An-N bonding in actinide complexes.

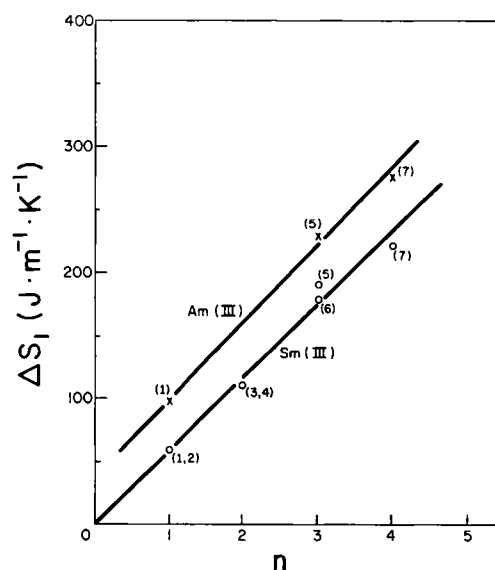
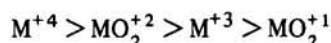


Fig. 5. The correlation of  $\Delta S$ , the entropy of complexation [35], and  $n$ , the number of carboxylate groups in the ligand:  $\circ$  = Sm(III);  $\times$  = Am(III); 1 = acetate; 2 =  $\alpha$ -picolinate; 3 = malonate; 4 = diphosphate; 5 = NTA; 6 = HEDTA; 7 = EDTA.

While optical spectroscopy and magnetic measurements have been of great value in the study of transition metal complexes, they are much more limited tools for the actinides since the  $f \rightarrow f$  transitions are much less sensitive to the effect of complexation. There is a class of spectral bands — the "hypersensitive bands" — which do show more significant perturbations upon complexation and some use has been made of these spectral transitions [37, 38, 39].

The radioactive nature of the transuranium elements places limitations on the techniques which can be used to study complexation in solution since the radiolysis accompanying macroscopic concentrations of the cations can perturb seriously the measurements. Consequently, many complexation studies have used tracer concentrations with a two-phase distribution technique such as ion-exchange or solvent extraction.

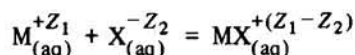
In studies where different oxidation states of an actinide have been complexed by the same ligand, the sequence of complexing strength most commonly observed is that discussed for the hydrolysis reactions; i.e.:



The sequence  $M^{+4} > M^{+3}$  is expected from the ionic nature of the  $M^{+n} \cdots X^{m-}$  interaction which should increase with  $n$  for constant  $m$ . The observation that the complexing strength of the  $MO_2^{+2}$  cations is greater than the  $M^{+3}$  cations can be understood by assuming that the central metal atom,  $M$ , in the linear  $[O-M-O]^{+2}$  cation has an effective charge that is greater than +3. It is this effective charge that determines the strength of complexing since the ligand binds in the equatorial positions about the linear  $MO_2^{+2}$ . WADT [40] recently analyzed  $UO_2^{+2}$  by the relativistic core potential method and obtained a value of +2.4 for the atomic charge on the uranium. However, the effective charge in the equatorial plane would be expected to exceed this value and an estimate of an effective charge of +3.3 ( $\pm 0.1$ ) was obtained from analysis of complexation by  $F^-$  anions [41]. Similar evaluation of the stability constants for  $NpO_2F$  and  $NpO_2SO_4^{-1}$  lead to an estimated effective charge on the Np atom in the linear  $NpO_2^+$  species of  $2.3 \pm 0.2$ .

### The free energy

The ionic nature of actinide complexes is supported by the correlation between the experimental free energy of complexation and that calculated by an equation which is based on electrostatic interaction between cation and anion. MUNZE [42] proposed the use of a modified BORN equation which included a temperature dependent dielectric constant. In our laboratory we use this equation but with an empirical dielectric constant which is dependent only on the cationic charge. For the complexation reaction:



the equation has the form ( $\Delta G$  in  $\text{kJ} \cdot \text{m}^{-1}$ ):

$$\Delta G = -\frac{(1.387 \times 10^3) Z_1 Z_2}{D_e d_{12}} - RT \nu \ln 55.5 + RT \Sigma \ln f \quad (1)$$

$$\begin{aligned} D_e &= \text{effective dielectric constant} \\ Z_1, -Z_2 &= \text{ionic charges of cation and anion} \\ \nu &= -1 \end{aligned}$$

$d_{12}$  = internuclear distance in the ion pair  $M-X$  in  $\text{\AA}$  ( $= r_1 + r_2$ )

$$\Sigma \ln f = \frac{-\Delta Z^2 0.511 I^{1/2}}{1 + Ba I^{1/2}} - Cl^{1/2} - DI$$

$$\Delta Z^2 = Z_{MX}^2 - (Z_1^2 + Z_2^2)$$

$$B = 0.33, C = 0.75, D = -0.015, a = 4.3$$

The second term ( $RT \nu \ln 55.5$ ) accounts for the effect of two species reducing to one ('cratic effect') and the final term corrects for the ionic strength of the solution. The correlation of experimental values with the calculation of  $-\Delta G_1$  by equation 1 for fluoride complexation ( $Z_2 = 1.0$ ) is shown in Fig. 6 [41] where  $D_e = 80$  for  $M^{+2}$  cations, 57 for  $M^{+3}$  and 41 for  $M^{+4}$ .

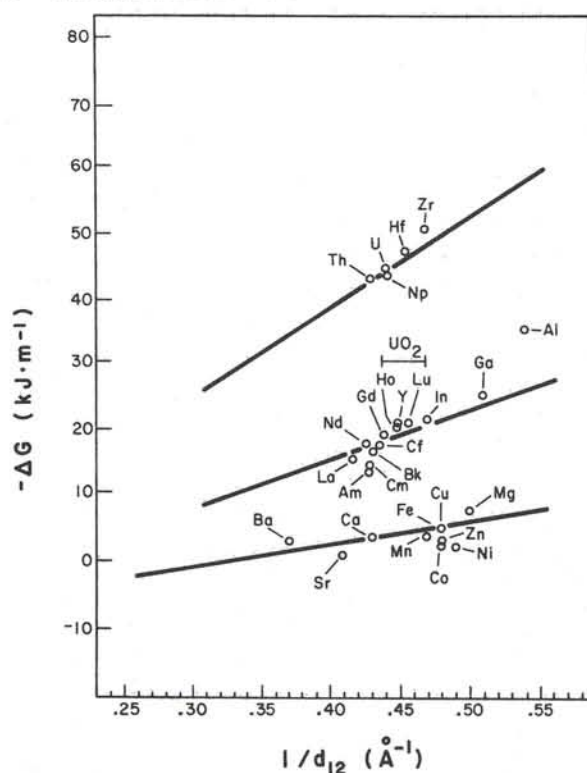


Fig. 6. The correlation of experimental values of  $-\Delta G$  for formation of  $MF$  complexes with the values calculated by equation (1). The solid lines show the calculated values as a function of  $1/d_{12}$  (ref. [41]).

Equation 1 has been found to be useful also for calculation of the free energy of complexation by organic ligands. In these systems, the value of  $Z_2$  is set proportional to the acid constant of the donor sites (or to  $\Sigma pK_{a_n}$  for polydentate ligands). Fig. 7 is the relation between  $Z_2$  and  $\Sigma pK_{a_n}$  which we obtained by using equation (1) with experimental free energies of protonation, holding all values constant except  $Z_2$ . These values of  $Z_2$ , in turn, were used with equation (1) to estimate the  $\Delta G_1$  of complexation of Am(III) and Np(IV) by aminocarboxylate ligands, of Am(III) and Th(IV) by acetate and of Th(IV) by malonate. The comparison of experimental and cal-



Denoting step (1) as  $d$  (= dehydration) and step (2) as  $c$  (= complexation), we can write:

$$-\Delta G = -\Delta G^d - \Delta G^c = -\Delta H^d - \Delta H^c + T\Delta S^d + T\Delta S^c$$

The compensation effect assumes  $-\Delta G^d \approx 0$  (since all the hydrated systems remain in equilibrium with bulk solvent [44]), thus

$$\Delta H^d \approx T\Delta S^d$$

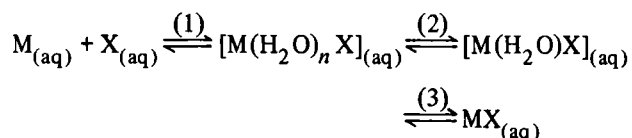
Moreover, since  $\Delta H$  and  $\Delta S$  are positive for most complexation reactions,

$$|\Delta H^d| > |\Delta H^c| \text{ and } |\Delta S^d| > |\Delta S^c|.$$

This leads to the interesting situation in which the entropy and enthalpy changes are reflective primarily of step (1), (the dehydration), while  $\Delta G$  is related almost completely to step (2), (the complexation). This model also explains why eq. (1) is so successful even though it seemingly ignores the dehydration part of the reaction.

#### Inner vs. outer sphere formation

EIGEN [45] has proposed that the formation of complexes proceeds sequentially as:



The first step is diffusion controlled while the second represents the formation of an "outer sphere" complex in which the metal ion and the ligand are separated by at least one molecule of water. In the final step, this outer sphere complex ejects the water and forms an "inner sphere" complex in which the metal and ligand are directly associated. Some ligands cannot displace the water and complexation apparently terminates with the formation of the outer sphere complex. Actinide cations form both inner and outer sphere complexes.

For the labile actinide complexes, it is often quite difficult to distinguish between inner and outer sphere complexes. This situation is complicated further by the fact that formation constants for some of these complexes when determined by optical spectrometry are often lower than those of the same system determined by other means such as potentiometry, solvent extraction, etc. This has led some authors to identify the former as "inner sphere" constants and the latter as "total" constants. However, others have shown that such assignments cannot be correct [46, 47] even if the optical spectra of the solvated cation and the outer sphere complex are indistinguishable while that of the inner sphere complex is different. In all these techniques, the "total" stability constant should be obtained and, as yet, no explanation can be given for the

different values by different techniques. Based on the previous discussion of the thermodynamic parameters,  $\Delta H$  and  $\Delta S$  values can be used, with caution, to obtain insight into the outer vs. inner nature of actinide complexes. For inner sphere complexation, the hydration sphere is insufficiently disrupted and the net entropy and enthalpy changes are usually positive. This is particularly true for polydentate chelation. In outer sphere complexes, the dehydration sphere appears to be only partially disrupted, since the net enthalpy is exothermic. The corresponding entropy change is also negative due to the ordering of ionic charges without a compensating disordering which could result from extensive disruption of the hydration sphere.

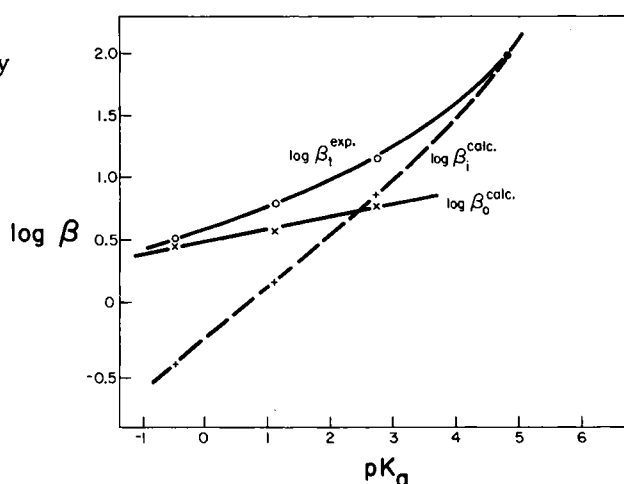


Fig. 10. Relationships between  $\log \beta_{\text{total}}$  (experimental),  $\log \beta_{\text{inner}}$  (calculated) and  $\log \beta_{\text{outer}}$  (calculated) and the  $pK_a$  for the ligands  $Cl_n CH_3-n CO_2^-$  ( $n = 0-3$ ).

These considerations lead, for trivalent actinides, to assignment of a predominant outer sphere character to the halide, nitrate, sulfonate and trichloroacetate complexes and an inner sphere character to the fluoride, iodate, sulfate and acetate complexes. The complexes of  $Cl_n CH_3-n CO_2^-$  ligands were studied by  $^{139}\text{La(III)}$  nmr spectroscopy [48] and the estimated fraction of inner sphere complexation agreed well with that calculated using a value of  $\beta(\text{inner})$  obtained with equation (1). For  $\text{Am(III)}$ , the  $\log \beta_i$  ( $i = \text{inner}$ ) calculated by eq. (1) allowed estimation of  $\log \beta_o$  ( $o = \text{outer}$ ) from:  $\beta_T$  (experimental) =  $\beta_i + \beta_o$ . The curves in Fig. 10 are based on the  $\beta_i$  and  $\beta_o$  so calculated and indicate that for monobasic ligands with  $pK_a \lesssim 2$ , outer sphere complexation is dominant for trivalent actinides while for  $pK_a \gtrsim 2$ , an inner sphere nature is expected. A similar study of complexation by these same ligands of other actinide cations [49] indicates that the change from predominantly inner sphere to predominantly outer sphere complexation is associated with ligand  $pK_a$  as follows:

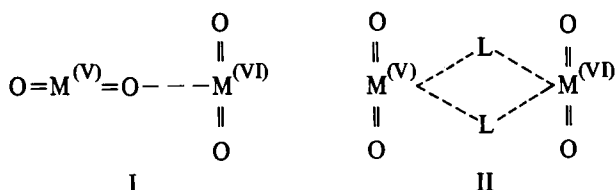
	outer sphere	$pK_a$	inner sphere
M(IV):		< ~ 1.0 >	
$MO_2^{+2}$ :		< ~ 1.7 >	
M(III):		< ~ 2 >	

Since the  $|\Delta H|$  and  $|\Delta S|$  values for inner sphere complexation are larger than for outer sphere formation, the experimental values would be likely to be endothermic for systems in which both types of complexes are present unless the inner sphere complex is present to less than 10–30% of the total complexation.

### Cation-cation complexes

A rather unique aspect of actinide solution chemistry is the formation of “cation-cation” complexes. SULLIVAN *et al.* [50] first reported the existence of complexes between pentavalent actinides,  $\text{MO}_2^{+1}$ , and multiply charged cations such as Cu(II), Fe(III), Th(IV), as well as oxygenated species like  $\text{UO}_2^{+2}$ . A recent study using Raman spectroscopy [51] confirmed the existence of these complexes as well as demonstrating the presence of  $\text{NpO}_2^{+2}$  dimers in acidic solutions. These dimers are not sensitive to pH and, obviously, are not hydrolytic polymers of the type formed in  $\text{MO}_2^{+2}$  solutions.

Two models for these cation-cation complexes have been proposed:



Model I has been supported by SULLIVAN [52] and VADAVATOV [53]. The second structure is that proposed in solution and in the solid for the hydrolytic dimers of  $\text{MO}_2^{+2}$  species where  $L = \text{OH}^-$  or  $\text{H}_2\text{O}$ . However, the experimental data, including recent studies by wide angle X-ray scattering [54], do not provide a firm basis to choose either model.

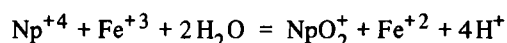
## VI. Kinetics

### Redox

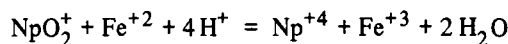
Generally, redox reactions of actinide species have, for discussion of kinetic effects, been divided into two groups – those which involve electron transfer only (e.g.  $\text{Pu}^{+3} \rightarrow \text{Pu}^{+4}$ ) and those which also require formation and/or rupture of metal-oxygen bonds (e.g.  $\text{Pu}^{+4} \rightarrow \text{PuO}_2^{+1}$ ). In most systems studied, the first group of reactions of simple electron exchange are fast. By contrast, these redox reactions which also involve metal-oxygen bond changes tend to be slower. These are, indeed, generalizations and reactions observed in the first group (e.g.  $\text{Pu}^{+3} + \text{PuO}_2^{+2} \rightarrow \text{Pu}^{+4} + \text{PuO}_2^{+1}$ ) can be slower than some in the second group (e.g.  $\text{U}^{+4} + \text{NpO}_2^{+2} = \text{UO}_2^{+2} + \text{NpO}_2^{+2}$ ). The wide variation in rates within the second group can be illustra-

ted by the disproportionation reaction  $2\text{MO}_2^{+2} \rightarrow \text{M}^{+4} + \text{MO}_2^{+1}$  in 1.0 M acid:  $\text{UO}_2^{+2}$ ,  $k = 4 \times 10^2$ ;  $\text{NpO}_2^{+2}$ ,  $k = 9 \times 10^{-9}$ ;  $\text{PuO}_2^{+2}$ ,  $k = 3.6 \times 10^{-3}$  [55, 56, 57].

The simple electron exchange reactions would be expected to show no rate dependency on hydrogen ion concentration. However, in some reactions studied, it seems probable that the activated complex involves a bridged hydrolyzed species, e.g.  $[\text{M}^{+3}(\text{OH})_2\text{Fe}^{+3}]$  – which could have some dependency on the pH of the medium. For the second type of redox reactions, if formation of a metal-oxygen bond occurs, a negative dependency on  $(\text{H}^+)$  is expected. Such a reaction would be:

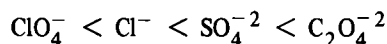


for which the rate expression is found to have a  $(\text{H}^+)^{-3}$  term [58]. By contrast, reactions in which M–O bonds are broken are found to have rate expressions in which a term for hydrogen ion concentration occurs with a positive exponent as, e.g.,



whose rate expression has a  $(\text{H}^+)^{+1}$  term [58].

In the presence of complexing anions an acceleration of the reaction rate is observed. The degree of acceleration is found to follow that of the tendency to form complexes, i.e.:



The complexation of reactants would facilitate the formation of binuclear bridged activated complexes (e.g.,  $\text{M}^{+3} \cdots \text{Cl} \cdots \text{MO}_2^{+2}$ ) by reducing the cation-cation electrostatic repulsion, thereby lowering  $\Delta G^\ddagger$  and increasing the forward rate. In weakly complexing systems such as perchlorate, hydroxyl bridging accomplishes this. Complexation of the products also would increase the net rate of the forward reaction by decreasing the reverse reaction.

It has been shown that a correlation exists between  $\Delta G^0$  (standard reaction free energy) and  $\Delta G^\ddagger$  (activation free energy) when formation or rupture of M–O bonds are involved in the redox reaction [59]. However, no such correlation exists for simple electron exchange reactions. However, for both groups of reactions, there is a strong “compensation” effect between  $\Delta H^\ddagger$  and  $\Delta S^\ddagger$ . As a result,  $\Delta G^\ddagger$  does not vary greatly for the majority of the actinide redox systems studied. This relative constancy of  $\Delta G^\ddagger$  is important as it means that various competing reaction mechanisms are likely to have similar values of  $\Delta G^\ddagger$  (and, hence, similar rates). A set of similar values of  $\Delta G^\ddagger$  explains the fractional exponents often observed for various terms in actinide redox rate equations as any particular system may have several paths, each contributing significantly to the total rate. Also, reactions which are apparently similar may have quite dissimilar rates if the possible paths are influenced differently by relatively “minor” effects (the rate for  $\text{Np}^{+3} + \text{NpO}_2^{+2}$  is almost 10 times greater than that for  $\text{Pu}^{+3} + \text{NpO}_2^{+2}$ ). This possibility of

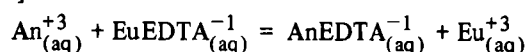
several competing paths and of significant variation in the contribution of each in apparently similar systems makes the study and interpretation of actinide redox reactions complicated indeed.

The formation of the cation-cation complexes discussed earlier no doubt plays a role in the redox reactions of such systems but this role remains to be explored and defined.

### Complexation

The rate determining step in the EIGEN mechanism for the formation of complexes is assumed to be a transition from outer sphere to inner sphere. Although problems of radioactivity, etc., make it very difficult to verify the validity of this mechanism for formation of actinide complexes of simple ligands, it is reasonable to assume such validity since the lanthanides seem to follow this mechanism [60, 61].

The kinetics of slower systems have been studied in a few cases. A tracer method was used to study the reaction [62]:



where An = Am, Cm, Bk and Cf.

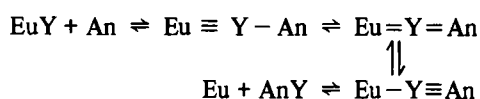
The exchange of An(III) with EuEDTA<sup>-</sup> is a first-order reversible reaction and the forward and reverse rate constants each contain an acid-dependent and an acid-independent term:

$$k_F = k_A \frac{[\text{EuEDTA}^{-}] [\text{An}^{+3}] [\text{H}^+]}{[\text{Eu}^{3+}]}$$

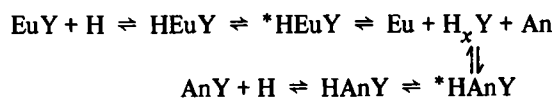
$$+ k_B [\text{EuEDTA}^{-}] [\text{An}^{+3}]$$

$$k_R = k_C [\text{H}^+] [\text{AnEDTA}^{-}] + k_D [\text{Eu}^{+3}] [\text{AnEDTA}^{-}]$$

may be represented schematically as follows (where EDTA is represented by Y):



The lines between Y and the cations indicate the number of carboxylate groups which are bonded to each metal ion (ionic charges have been omitted). For the acid-catalyzed mechanism it was proposed that the first step is a rapid equilibrium in which one of the carboxylate groups of the EDTA complex is protonated. The slow step is either (1) the dissociation of a second carboxylate group from the metal ion or (2) the transfer of a proton from the carboxylate oxygen to the nitrogen. The ligand is then able to dissociate rapidly from the metal ion. In either case the free europium and actinide ions compete for the free, protonated EDTA. Schematically this mechanism is given by:



Macroscopic level concentrations of Am(III) were used to study the rates of formation and dissociation of AmDCTA<sup>-</sup> (DCTA = trans, 1,2-diaminocyclohexanetetraacetate), respectively, by stopped-flow and conventional spectrophotometric methods [63]. A mechanism was proposed which involves coordination of Am(III) to three acetate groups of H<sub>n</sub>(DCTA)<sup>n-4</sup> to form the relatively long-lived intermediate \*AmHDCTA which subsequently loses a proton. The slow step of the formation reaction was postulated to be associated with the formation of an americium-donor nitrogen bond.

### VII. Conclusions

This review has attempted to provide some understanding of the diversity and complexity of actinide solution chemistry. It is obvious that significant progress has been made in all areas of this field but it is equally obvious that much remains to be done. The problems of working with radioactivity unfortunately has limited the number of laboratories which study these elements. Nevertheless, continuing and vigorous research programs in actinide solution chemistry are needed to further our fundamental knowledge and to answer the questions in applied areas.

The preparation of this review was supported in part by contracts with the U.S.D.O.E. Offices of B.E.S. and H.E.R.

### References

1. FORMAN, J. K., SMITH, T. D.: *J. Chem. Soc.* 1957, 1752.
2. CONNICK, R. E.: *The Actinide Elements*, Ch. 8, G. T. SEABORG and J. J. KATZ, eds., McGraw Hill Book Co., New York 1954.
3. AHLRAND, S., LILJENZIN, J. O., RYDBERG, J.: *Comprehensive Inorganic Chemistry*, Vol. 5., Pergamon Press, 1975, pp. 665 - 635.
4. MYASOEDOV, B. F., *Actinides in Perspective*, N. EDELSTEIN, ed., Pergamon Press, 1982, p. 509.
5. BILLON, A.: *Analysis* 8, 327 (1980).
6. MIKHEEV, N. B., SPITSYN, V. I., KAMENSKAYA, A. N., RUMER, I. A., GVOYDEV, B. A., ROSENKEVITCH, N. A., AUERMAN, L. N.: *Dokl. Acad. Nauk SSSR* 208, 1146 (1973), MIKULSKI, J., and PETRYNA, T., *Radiochem. Radioanal. Lett.* 43, 85 (1980).
7. HULET, E. K., LOUGHEED, R. W., BAISDEN, P. A., LANDRUM, J. H., WILD, J. F., LUNDQUIST, R. F. D.: *J. Inorg. Nucl. Chem.* 41, 1743 (1979); SAMHOUN, K., DAVID, F., HAHN, R. L., O'KELLEY, G. D., and TARRANT, J. R., *J. Inorg. Nucl. Chem.* 41, 1749 (1979).
8. PIKAEV, A. K., SHILOV, V. P., SPITSYN, V. I.: *Izv. Akad. Nauk SSSR* 232, 287 (1977).
9. GORDON, S., MULAC, W. A., SCHMIDT, K. N., SJOBLUM, R.: *Inorg. Chem.* 17, 294 (1978).
10. GUILLAUMONT, R., BOUISSIERES, G., MUXART, R.: *Actinides Rev.* 1, 135 (1968).
11. *Transuranics in the Environment*, HANSON, W. C., ed., (1980) DOE/TIC-22800, U.S.D.O.E.
12. SHILOV, V. P.: *Radiokhimiya* 18, 659 (1976).
13. SULLIVAN, J.: Private communication.
14. AHLRAND, S.: Private communication.
15. TOTH, T. M., BELL, J. T., FRIEDMAN, H. A.: *Actinide Separations*, J. D. NAVRATIL and W. W. SCHULZ, eds., (1980) ACS Symposium Series 117, Washington, D. C., pp. 253 - 266.
16. ALLARD, B., KIPATSI, H., LILJENZIN, J. O.: *J. Inorg. Nucl. Chem.* 42, 1015 (1980).

17. CHOPPIN, G. R.: *Pure Appl. Chem.* **27**, 23 (1971).
18. RAYMOND, K. N., EIGENBROT, C. W.: *Acc. Chem. Res.* **13**, 276 (1980).
19. SHANNON, R. D.: *Acta Crystallog.* **A32**, 751 (1976).
20. LEBEDEV, I. A.: *Radiokhimiya* **20**, 641 (1978).
21. FUGER, J., OETTING, F. L.: *The Chemical Thermodynamics of Actinide Elements and Compounds; Part 2, The Actinide Aqueous Ions* (1976), Inter. At. Ener. Agen., Vienna.
22. GOLDMAN, S., MORSS, L. R.: *Can. J. Chem.* **53**, 2695 (1975).
23. LUNDQUIST, R., HULET, E. K., BAISDEN, P. A.: *Acta Chem. Scand.* **A35**, 653 (1981).
24. CHOPPIN, G. R., STRAZIK, W. F.: *Inorg. Chem.* **4**, 1250 (1965).
25. HABENSCHUSS, A., SPEDDING, F. H.: *J. Chem. Phys.* **70**, 2797, 3758 (1979).
26. DE HORROCKS, JR., W., SUDNICK, D. R.: *Am. Chem. Soc.* **101**, 334 (1979).
27. FRANK, H., EVANS, O.: *J. Phys. Chem.* **13**, 507 (1945).
28. SVORONOS, D. R., ANTIC-FIDANCEV, E., LEMAITRE-BLAISE, M., CARO, P.: *Nouv. J. Chim.* **5**, 547 (1981).
29. JONES, A. D., CHOPPIN, G. R.: *Actinides Rev.* **1**, 311 (1969).
30. SCHMIDT, K. H., SULLIVAN, J. C., GORDON, S., THOMPSON, R. C.: *Inorg. Nucl. Chem. Lett.* **14**, 429 (1978); *ibid.* *J. Inorg. Nucl. Chem.* **42**, 611 (1980).
31. CACECI, M. S., CHOPPIN, G. R.: *Radiochim. Acta*, accepted for publication.
32. SULLIVAN, J. C., HINDMAN, J. C.: *J. Phys. Chem.* **63**, 1332 (1959).
33. BAES, C. F., MESMER, R. E.: *The Hydrolysis of Cations*, J. Wiley & Sons, New York (1976).
34. CHOPPIN, G. R., GOEDKIN, M. P., GRITMAN, T. F.: *J. Inorg. Nucl. Chem.* **39**, 2025 (1977).
35. MARTELL, A. E., SMITH, R. M.: *Critical Stability Constants*, Vol. 1–5. Plenum Press, N. Y., 1974–82.
36. BAISDEN, P. A., CHOPPIN, G. R., GARRETT, B. B.: *Inorg. Chem.* **16**, 1367 (1977).
37. RYAN, R. L.: *Inorganic Chemistry: Lanthanides and Actinides*, Vol. 7, K. W. BAGNALL, ed., Butterworths London, 1972, Chapter 9.
38. HENRIE, D. E., FELLOWS, R. L., CHOPPIN, G. R.: *Coord. Chem. Rev.* **18**, 199 (1976).
39. JUDD, B. R.: *Lanthanides and Actinide Chemistry and Spectroscopy*, N. M. EDELSTEIN, ed. ACS Symposium Series 131, Am. Chem. Soc., Washington, 1970, p. 267.
40. WADT, W. R.: *J. Am. Chem. Soc.* **103**, 6053 (1981).
41. CHOPPIN, G. R., UNREIN, P. J.: *Transplutonium Elements*, W. MULLER and R. LINDNER, eds., North-Holland, Amsterdam, 1976, p. 97.
42. MUNZE, R.: *J. Inorg. Nucl. Chem.* **34**, 661 (1972).
43. DUNCAN, J. F., KEPER, D. L.: *The Structure of Electrolyte Solutions*, W. J. HAMER, ed., Wiley, New York 1959, p. 380.
44. IVES, D. J. G., MARSDEN, P. D.: *J. Chem. Soc.* **1965**, 649.
45. EIGEN, M., WILKINS, R.: *Adv. Chem. Ser.*, Am. Chem. Soc., No. 49, 55 (1965).
46. BECK, M. R.: *Coord. Chem. Rev.* **3**, 91 (1968).
47. JOHANSSON, L.: *Acta Chem. Scand.* **25**, 3479 (1971).
48. CHOPPIN, G. R.: *Lanthanide and Actinide Chemistry and Spectroscopy*, N. M. EDELSTEIN, ed., ACS Symposium Series 131, Am. Chem. Soc., Washington 1980, p. 173.
49. KHALILI, F. I., CHOPPIN, G. R.: to be published.
50. SULLIVAN, J. C., HINDMAN, J. C., ZIELAN, A. J.: *J. Am. Chem. Soc.* **83**, 3373 (1961).
51. GIULLAUME, B., BEGUN, G. M., HAHN, R. L.: *Inorg. Chem.* **21**, 1159 (1982).
52. SULLIVAN, J. C.: *J. Am. Chem. Soc.* **84**, 4256 (1962).
53. VADOVATOV, V. A., *et al.*: *Radiokhimiya* **17**, 889 (1975); **21**, 830 (1979).
54. GIULLAUME, B., NARTEN, A. H., HAHN, R. L.: *Abstr. Actinides*, '81, N. EDELSTEIN, ed., LRL-Berkeley.
55. NEWTON, T. W., BAKER, F. B.: *Inorg. Chem.* **4**, 1166 (1965).
56. HINDMAN, J. C., SULLIVAN, J. C., COHEN, D.: *J. Am. Chem. Soc.* **76**, 3278 (1954).
57. RABIDEAU, S. W.: *J. Am. Chem. Soc.* **79**, 6350 (1957).
58. HUIZENGA, J. R., MAGNUSSON, L. B.: *J. Am. Chem. Soc.* **73**, 3202 (1951).
59. NEWTON, T. W., BAKER, F. B.: *Lanthanide/Actinide Chemistry*, P. R. FIELDS and T. MOELLER, eds., *Adv. in Chem. Series* 71, Am. Chem. Soc., Washington 1967, p. 268.
60. PURDIE, N., VINCENT, C. A.: *Trans. Faraday Soc.* **63**, 2745 (1967).
61. GEIER, G.: *Ber. Bunsenges. Phys. Chem.* **69**, 617 (1965).
62. CHOPPIN, G. R., WILLIAMS, K. R.: *J. Inorg. Nucl. Chem.* **35**, 4255 (1978); *ibid.* **36**, 1849 (1974).
63. SULLIVAN, J. C., NASH, K. L., CHOPPIN, G. R.: *Inorg. Chem.* **17**, 3374 (1978).



## Recent Analytical Chemistry of the Transplutonium Elements

By B. F. MYASOEDOV and I. A. LEBEDEV, V. I. Vernadsky Institute of Geochemistry and Analytical Chemistry, Academy of Sciences of the USSR, Moscow U.S.S.R.

(Received March 10, 1982)

*Transplutonium elements / Nuclear properties / Oxidation states / Separation methods / Determination methods*

### Abstract

The modern state of the analytical chemistry of the transplutonium elements (TPE) ranging from Americium to Lawrencium are reviewed. The main characteristics of the most important isotopes are given, and properties of metals and oxides are discussed. Special attention is paid to the TPE properties in unusual oxidation states in solutions, the methods of production and stabilization, and current methods of isolating and separating of these elements. In conclusion the principal methods of determining TPE and impurities in them are considered.

### I. Introduction

Studies on TPE are currently in progress in different countries. This is due to the great scientific interest in the elements, the chemical and physical properties of which have not been studied in detail and also to the great progress of nuclear power.

TPE are produced in connection with the processing of highly radioactive materials containing a mixture of heavier elements in special reactors. For this reason effective and simple highly sensitive and selective methods of TPE determination in different samples including natural ones, are of great importance. The problems of the analytical chemistry of TPE have been most fully systematized in previously published monographs [1–3], and specific questions have been discussed in transactions of different conferences [4–6].

In the present survey the authors tended to generalize recent achievements in analytical chemistry of TPE, especially in connection with the discovery of the capacity of some of those elements to exist in unusual oxidation states (both the highest, and the lowest ones).

### II. TPE general characteristics

#### 1. Isotopes and their properties

About 170 nuclides among elements with  $z = 95–103$  are known. They are all radioactive and have half-lives from several ns to  $\sim 10^7$  years [7, 8]. Table 1 gives the nuclear properties of some isotopes used in practice. (The table also shows isotopes Np and Pu since these elements are impurities or daughter decay products during TPE analysis.) The overwhelming majority of nuclides given in Table 1, decay by emitting  $\alpha$ -rays with energy within a

range 4.6–7.2 MeV; thus the main radiometric method of quantitative determination of TPE is to measure their  $\alpha$ -activity (total counting and  $\alpha$ -spectrometry). Only a few nuclides have no  $\alpha$ -rays ( $^{238}\text{Np}$ ,  $^{239}\text{Np}$ ) or have small probability of  $\alpha$ -decay ( $^{241}\text{Pu}$ ,  $^{249}\text{Bk}$ ), in this case  $\beta$ -activity counting methods are used for their quantitative determination. About half the nuclides have practically noticeable rate of spontaneous fission, allowing them to be determined on the basis of counting the neutrons or fission fragments. The emission of characteristic  $\gamma$ -ray quanta (X-ray or nuclear) takes place in the process of all the nuclides decay, and this also used in their qualitative and quantitative determination. Experiments were recently carried out in some countries to introduce clarity into the half-life of a number of important isotopes of U, Pu, Am, Cm, Bk, Cf. As a result of using improved measuring apparatus and perfectly pure specimens of nuclides, it became possible to measure those values with errors less than a portion of a per cent.

#### 2. Metals and oxides

Only Am, Cm, Bk, Cf and Es are obtained in metallic states as yet. They all represent shining silver metals, well-dissolving in acids [2]; the main physical properties of TPE metals are given in Table 2.

The thermodynamic properties of TPE metals are characterized in detail in [49].

These elements form two main types of oxides: dioxide ( $\text{MO}_2$ ) and sesquioxide ( $\text{M}_2\text{O}_3$ ). Dioxides are stable at low temperatures and are formed as a result of air calcination of many TPE compounds, oxalates, for instance. They represent dark powders, which once heated, hardly dissolve in acids. In the case of californium, air calcination of  $\text{Cf}_2\text{O}_3$  results in oxide composition  $\text{Cf}_7\text{O}_{12}$ , which is isostructural with  $\text{Tb}_7\text{O}_{12}$  [63]. The reduction of dioxides by hydrogen with strong calcination forms weak-coloured sesquioxides, which are easily dissolved in acids [64–68] and melt without decomposition (the melting point of  $\text{Cm}_2\text{O}_3$  is  $2260^\circ\text{C}$ ,  $\text{Bk}_2\text{O}_3$  –  $1920^\circ\text{C}$ ,  $\text{Cf}_2\text{O}_3$  –  $1750^\circ$  [65].

#### TPE Properties in aqueous solutions

The 5f-series elements, namely transplutonium elements are characterized by a much greater number of oxidation states, than the analogous 4f-elements-lanthanides (Table 3). In acidic aqueous media without oxidizers and reducers

Table 1. Nuclear properties of some TPE isotopes

Nuclide	Atomic mass <sup>1</sup>	Half-life <sup>2</sup>	Specific activity, Bq/mg	Mode and energy of particles, MeV (yield, %) <sup>3</sup>	Energy of principal gamma-quanta, keV (yield, %) <sup>4</sup>	Neutron activity, n/(s·mg) <sup>5</sup>	Reference (addition.)
1	2	3	4	5	6	7	8
<sup>237</sup> Np	237.048	2.14 · 10 <sup>6</sup> y	2.607 · 10 <sup>4</sup>	α: 4.769	29.6(13); 86.6(13)	—	—
<sup>238</sup> Np	238.051	2.117 d	9.587 · 10 <sup>12</sup>	β: 1.26(45)	984(24); 1028(17.4)	—	—
<sup>239</sup> Np	239.053	2.35 d	8.60 · 10 <sup>12</sup>	β: 0.33(42); 0.44(35)	106(27.8); 278(14.5)	—	—
<sup>236</sup> Pu	236.046	2.851 y	1.965 · 10 <sup>10</sup>	α: 5.755	47.6(0.03); 109(0.012)	33.8	—
<sup>237</sup> Pu	237.048	45.4 d	4.489 · 10 <sup>11</sup>	α: 5.36+5.65 (0.0033)	59.6(5)	—	—
<sup>238</sup> Pu	238.050	87.58 y	6.344 · 10 <sup>8</sup>	α: 5.487	43.5(0.04); 99.9(0.007)	2.675	[17–21]
<sup>239</sup> Pu	239.052	24111 y	2.295 · 10 <sup>6</sup>	α: 5.148	51.6(0.02); 38.7(0.006)	2.2 · 10 <sup>-5</sup>	[22–27]
<sup>240</sup> Pu	240.054	6537 y	8.429 · 10 <sup>6</sup>	α: 5.157	45.2(0.045); 104(0.007)	0.897	—
<sup>241</sup> Pu	241.057	14.44 y	3.800 · 10 <sup>9</sup>	β: 0.0208 α: 4.89(2.3 · 10 <sup>-3</sup> )	148(0.022); 103.5(0.01)	—	[21, 28–32]
<sup>242</sup> Pu	242.059	3.755 · 10 <sup>5</sup> y	1.455 · 10 <sup>5</sup>	α: 4.889	44.9(0.033); 103.5(0.007)	1.71	[33–35]
<sup>244</sup> Pu	244.064	8.26 · 10 <sup>7</sup> y	6.561 · 10 <sup>2</sup>	α: 4.580	44(0.015)	1.878	—
<sup>241</sup> Am	241.057	432.6 y	1.268 · 10 <sup>8</sup>	α: 5.480	59.54(35.9); 101(0.054)	1.2 · 10 <sup>-3</sup>	[36–39]
<sup>242m</sup> Am	242.060	141 y	3.88 · 10 <sup>8</sup>	α: 5.20+5.37(0.45)	49.3(0.2); 86.7(0.038)	0.15	[40]
<sup>243</sup> Am	243.061	7369 y	7.385 · 10 <sup>6</sup>	α: 5.270	74.7(66); 43.5(5.5)	4.3 · 10 <sup>-3</sup>	[37, 41, 42]
<sup>242</sup> Cm	242.059	162.8 d	1.226 · 10 <sup>11</sup>	α: 6.089	44.1(0.03); 101.9(0.004)	2.09 · 10 <sup>4</sup>	—
<sup>243</sup> Cm	243.061	28.5 y	1.909 · 10 <sup>9</sup>	α: 5.779(87); 6.03(13)	277.6(14); 228.2(10.6)	—	—
<sup>244</sup> Cm	244.063	18.11 y	2.992 · 10 <sup>9</sup>	α: 5.795	42.8(0.02); 99(0.0013)	1.08 · 10 <sup>4</sup>	—
<sup>245</sup> Cm	245.065	8532 y	6.326 · 10 <sup>6</sup>	α: 5.355	174(14); 133(13.7)	—	—
<sup>246</sup> Cm	246.067	4730 y	1.136 · 10 <sup>7</sup>	α: 5.376	44.5(0.024)	8.72 · 10 <sup>3</sup>	—
<sup>247</sup> Cm	247.070	1.56 · 10 <sup>7</sup> y	3.43 · 10 <sup>3</sup>	α: 4.866(79); 5.24(21)	402.4(72); 84(23)	—	—
<sup>248</sup> Cm	248.072	3.39 · 10 <sup>5</sup> y	1.57 · 10 <sup>5</sup>	α: 5.070(91.74)	45(0.02)	4.09 · 10 <sup>4</sup>	—
<sup>249</sup> Bk	249.075	327 d	5.93 · 10 <sup>10</sup>	β: 0.124 α: 5.41(1.45 · 10 <sup>-3</sup> )	327(0.000024)	94.6	[43,44]
<sup>249</sup> Cf	249.075	351 y	1.513 · 10 <sup>8</sup>	α: 5.82(96); 6.19(4)	388.3(66); 333.4(14.4)	2.675	—
<sup>250</sup> Cf	250.076	13.08 y	4.044 · 10 <sup>9</sup>	α: 6.024	42.9(0.016)	1.09 · 10 <sup>7</sup>	—
<sup>251</sup> Cf	251.079	900 y	5.853 · 10 <sup>7</sup>	α: 5.916(50); 5.68(50)	177(19); 225(7.4)	—	—
<sup>252</sup> Cf	252.082	2.631 y	1.994 · 10 <sup>10</sup>	α: 6.111(96.9)	43.4(0.015); 100.2(0.013)	2.30 · 10 <sup>9</sup>	[45–48]
<sup>253</sup> Es	253.085	20.47 d	9.326 · 10 <sup>11</sup>	α: 6.627	42(0.038); 388(0.05)	3.2 · 10 <sup>5</sup>	—
<sup>254</sup> Es	254.088	276 d	6.89 · 10 <sup>10</sup>	α: 6.427	63(2)	—	—
<sup>255</sup> Es	255.090	39.8 d	4.76 · 10 <sup>11</sup>	β: 0.38(91.5) α: 6.3(8.5)	—	7.1 · 10 <sup>7</sup>	—
<sup>254</sup> Fm	254.087	3.24 h	1.41 · 10 <sup>14</sup>	α: 7.185	41(0.2)	3.3 · 10 <sup>11</sup>	—
<sup>255</sup> Fm	255.090	20.07 h	2.26 · 10 <sup>13</sup>	α: 7.02	81.3(1.1); 58.4(0.78)	2.2 · 10 <sup>7</sup>	—
<sup>256</sup> Fm	256.092	2.63 h	1.72 · 10 <sup>14</sup>	α: 6.905(8.1)	—	5.9 · 10 <sup>14</sup>	—
<sup>257</sup> Fm	257.095	100.5 d	1.87 · 10 <sup>11</sup>	α: 6.517(96); 6.70(3.8)	242(10); 180(8.5)	1.5 · 10 <sup>9</sup>	—
<sup>256</sup> Md	256.093	1.25 h	3.62 · 10 <sup>14</sup>	α: 7.19(9) et al.	400(10)	—	—
<sup>257</sup> Md	257.095	5.0 h	9.0 · 10 <sup>13</sup>	α: 7.064(10)	—	—	—
<sup>258</sup> Md	258.098	56 d	3.3 · 10 <sup>11</sup>	α: 6.74	—	—	—
<sup>255</sup> No	255.093	3.1 m	8.8 · 10 <sup>15</sup>	α: 8.11(36); 7.94(14)	187.2(5.5)	—	—
<sup>256</sup> Lr	256.098	27 s	6.0 · 10 <sup>16</sup>	α: 8.44	—	—	—

s - second, m - minute, h - hour, d - day, y - year

Notes: 1) The calculation is done on the defects of masses values, shown in [2]. 2) Mainly on [7–9]. Some new data on the half-life of isotopes Pu(238–242), Am(241–243), Bk(249) and Cf(252) are taken from the papers, named in column 8, and averaged. 3) See [7]. The average energy value of the α-particles, which are not resolved in the SSD-spectrum is given. The yield, if not indicated, is 100%. 4) See [7, 10]. Some new data on Am, Cm, Cf isotopes are taken from [11–14]. 5) The spontaneous fission yields are taken from [8, 9], the average number of neutrons per fission – from [15, 16].

Table 2. Physical properties of TPE metals

	Am	Cm	Bk	Cf	Es, Fm, Md
Density (room, t°), g/cm <sup>3</sup>	13.78* [50]	13.71** [51]	14.80 [52]	15.12 [53]	—
Melting point, °C	1177 [49]	1358 [54]	1050 [55]	900 [56]	—
Boiling point, °C	2011 [57]	3110 [54]	2587 [55]	1472 [58]	—
Metallic radius, nm	0.173 [59]	0.174 [60]	0.170 [60]	0.169 [60]	—
Metallic valence	+3 [61]	+3 [61]	+3 [61]	+3 [61] +2 [62]	+2 [61, 62]

\* <sup>243</sup>Am

\*\* <sup>244</sup>Cm

Table 3. Oxidation states of TPE

	Am	Cm	Bk	Cf	Es	Fm	Md	No	Lr
+1							±		
+2	±	±	±	±	±	±	+	⊕	
+3	⊕	⊕	⊕	⊕	⊕	⊕	⊕	+	⊕
+4	+	±	+	±	±				
+5	+			±					
+6	+	±							
+7	±								

⊕ – the most stable oxidation state in aqueous solutions;

+

± – unstable oxidation state, exist in specific conditions, or is produced by special methods, or is known in solid state.

most TPE are in a trivalent oxidation state, however Am, Cm, Bk, Cf may exist in the highest oxidation states, though Md reduces rather easily to  $Md^{2+}$ . The most stable oxidation state for No in aqueous solutions is +2. Recently the existence of Am(VII) [69], Cm(VI) [70], Cf(IV) [71] and Cf(V) [72], Es(IV) [73], Md(I) [74, 75] in different conditions has been proved.

Most solvent extraction and sorption methods of TPE separation are based on the small difference in the properties of those elements in the +3 oxidation state and this difference usually increases due to the complex formation. Information on the TPE complex-formation is given in the monograph [76]. A more efficient TPE separation is ensured by methods based on their different oxidation state, which are discussed below.

Americium may exist as Am(III), Am(IV), Am(V) and Am(VI) in acidic aqueous media. In a highly alkaline solution Am(VII) is produced [69, 77–79]; in a non-aqueous medium (acetonitrile) [80] and in a chloride melt [81] – Am(II) is found. The existence of the unstable Am(II), which is produced by pulse-radiolysis of perchlorate solutions of Am, containing butanol, is shown in [82–84]. The most stable oxidation state in solutions is Am(III), which is produced at the solution of a metal or Am oxides in acids, and by the reduction of other oxidation states. The possibilities of Am(III) oxidation to the highest oxidation states can be estimated with the help of the formal oxidation potential values, which are given in Table 4.

Americium(IV), which practically does not exist in strong acid media due to its immediate disproportionation [2], can be stabilized in the presence of strong complexing agents. In recent years convenient practical methods of Am(III) oxidation up to Am(IV) in 8–15 M  $H_3PO_4$  electrochemically [107, 108] and by the mixture  $Ag_3PO_4 + (NH_4)_2S_2O_8$  [108–112] have been worked out, and the stability of Am(IV) in phosphoric acid solutions has been studied in detail [109–110, 112, 113]. The oxidation of Am(III) up to Am(IV) can also be carried out in solutions of unsaturated heteropolytungstates  $K_7PW_{11}O_{39}$  or  $K_{10}P_2W_{17}O_{61}$  – by persulfate-ions on heating [114–116], or by the electrochemical method [116]. In these conditions Am(IV) is stable in the presence of an oxidizer during several days [114]; without an oxidizer it reduces

at a low speed (about 1% per hour) [116, 117], probably by the radiolysis products and water [118].

It has also been proved that Am(III) can be oxidized up to Am(IV) by the mixture of  $AgNO_3 + (NH_4)_2S_2O_8$  without heating in 0.1–6 M  $HNO_3$  solutions, containing  $K_{10}P_2W_{17}O_{61}$  (4-fold is in excess of Am) [119]; in such solutions (with the  $HNO_3$  concentration  $\leq 3$  M) Am(IV) is stable during 5–7 days. Obtaining of the stable Am(IV) in phosphotungstate solutions undoubtedly gives the opportunity to use it for analytical purposes. The possibility of Am(III) electrochemical oxidation up to Am(IV) in carbonate solutions has also been shown [103]. In diluted solutions of  $Am(ClO_4)_3$  containing  $N_2O$ ,  $S_2O_8^{2-}$  or  $XeO_3$ , under the influence of  $\gamma$ -rays or the pulse of electrons, a non-stable Am(IV) can appear, which transforms into Am(V) and Am(VI) very quickly ( $\sim 10^{-3}$  s) [82, 84, 120–122].

The oxidation of Am(III) up to Am(V) and Am(VI) is used in a number of methods of americium isolation and determination, which have been described [3]. Recently new methods of producing Am(VI) in  $HNO_3$  solutions by sodium bismuthate oxidation [123], in phosphoric acid media by the electrochemical method [107, 108] and oxidation with the mixture of  $Ag_3PO_4 + (NH_4)_2S_2O_8$  [108, 110, 124], in  $HClO_4$  solutions with a small addition of  $H_3PO_4$  – by the electrochemical method [125]; and in  $HNO_3$  solutions with an addition of  $K_{10}P_2W_{17}O_{61}$  – by the mixture of  $AgNO_3 + (NH_4)_2S_2O_8$  [119] have been worked out. The studies on Am(VI) stability in aqueous solutions of various chemical composition [119, 123–132] have proved that in most cases Am(VI) gradually reduces up to Am(V) by own  $\alpha$ -radiation. In  $H_3PO_4$  solutions [132] and in the presence of  $K_{10}P_2W_{17}O_{61}$  [119, 130] Am(VI) is most stable, in the latter case it practically does not reduce for several days. A convenient method of electrochemical production of Am(V) by reduction of Am(VI) in diluted  $HClO_4 + H_3PO_4$  solutions [125] has been worked out. In weak acid solutions Am(V) is generally more stable than Am(VI) [126–129, 133], but with increasing acidity the stability of Am(V) falls due to the increasing disproportionation rate (the same effect is observed with increasing  $PO_4^{3-}$ -ion concentration [134]). The trace amounts of Am(V) reduce quickly in the presence of  $CH_3COO^-$ ,  $SO_4^{2-}$ ,  $Cl^-$ ,  $BrO_3^-$ ,  $I^-$ ,  $SO_3^{2-}$ -ions and  $H_2O_2$  [133]. In the solutions of most acids Am(V) is immediately oxidized by Am(IV) up to Am(VI) [135], but in  $K_{10}P_2W_{17}O_{61}$  solution this reaction does not come to an end, and it is possible to observe the existence of Americium in four oxidation states III, IV, V and VI simultaneously [99, 130]. In 5 M NaOH, Am(III) fully oxidizes by the electrochemical method up to Am(V) (the anode potential is +1 V) and then up to Am(VI) [104]. The interaction between  $H_2O_2$  and Am(V, VI) in 1 M NaOH results in unstable Am(V) peroxide, which transforms into insoluble Am(IV) peroxide [136]. Al metal reduces Am(VI) in 1 M NaOH up to Am(III) [137]. The Am(III) oxidation by persulphate-ions on heating in carbonate solutions results in Am(V) and Am(VI), the kinetics of the process

Table 4. The formal redox potentials of TPE reversible pairs in aqueous solutions (V, vs' NHE), at 20–25°C. Values in parentheses are the solution concentrations

Medium	Americium			Curium	Berkelium
	IV/III	VI/V	VII/VI	IV/III	IV/III
HClO <sub>4</sub>	–	1.60 (1 M) [2]	–	–	1.59–1.74 (1–9 M) [85, 86]
HNO <sub>3</sub>	–	–	–	–	1.54–1.60 (1–16 M) [85, 87–90]
H <sub>2</sub> SO <sub>4</sub>	–	–	–	–	1.43–1.33 (0.05–10 M) [87, 91–93]
H <sub>3</sub> PO <sub>4</sub>	1.79–1.75 (10–15 M) [94, 95]	1.58–1.45 (1–5 M) [94, 96]	–	–	1.12 (7.5 M) [88]
K <sub>10</sub> P <sub>2</sub> W <sub>17</sub> O <sub>61</sub>	1.65–1.40 (6–13 mM, pH = 0–6) [97, 98]	1.52 (0.016 M, pH = 0.7) [99]	–	2.1–2.3 [98]	0.85–0.64 (6 mM, pH = 0–6) [98]
K <sub>2</sub> CO <sub>3</sub>	0.86 (1 M) [100]	0.97–0.77 (0.1–2.7 M) [101, 102]	–	1.6 (1 M) [100]	0.26 (2 M) [88]
Na <sub>2</sub> CO <sub>3</sub>	0.92 (2 M) [103]	0.90 (0.2–2.1 M) [102]	–	–	–
NaOH	0.25–0.18 (1–10 M) [104]	0.68–0.63 (1–10 M) [104, 105]	1.05 (1 M) [79, 106]	–	–

have been studied in detail [138]. The electrochemical oxidation of Am(III) in 1 M K<sub>2</sub>CO<sub>3</sub> (the potential is +1 V) produces Am(VI), which by the electrochemical method reduces to Am(V) under +0.9 V [101]. A partial oxidation of Am(III) to Am(V) and Am(VI) in 3–5.5 M K<sub>2</sub>CO<sub>3</sub> by acute irradiation of the solution has also been observed [139].

**Curium** is very stable in aqueous solutions in +3 state of oxidation, and in most cases it is not oxidized in the conditions when Am(III) oxidation is observed. This can be explained by the high values of the oxidation potential of the Cm(IV)/Cm(III) pair – which is about 0.7–0.8 V higher than that of the Am(IV)/Am(III) pair (see Table 4). This factor is widely used in the methods of separation of Cm from Am, Bk and lighter actinides. However Cm(III) can be oxidized to Cm(IV) by potassium persulphate on heating in K<sub>10</sub>P<sub>2</sub>W<sub>17</sub>O<sub>61</sub> solution [114, 116]; though the stability of Cm(IV) in such conditions is not strong, it fully reduces in 1.5–3 hours. The appearance of a very unstable (~ 10<sup>-5</sup> s) Cm(IV) resulting from irradiation by the electrons of the Cm(III) perchlorate solution saturated with N<sub>2</sub>O has also been observed [82]. In the presence of tert-butyl alcohol, which connects the oxidizers (OH-radicals), the irradiation of Cm(III) solution by electrons results in the appearance of unstable Cm(II) (10<sup>-6</sup> s) [82].

According to the theoretical calculations [140], the standard oxidation potential of the Cm(VI)/Cm(V) pair is not high (+1.5 V), and Cm(VI) can exist in aqueous solutions. But its direct production by Cm(III) oxidation is difficult due to the high potential of the Cm(IV)/Cm(III) pair. It has been proved [70] that Cm(VI) (in form of CmO<sub>2</sub><sup>2+</sup>) appears as a result of <sup>242</sup>AmO<sub>2</sub><sup>+</sup> β<sup>-</sup>-decay in solid

K<sub>3</sub>AmO<sub>2</sub>(CO<sub>3</sub>)<sub>2</sub> and exists in the solution after the dissolving of americium carbonate in 0.1 M NaHCO<sub>3</sub>.

**Berkelium** like cerium can be oxidized rather easily to Bk(IV) in aqueous solutions by various oxidizers [3]. Recently some new methods of Bk(III) oxidation have been suggested, many of which have been studied on large quantities of Bk. Berkelium can be oxidized by ozone in HNO<sub>3</sub> [89, 141, 142], K<sub>2</sub>CO<sub>3</sub> [141] and H<sub>2</sub>SO<sub>4</sub> [143] media by KBrO<sub>3</sub> on heating or without heating in HNO<sub>3</sub>, H<sub>2</sub>SO<sub>4</sub> and HCl solutions (not completely) [89, 144, 145]; by AgO or the mixture of AgNO<sub>3</sub> + (NH<sub>4</sub>)<sub>2</sub>S<sub>2</sub>O<sub>8</sub> in solutions of HNO<sub>3</sub> [112, 146–148] and H<sub>2</sub>SO<sub>4</sub> [149]; by (NH<sub>4</sub>)<sub>2</sub>S<sub>2</sub>O<sub>8</sub> on heating; by K<sub>2</sub>Cr<sub>2</sub>O<sub>7</sub>, NaBiO<sub>3</sub> and PbO<sub>2</sub> in HNO<sub>3</sub> solutions [145, 148]; by the electrochemical method in HNO<sub>3</sub> solutions [85, 88, 90, 142], K<sub>2</sub>CO<sub>3</sub> [88], H<sub>2</sub>SO<sub>4</sub> [93] and K<sub>10</sub>P<sub>2</sub>W<sub>17</sub>O<sub>61</sub> [98]. In acidic solutions in the presence of such oxidizers as KBrO<sub>3</sub>, (NH<sub>4</sub>)<sub>2</sub>S<sub>2</sub>O<sub>8</sub>, ozone, Bk(IV) is stable during several days [142, 144, 146], and in pure solutions of HNO<sub>3</sub> and H<sub>2</sub>SO<sub>4</sub> it reduces as a result of its interaction with radiolysis products and water at the rate of 15–20% per hour [93, 142]. The stability of Bk(IV) in HNO<sub>3</sub> solutions in the presence of AgNO<sub>3</sub> + (NH<sub>4</sub>)<sub>2</sub>S<sub>2</sub>O<sub>8</sub> decreases greatly while increasing the temperature [112]. In K<sub>2</sub>CO<sub>3</sub> solution the oxidation potential of the Bk(IV)/Bk(III) pair is so low (see Table 4), that a radiolytic oxidation of Bk(III) to Bk(IV) is observed [88].

Various reductants are used to reduce Bk(IV) to Bk(III): hydrogen peroxide [89, 145], hydroxylamine, ascorbic acid [89] – in HNO<sub>3</sub> solutions, hydrazine-nitrate [150] – for Bk(IV) reextraction from HDEHP solutions. The elec-

trochemical reduction of Bk(IV) in  $\text{HNO}_3$  [90, 142] and  $\text{H}_2\text{SO}_4$  [93] solutions has also been studied.

In the melt of chlorides ( $\text{NdCl}_2 + \text{NdCl}_3 + \text{SrCl}_2$ ) the cocrystallization of Bk with  $\text{Nd}^{3+}$  (in the form of  $\text{NdOCl}$ ) decreases while increasing the ratio of Nd(II) to Nd(III), that indicates the reduction of Bk to Bk(II) [81].

**Californium, Einsteinium and Fermium** in aqueous solutions under ordinary conditions are stable only in the +3 oxidation state like curium. However, in acidic aqueous-ethanol solutions (1–8 M  $\text{H}_2\text{O}$ , 0.2–7 M HCl) those elements are reduced by Mg metal to divalent state [151, 152]. The stability of +2 state of oxidation on the whole increases with rising TPE atomic number [151], and the Fm(III)/Fm(II) pair has the same oxidation potential as the Yb(III)/Yb(II) pair [153]. It has been shown [154] that Fm(III) can be reduced to Fm(II) by electrolysis on mercury cathode.

On the other hand, Cf(III) is oxidized to Cf(IV) by heating with  $\text{K}_2\text{S}_2\text{O}_8$  in  $\text{K}_{10}\text{P}_2\text{W}_{17}\text{O}_{61}$  solution [71, 116], but as in the case of Cm(IV), Cf(IV) is unstable and reduces completely during 2–3 hours [116].

In accordance with Cm(VI) the existence of Cf(V) was proved as a result of  $\beta^-$ -decay of  $^{249}\text{Bk}(\text{IV})$  [72]. Using TPE gaseous fluorides on the thermochromatograph column has proved that in such conditions Es is an analogue to Pu, Am, Cm, Bk, Cf, which form tetrafluorides, i.e. it probably has the +4 oxidation state [73].

**Mendelevium**, much like the previous TPE, is most stable in aqueous solutions in the +3 oxidation state, though many strong reducers (Zn,  $\text{Cr}^{2+}$ ,  $\text{V}^{2+}$ ,  $\text{Yb}^{2+}$ ,  $\text{Eu}^{2+}$ ) in HCl solution reduce it to Md(II) [2]. The electrochemical reduction of Md(III) on mercury cathode in the presence of acetate- or citrate-ions also results in producing Md(II), which later reduces to the metallic state [155]. The most interesting property of Md is its capacity to reduce to Md(I) in ethanol HCl solutions by Mg,  $\text{Eu}^{2+}$  and  $\text{Yb}^{2+}$  [74, 75, 156]. Md(I) has the ionic radius 0.117 nm [157] and does not form either stable complexes with  $\text{Cl}^-$ -ions or low-soluble chloride, similar to alkaline cations [75, 157]. The attempts to oxidize Md(III) to Md(IV) by  $\text{NaBiO}_3$  failed [158].

**Nobelium**, which ends the 5f-shell formation is the most stable in aqueous solutions in the +2 oxidation state (an ion with the  $5f^{14}$  electron configuration). The usual strong oxidizers (persulphate in the presence of  $\text{Ag}^+$  ions, bromate, etc.) oxidize No(II) to No(III) [2]. The existence of nobelium in the form of No(II) in aqueous solutions has been proved by the study of its extraction and ion-exchange properties [159]; these data have made it possible to measure the  $\text{No}^{2+}$  ionic radius (0.10–0.11 nm). These results, as well as the study of No(II) complexing with citrate- and oxalate-ions [160] have proved that  $\text{No}^{2+}$ -ion has identical properties with the  $\text{Ca}^{2+}$ - and  $\text{Sr}^{2+}$ -ions.

**Lawrencium**, the last element in the actinide series, should theoretically only exist in the +3 oxidation state in aqueous solutions. The chemistry of Lr has not been studied in depth, the data of its extraction from acidic solutions prove its existence in the form of the  $\text{Lr}^{3+}$ -ion [2]. According to new calculations [161], the Lr main atomic configuration is not  $5f^{14}7s^26d$  (by analogy with Lutecium), but  $5f^{14}7s^27p$ .

#### Separation methods of some TPE in the radiochemical pure state

Modern analytical methods, such as radiometric, neutron-activation, spectral, electrochemical and several other methods, especially in combination with the automatic experimental data processing on the electron computer make possible the direct determination some TPE isotopes in various objects. However, while solving numerous practical problems connected with TPE determination, the essential preliminary step is to separate, concentrate and isolate them from other elements. Extraction and chromatography, extraction chromatography, deposition and co-deposition, chromatography on paper, the methods of sublimation and electrophoresis are mainly used with that end in view [2, 3]. However, the best effect in the separation is produced by the methods based on using different TPE oxidation states [162].

Extraction methods using Am(V) and Am(VI) are the most effective to separate americium from other TPE and fission products. Such methods are especially promising for the separation of Am(V) tracers for further determination [163, 164]. Am(V) can be recovered from aqueous solutions by the extraction of TTA [165], PMBP [166] and by ammonium pyrrolidinedithiocarbamate [167]. The solvent extraction of tri- and tetravalent actinide ions is completely suppressed in the presence of potassium phosphotungstate but penta- and hexavalent americium extract quantitatively into the organic phase (0.05 M PMBP in iso-butanol). The separation factor of Am and Cm makes  $\sim 2.5 \cdot 10^3$  [168]. Am(V) can be separated from actinide and lanthanide elements by mixtures of picronic acid and sulphoxides from nitric acid solutions, as Am(V) extraction is negligible in such conditions [169].

The hexavalent americium having a concentration of  $\geq 2$  mg/ml, extracts by solutions of HDEHP [173–176], TOPO [176], d-(2,6-dimethyl-4-heptil) phosphoric acid [170] and by mixture of HDEHP and TBP [171] or TOPO [172] in cyclohexane. On using mixtures of PMBP and TOPO [164] and TTA and TOPO [172] in cyclohexane as extractants Am and Cm can be separated. The americium is previously oxidized up to the hexavalent state; during extraction it reduces to the unextracted pentavalent state; and curium and other tri-valent elements with a high distribution coefficient in such, transfer into organic phase. The method provides quantitative extraction of americium and a high degree of its purification from curium ( $> 10^3$ ) and fission fragments [164]. Using electrochemi-

cal oxidation of americium instead of oxidation by persulphate-ions, the radiometric determination of americium becomes more exact [125].

For the determination of americium and plutonium in natural samples the combined methods are described [177]. Pu and Am together with rare earths and other actinides are isolated from the solution analysed by coprecipitation on  $\text{BaSO}_4$ . Then the actinides are extracted by 15% HDEHP in *n*-heptane, and due to reextraction of 4 M  $\text{HNO}_3$ , Pu remains in the organic phase. The actinides and rare earths are separated from Am chromatographically. The purification factor of Pu and Am both from each other and from Th, U, Po and Pa is  $10^4 - 10^5$ . The method is used to determine the contents of americium and plutonium in soils, dust sediments and natural water.

A synergistic extraction of tri-valent Am, Cm, Bk and Cf by a mixture of TTA and TBP has been studied in the paper [178].

Lately, for the selective isolation of berkelium a number of effective methods, based on the extraction of berkelium in the tetra-valent state have been worked out. The conditions of tetravalent berkelium extraction by HDEHP [89, 179] and the conditions of its reextraction from the organic phase have been studied in detail [150]. TOPO and TPPO solutions extract Bk(IV) quantitatively from 1–12 M  $\text{HNO}_3$  [180], and TBP solutions – from 8–12 M  $\text{HNO}_3$  [181]. The extraction of Bk(IV) by TOPO from sulphuric acid solutions is less efficient, and TBP practically do not extract it at all. The high-molecular amines are also used for the extraction of Bk(IV). The influence of the acid concentration and the nature of the oxidizer and diluent on the completeness of Bk(IV) extraction by TOA [149, 182] and by aliquate-336 [183] has been studied. Potassium bromate and bichromate as well as the mixture of silver nitrate and ammonium persulphate [184] have been used as oxidizers in those works. The quantitative extraction of berkelium after its oxidation by bichromate-ions of 0.4 M TOA in  $\text{CCl}_4$  takes place in 10 M  $\text{HNO}_3$ . The usage of the mixture of silver nitrate and persulphate-ions for the extraction by TOA makes it possible to separate berkelium from cerium as in these conditions berkelium reduces to the tri-valent state and remains in aqueous phase. During the extraction of berkelium by 30% aliquate in  $\text{CCl}_4$  from 10–12 M  $\text{HNO}_3$ , after its oxidation by bichromate-ions, a separation from the other TPE and rare earths is achieved. In the presence of heteropolianions Bk(IV) is quantitatively extracted from nitric acid solutions by the primary, secondary, tertiary amines and quaternary ammonium bases. Heteropolianions do not only stabilize the tetra-valent berkelium but also enter the composition of extracted compounds.

One of the efficient methods of TPE separation is extraction chromatography. On using of HDEHP as an extractant applying on different supports americium and curium separation [133, 173] and of selective extraction of Bk(IV) [179, 185] have been worked out. During the quantitative extraction of americium and curium the separation factor of Am(VI) from Cm is  $2 \cdot 10^2$  and that of Cm

from Am –  $10^2$ . Using penta-valent americium the purification from Cm is  $\sim 5 \cdot 10^3$ , and the purification of Cm from Am is worse ( $\sim 60$ ) [173]. As a stationary phase a mixture of TTA and TBP was used [187] for the rapid separation of tri-valent Am and Eu [186] and the complex mixture of elements including Am, Cm, Cf, U, Th and others.

The separation of Am(V) and Cm(III) on Dowex-A 1 × 8 resin has been studied in the work [188]. It was proved that the separation coefficient of Am and Cm strongly increases with increasing pH from 2.5 to 3.2, and with falling temperature and with increasing the quantity of resin. The mechanism of Bk(IV) and Ce(IV) separation on Dowex-I-anionite has been studied in the work [189]. The separation of TPE in tri-valent state on the ion-exchange resins using aqueous organic solutions has given the most interesting results [190, 191]. In aqueous alcoholic solutions in the presence of  $\alpha$ -oxybutyric acid the separation factor of americium and curium on Dowex-I × 8 resin is  $\sim 6$  [192].

Zirconium phosphate is most widely spread among the inorganic sorbents which separate TPE. This sorbent has been used to separate Am(IV) [193], Am(V) [194–197] and Am(VI) [195] from curium, and for selective isolation Bk(IV) from mixture of actinide elements and fission products [198]. The separation of Am(VI) and Cm(III) on the calcium fluoride sediment ( $t^0 = 800^\circ\text{C}$ ) is described in the work [199].

To separate TPE in different states the methods of precipitation and co-precipitation are also useful. The study of Am (III, V, VI) co-precipitation on sediments of lanthanum, thorium and cerium fluorides, and on bismuth and zirconium phosphates [200] has proved that all the sediments studied, except as zirconium phosphate, fully capture Am(III), and Am(VI) remains in the solution. Am(V) is partially captured by the sediments of lanthanum and thorium fluorides. A different method of americium separation in different oxidation has been used to study its stability in the presence of oxidizers [128]. The penta-valent americium can be separated from Am(III) and Am(IV) in acetate solutions by co-precipitation with the sediment of pyrrolidinedithiocarbamate [167].

For the separation of fermium from Cf, Es and lanthanide, an efficient method has been suggested, which is based on the co-crystallization of Fm, reduced in the presence of Yb(II), with sodium chloride from aqueous ethanolic solutions. When a practically quantitative extraction of Fm is going on, the degree of purification from most attendant elements achieves  $10^3 - 10^4$  [201]. In the presence of di-valent europium Md(I) is fully recovered, with sediments of chlorides K or Na, the purification from the other actinides and lanthanides reaches  $\sim 5 \cdot 10^2$  [202].

## Methods of TPE determination

### Radiometrical methods

Thanks to a considerable improvement in measuring equip-

ment and half-life revision, the radiometric methods of TPE determination achieve at present the precision methods level. First of all this relates to the methods of TPE determination using  $\alpha$ -activity in which the best metrological characteristics (low detection limit, high efficiency and small errors) are reached using the silicon semiconductor detector and liquid scintillator. The alpha-spectrometer with a semiconductor detector (area 1–3 cm<sup>2</sup>) has an efficiency of nearly 50% and the detection limit 10<sup>-3</sup> Bq (in sample) [203–204]; the efficiency is 85% using two detectors [205]. As the energy resolution of such detectors reaches 20–30 keV, it is possible to determine the usual mixture of americium and curium (<sup>241</sup>Am, <sup>243</sup>Am, <sup>242</sup>Cm, <sup>244</sup>Cm) without separation of those elements. In case of complex  $\alpha$ -spectra with superposing lines, different mathematical methods processing are used [206, 207]. A number of methods, based on precipitation, extraction and ion-exchange procedures have been worked out to isolate TPE from the environment, irradiated nuclear fuel industrial solutions, etc. [177, 203, 204, 207–210]. The electrodeposition of radionuclides on the backing from aqueous [211–213] or organic solutions (ethanolic [205], iso-propanolic [214, 215], iso-butanolic [216] or mixed [217] solutions) solutions) which gives the thin uniform coating on target and the high resolution under measuring  $\alpha$ -particles, is used more often on target for  $\alpha$ -spectrometry. However, good samples can be received without electrodeposition if a fine membrane filter is used as a backing [208]. If the  $\alpha$ -activity of analysed solution is high enough, the use of  $\alpha$ -counter (on the basis of SSD) with a small solid angle gives good results: for example, while determining Am in a solution with americium content  $\sim 1.7 \cdot 10^{-4}$  mg/ml by a counter with the solid angle of  $6 \cdot 10^{-3}$  steradian, the analysis reproducibility is 0.34 per cent with a systematic error of less than 0.5% [218].

If a sample contains only one  $\alpha$ -active nuclide, or one  $\alpha$ -active element with a certain isotopic compound (or a total  $\alpha$ -activity is determined), it is possible to use the methods of integral  $\alpha$ -counting. The methods in which the active sample is placed into the detector are most efficient: a flow proportional  $2\pi$ - or  $4\pi$ -counter for dry samples, a liquid scintillation counter for solutions. The proportional counters have a count efficiency of 50% and a very low background (about 10<sup>-3</sup> c/s) making it possible to measure the absolute  $\alpha$ -activity with an error of 0.3% [219]. Though the LS-counter demands a high activity of the sample measured (as its background is over  $\sim 10$  fold the background of the proportional counter), it is also used in measuring the  $\alpha$ -activity of the TPE isotopes. The advantages of the LS-method consists in the high efficiency of the counting (practically 100 per cent) and in the elimination of such a labour-consuming stage as the preparation of a dry sample for measuring. There are two methods of samples preparing for LS-measuring: (1) directly adding the aqueous or organic solution of sample to LS; (2) an extraction of the radionuclide from the sample by LS. In the latter case an extractant is added to the LS solution. The mixtures containing the scintillating materials such

as 5 g/l p-terphenyl and 0.05 g/l POPOP, and as extractants 20% HDEHP [220, 221], or 43.5% nonylphosphate [222] (diluent-toluene) are used for TPE determination. Such LS makes it possible to concentrate the element as well, and to separate it from impurities. For instance, LS together with HDEHP extract Pu from the solutions with high content of HCl or HNO<sub>3</sub>, isolating it from most non-active impurities [220] and Am, Cm [222]. This LS extracts Am, Cm and Cf from solutions with low acidity, separating them from anions [221]. LS with nonylphosphate can completely extract Am and Cm from NHO<sub>3</sub> solutions up to 2 M; the methods of the analysis on Am and Cm content in the biological samples with the help of the LS is characterized by the detection limit up to  $3 \cdot 10^{-3}$  Bq/ml [222].

To determine of small quantities of Pu, Am and Cm in aqueous solutions, the co-precipitation of these elements with the lanthanum hydroxide in the presence of a solid scintillator (ZnS, activated Ag) is suggested [223]. The glass with a thin layer of sediment on the bottom, in which the radionuclides are fully mixed with the scintillator, put on the photocathode of the photomultiplier and measure the count rate. The counting efficiency reaches 80%, the detection limit (if the volume of the initial sample is 1 l) is  $4 \cdot 10^{-5}$  Bk/ml.

Lately, for the determination of  $\alpha$ -active TPE directly in solutions, "immersed" SSD has been widely used [224–228]. An ordinary silicon SD (without the gold coat) in a glass [225] or stainless steel [228] casing, is immersed into the solution containing the nuclides under determination, and the counting rate is measured, which is proportional to the nuclide concentration (the proportionality factor depends on the  $\alpha$ -particle energy). Such a detector has a small counting efficiency (1 per cent or less) and is convenient for measuring high  $\alpha$ -activity; the polished surface of silicon is fully purified from  $\alpha$ -active pollution by HNO<sub>3</sub> solution. The presence of non-volatile macro-impurities in the solution usually prevents the preparation of samples with a thin layer for  $\alpha$ -counting, it practically does not effect measuring with an "immersed" detector. In combination with the multichannel analyzer, the "immersed" SSD makes it possible to do a  $\alpha$ -spectrometrical analysis: a separate determination of  $\alpha$ -active nuclides in solutions containing such mixtures as <sup>244</sup>Cm, <sup>252</sup>Cf, <sup>253</sup>Es [226] or <sup>241</sup>Am, <sup>243</sup>Am, <sup>242</sup>Cm, <sup>244</sup>Cm [227, 228] is described. An energy resolution of such an  $\alpha$ -spectrometer is usually 50–100 keV [226, 228], though it can reach 18–20 keV [226]. Determination is possible in solutions containing NaNO<sub>3</sub> up to 7 M [228].

The possibility of applying the  $\alpha$ -spectrometric method to the analysis of the mixture of  $\alpha$ -active nuclides is usually restricted by two factors: the difference in  $\alpha$ -particles energy and the correlation of nuclides activity. The analysis becomes practically impossible if the peaks made in the  $\alpha$ -spectrum by two or more nuclides, are overlapped strongly enough. Such mixtures as <sup>238</sup>Pu and <sup>241</sup>Am, <sup>242</sup>Cm and <sup>250,252</sup>Cf, <sup>244</sup>Cm and <sup>249</sup>Cf may serve as an example. The possibility of determining of one of the elements de-

teriorates in the presence of an element with higher energy and intensity of  $\alpha$ -rays, as a low-energetic  $\alpha$ -peak slope with a higher energy increases to a great extent the background in the  $\alpha$ -peak field with a lower energy. In some cases the method of  $\alpha$ - $\gamma$ -coincidences is used. The design for the measurement of the spectrum of  $\alpha$ - $\gamma$ -coincidences [229] consists of an ordinary semiconductor  $\alpha$ -spectrometer combined with a unichannel  $\gamma$ -spectrometer, tuned in the  $\gamma$ -rays of the nuclide with the lower  $\alpha$ -particles energy. With such a method one may determine  $^{243}\text{Am}$  in  $^{243}\text{Am}$  and  $^{244}\text{Cm}$  mixtures up to 1% ( $3 \cdot 10^{-3}$  %  $^{243}\text{Am}$  according to the  $\alpha$ -activity), even in the presence of  $\gamma$ -active fission products [229]. The method of  $\alpha$ - $\gamma$ -coincidences is also used to measure the absolute  $\alpha$ -activity of nuclides, ex.  $^{241}\text{Am}$  with a very small error (0.1–0.2%) [218, 219].

In the process of radiometric determination a nuclide as an impurity is preliminarily separated. The most effective separation is achieved using the different oxidation states of elements. Thus, for instance, to determine  $^{243}\text{Am}$  in the mixture with  $^{244}\text{Cm}$ , americium should be electrochemically oxidated up to Am(VI) and curium should be removed by extraction, then the  $\alpha$ -spectrum determination of americium becomes possible [125]. If the solution of 0.05 M phenyl-methyl-benzoyl-pyrazolone and 0.025 M tributylphosphineoxide in cyclohexane is used for the extraction, the double extraction provides the purification of Am from Cm over  $3 \cdot 10^4$ -fold, with about 2%-loss of americium.

The counting problem of  $\beta$ -particles with low energy comes up in the analytical chemistry of TPE in connection with the analysis of samples containing  $^{249}\text{Bk}$ . As a rule the proportional flow counter (the counting efficiency is 50–100%, the background is about 1 c/s) or the LS counter is used for this purpose. The use of the LS-method for  $^{249}\text{Bk}$  determination is complicated by the fact that most substances quench relatively weak scintillations, induced by  $\beta$ -particles of  $^{249}\text{Bk}$ . The dependence of count coefficient of  $^{249}\text{Bk}$  by the LS-counter upon  $\text{HNO}_3$  and  $\text{H}_2\text{SO}_4$  concentration has been determined [230]. For the  $\beta$ -spectrometric determination of  $^{249}\text{Bk}$ , an "immersed" drift (Si(Li)-detector may be used, the detection limit of berkelium in the solution is  $\sim 2 \cdot 10^4$  Bq/ml [226].

The convenient determination method for nuclides with spontaneous fission is to measure the neutron activity. Even isotopes of plutonium, curium and californium are regarded to be nuclides with high neutron activity. The neutron counting method makes it possible to determine the content of those nuclides in samples of various configurations without destroying them. The influence of other  $\alpha$ -active nuclides are taken into account which give the additional flux of neutrons at the expense of nuclear reactions on light nucleus of mode ( $\alpha, n$ ). Counters of neutron-neutron coincidences do not have those drawbacks, as they exclude the background of ( $\alpha, n$ )-reactions and provide the identification of distinct neutron-active nuclides as for the value of the average number of neutrons per fission [231, 232]. The determination of microgrammic quantities of  $^{244}\text{Cm}$  is described with the help of those plants

in samples containing only this nuclide [231, 232], and in the mixture with  $^{240}\text{Pu}$  [231]. The error in the determination of neutron-active nuclides by this method is 1–2% [231, 232], the detection limit of  $^{244}\text{Cm}$  is  $3 \cdot 10^{-9}$  g [232]. In the analysis of the mixture of neutron-active nuclides rather precise results are gained if the specific neutron activity of all the nuclides is nearly equal in quantity [231].

## Physical methods

### X-ray spectral and X-ray fluorescence methods

The presence of X-radiation of the daughter nuclide appearing during the decay of the mother radionuclide is the specific peculiarity of radioactive elements. The  $\alpha$ -decay of americium isotopes is followed by the characteristic X-radiation of Np, the  $\alpha$ -decay of curium isotopes – by Pu etc. Energies of the most intensive X-quanta of transuranium elements are presented in Table 5. (On the whole, the values are calculated from the bond energies of electrons [233], the data for the K-series are taken from the paper [234], for the  $L_\alpha$ -radiation of Np-Am – from [235], for the M-series of Np-Am – from [236].) Their relative yields are given in parentheses [234, 237, 238], they are considerably dependent upon the type and energy of the decay of the mother nuclide.

X-radiation can be used both for qualitative identification of individual nuclides and for their quantitative determination. The analysis method of  $^{249}\text{Bk}$  and  $^{249}\text{Cf}$  mixture using  $L_\alpha$ -band of californium has been described [238]. The X-ray spectrometer with silicon detector, possessing the counting efficiency of about 1% and energy resolution 170–300 eV in the area of 5.9–26.4 keV is used for the detection of X-radiation. This method permits determination to 0.01  $\mu\text{g}$  of  $^{249}\text{Bk}$  in 1  $\mu\text{g}$  of  $^{249}\text{Cf}$ .

The ordinary X-ray fluorescence method can be applied for the determination of TPE. The fluorescence yields of the K-level for Np-Es are about 97.2% [239]. The relative yields of X-rays of M-series for Np-Am have been determined in the paper [236]. It is recommended to use M-series for X-ray fluorescence determination of americium, so this radiation is in the low background region of the X-ray tube [235]. The detection limit of americium in this case reaches 0.046  $\mu\text{g}$ , while it is equal to 0.93  $\mu\text{g}$  in the determination of  $L_\alpha$ -lines.

### Mass spectrometric analysis

Sensitive techniques of mass-spectrometric determination of TPE in the samples of uranium, plutonium, americium, curium, berkelium and californium have been developed [240–242]. If the mass of analysed sample is equal to 0.1–10  $\mu\text{g}$ , it is possible to determine plutonium and americium in curium at the level of  $10^{-2}$  %, and plutonium, americium and curium in berkelium and californium – at the level of 0.5%. In this case the detection error is

Table 5. X-ray of TPE (energy, keV, and yield, per cent)

Line	Np	Pu	Am	Cm	Bk	Cf	Es	Fm	Md
$K_{\alpha_1}$	101.05	103.71	106.43	109.3 (100)	112.1 (100)	115.0 (100)	118.0 (100)	120.75	123.77
$K_{\alpha_2}$	97.06	99.50	101.99	104.6 (63.2)	107.2 (64.3)	109.8 (65.7)	112.5 (66.6)	115.06	117.80
$K_{\beta_1}$	114.24	117.20	120.24	123.4 (23.0)	126.6 (22.2)	129.8 (25.9)	133.2 (24.2)	136.24	139.61
$K_{\beta_3}$	113.31	116.22	119.2	122.3 (11.2)	125.5 (12.6)	128.6 (13.3)	131.8 (13.4)	134.89	138.19
$L_{\alpha}$	13.759– –13.942 (13.2–27.5)	14.084– –14.276 (3.33–49.8)	14.411– –14.615	14.74– –14.96 (3.09–5.3)	15.09– –15.32	15.43– –15.67 (0.0055)	15.78– –16.03	16.13– –16.40	16.49– –16.77
$L_{\beta}$	16.838– –17.992 (19.25–30.6)	17.255– –18.540 (3.71–47.6)	17.676– –19.105	18.10– –19.68 (3.80–3.85)	18.55– –20.27	18.98– –20.86 (0.0027)	19.44– –21.48	19.89– –22.10	20.36– –22.75
$L_{\gamma}$	20.828– –21.338 (4.85–7.69)	21.465– –21.981 (0.86–12.5)	22.116– –22.638	22.78– –23.31 (0.85–0.93)	23.46– –24.00	24.15– –24.69	24.86– –25.41	25.58– –26.14	26.33– –26.89
$L_I$	11.882 (0.86–1.8)	12.139 (0.21–3.2)	12.389	12.65 (0.21–0.23)	12.92	13.18	13.45	13.72	13.99
$L_n$	15.872	16.349	16.829	17.33	17.83	18.35	18.87	19.41	19.96
$M_{\alpha_1}$	3.263	3.350	3.442	3.536	3.635	3.734	3.842	3.940	4.048
$M_{\beta}$	3.436	3.532	3.633	3.737	3.842	3.947	4.062	4.177	4.292

about 10–20% [241, 242], but in the case of a higher content of the analysed element (about 1% of plutonium and curium in the americium) error can be reduced up to 4–5%.

Determination of Bk by neutron-activation analysis [243]

$^{250}\text{Bk}$  with half-life of 3.32 h, and intensive  $\gamma$ -radiation ( $E_{\gamma} = 989$  keV, yield 45.6%) is produced during the irradiation of  $^{249}\text{Bk}$  by thermal neutrons, the activation cross-section being equal to 1400–1700 barns. The sensitive method of  $^{249}\text{Bk}$  determination in the mixture with curium and californium is based on this phenomenon. The mixture is irradiated by thermal neutron flux with a density of  $1 \cdot 10^{13}$  n/(cm<sup>2</sup>·sec) for several hours, and after a short time the intensity of  $\gamma$ -line of 989 keV is measured on a  $\gamma$ -spectrometer with semiconductor detector. The detection limit of berkelium in samples of 2  $\mu\text{g}$  is equal to  $1.8 \cdot 10^{-4}$  %.

Neutron-spectrometric determination of transplutonium elements [244]

This method is based on the fact, that nuclei of heavy elements selectively absorb neutrons of definite energy in the range of 0.1–30 eV. The neutron “absorption spectrum” of a sample containing transplutonium elements has characteristic peaks, their height being proportional

to the content of the corresponding nuclides. The neutron spectrometer is used for this purpose. It permits working with 5–100 mg of substance, the detection limit of  $^{244}\text{Cm}$  reaches 0.2 mg/cm<sup>2</sup>,  $^{243}\text{Am}$  – 3 mg/cm<sup>2</sup>. The accuracy of determination is limited by the accuracy of resonance parameters of the corresponding nucleus and in the case of americium and curium is about 5–10%.

Determination of americium in curium by the emission spectrometry method [245]

The spectrographic method of americium detection using hot hollow cathode is based on the measurement of the intensity of the Am emission line of 351,013 nm. Nitric acid solution, containing to 0.1 mg of curium, is introduced inside the carbon hollow electrode and after drying, the emission spectrum is made in the He atmosphere (7 mm of Hg). The detection limit of americium is equal to  $1 \cdot 10^{-7}$  g, error is not more than 25%. As the intensity of the americium line depends on the curium content, it is necessary to use standards with a known content of curium.

**Chemical methods**

Coulometric determination of americium and curium

In most cases americium determination is carried out by

the method of coulometry, with the potential controlled by pair Am(VI)/Am(V). In the determination of americium in sulphuric acid solution [246, 247] the detection limit is about 0.4 mg, the interference of curium is noticed. U, Np and Pu interfere in the determination americium in carbonate solution (oxidation of Am(III) to Am(V) [248]).

Americium determination in the solution of 2 M  $H_3PO_4 + 0.1$  M  $HClO_4$ , allowing determination to 5–10  $\mu g$  of Am in the sample [249] is elaborate. Am(III) is electrochemically oxidized to Am(VI) under the anode potential of 2.0 V and then the coulometric determination is carried out, reducing Am(VI) to Am(V) under the potential of 1.27 V. Hundred-fold quantities of Al, Ni, Cu, Cr, Zr, lanthanides (except Ce), commensurable quantities of Pu, Cd, Fe do not interfere to determine americium. The great quantities of curium usually interfere with the determination of americium [246, 247], due to the reduction of Am(VI) by the  $\alpha$ -radiation of curium. Curium does not interfere in phosphoric acid solutions, since the formation of reductants during  $\alpha$ -radiolysis of these solutions is negligible [250]. The determination error of 10–20  $\mu g$  of Am is 3–4%, and it decreases to 1.5% if the americium content in the sample exceeds 30  $\mu g$ .

It is possible to determine americium from 5 to 100  $\mu g$  by pair Am(IV)/Am(III) in  $6 \cdot 10^{-3}$  M  $K_{10}P_2W_{17}O_{61} + 0.1$  M  $HClO_4$  solution [251]. In this solution Am(III) is completely oxidized to Am(IV) for 15 minutes under potential 1.7 V. Coulometric determination is carried out reducing Am(IV) to Am(III) under 1.17 V. Am(IV) is very stable in  $K_{10}P_2W_{17}O_{61}$  solution, so ten-fold excess of curium does not interfere. Many of the elements being oxidized in these conditions (Pu, Ce, and others) also do not interfere, since they are not reduced below the potential of 1.17 V. The determination error does not exceed 3% even in the presence of 100-fold quantities of other metals.

An indirect coulometric method of americium determination with high accuracy has been suggested [252]. This method is based on the substitution reaction of  $Hg^{2+}$  by Am from its complex with EDTA, with the next coulometric determination of mercury (reduction to metal). The analysis time is 1 hour, the determination error of 0.3–0.7 mg of Am is 0.1–0.2%. This method can be recommended for the standardization of pure solutions of americium, since it is not distinguished by selectivity; all the lanthanides, actinides in oxidation states +3 and +4, many of divalent cations ( $Pb^{2+}$ ,  $Zn^{2+}$ ,  $Cd^{2+}$ ,  $Cu^{2+}$  etc.) as well as anions, forming stable complexes with  $Am^{3+}$ , interfere in the determination of americium.

An analogous method has been used for the accurate determination of  $\sim 100 \mu g$  of  $^{248}Cm$  in nitric acid solution [253]. In this case the known quantity of EDTA (in the excess) was added to the solution of curium in an acetate buffer, and uncomplexed EDTA was titrated with  $Hg^{2+}$  electrochemically generated from metallic mercury. The curium content in the sample was calculated from the quantity of electricity necessary for the generation of  $Hg^{2+}$ . The determination error does not exceed 1%.

### Titrimetric methods

Complexometric titration is most frequently used for the determination of macro amounts of TPE. Americium and curium are known to form very stable complexes with the usually applied complexons – EDTA ( $\beta = 10^{17}$  [254]), DTPA ( $\beta = 10^{22} - 10^{23}$  [255]). By titration with solution of EDTA in the presence of xylenol orange as an indicator and spectrophotometric fixation of the end point, it is possible to determine about 1 mg of americium and curium in a sample with an accuracy of about 1.4  $\mu g$  [256].

Methods of determination of microgram amounts of americium and curium by titration with a solution of DTPA have been developed [257, 258]. By potentiometric indication of end point, the determination error is  $\sim 2\%$ , by spectrophotometric indication – 0.5% [257]. In another version of this method, an electrochemically generated complex of Fe(II) with DTPA serves as a titrant, permitting out analysis with the help of an automatic coulometric titrator [259]. The determination error of 20–200  $\mu g$  of americium is about 3–5% [258].

Spectrophotometric titration is used for the quantitative determination of americium (VI, V and III) when they are jointly present [260]. Titration is executed in nitric acid solution. Firstly Am(VI) is titrated with standard solution of  $NaNO_2$ , the end of titration is detected by the change of optical density under 996 nm (Am(VI)) or 717 nm (Am(V)). In this case Am(VI) is reduced to Am(V), which is stable in these conditions. The total amount of Am(V) is titrated by the solution of U(IV), which reduces Am(V) to Am(III) and from this the content of Am(V) in the original sample is calculated. The americium(III) content at the end of titration is found from the optical density of 813 nm. The determination error is 2–3% if the americium concentration in the solution is  $\sim 6 \cdot 10^{-3}$  M (1.5 mg / ml).

### Methods determining impurities in transplutonium elements

Spectrographic determination of impurities in Am-Cf [261]. An emission spectrographic method to determine impurities at the level of  $10^{-3} - 10^{-2} \%$  has been developed for quality characterizing TPE samples produced for use in different branches of science and technology. The method is used in two versions: direct spectrophotometric determination (for Am and Cm samples) and determination with preliminary separation of the main component, allowing the limits of detection to be decreased considerably. In the first case the sample of 0.05 ml volume, containing 0.2 mg of the main substance is applied on carbon electrode and then an emission spectrum, irritated in an alternating current arc, is taken in the range of 250–450 nm. Analyzed elements and their limits of detection are given in Table 6. In the second case impurities are isolated from analyzed samples of TPE (mass of 5–10 mg) by the extraction – chromatography method on silica gel with HDEHP. Separation of TPE from rare-earth elements is

Table 6. Limits of detection of impurities in americium and curium oxides by direct spectrographic method [261]

Element	Al	Si	Cd	B	Na	Ca	Mg	Ni	Cr
Limit of detection, weight %	0.0025	0.005	0.025	0.006	0.025	0.005	0.002	0.008	0.008
	Fe	Ce	Pr	Nd	Sm	Eu	Gd		
	0.008	0.08	0.07	0.05	0.07	0.02	0.008		

executed by the solution of 0.03 M DTPA + 0.3 M citric acid (pH = 2.9). Fractions, containing impurities are evaporated and then analyzed. In this case, the limits of detection average one-fifth of their previous values, and besides the elements, enumerated in Table 6, Li, K, Pb, Cs, Sr, Ba, Be, Y, La, Mn and Co are determined as well. The determination error is about 4–20%.

#### Determination of impurities of rare-earth elements

In mass-spectrometric analysis of TPE samples [240–242] La, Ce, Pr, Nd, Sm and Eu are determined simultaneously with Pu, Am and Cm. If the weight of the Cm and Am sample is 5–10  $\mu\text{g}$ , lanthanides are determined at the level of  $10^{-3}\%$  [241, 262], for Bk and Cf samples equal to 0.1  $\mu\text{g}$  – on the level of  $3 \cdot 10^{-2}\%$  [242]. The determination error is 10–20%.

During the complexometric determination of Am(III) and Cm(III) [257] in the presence of lanthanides in solution, titration gives the total content of TPE and lanthanides. It is possible to calculate the content of lanthanides proceeding from the difference, if the content of Am and Cm is determined by another means (spectrophotometry, radiometry). Nd concentration found in this way in the solution containing  $1.935 \cdot 10^{-3}$  M of Am, Cm and Nd (including  $0.279 \cdot 10^{-3}$  M of Nd), differed from the true one by 0.4%.

#### Determination of Pu

The determination of small quantities of plutonium in samples of TPE represents an important problem, since in most cases in real mixtures  $\alpha$ - and  $\gamma$ -activities of transplutonium elements are greater those of plutonium. It was mentioned above that mass-spectrometric analysis permitted to determine to  $10^{-2}\%$  of plutonium in the preparation of Cm [122] and to 0.3% in the preparation of Bk and Cf [242]. For plutonium determination in  $^{241}\text{Am}$ , the method based on registration of neutron-neutron coincidences of spontaneous fission of  $^{238}\text{Pu}$ ,  $^{240}\text{Pu}$  and  $^{242}\text{Pu}$  has been suggested [263]. Such determination is possible in solids and solutions containing  $> 1 \mu\text{g/ml}$  of Pu, in the presence of comparable quantities of americium. Determination of very small quantities of plutonium in  $^{241}\text{Am}$  can be carried out after chemical separation of plutonium by sorption on i-okthylmethyl-phosphonate of Fe(III) [264]. Pu is isolated from nitric acid solution by 30 mg of sorbent with subsequent washing and  $\alpha$ -radiometric determination of plutonium. Purification of Pu from Am exceeds  $10^5$ , detection limit of  $^{249}\text{Pu}$  is equal to  $3 \cdot 10^{-4}$

$\mu\text{g}$ . It is possible to determine to 0.05% of  $^{239}\text{Pu}$  in  $^{241}\text{Am}$ .

The neutron-spectrometric method of heavy elements determination [244] allows the non-destructive determination of plutonium isotopes in TPE samples. The detection limit of  $^{240}\text{Pu}$  is close to the detection limit of  $^{244}\text{Cm}$ , that of  $^{249}\text{Pu}$  to the detection limit of  $^{243}\text{Am}$ . It is possible to determine quantities of Pt and Sm comparable with quantities of  $^{243}\text{Am}$ . The determination error of plutonium isotopes reaches 2–5%.

#### References

- METZ, CH. F., WATERBARY, G. R.: Treatise in analytical chemistry, p. II, sect. A, v. 9. *The transuranium actinide elements*. New York-London: Interscience Publ. 1962.
- KELLER, C.: *The chemistry of the transuranium elements*. Verlag Chemie GmbH, 1971.
- MYASOEDOV, B. F., GUSEVA, L. I., LEBEDEV, I. A. *et al.*: *Analiticheskaya khimiya transplutoniyevykh elementov* (Analytical chemistry of the transplutonium elements). Moscow: Nauka Publishers 1972.
- Transplutonium-1975*. Ed. MULLER, W., LINDNER, R. Amsterdam: North-Holland Publ. Company 1976.
- Transplutonium elements – production and recovery*. Ed. NAVRATIL, G. D., SCHULZ, W. W., Amer. Chem. Soc. symp. ser. 161. Washington, D.C. 1981.
- Actinide separations*. Ed. NAVRATIL, G. D., SCHULZ, W. W., Amer. Chem. Soc. symp. ser. 117. Washington, D.C. 1980.
- ZAMYATNIN, YU. S.: *Radioaktivnyi raspad i skhemy urovnei yader tyazhelykh elementov* (Radioactive decay and level schemes of heavy element nuclei). Moscow: Atomizdat 1974.
- Nuclear Wallet Cards*. Ed. SHIRLEY, V. S., LEDERER, C. M. 1979.
- EWBANK, W. B., ELLIS, Y. A., SCHMORAK, M. R.: Nucl. Data Sheets 26(1), 1 (1979).
- GUSEV, N. G., DMITRIEV, P. P.: *Kvantovoe izluchenie radioaktivnykh nuklidov* (Quantum radiation of radioactive nuclides). Moscow: Atomizdat 1974.
- CAMPBELL, J. L., MCNELLES, L. A.: Nucl. Instrum. Methods 117(2), 519 (1974).
- AHMAD, I., WAHLGREN, M.: Nucl. Instrum. Methods 99(2), 333 (1972).
- GENOUX-LUBAIN, A., ARDISSON, G.: Radiochem. Radioanal. Lett. 33(1/2), 59 (1978).
- BARANOV, S. A., SHESTOPALOVA, S. A., UCHEVATKIN, I. F., SHATINSKIY, V. M.: Izv. Akad. Nauk SSSR, Ser. Fiz. 41(6), 1258 (1977).
- GORBACHEV, V. M., ZAMYATNIN, YU. S., LBOV, A. A.: *Vzaimodeistvie izlucheniya s yadrami tyazhelykh elementov i delenie yader* (Interaction of radiation with heavy element nuclei and nuclear fission). Moscow: Atomizdat 1976.
- HOFFMAN, D. C., FORD, G. P., BALAGNA, J. P., VEESER, L. R.: Phys. Rev. C21(2), 637 (1980).
- POLYUKHOV, V. G., TIMOFEEV, G. A., PRIVALOVA, P. A. *et al.*: At. Energ. 40(1), 61 (1976).
- AGGARWAL, S. K., JADHAV, A. V., CHITAMBER, S. A. *et al.*: Radiochem. Radioanal. Lett. 46(1/2), 69 (1981).
- GAY, R. R.: Thesis, Univ. Stanford, 1975. Nucl. Sci. Abstr. 32(7), 18679 (1975).
- GAY, R., SHER, R.: Natl. Bur. Stand. USA, spec. publ. N 425, 587 (1975) INIS Atomindex 7(20), 267516 (1976).
- STROHM, W. W., JORDAN, K. C.: Trans. Am. Nucl. Soc. 18(1), 185 (1974).

22. GUNN, S. R.: *Int. J. Appl. Radiat. Isot.* **29**(8), 497 (1978).
23. JAFFEY, A. H., DIAMOND, H., BENTLEY, W. C. *et al.*: *Phys. Rev. C* **16** (1), 354 (1977).
24. JAFFEY, A. H., DIAMOND, H., BENTLEY, W. C. *et al.*: *Int. J. Appl. Radiat. Isot.* **29** (8), 505 (1978).
25. LUCAS, L. L., NOYCE, J. R., COURSEY, B. M.: *Int. J. Appl. Radiat. Isot.* **29** (8), 501 (1978).
26. PRINDLE, A., EVANS, J., DUPZYK, R. *et al.*: *Int. J. Appl. Radiat. Isot.* **29** (8), 517 (1978).
27. SEABAUGH, P. W., JORDAN, K. C.: *Int. J. Appl. Radiat. Isot.* **29** (8), 489 (1978).
28. AGGARWAL, S. K., JAIN, H. C.: *Phys. Rev. C* **21** (5), 2033 (1980).
29. AGGARWAL, S. K., ACHARYA, S. N., PARAB, A. R., JAIN, H. C.: *Phys. Rev. C* **23** (4), 1748 (1981).
30. JACKSON, D. D., MARSH, S. F.: Report LA-UR-79-3190 (1979). *INIS Atomindex* **11** (11), 529131 (1980).
31. MARSH, S. F., ABERNATHEY, R. M., BECKMAN, R. J., REIN, J. E.: *Int. J. Appl. Radiat. Isot.* **31** (10), 629 (1980).
32. VANINBROUKX, R.: *INIS Atomindex* **11** (9), 520619 (1980).
33. AGGARWAL, S. K., ACHARYA, S. N., PARAB, A. R., JAIN, H. C.: *Phys. Rev. C* **20** (3), 1135 (1979).
34. MEADOWS, J. W.: Report ANL/NDM-38 (1977). *INIS Atomindex* **9** (16), 390809 (1978).
35. OSBORNE, D. W., FLOTOW, H. E.: *Phys. Rev. C* **14** (3), 1174 (1976).
36. POLYUKHOV, V. G., TIMOFEEV, G. A., PRIVALOVA, P. A., BAKLANOVA, P. F.: *At. Energ.* **36** (4), 319 (1974).
37. BROUN, L. C., PROPST, R. C.: *J. Inorg. Nucl. Chem.* **30** (10), 2591 (1968).
38. OETTING, F. L., GUNN, S. R.: *J. Inorg. Nucl. Chem.* **29** (11), 2659 (1967).
39. RAMTHUN, H., MILLER, W.: *Int. J. Appl. Radiat. Isot.* **26** (10), 589 (1975).
40. ZELENKOV, A. G., PCHELIN, V. A., RODIONOV, YU. F. *et al.*: *At. Energ.* **47** (6), 405 (1979).
41. AGGARWAL, S. K., PARAB, A. R., JAIN, H. C.: *Phys. Rev. C* **22** (2), 767 (1980).
42. POLYUKHOV, V. G.: *At. Energ.* **37** (4), 357 (1974).
43. GLAZOV, V. M., BORISOVA, R. I., SHAFIEV, A. I.: *At. Energ.* **37** (1), 78 (1974).
44. POLYUKHOV, V. G., TIMOFEEV, G. A., LEVAKOV, B. I.: *Radiokhimiya* **23** (6), 884 (1981).
45. MOZHAEV, V. K.: *At. Energ.* **40** (2), 174 (1976).
46. TSCHEBOLEV, V. T., RAMENDIK, Z. A., SHLYAMIN, E. A.: *At. Energ.* **36** (5), 399 (1974).
47. SPIEGEL, V.: *Nucl. Sci. Eng.* **53** (3), 326 (1974).
48. DE VOLPI, A., PORGES, K. G.: *Inorg. Nucl. Chem. Lett.* **5** (2), 111; (7), 699 (1969).
49. OETTING, F. L., RAND, M. H., ACKERMANN, R. G.: *The chemical thermodynamics of actinide elements and compounds*. Part 1. The actinide elements. IAEA, Vienna 1976.
50. SELEZNEV, A. G., SHUSHAKOV, V. D., KOSULIN, N. S.: *Fiz. Met. Metalloved.* **46** (5), 1109 (1978).
51. STEVENSON, J. N., PETERSON, J. R.: *J. Less-Common Met.* **66**, 201 (1979).
52. PETERSON, J. R., FAHEY, J. A., BAYBARZ, R. D.: *J. Inorg. Nucl. Chem.* **33** (10), 3345 (1971).
53. HAIRE, R. G., ASPREY, L. B.: *Inorg. Nucl. Chem. Lett.* **12** (1), 73 (1976).
54. WARD, J. W., OHSE, R. W., REUL, R.: *J. Chem. Phys.* **62** (6), 2366 (1975).
55. WARD, J. W., KLEINSCHMIDT, P. D., HAIRE, R. G.: In: *Actinides-1981*. Abstracts, 1981, Berkeley, p. 260.
56. HAIRE, R. G., BAYBARZ, R. D.: *J. Inorg. Nucl. Chem.* **36** (6), 1295 (1974).
57. WARD, J. W., MÜLLER, W., KRAMER, G. F.: In: *Transplutonium-1975*, p. 161.
58. WARD, J. W., KLEINSCHMIDT, P. D., HAIRE, R. G.: *J. Phys.* **40** (4), C4-333 (1979).
59. BAYBARZ, R. D., BOHET, J., BUIJS, K. *et al.*: In: *Transplutonium-1975*, p. 61.
60. NOE, M., PETERSON, J. R.: In: *Transplutonium-1975*, p. 69.
61. NUGENT, L. J., BURNETT, J. L., MORSS, L. R.: *J. Chem. Thermodyn.* **5** (5), 665 (1973).
62. HÜBNER, S.: *Radiochem. Radioanal. Lett.* **44** (2), 79 (1980).
63. TURCOTTE, R. P., HAIRE, R. G.: In: *Transplutonium-1975*, p. 267.
64. MORSS, L. R., FUGER, G., GOFFART, J., HAIRE, R. G.: In: *Actinides-1981*. Abstracts, 1981, Berkeley, p. 263.
65. BAYBARZ, R. D.: *J. Inorg. Nucl. Chem.* **35** (12), 4149 (1973).
66. SUDAKOV, L. V., KAPSHUKOV, I. I.: *Radiokhimiya* **17** (2), 316 (1975).
67. SUDAKOV, L. V., ERIN, E. A., BARANOV, A. YU. *et al.*: *Radiokhimiya* **17** (2), 200 (1975).
68. SUDAKOV, L. V., KAPSHUKOV, I. I., SHIMBAREV, E. V., BARANOV, A. YU.: *Radiokhimiya* **17** (3), 446 (1975).
69. KROT, N. N., GELMAN, A. D., MEFODYEVA, M. P. *et al.*: *Semivalentnoe sostoyanie neptuniya, plutoniya, ameritsiya* (Heptavalent state of neptunium, plutonium, americium). Moscow: Nauka Publishers 1977.
70. PERETRUKHIN, V. F., ERIN, E. A., DZYUBENKO, V. I. *et al.*: *Dokl. Akad. Nauk SSSR* **242** (6), 1359 (1978).
71. KOSYAKOV, V. N., TIMOFEEV, G. A., ERIN, E. A. *et al.*: *Radiokhimiya* **19** (1), 82 (1977).
72. KOSYAKOV, V. N., ERIN, E. A., VITYUTNEV, V. M. *et al.*: *Radiokhimiya* **24** (5) 551 (1982).
73. BOUISSIERES, G., JOUNIAUX, B., LEGOUX, Y. *et al.*: *Radiochem. Radioanal. Lett.* **45** (2), 121 (1980).
74. MIKHEEV, N. B., SPITSYN, V. I., KAMENSKAYA, A. N. *et al.*: *Dokl. Akad. Nauk SSSR* **208** (5), 1146 (1973).
75. MIKHEEV, N. B., KAMENSKAYA, A. N., SPITSYN, V. I. *et al.*: *Radiokhimiya* **23** (5), 736 (1981).
76. MOSKVIN, A. I.: *Koordinatsionnaya khimiya aktinoidov* (Coordination chemistry of actinides). Moscow: Atomizdat 1975.
77. KROT, N. N., SHILOV, V. P., NIKOLAEVSKIY, V. B. *et al.*: *Dokl. Akad. Nauk SSSR* **217** (3), 589 (1974).
78. NIKOLAEVSKIY, V. B., SHILOV, V. P., KROT, N. N., PERETRUKHIN, V. F.: *Radiokhimiya* **17** (3), 431 (1975).
79. SHILOV, V. P.: *Radiokhimiya* **18** (4), 659 (1976).
80. MYASOEDOV, B. F., KULYAKO, YU. M., SKLYARENKO, I. S.: *J. Inorg. Nucl. Chem.* **38** (4), 827 (1976).
81. DJACHKOVA, R. A., AUERMAN, L. N., MIKHEEV, N. B., SPITSYN, V. I.: *Radiokhimiya* **22** (3), 316 (1980).
82. SULLIVAN, J. C., GORDON, S., MULAC, W. A. *et al.*: *Inorg. Nucl. Chem. Lett.* **12** (8), 599 (1976).
83. PIKAEV, A. K., SHILOV, V. P., SPITSYN, V. I.: *Izv. Akad. Nauk SSSR, Ser. Chim.* (12), 2840 (1976).
84. GORDON, S., MULAC, W. A., SCHMIDT, K. H., SJOBLOM, R. K.: *Inorg. Chem.* **17** (2), 294 (1978).
85. SIMAKIN, G. A., KOSYAKOV, V. N., BARANOV, A. A. *et al.*: *Radiokhimiya* **19** (3), 366 (1977).
86. SIMAKIN, G. A., BARANOV, A. A., KOSYAKOV, V. N. *et al.*: *Radiokhimiya* **19** (3), 373 (1977).
87. MUSICAS, C., BERGER, R.: *Adv. Chem. Ser.* **71**, 296 (1967).
88. STOKELY, J. R., BAYBARZ, R. D., PETERSON, J. R.: *J. Inorg. Nucl. Chem.* **34** (1), 392 (1972).
89. KAZAKOVA, G. M., KOSYAKOV, V. N., ERIN, E. A.: *Radiokhimiya* **17** (2), 311 (1975).
90. BARANOV, A. A., SIMAKIN, G. A., ERIN, E. A. *et al.*: *Radiokhimiya* **21** (1), 59 (1979).
91. STOKELY, J. R., BAYBARZ, R. D., SHULTZ, W. D.: *Inorg. Nucl. Chem. Lett.* **5** (11), 877 (1969).
92. PROPST, R. C., HYDER, M. L.: *J. Inorg. Nucl. Chem.* **32** (7), 2205 (1970).
93. KULYAKO, YU. M., FRENKEL, V. YA., LEBEDEV, I. A. *et al.*: *Radiochim. Acta* **28** (3), 119 (1981).
94. YANIR, E., GIVON, M., MARCUS, Y.: *Inorg. Nucl. Chem. Lett.* **6** (4), 415 (1970).
95. LEBEDEV, I. A., FRENKEL, V. YA., KULYAKO, YU. M., MYASOEDOV, B. F.: *Radiokhimiya* **21** (6), 809 (1979).
96. LEBEDEV, I. A., FRENKEL, V. YA., KULYAKO, YU. M., MYASOEDOV, B. F.: *Radiokhimiya* **21** (6), 817 (1979).
97. SAPRYKIN, A. S., SPITSYN, V. I., KROT, N. N.: *Dokl. Akad. Nauk SSSR* **228** (3), 649 (1976).
98. BARANOV, A. A., SIMAKIN, G. A., KOSYAKOV, V. N. *et al.*: *Radiokhimiya* **23** (1), 127 (1981).
99. KULYAKO, YU. M., LEBEDEV, I. A., FRENKEL, V. YA. *et al.*: *Radiokhimiya* **23** (6), 839 (1981).
100. FEDOSEEV, A. M., PERETRUKHIN, V. F., KROT, N. N.: *Dokl. Akad. Nauk SSSR* **244** (5), 1187 (1979).
101. SIMAKIN, G. A., VOLKOV, YU. F., VISYATSCHEVA, G. I. *et al.*: *Radiokhimiya* **16** (6), 859 (1974).
102. SIMAKIN, G. A.: *Radiokhimiya* **19** (4), 518 (1977).

103. HOBART, D. E., SAMHOUN, K., BOURGES, J. Y. *et al.*: In: *Actinides-1981*. Abstracts, 1981, Berkeley, p. 269.
104. PERETRUKHIN, V. F., NIKOLAEVSKIY, V. B., SHILOV, V. P.: *Radiokhimiya* 16 (6), 833 (1974).
105. NIKOLAEVSKIY, V. B., SHILOV, V. P., KROT, N. N.: *Radiokhimiya* 16 (1), 122 (1974).
106. NIKOLAEVSKIY, V. B., SHILOV, V. P., KROT, N. N., PERETRUKHIN, V. F.: *Radiokhimiya* 17 (3), 426 (1975).
107. MYASOEDOV, B. F., MIKHAILOV, V. M., LEBEDEV, I. A. *et al.*: *Radiochem. Radioanal. Lett.* 14 (1), 17 (1973).
108. MYASOEDOV, B. F., LEBEDEV, I. A., MILYUKOVA, M. S.: *Rev. Chim. Miner.* 14 (2), 160 (1977).
109. MYASOEDOV, B. F., MILYUKOVA, M. S., LITVINA, M. N.: *Radiochem. Radioanal. Lett.* 25 (1), 33 (1976).
110. MILYUKOVA, M. S., LITVINA, M. N., MYASOEDOV, B. F.: *Radiokhimiya* 19 (3), 349 (1977).
111. LEBEDEV, I. A., MAZUR, YU. F., MYASOEDOV, B. F.: *Radiokhimiya* 20 (2), 207 (1978).
112. LITVINA, M. N., MALIKOV, D. A., MILYUKOVA, M. S., MYASOEDOV, B. F.: *Radiokhimiya* 22 (5), 653 (1980).
113. LEBEDEV, I. A., FRENKEL, V. YA., MYASOEDOV, B. F.: *Radiokhimiya* 19 (4), 570 (1977).
114. SAPRYKIN, A. S., SHILOV, V. P., SPITSYN, V. I., KROT, N. N.: *Dokl. Akad. Nauk SSSR* 226 (4), 853 (1976).
115. SAPRYKIN, A. S., SPITSYN, V. I., KROT, N. N.: *Dokl. Akad. Nauk SSSR* 231 (1), 150 (1976).
116. KOSYAKOV, V. N., TIMOFEEV, G. A., ERIN, E. A. *et al.*: *Radiokhimiya* 19 (4), 511 (1977).
117. SHILOV, V. P., BUKHTIYAROVA, T. N., SPITSYN, V. I., KROT, N. N.: *Radiokhimiya* 19 (4), 565 (1977).
118. ERIN, E. A., KOPYTOV, V. V., VASILYEV, V. YA., RYKOV, A. G.: *Radiokhimiya* 23 (5), 727 (1981).
119. MILYUKOVA, M. S., LITVINA, M. N., MYASOEDOV, B. F.: *Radiochem. Radioanal. Lett.* 44 (4), 259 (1980).
120. NIKOLAEVSKIY, V. B., SHILOV, V. P., KROT, N. N., PIKAEV, A. K.: *Radiokhimiya* 18 (3), 368 (1976).
121. PIKAEV, A. K., SHILOV, V. P., NIKOLAEVSKIY, V. B. *et al.*: *Radiokhimiya* 19 (5), 720 (1977).
122. PIKAEV, A. K., SHILOV, V. P., SPITSYN, V. I.: *Dokl. Akad. Nauk SSSR* 232 (2), 387 (1977).
123. HARA, M., SUZUKI, S.: *J. Radioanal. Chem.* 36 (1), 95 (1977).
124. MILYUKOVA, M. S., LITVINA, M. N., MYASOEDOV, B. F.: *Radiochem. Radioanal. Lett.* 42 (1), 21 (1980).
125. FRENKEL, V. YA., KULYAKO, YU. M., LEBEDEV, I. A., MYASOEDOV, B. F.: *Zh. Anal. Khimii* 34 (2), 330 (1979).
126. MYASOEDOV, B. F., LEBEDEV, I. A., FRENKEL, V. YA., VYATKINA, I. I.: *Radiokhimiya* 16 (6), 822 (1975).
127. VLADIMIROVA, M. V., RYABOVA, A. A., KULIKOV, I. A., MILOVANOVA, A. S.: *Radiokhimiya* 19 (5), 725 (1977).
128. HARA, M., SUZUKI, S.: *Bull. Chem. Soc. Japan* 52 (4), 1041 (1979).
129. ERMAKOV, V. A., FROLOV, A. A., RYKOV, A. G.: *Radiokhimiya* 21 (1), 68; (4), 615 (1979).
130. ERIN, E. A., KOPYTOV, V. V., RYKOV, A. G., KOSYAKOV, V. N.: *Radiokhimiya* 21 (1), 63 (1979).
131. KULIKOV, I. A., FRENKEL, V. YA., VLADIMIROVA, M. V. *et al.*: *Radiokhimiya* 21 (6), 839 (1979).
132. FRENKEL, V. YA., LEBEDEV, I. A., MYASOEDOV, B. F.: *Radiokhimiya* 22 (1), 75 (1980).
133. HARA, M., SUZUKI, S.: *Bull. Chem. Soc. Japan* 47 (3), 635 (1974).
134. FRENKEL, V. YA., LEBEDEV, I. A., TIKHONOV, M. F. *et al.*: *Radiokhimiya* 23 (6), 846 (1981).
135. FRENKEL, V. YA., LEBEDEV, I. A., KULYAKO, YU. M., MYASOEDOV, B. F.: *Radiokhimiya* 21 (6), 836 (1979).
136. MUSICAS, C.: *J. Inorg. Nucl. Chem.* 38 (1), 171 (1976).
137. DZYUBENKO, V. I., PERETRUKHIN, V. F.: *Radiokhimiya* 19 (6), 832 (1977).
138. CHISTYAKOV, V. M., ERMAKOV, V. A., MOKROUSOV, A. D., RYKOV, A. G.: *Radiokhimiya* 16 (6), 810 (1974).
139. OSIPOV, S. V., ANDREICHUK, N. N., VASILYEV, V. YA., RYKOV, A. G.: *Radiokhimiya* 19 (4), 522 (1977).
140. SPITSYN, V. I., IONOVA, G. V.: *Radiokhimiya* 20 (3), 328 (1978).
141. CHEPOVOY, V. I., LEBEDEV, I. A., MYASOEDOV, B. F.: *Radiokhimiya* 19 (4), 478 (1977).
142. CHEPOVOY, V. I., LEBEDEV, I. A., KULYAKO, YU. M., MYASOEDOV, B. F.: *Radiokhimiya* 22 (5), 658 (1980).
143. CHEPOVOY, V. I., LEBEDEV, I. A., MYASOEDOV, B. F.: *Radiokhimiya* 19 (2), 256 (1977).
144. MALIKOV, D. A., ALMASOVA, E. V., MILYUKOVA, M. S., MYASOEDOV, B. F.: *Radiochem. Radioanal. Lett.* 44 (5), 297 (1980).
145. SHAFIEV, A. I., EFREMOV, YU. V., YAKOVLEV, G. N.: *Radiokhimiya* 16 (1), 34 (1974).
146. MILYUKOVA, M. S., MALIKOV, D. A., MYASOEDOV, B. F.: *Radiochem. Radioanal. Lett.* 29 (3), 93 (1977).
147. ERIN, E. A., KOPYTOV, V. V., VITYUTNEV, V. M.: *Radiokhimiya* 18 (4), 514 (1976).
148. KOSYAKOV, V. N., YAKOVLEV, N. G., KAZAKOVA, G. M. *et al.*: *Radiokhimiya* 19 (4), 486 (1977).
149. MILYUKOVA, M. S., MALIKOV, D. A., MYASOEDOV, B. F.: *Radiokhimiya* 20 (6), 893 (1978).
150. ERIN, E. A., VITYUTNEV, V. M., KOPYTOV, V. V., VASILYEV, V. YA.: *Radiokhimiya* 21 (4), 560 (1979).
151. MIKHEEV, N. B., SPITSYN, V. I., DJACHKOVA, R. A., AUERMAN, L. N.: *Dokl. Akad. Nauk SSSR* 246 (3), 622 (1979).
152. MIKHEEV, N. B. *et al.*: The USSR Inventor's Certificate N 371780, 371781, 371782. *Izobreteniya v SSSR i za rubezhom* 49 (2), 1 (1980).
153. MIKHEEV, N. B., SPITSYN, V. I., KAMENSKAYA, A. N. *et al.*: *Inorg. Nucl. Chem. Lett.* 13 (12), 651 (1977).
154. DAVID, F., SAMHOUN, K., GUILLAUMONT, R.: *Rev. Chim. Miner.* 14 (2), 199 (1977).
155. SAMHOUN, K., DAVID, F., HAHN, R. L. *et al.*: *J. Inorg. Nucl. Chem.* 41 (12), 1749 (1979).
156. MIKHEEV, N. B., SPITSYN, V. I., KAMENSKAYA, A. N. *et al.*: *Radiochem. Radioanal. Lett.* 43 (2/3), 85 (1980).
157. MIKHEEV, N. B., KAMENSKAYA, A. N., BERDONOSOV, S. S., KLIMOV, S. I.: *Radiokhimiya* 23 (6), 793 (1981).
158. HULET, E. K.: Report UCRL-85169, 1980. *INIS Atomindex* 12 (7), 591083 (1981).
159. SILVA, R. J., MCDOWELL, W. J., KELLER, O. L., TARRANT, J. R.: *Inorg. Chem.* 13 (9), 2233 (1974).
160. MCDOWELL, W. J., KELLER, O. L., DITTNER, P. E. *et al.*: *J. Inorg. Nucl. Chem.* 38 (6), 1207 (1976).
161. DESCLAUX, J.-P., FRICKE, B.: *J. Phys. (Paris)* 41 (9), 943 (1980).
162. MYASOEDOV, B. F.: *J. Inorg. Nucl. Chem.* 38 (supplement), 151 (1976).
163. STOKELY, J. R., MOORE, F. L.: *Analyt. Chem.* 39 (8), 994 (1967).
164. MYASOEDOV, B. F., MOLOCHNIKOVA, N. P., LEBEDEV, I. A.: *Zh. Anal. Khim.* 26 (10), 1984 (1971).
165. HARA, M.: *Bull. Chem. Soc. Japan* 43 (1), 89 (1970).
166. MYASOEDOV, B. F., MOLOCHNIKOVA, N. P.: *Radiochem. Radioanal. Lett.* 18 (1), 33 (1974).
167. MYASOEDOV, B. F., MOLOCHNIKOVA, N. P., DAVIDOV, A. V.: *Radiokhimiya* 21 (3), 400 (1979).
168. MOLOCHNIKOVA, N. P., FRENKEL, V. YA., MYASOEDOV, B. F., LEBEDEV, I. A.: *Radiokhimiya* 24 (3), 303 (1982).
169. MYASOEDOV, B. F., MOLOCHNIKOVA, N. P., KUVATOV, YU. G., NIKITIN, YU. E.: *Radiokhimiya* 23 (1), 43 (1981).
170. MASON, G. W., BOLLMEIER, A. F., PEPPARD, D. F.: *J. Inorg. Nucl. Chem.* 32 (3), 1011 (1970).
171. ZANGEN, M.: *J. Inorg. Nucl. Chem.* 28 (8), 1693 (1966).
172. FARDY, J. J., BUCHANAN, J. M.: *J. Inorg. Nucl. Chem.* 38 (1), 149 (1976).
173. KOSYAKOV, V. N., YAKOVLEV, N. G., KAZAKOVA, G. M.: *Radiokhimiya* 21 (2), 262 (1979).
174. TIMOFEEV, G. A., LEVAKOV, B. I., VLADIMIROVA, N. A.: *Radiokhimiya* 17 (1), 124 (1975).
175. TIMOFEEV, G. A., LEVAKOV, B. I., ANDREEV, V. I.: *Radiokhimiya* 19 (4), 525 (1977).
176. MUSICAS, C., GERMAIN, M., BATHELLIER, G.: In: *Actinide separations*, 1980, p. 157.
177. BERNABEE, R. P., PERCIVAL, D. R., HINDMAN, F. D.: *Anal. Chem.* 52 (14), 2351 (1980).
178. KHOPKAR, P. K., MATHUR, J. N.: *J. Radioanal. Chem.* 60 (1), 131 (1980).
179. KOSYAKOV, V. N., YAKOVLEV, N. G., KAZAKOVA, G. M. *et al.*: *Radiokhimiya* 19 (4), 486 (1977).
180. MILYUKOVA, M. S., MALIKOV, D. A., KUZOVKINA, E.

- V., MYASOEDOV, B. F.: *Radiokhimiya* 25 (2), 173 (1983).
181. MILYUKOVA, M. S., MALIKOV, D. A., KUZOVKINA, E. V., MYASOEDOV, B. F.: *Radiochem. Radioanal. Lett.* 48 (6), 355 (1981).
  182. MILYUKOVA, M. S., MYASOEDOV, B. F.: *Radiokhimiya* 20 (3), 378 (1978).
  183. MILYUKOVA, M. S., MALIKOV, D. A., MYASOEDOV, B. F.: *Radiokhimiya* 22 (3), 352 (1980).
  184. MILYUKOVA, M. S., MALIKOV, D. A., MYASOEDOV, B. F.: *Radiochem. Radioanal. Lett.* 29 (3), 93 (1977).
  185. ERIN, E. A., VITYUTNEV, V. M., KOPYTOV, V. V., VASILYEV, V. YA.: *Radiokhimiya* 21 (1), 100 (1979).
  186. KOROTKIN, YU. S.: *Radiokhimiya* 23 (2), 174 (1981).
  187. KOROTKIN, YU. S.: *Radiokhimiya* 23 (2), 181 (1981).
  188. EL-SWEIFY, F., ALY, S. A.: *J. Radioanal. Chem.* 60 (2), 353 (1980).
  189. SHAFIEV, A. I., EFREMOV, YU. V.: *Radiokhimiya* 14 (5), 735 (1972).
  190. GUSEVA, L. I., LEBEDEV, I. A., MYASOEDOV, B. F., TIKHOMIROVA, G. S.: *J. Radioanal. Chem.* 38 (supplement), 55 (1976).
  191. LEBEDEV, I. A., MYASOEDOV, B. F., GUSEVA, L. I.: *J. Radioanal. Chem.* 21 (1), 259 (1974).
  192. GUSEVA, L. I., TIKHOMIROVA, G. S.: *J. Radioanal. Chem.* 52 (2), 369 (1979).
  193. ERIN, E. A., SHAFIEV, A. I., YAKOVLEV, G. N.: *Radiokhimiya* 17 (1), 93 (1975).
  194. MOORE, F. L.: *Anal. Chem.* 43 (3), 487 (1971).
  195. SHAFIEV, A. I., EFREMOV, YU. V., NIKOLAEV, V. M., YAKOVLEV, G. N.: *Radiokhimiya* 13 (1), 129 (1971).
  196. SHAFIEV, A. I., EFREMOV, YU. V., ANDREEV, V. I.: *Radiokhimiya* 15 (2), 265 (1973).
  197. SHAFIEV, A. I., EFREMOV, YU. V., YAKOVLEV, G. N.: *Radiokhimiya* 17 (4), 498 (1975).
  198. MYASOEDOV, B. F., BARSUKOVA, K. V.: *Radiochem. Radioanal. Lett.* 7 (5/6), 269 (1971).
  199. SHAFIEV, A. I., GONCHAROV, V. A., BEVZ, A. S., YAKOVLEV, G. N.: *Radiokhimiya* 14 (5), 778 (1972).
  200. HARA, M., SUZUKI, S.: *Bull. Chem. Soc. Japan* 48 (5), 1431 (1975).
  201. MIKHEEV, N. B., KAMENSKAYA, A. N., KONOVALOVA, N. A. *et al.*: *Radiokhimiya* 24 (3) (1982).
  202. MIKHEEV, N. B., KAMENSKAYA, A. N., MIKULSKI, J. *et al.*: *Radiokhimiya* 23 (6), 927 (1981).
  203. HOLM, E., FUKAI, R.: *Talanta* 23 (11/12), 853 (1976).
  204. HOLM, E., FUKAI, R.: *Talanta* 24 (11), 659 (1977).
  205. NOAKES, J. E., DUGGAN, J. L.: *J. Radioanal. Chem.* 43 (2), 399 (1978).
  206. BASOVA, B. G., RABINOVICH, A. D., POLYUKHOV, V. G., TIMOFEEV, G. A.: *Radiokhimiya* 21 (3), 430 (1979).
  207. AGGARWAL, S. K., ALMAULA, A. T., SHAH, P. M. *et al.*: *Radiochem. Radioanal. Lett.* 45 (1), 73 (1980).
  208. SILL, C. W., WILLIAMS, R. L.: *Anal. Chem.* 53 (3), 412 (1981).
  209. VECERNIK, J., SUS, F., KRTEL, J. *et al.*: *Radiochem. Radioanal. Lett.* 47 (5), 275 (1981).
  210. MATHEW, E., MATKAR, V. M., PILLAI, K. C.: *J. Radioanal. Chem.* 62 (1/2), 267 (1981).
  211. TALVITIE, N. A.: *Anal. Chem.* 44 (2), 280 (1972).
  212. JOSHI, S. R., ROY, J. C.: *Nucl. Instr. Methods* 115 (1), 303 (1974).
  213. KRESSIN, I. K.: *Analyt. Chem.* 49 (6), 842 (1977).
  214. RAMASWARI, A., DANGE, S. P., PRAKASH, S.: *Radiochim. Acta* 19 (1), 46 (1973).
  215. MÜLLEN, G., AUMANN, D. C.: *Nucl. Instrum. Methods* 128 (3), 425 (1975).
  216. KOROTKIN, YU. S.: *Radiokhimiya* 16 (3), 377 (1974).
  217. HARDCASTLE, J. E., LEVINE, N. E.: *Radiochim. Acta* 18 (1), 59 (1972).
  218. AMOUDRY, F.: *Analisis* 8 (10), 463 (1980).
  219. KARAVAEV, F. M.: *Izmereniya aktivnosti nuklidov* (Measurements of nuclide activity). Moscow: Standard Publ. 1972.
  220. KEOUGH, R. F., POWERS, G. J.: *Anal. Chem.* 42 (3), 419 (1970).
  221. KHOPKAR, P. K., MATHUR, J. N.: *J. Inorg. Nucl. Chem.* 42 (1), 109 (1980).
  222. HAM, G. J., STRADLING, G. N., BREADMORE, S. E.: *Anal. Chem.* 49 (8), 1268 (1977).
  223. KAPUSTIN, V. K., LEONOV, V. V., SOKOLIKOV, A. V.: *Radiokhimiya* 20 (1), 150 (1978).
  224. MARKOV, V. K., YABLOCHKIN, A. A., KRAPIVIN, M. I., NADEIN, V. I.: *Radiokhimiya* 18 (5), 751 (1976).
  225. PEVTSOV, V. V.: *Prib. Tekh. Eksp.*, (4), 78 (1976).
  226. PEVTSOV, V. V., TIMOFEEV, G. A.: *Radiokhimiya* 19 (4), 450 (1977).
  227. KRAPIVIN, M. I., LEBEDEV, I. A., MYASOEDOV, B. F. *et al.*: *Zh. Anal. Khim.* 33 (10), 1911 (1978).
  228. KRAPIVIN, M. I., LEBEDEV, I. A., MYASOEDOV, B. F. *et al.*: *Radiokhimiya* 21 (2), 321 (1979).
  229. MYASOEDOV, B. F., CHERNOV, G. M., MYAGKOV, A. P., LEBEDEV, I. A.: *Zh. Anal. Khim.* 28 (2), 294 (1973).
  230. CHEPOVOY, V. I., LEBEDEV, I. A., KAZAKOV, I. A., MYASOEDOV, B. F.: *Zh. Anal. Khim.* 33 (7), 1302 (1978).
  231. VORONKOV, A. A., KAZARINOV, N. M., KORENKOV, A. G., MAEVSKIY, V. A.: *Radiokhimiya* 20 (6), 924 (1978).
  232. BERDIKOV, V. V., TRIUMFOV, N. G., TSVETKOV, O. S.: *Radiokhimiya* 21 (2), 289 (1979).
  233. *Alpha-, beta- and gamma-ray spectroscopy*. Ed. SIEGBAHN, K., Amsterdam: North-Holland Publ. Company, 1965, v. 1.
  234. DITTNER, P. F., BEMIS, C. E.: *Phys. Rev. A* 5 (2), 481 (1972).
  235. MILLER, A. G.: *Anal. Chem.* 48 (1), 176 (1976).
  236. KLEYKAMP, H.: In: *Actinides-1981*. Abstracts, 1981, p. 298.
  237. BEMIS, C. E., TUBBS, L.: Report ORNL-5297, Oak-Ridge, 1977, p. 93.
  238. BUKLANOV, G. V., KHARITONOV, YU. P.: *At. Energ.* 48 (2), 106 (1980).
  239. AHMAD, I.: *Z. Phys. A* 290 (1), 1 (1979).
  240. CHETVERIKOV, A. P., GABESKIRIYA, V. YA., TIKHOMIROV, V. V.: *Radiokhimiya* 21 (1), 132 (1979).
  241. TIKHOMIROV, V. V., GABESKIRIYA, V. YA., CHETVERIKOV, A. P.: *Radiokhimiya* 23 (4), 595 (1981).
  242. TIKHOMIROV, V. V., CHETVERIKOV, A. P., GABESKIRIYA, V. YA.: *Radiokhimiya* 23 (6), 896 (1981).
  243. IVANOV, O. I., KRAINOV, E. V., SVIRIDOV, A. F.: *At. Energ.* 45 (3), 231 (1978).
  244. BABICH, S. I., ZAMYATNIN, YU. S., IVANOV, V. M. *et al.*: *Radiokhimiya* 22 (3), 442 (1980).
  245. ZAKHAROV, E. A., MYASOEDOV, B. F., LEBEDEV, I. A.: *Zh. Anal. Khim.* 30 (7), 1344 (1975).
  246. KOEHLI, G.: *Anal. Chim. Acta* 33 (4), 418 (1965).
  247. STOKELY, J. R., SHULTS, W. D.: *Anal. Chim. Acta* 45 (3/4), 417 (1969).
  248. PROPST, R. C.: *Anal. Chem.* 41 (7), 910 (1969).
  249. FRENKEL, V. YA., KULYAKO, YU. M., LEBEDEV, I. A. *et al.*: *Zh. Anal. Khim.* 35 (9), 1759 (1980).
  250. KULIKOV, I. A., FRENKEL, V. YA., VLADIMIROVA, M. V. *et al.*: *Radiokhimiya* 21 (6), 839 (1979).
  251. KULYAKO, YU. M., TROFIMOV, T. I., FRENKEL, V. YA. *et al.*: *Zh. Anal. Khim.* 36 (12), 2343 (1981).
  252. BERGEY, C., FOUCHARD, L.: *Talanta* 26 (6), 445 (1979).
  253. MCCRACKEN, J. E., STOKELY, J. R., BAYBARZ, R. D. *et al.*: *J. Inorg. Nucl. Chem.* 33 (10), 3251 (1971).
  254. LEBEDEV, I. A., MAKSIMOVA, A. M., STEPANOV, A. V., SHALINETS, A. B.: *Radiokhimiya* 9 (6), 707 (1967).
  255. PISKUNOV, E. M., RYKOV, A. G.: *Radiokhimiya* 14 (4), 638, 641 (1972).
  256. BUIJS, K., BARTSCHER, W.: *Anal. Chim. Acta* 88 (2), 403 (1977).
  257. TIMOFEEV, G. A., SIMAKIN, G. A., BAKLANOVA, P. F. *et al.*: *Zh. Anal. Khim.* 31 (12), 2337 (1976).
  258. SIMAKIN, G. A., TIMOFEEV, G. A., VLADIMIROVA, N. A.: *Radiokhimiya* 19 (4), 560 (1977).
  259. SIMAKIN, G. A., BAKLANOVA, P. F., KUZNETSOV, G. F., CHERNOV, A. V.: *Zh. Anal. Khim.* 29 (8), 1585 (1974).
  260. KORNILOV, A. C., CHISTYAKOV, V. M., FROLOV, A. A. *et al.*: *Radiokhimiya* 23 (5), 731 (1981).
  261. BARINOV, V. M., ADAIKIN, N. A., SAVCHENKO, V. E., FILIMONOV, V. T.: *Radiokhimiya* 21 (1), 121 (1979).
  262. TIKHOMIROV, V. V., CHETVERIKOV, A. P., GABESKIRIYA, V. YA.: *Radiokhimiya* 22 (3), 435 (1980).
  263. EDELINE, J. C.: *Analisis* 8 (10), 466 (1980).
  264. TSVETAeva, N. E., FEDOSEEV, D. A., IVANOVA, L. A. *et al.*: *Radiokhimiya* 21 (2), 252 (1979).

## Lower Oxidation States of Actinides

By N. B. MIKHEEV, Institute of Physical Chemistry of the Academy of Sciences of the USSR, Moscow, USSR

(Received January 4, 1982)

*Actinides / Lanthanides / Valency / Cocrystallization / Oxidation potentials*

### Abstract

The paper deals with the latest data on physico-chemical properties of actinides in the lower oxidation states. Based on the measurements of the oxidation potentials of  $Me^{3+}/Me^{2+}$  couples it was proved that elements of the first half of lanthanides and the second half of actinides are characterized by similar changes in the 2+ oxidation state stability with an increase in the atomic number of an element. For actinides in this oxidation state show likeness with alkaline-earth elements. Of all actinides, up to now only mendelevium has been obtained in the 1+ oxidation state. The ionic radius of  $Md^{1+}$ , equivalent to 1.20 Å, lies within the range of those of  $K^+$  and  $Na^+$ , while the solubility product of  $MdCl$  in aqua-ethanolic solutions is close to that of  $KCl$ . Based on these and other data a certain similarity between  $Md^{1+}$  and alkaline metal ions was established.

According to SEABORG's actinide concept in which the actinide group is viewed as a second rare-earth series the oxidation state 3+ cannot be considered a lower one for elements of the actinide series since the 3+ oxidation state is basic for rare-earth elements. At the same time, it should be mentioned that of the elements of the first half of actinides, from thorium to americium, only the last element was, until recently, known in the oxidation state 2+. On the contrary, elements of the first half of lanthanides from cerium to europium are known in the divalent state. Such dissimilarity between the two element groups contradicts the "pair analogy" of the two families, formulated by SEABORG in his actinide concept [1]. It is only the "americium-europium" pair which coincides with the "pair"-analogy" principle. Thus, when considering the problem of lower oxidation states of actinides prime attention should be given to the second half of this family, i.e. to the elements from curium to nobelium.

Elements of the second half of actinides, unlike those of the first one, are characterized by less availability and shorter half-lives. They have also been less studied. While it is possible to carry out studies on elements from curium to californium using ultramicrochemical techniques and to operate with small, though weighable, quantities of these elements, such studies become more difficult in the case of einsteinium; and for elements from fermium to nobelium the use of weighable quantities appears impossible. That is why only trace quantities and radiochemical techniques are used for studying the chemistry of far actinides.

There are cocrystallization, extraction, chromatographic (including gas chromatography), and electrochemical methods applied in investigating far actinides in the lower oxidation states. Each of them has its merits and disadvantages. It should be taken into consideration, when assessing

either of these methods, that only nobelium is quite stable in the oxidation state 2+. All the remaining actinides show negative values of the  $E_{Me^{3+}/Me^{2+}}^0$  couple and, being present in trace quantities, can maintain a lower oxidation state in the solution only in the presence of a reducer. For actinides in the oxidation states from 4+ to 2+ lanthanides in respective oxidation states are the best carriers. Because studies on lower valence forms of actinides not only require water solutions but also non-water ones, and melted salts in some cases, the use of extraction and chromatographic methods is limited. In this regard, the cocrystallization method seems most universal [2]. This method makes it possible to identify the oxidation state of an actinide, determine the standard oxidation potential value of the  $E_{Me^{3+}/Me^{(3-n)+}}^0$  couple, the complex stability constant, the solubility product of an actinide salt, its volatility, ionic radius and many other characteristics.

At the same time, the use of the cocrystallization method for solving the above-mentioned problems requires the determination of equilibrium values of the cocrystallization coefficients and the cocrystallization mechanisms. In other words, there is the problem of whether the cocrystallization occurs due to the formation of isomorphous solid solutions (when actinide microquantities and carrier macroquantities are in the same oxidation state) or to the formation of anomalous mixed crystals when heterovalent macro- and microcomponents enter into the solid phase matrix. The recently developed methods enable us to successfully solve this problem which ensures the application of the cocrystallization technique in studies on the chemistry of actinides in the lower oxidation states.

### Regularity of Stability Change for Divalent Actinides with an Increase in Atomic Number

In the late 1960-s American scientists carried out studies on observing divalent nobelium [3] and mendelevium [4]. It was established on the basis of ion-exchange chromatographic techniques that the main oxidation state of nobelium is 2+. As for mendelevium it followed, based on extraction chromatographic experiments and data on coprecipitation of mendelevium with barium sulphate, that mendelevium reduces from the 3+ oxidation state in the presence of V(II). Based on the coprecipitation of reduced mendelevium with  $BaSO_4$ , the authors [4] came to the conclusion that in these conditions mendelevium is present in the divalent state. They did not consider the possibility of cocrystallization of mendelevium 1+, though alkaline metal ions are known to cocrystallize with  $BaSO_4$

forming anomalous mixed crystals [5]. Since thulium and ytterbium-electron analogues of mendelevium and nobelium are known in the divalent state it should be admitted, according to SEABORG's "pair analogy" concept, that Cf(II) can possibly exist because its electron analogue, dysprosium(II) also exists.

To prove the possibility of existence of divalent actinides French scientists provided studies on actinides and lanthanides extraction into the amalgam phase of alkaline metals from water solutions containing organic acids [6--9]. The authors proceeded from the fact that europium, ytterbium and samarium which are easily reduced to the divalent state, comparatively quickly transit into the amalgam phase. It should be mentioned, however, that this process takes place in thermodynamically nonequilibrium conditions and is accompanied by free hydrogen formation which results in permanently increasing pH of the solution. The extraction mechanism is complex and inadequately studied. There are a lot of factors influencing the transition of a microelement into the amalgam phase: the stability of microelement-organic acid complexes, the stability of microelement hydroxocomplexes, the kinetics of decomposition of the first and of formation of the latter, the energy of amalgam formation by a microelement, the value of the oxidation potential of a microelement, and its possibility to form intermediate oxidation states. Thus, not only the ability of a microelement to be reduced to the divalent state but rather a multitude of factors influence the kinetics of the extraction of a microelement by an amalgam. Since all these factors influencing the extraction process are difficult to consider, sometimes unexpected results may appear. So it was found out that in the lanthanide series the elements not obtained in the divalent state such as lanthanum and cerium are extracted by an amalgam far better than neodymium and thulium. Therefore, if the last three elements were not obtained in the divalent state then according to the data on alkaline metal extraction by an amalgam, the wrong conclusion – that for these elements the oxidation state 2+ is not realized, might be drawn.

Now considering the actinide group, based on the data on extraction into the amalgam phase, one would admit that the existence of divalent plutonium is more likely than that of americium since plutonium is extracted by an amalgam twice as easily as americium [6–7]. At the same time, experiments provided with macroquantities of both elements prove opposite results. By now various compounds of divalent americium [10, 11] have been obtained while many attempts to obtain divalent plutonium have failed. The same high extraction levels of actinium and californium make it possible, if based on data of work [8], to conclude that while californium reduces to the divalent state actinium must exist in the oxidation state 2+. But this contradicts reality [12].

Thus, based on high levels of actinide and lanthanide extraction into the amalgam phase the possibility of the existence of the 2+ oxidation state for them can only be supposed but not definitely states. To study the possibility

of the existence of californium, einsteinium and fermium in the divalent state the method of cocrystallization of these elements with samarium dichloride from acid ethanolic solutions was used [13--17]. So it was established that californium, einsteinium, fermium, as well as strontium and some other actinides and lanthanides, present in microquantities, cocrystallize with the solid phase of samarium dichloride. The cocrystallization coefficient value for each studied element was calculated relative to the cocrystallization of  $^{85}\text{Sr}$  microquantities with  $\text{SmCl}_2$  according to the equation:

$$\ln \frac{a}{a-x} = \lambda \ln \frac{b}{b-y} \quad (1)$$

where  $a$  and  $b$  – the content of microelement and strontium in system,  $x$  and  $y$  – their quantities in the solid phase and  $\lambda$  – cocrystallization coefficient.

In the conditions of complicated oxidation-reduction reactions, occurring in the system studied, such approach to calculating cocrystallization coefficients ensured reliable experimental result interpretation since the microelement behaviour in the cocrystallization process was compared each time with that of strontium microquantities, whose state in the solution left no doubts.

The data obtained (see Table 1) show that not only lanthanides and actinides, which are known in the divalent state and whose cocrystallization can occur due to true isomorphism or isodimorphism, but also certain elements unknown in the divalent state, cocrystallize with samarium dichloride. Obviously, the cocrystallization of the latter occurs due to the formation of anomalous mixed crystals without the lower mixing limit. Thus, in order to differentiate cases when actinides and/or lanthanides cocrystallization occurs due to isomorphism and through the formation of anomalous mixed crystals it was necessary to use the methods which enable a distinction between the two types of cocrystallization processes.

It was shown based on HAHN's works [18] that isostructural salts have a similar ability to form anomalous mixed crystals. Therefore, it was necessary to provide cocrystallization of lanthanide and actinide microquantities with the solid phase of a salt isostructural to samarium dichloride, though different from it by the fact that when it cocrystallizes no sufficiently low oxidation potential at which reduction of actinides can be expected is achieved.

In this regard, a most appropriate salt is europium dichloride whose crystal lattice parameters differ from those of samarium dichloride as in hundredths of an angstrom [19]. At the same time, the oxidation potential  $E_{\text{Eu}^{3+}/\text{Eu}^{2+}}^0 = -0.35$  V while  $E_{\text{Sm}^{3+}/\text{Sm}^{2+}}^0 = -1.55$  V [20]. In other words, at the europium reduction potential all actinides and lanthanides (except europium) will be present in the trivalent state.

The results obtained are given in Table 1. It follows from Table 1 that Cf, Es, Fm and Yb do not cocrystallize with  $\text{EuCl}_2$  though they transit into the solid phase of  $\text{SmCl}_2$ . So at the  $\text{Eu}^{2+} \rightarrow \text{Eu}^{3+} + e^-$  reduction potential all the above-mentioned elements do not reduce to the

Table 1. *Cocrystallization coefficients with SmCl<sub>2</sub> and EuCl<sub>2</sub> of microquantities of some actinide and lanthanide elements in respect to strontium microquantities*

Cocrystallizing element	Cocrystallization coefficient in the solid phase	
	SmCl <sub>2</sub>	EuCl <sub>2</sub>
Eu	1.3 ± 0.2	—
Yb	0.28 ± 0.02	0.005 ± 0.001
Fm	1.0 ± 0.2	0.015 ± 0.001
Es	0.15 ± 0.01	0.006 ± 0.002
Cf	0.026 ± 0.003	0.006 ± 0.002
Np	0.46 ± 0.03	0.23 ± 0.07
Pu	0.40 ± 0.08	0.11 ± 0.03
Am	0.13 ± 0.03	0.070 ± 0.005
Cm	0.11 ± 0.02	0.11 ± 0.05
La	0.55 ± 0.05	0.64 ± 0.03
Ce	0.27 ± 0.08	0.43 ± 0.01
Gd	0.004 ± 0.001	0.003 ± 0.001
Y	0.004 ± 0.001	—

divalent state, nor do they cocrystallize with europium dichloride. However, at the potential of reduction of samarium to the divalent state these elements reduce to the 2+ oxidation state and cocrystallize with SmCl<sub>2</sub> due to true isomorphic or isodimorphic cocrystallization.

On the contrary La, Ce, Np, Pu, Am, and Cm cocrystallize both with EuCl<sub>2</sub> and SmCl<sub>2</sub> in the oxidation state 3+ due to the formation of anomalous mixed crystals [21, 22]. All these elements, however, show different inclination to form anomalous mixed crystals. For the actinide series, for example, the ability of elements to form anomalous mixed crystals both with SmCl<sub>2</sub> and EuCl<sub>2</sub> declines with an increase in the atomic number. This results in the decreasing of the cocrystallization coefficient for the Np → Cm row, and getting down to Cf and the next elements this ability completely disappears.

Besides this method of proving isomorphic cocrystallization of Cf, Es, and Fm with SmCl<sub>2</sub>, another one — the independent criterium — was used. Anomalous mixed crystals without the lower mixing limit are known, in the majority of cases, to have the upper mixing limit. This is connected with the fact that when entering into the crystal lattice of an anomalously cocrystallizing component Schottky defects, whose number is limited, appear which, in turn, leads to a limited intrusion of a heterovalent ion into the macrocomponent lattice. In such cases the cocrystallization coefficient of an anomalously cocrystallizing component decreases with an increase in its concentration [23]. This shows well in the case of the cocrystallization of NpCl<sub>3</sub> with SmCl<sub>2</sub> [21, 22] (Table 2).

Table 2. *Influence of <sup>237</sup>Np concentration on its cocrystallization coefficient with SmCl<sub>2</sub>*

<sup>237</sup> Np concentration (mg/ml)	Cocrystallization coefficient
microquantity	0.46 ± 0.03
0.025	0.24 ± 0.02
0.05	0.09 ± 0.01

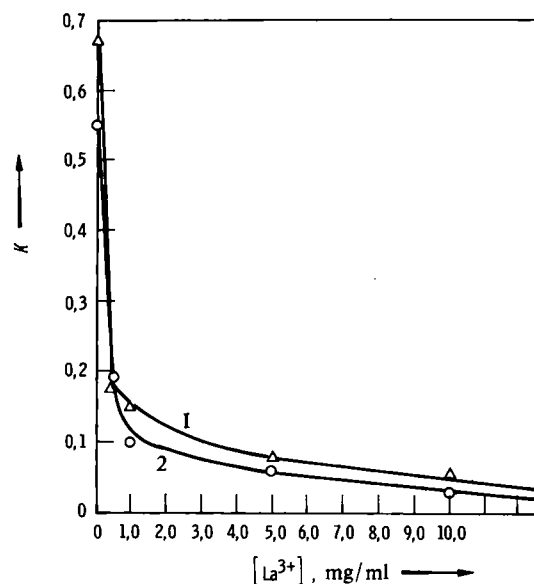


Fig. 1. The dependence of the coefficient of cocrystallization of LaCl<sub>3</sub> with SmCl<sub>2</sub> (1) and EuCl<sub>2</sub> (2) on its concentration

To prove the character of the cocrystallization of Cf, Es, and Fm with SmCl<sub>2</sub> the investigation on the dependence of the cocrystallization coefficient on the element concentration do not seem possible. However, it turned out possible to solve this problem by introducing LaCl<sub>3</sub> macroquantities into the system. Forming anomalous mixed crystals with SmCl<sub>2</sub> and EuCl<sub>2</sub> (Fig. 1) LaCl<sub>3</sub> competes with heterovalent elements leading to decreased coefficients of their cocrystallization. Nonetheless, the cocrystallization coefficient of isomorphically cocrystallizing components does not diminish (see Table 3). As it follows from Table 3, the coefficient of cocrystallization of Np, Pu, Am and Cm with SmCl<sub>2</sub> and EuCl<sub>2</sub> decreases in the presence of LaCl<sub>3</sub>, however, this does not occur in the case of Cf and Fm as well as Eu and Yb cocrystallization.

Table 3. *Cocrystallization coefficients with SmCl<sub>2</sub> of microquantities of some actinide and lanthanide elements in respect to cocrystallization of strontium microquantities*

Cocrystallizing microelement	Cocrystallization coefficients with SmCl <sub>2</sub> from the solution	
	without LaCl <sub>3</sub>	with concentration of La <sup>3+</sup> 1 mg/ml
Eu	1.3 ± 0.2	1.5 ± 0.3
Fm	1.0 ± 0.2	0.71 ± 0.1
Es	0.15 ± 0.01	0.26 ± 0.04
Cf	0.026 ± 0.003	0.048 ± 0.012
Np	0.46 ± 0.03	0.06 ± 0.01
Pu	0.40 ± 0.08	0.06 ± 0.01
Am	0.13 ± 0.03	0.04 ± 0.01
Cm	0.11 ± 0.02	0.007 ± 0.002
La	0.55 ± 0.05	0.15 ± 0.01
Ce	0.27 ± 0.08	0.06 ± 0.015
Gd	0.004 ± 0.007	0.003 ± 0.001
Y	0.004 ± 0.001	—

Thus, based on studies using two independent criteria, we can come to an explicit conclusion that Cf, Es and Fm cocrystallize with samarium dichloride by means of isomorphic cocrystallization i.e. these elements being present in the 2+ oxidation state.

The cocrystallization technique was also successfully applied for determining the  $E_{Me^{3+}/Me^{2+}}^0$  oxidation potentials for actinides. The use of this technique may be illustrated by determining  $E_{Fm^{3+}/Fm^{2+}}^0$  [24]. In order to solve this problem the cocrystallization of Fm(II) with  $SrCl_2$  was studied. The latter compound was precipitated by lithium chloride from the  $SrCl_2$ -saturated aqua-ethanolic solution containing Yb(II) as a reducer. So it was established that Fm(III) as well as Yb(II) and Yb(III) are not captured by the  $SrCl_2$  precipitate.

The HENDERSON-KRACEK equation could be used to calculate the coefficient of cocrystallization of Fm(II) with  $SrCl_2$  if full reduction of Fm(III) to Fm(II) and equilibrium between the crystal phase and the solution are achieved.

$$D = \frac{x_{FmCl_2} \cdot m_{SrCl_2}}{x_{SrCl_2} \cdot m_{FmCl_2}} \quad (2)$$

where  $x$  – the components content in the solid phase,  
 $m$  – the components quantity in the solution.

If under these conditions, fermium is only partly reduced to the divalent state its distribution coefficient is expressed by equation 3:

$$K = \frac{x_{FmCl_2} \cdot m_{SrCl_2}}{x_{SrCl_2} (m_{FmCl_2} + m_{FmCl_3})} \quad (3)$$

As it follows from equation 2 and 3,

$$\frac{1}{K} = \frac{1}{D} \left( 1 + \frac{m_{FmCl_3}}{m_{FmCl_2}} \right) \quad (4)$$

Therefore,

$$\frac{m_{FmCl_3}}{m_{FmCl_2}} = \frac{D}{K} - 1 \quad (5)$$

Because for the state of equilibrium

$$\begin{aligned} E_{Yb^{3+}/Yb^{2+}}^0 + \frac{RT}{F} \ln \frac{a_{YbCl_2}}{a_{YbCl_3}} &= \\ &= E_{Fm^{3+}/Fm^{2+}}^0 + \frac{RT}{F} \ln \frac{a_{FmCl_2}}{a_{FmCl_3}} \end{aligned}$$

it follows that

$$\begin{aligned} \exp \left( \frac{\Delta E_{Fm, Yb}^0}{RT/F} \right) &= \\ &= \frac{m_{FmCl_2} \cdot m_{YbCl_2}}{m_{YbCl_2} \cdot m_{FmCl_3}} \cdot \left( \frac{\gamma_{\pm FmCl_2}}{\gamma_{\pm YbCl_2}} \right)^3 \cdot \left( \frac{\gamma_{\pm YbCl_3}}{\gamma_{\pm FmCl_3}} \right)^4 \end{aligned} \quad (6)$$

With the help of equations 5 and 6 the difference between the oxidation potentials of fermium and ytterbium can be determined:

$$\Delta E_{Fm, Yb}^0 = E_{Fm^{3+}/Fm^{2+}}^0 - E_{Yb^{3+}/Yb^{2+}}^0$$

To do so it is necessary to know, besides  $D$ , the value of  $K$  which corresponds to respective ratios of  $Yb^{3+}/Yb^{2+}$  concentration in the solution. Table 4 shows  $K$  values at various  $Yb^{3+}/Yb^{2+}$  ratios.

The processing of experimental data, given in Table 4, by use of the least squares method gave the value of  $D = 0.55 \pm 0.05$  V and  $E_{Fm, Yb}^0 = 0.003 \pm 0.002$  V. It may be assumed, considering the closeness of the ionic radii of Fm and Yb in the same oxidation states, that the product of their activity coefficient ratios (Equation 6) is close to one. Even if to assume that the product of these ratios is in the interval of 0.5–2 the error in the difference of standard oxidation potentials of fermium and ytterbium would only be  $\pm 0.02$  V. Thus, since the standard oxidation potential  $E_{Yb^{3+}/Yb^{2+}}^0 = -1.15$  V it follows that the standard oxidation potential  $E_{Fm^{3+}/Fm^{2+}}^0 = 1.15 \pm 0.02$  V.

Table 4.  $K_{Fm, SrCl_2}$  values at different concentration relationship of bivalent and trivalent ytterbium

Relationship $m_{Yb^{3+}}/m_{Yb^{2+}}$	$K_{Fm, SrCl_2}$
0.088	$0.62 \pm 0.24$
0.091	$0.78 \pm 0.45$
0.130	$0.45 \pm 0.04$
0.160	$0.64 \pm 0.24$
1.57	$0.24 \pm 0.03$
2.87	$0.15 \pm 0.03$
10.20	$0.05 \pm 0.01$

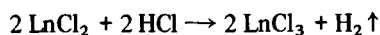
Getting back to the Table 1 data, one cannot help noticing an essential difference in the coefficients of cocrystallization of Cf, Es, and Fm with  $SmCl_2$ . This can only be accounted for by the fact that in the presence of Sm(II) Cf and Es, unlike fermium, do not completely reduce. Based on the Cf, Es, and Fm cocrystallization coefficient values we calculated oxidation potentials  $E_{Es^{3+}/Es^{2+}}^0 = -1.5$  V and  $E_{Cf^{3+}/Cf^{2+}}^0 = -1.6$  V [25].

Some time later the oxidation potential  $E_{Cf^{3+}/Cf^{2+}}^0$  was determined by American scientists [26] with the use of the polarography technique and operating with weighable quantities of californium. The value obtained by them  $E_{Cf^{3+}/Cf^{2+}}^0 = -1.58$  V is close to the value determined by us.

It is difficult to study the possibility of the existence of the oxidation state for elements with atomic number less than that of californium by using water and non-water solutions since the oxidation potential  $E_{An^{3+}/An^{2+}}^0$  for these elements is substantially lower than that of californium. In this regard, melted salt systems with divalent neodymium and praseodymium, acting as a reducer, were used in order to clarify the possibility of existence of the 2+ oxidation state for these elements.

As a result of studying many systems trivalent lanthanides and actinides were established to cocrystallize with lanthanide oxichlorides (LnOCl), however, oxichloride precipitates do not, practically, capture these elements in an oxidation state lower than 3+. So we can identify lower oxidation states of actinides and lanthanides and determine the standard oxidation potential value for the  $Me^{3+}/Me^{2+}$  couple based on the cocrystallization coefficient changes depending on the oxidation potential of the system.

Seemingly, it is important to consider the methodology of experimenting with melted salts. All the experiments were provided in hermetic molybdenum crucibles in argon atmosphere at the temperature of 1173°K. The mixture containing lanthanide oxichloride, di-, and trichlorides, the studied actinide or lanthanide, and  $SrCl_2$  (which was introduced to keep the constant  $Me^{3+}/Me^{2+}$  ratio in different experiments) were melted for 20 minutes. So, as a result of multiple recrystallization the oxichloride solid phase came in equilibrium with the melted salt phase. After cooling the crucible the content was taken out in an argon-filled chamber and dissolved in 0.1 M HCl. In these conditions an oxichloride of a rare-earth element does not dissolve while a lanthanide chloride, strontium chloride and a microelement portion, present in the melt phase, transit into the solution. The amount of divalent lanthanide was determined according to the hydrogen quantity formed, when the dichloride dissolving occurred as in the reaction:



An equilibrium distribution of the microcomponent between a lanthanide oxichloride and the melt containing lanthanide di- and trichloride mixture is described by the following equation:

$$K = \left[ \frac{An^{3+}}{Ln^{3+}} \right]_{LnOCl} \times \left[ \frac{Ln^{3+} + Ln^{2+}}{An^{3+} + An^{2+}} \right]_{melt} \quad (7)$$

The microcomponent distribution in the absence of reducer is described by a well-known HENDERSON-KRAČEK equation:

$$D = \left[ \frac{An^{3+}}{Ln^{3+}} \right]_{LnOCl} \times \left[ \frac{Ln^{3+}}{An^{3+}} \right]_{melt} \quad (8)$$

Based on equation 7 and 8 and NERNST's equation for the oxidation potential of a system, the difference of standard oxidation potentials  $\Delta E_{Ln, An}^0 = E_{Ln^{3+}/Ln^{2+}}^0 - E_{An^{3+}/An^{(3-n)^+}}^0$  and the number of electrons ( $n$ ) taking part in the reaction of microcomponent reduction  $An^{3+} + ne = An^{(3-n)^+}$ , can be determined according to equation 9:

$$\ln \left( \frac{1 + \frac{[Ln^{2+}]}{[Ln^{3+}]}}{K} - \frac{1}{D} \right) = n \ln \frac{[Ln^{2+}]}{[Ln^{3+}]} + \ln \frac{1}{D \exp \frac{\Delta E_{Ln, An}^0}{RT/nF}} \quad (9)$$

With the help of calculations it is possible to find the oxidation state of a reduced microelement and the difference in standard oxidation potentials  $\Delta E_{Ln, An}^0$ . Obviously, the closer the standard oxidation potentials of the potential-determining lanthanide and the studied microelement are, the smaller would be the error in determining  $\Delta E^0$ . In this regard, while studying Bk, Am, and Pu, Nd(II) was used as a reducer ( $E_{Nd^{3+}/Nd^{2+}}^0 = -2.62$  V [27]), and for studying Cm and Pu-Pr (2+) was chosen as a reducer ( $E_{Pr^{3+}/Pr^{2+}}^0 = -2.84 \pm 0.04$  V [28]). Finally as a result of numerous studies the existence of all elements from Bk to Pu in the oxidation state 2+ was established and the value of  $\Delta E^0$  for them was determined. The data obtained are given in Table 5.

Table 5. Difference of oxidation potentials  $\Delta E = E_{Me^{3+}/Me^{2+}} - E_{me^{3+}/me^{2+}}$  in molten salts (Me - macroelement, me - microelement)

Pairs of elements	$\Delta E = E_{Me^{3+}/Me^{2+}} - E_{me^{3+}/me^{2+}}$
Pr - Nd	-0.22 ± 0.04
Pr - Ce	+0.08 ± 0.04
Pr - Pu	-0.20 ± 0.01
Pr - Cm	-0.06 ± 0.02
Pr - Gd	+0.01 ± 0.03
Pr - Tb	-0.01 ± 0.03
Nd - Pm	-0.18 ± 0.03
Nd - Am	-0.34 ± 0.02
Nd - Bk	-0.10 ± 0.01
Nd - Pu	-0.04 ± 0.03

Table 6. Difference of oxidation potentials  $E_{Ln^{3+}/Ln^{2+}}$  of samarium, ytterbium and europium in aqueous solutions and melts

Pairs of elements	Difference of Oxidation Potentials	
	in solution	in melts
Sm - Yb	-0.40	-0.36
Sm - Eu	-1.20	-1.18
Yb - Eu	-0.80	-0.82

Based on the values of  $E_{Me^{3+}/Me^{2+}}^0$  and those of the standard oxidation potentials  $E_{Nd^{3+}/Nd^{2+}}^0$  and  $E_{Pr^{3+}/Pr^{2+}}^0$  it becomes possible to calculate the values of  $E_{Me^{3+}/Me^{2+}}^0$  for elements given in Table 5 if  $\Delta E^0$  for melts and water solutions is the same. In work [29] the values of oxidation potentials  $E_{Me^{3+}/Me^{2+}}^0$  for Eu, Yb, and Sm in systems containing melted chlorides were determined. As can be seen from Table 6 the  $\Delta E^0$  values obtained in systems with melted chlorides practically coincide with the  $\Delta E^0$  values obtained in water solutions for the same element couples. Thus, this gives ground to calculate  $E_{Me^{3+}/Me^{2+}}^0$  for all studied elements and to compile a table of the  $E_{Me^{3+}/Me^{2+}}^0$  standard oxidation potential values for actinides and lanthanides using the values of  $E_{Me^{3+}/Me^{2+}}^0$  obtained for water solutions, and  $\Delta E_{Me^{3+}/Me^{2+}}^0$  found for chloride melts (see Table 7).

The data on plutonium (3+) reduction to the divalent state are of special interest [30]. Attempts to obtain divalent plutonium by the interaction between melted

Table 7. Oxidation potential values  $E_{\text{Me}^{3+}/\text{Me}^{2+}}^{\circ}$  of actinides and lanthanides

Element	Experimental data	Nugent's data [38]	Element	Experimental data	Nugent's data [38]
Ac	Unknown	$-4.9 \pm 0.2$	La	Unknown	$-3.1 \pm 0.2$
Th	Unknown	$-4.9 \pm 0.2$	Ce	$-2.9 \pm 0.08$ [33]	$-3.2 \pm 0.2$
Pa	Unknown	$-4.7 \pm 0.2$	Pr	$-2.84 \pm 0.04$ [28]	$-2.7 \pm 0.2$
U	Unknown	$-4.7 \pm 0.2$	Nd	$-2.6$ [27]	$-2.6 \pm 0.2$
Np	Unknown	$-4.7 \pm 0.2$	Pm	$-2.44 \pm 0.02$ [31]	$-2.6 \pm 0.2$
Pu	$-2.6$ [30]	$-3.5 \pm 0.2$	Sm	$-1.55$ [20]	$-1.6 \pm 0.2$
Am	$-2.28 \pm 0.03$ [31]	$-2.3 \pm 0.2$	Eu	$-0.35$ [20]	$-0.3 \pm 0.2$
Cm	$-2.78 \pm 0.07$ [32]	$-4.4 \pm 0.2$	Gd	$-2.85 \pm 0.05$ [34]	$-3.9 \pm 0.2$
Bk	$-2.52 \pm 0.01$ [31]	$-2.8 \pm 0.2$	Tb	$-2.83 \pm 0.06$ [34]	$-3.7 \pm 0.2$
Cf	$-1.60$ [25, 26]	$-1.6 \pm 0.2$	Dy	$-2.45 \pm 0.2$ [35]	$-2.6 \pm 0.2$
Es	$-1.55$ [25]	$-1.3 \pm 0.2$	Ho	$-2.7 \pm 0.2$ [35]	$-2.9 \pm 0.2$
Fm	$-1.15$ [24]	$-1.1 \pm 0.2$	Er	$-2.8 \pm 0.2$ [35]	$-3.1 \pm 0.2$
Md	$-0.2$ [4]	$0 \pm 0.2$	Tm	$-2.3 \pm 0.2$ [38]	$-2.3 \pm 0.2$
No	$+1.5$ [38]	$+1.3 \pm 0.2$	Yb	$-1.15$ [20]	$-1.1 \pm 0.2$

metallic plutonium and its melted trichloride turned out unsuccessful [31]. In another work [32] the same system was used for reducing microquantities of Am(III) to Am(II). It was shown that melted metallic plutonium reduces Am(III) to the divalent state. Therefore, the electrode potential of the  $\text{Pu}^{3+}/\text{Pu}^0$  couple approximately equals  $E_{\text{Am}^{3+}/\text{Am}^{2+}}^{\circ} = -2.28$ . So using NERNST's equation we are able to assess the  $\text{Pu}^{3+}/\text{Pu}^{2+}$  ratio in equilibrium with melted metallic plutonium:

$$-2.28 = -2.6 + \frac{RT}{F} \ln \frac{[\text{Pu}^{3+}]}{[\text{Pu}^{2+}]} \quad (10)$$

This ratio  $\text{Pu}^{3+}/\text{Pu}^{2+} = 24.5$ . Thus, the melt of plutonium tri- and dichloride, being in equilibrium with melted metallic plutonium contains about 4 mole percent of plutonium dichloride.

Table 7 shows experimentally-obtained values of  $E_{\text{Me}^{3+}/\text{Me}^{2+}}^{\circ}$  and the oxidation potentials theoretically calculated by NUGENT [38] based on the excitation energy of an ion when transiting from an  $f^n$  into  $f^{n-1}d$  state. For a majority of actinides and lanthanides (see Table 7) the calculated and the experimentally obtained oxidation potential values satisfactorily coincide. Substantial differences between these two kinds of data for actinides are in the cases of Bk and Pu especially Cm and for lanthanides — in the cases of Gd, Tb and Ce. All these elements are characterized by relatively low values of the energy of excitation of double charged ions from an  $f^n$  into  $f^{n-1}d$  state. This causes delocalization of f-electrons which results in the appearance of metallic conductivity for  $\text{CeJ}_2$ ,  $\text{ThJ}_2$ , and some other dihalogenides in the solid phase.

The calculation of hybridization energy for divalent actinides [39] shows that for all elements from Bk to Md the sp-hybridization state is more preferable than the sd-state (Table 8). Because the difference between the sp- and sd-hybridization states is slight for Bk it, apparently, has along with the sp-hybridization also the spd- and sd-hybridizations. The appearance of the spd and/or sd-hybridization for near actinides would influence the geometrical shape of molecules. Instead of the linear shape

Table 8. Excitation (transition) energy  $s^2 \rightarrow sp$  and  $s^2 \rightarrow sd$  (Kcal/mole)

Transition	Bk	Cf	Es	Fm	Md
$s^2 \rightarrow sp$	49	51	54	55	57
$s^2 \rightarrow sd$	54	60	65	74	80

(corresponding to the sp-hybridization) the molecule would become angled. All the above-mentioned features cannot help leading to differences in chemical properties of near and far actinides in the same oxidation state 2+. Thus, similarities in chemical properties of divalent elements should, in the case of actinides, be expected in the row from Cf to No, and in the case of lanthanides — from Pr to Eu, and from Dy to Yb.

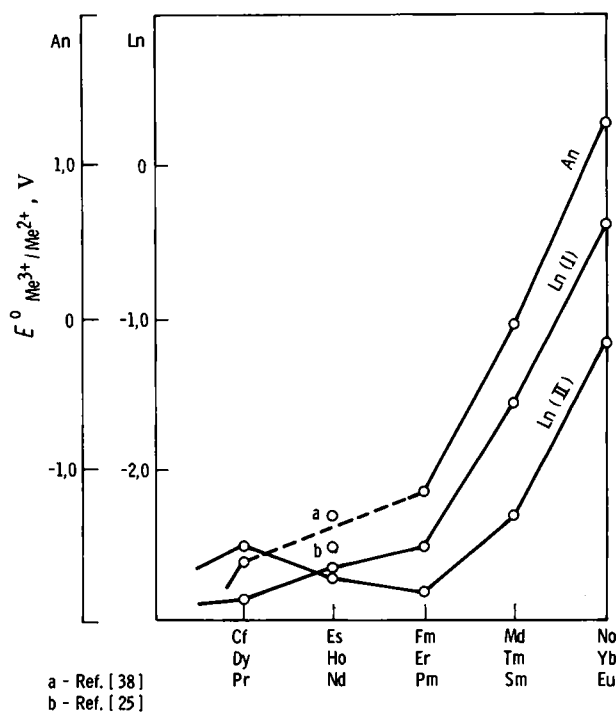


Fig. 2. Regularity of the change in the  $E_{\text{Me}^{3+}/\text{Me}^{2+}}^{\circ}$  with an increase in the atomic number for the second half of actinides, as well as for the first and second halves of lanthanides

Since lanthanide terms in  $f^n$  or  $f^{n+7}$  configurations coincide with those of actinides in an  $f^{n+7}$  configuration, the actinide group from Cf to No can be compared with elements of the second half of lanthanides from Dy to Yb. Fig. 2 shows changes in  $E_{\text{Me}^{3+}/\text{Me}^{2+}}^0$  with an increase in atomic number of an element for actinides and lanthanides.

It follows from the figure that elements of the second half of actinides and those of the first half of lanthanides complete likeness in the increase of the 2+ oxidation state stability with an increase in the atomic number of an element which is not observed when comparing the above-mentioned groups of elements with elements of the second half of lanthanides. The found regularity in likeness between elements of the first half of lanthanides and the second half of actinides is accounted for by a similar lowering of f-electron energy with an increase in the atomic number of an element. Therefore, it would be interesting to consider the f-electron energy change for lanthanide

Table 9. Transition energy of  $\text{Ln}^+$  from the  $f^{n+1}s^0$  electron configuration to  $f^n s^1$

Ln	n	$E_{\text{cal}} \cdot 10^{-3}$ $\text{cm}^{-1}$	$E_{\text{meas}} \cdot 10^{-3}$ $\text{cm}^{-1}$
La	1	-41.36	-40.959
Ce	2	-33.84	-34.341
Pr	3	-34.20	
Nd	4	-34.87	
Pm	5	-27.87	
Sm	6	-18.40	-18.289
Eu	7	-56.85	
Gd	8	-46.91	
Tb	9	-40.44	
Dy	10	-42.74	
Ho	11	-45.46	
Er	12	-39.79	
Tm	13	-30.71	

Table 10. Transition energy of  $\text{An}^+$  from the  $f^{n+1}s^0$  electron configuration to  $f^n s^1$

An	n	$E_{\text{cal}} \cdot 10^{-3}$ $\text{cm}^{-1}$
Ac	1	-38.4
Th	2	-29.9
Pa	3	-27.4
U	4	-25.3
Np	5	-17.8
Pu	6	-9.6
Am	7	-28.4
Cm	8	-18.7
Bk	9	-11.7
Cf	10	-11.4
Es	11	-11.5
Fm	12	-5.6
Md	13	+2.7

Table 11. Energy differences ( $\Delta E \cdot 10^{-3}, \text{cm}^{-1}$ ) of monocharged ions of lanthanides and actinides in the  $f^n s^1$  and  $f^{n+1} s^0$  states

Ln-An	$E_{\text{I-II}}$	Ln-Ln	$E_{\text{I-II}}$	An-An	$E_{\text{I-II}}$	Ln-An	$E_{\text{I-II}}$	Ln-An	$E_{\text{I-II}}$	Ln-An	$E_{\text{I-II}}$
La-Cm	-22.7	Gd-La	-5.55	Ac-Cm	-19.7	La-Ac	-2.9	Gd-Cm	-28.2	Gd-Ac	-8.5
Ce-Bk	-22.1	Tb-Ce	-6.60	Th-Bk	-18.2	Ce-Th	-3.9	Tb-Bk	-28.7	Tb-Th	-10.5
Pr-Cf	-22.8	Dy-Pr	-8.54	Pa-Cf	-16.0	Pr-Pa	-6.8	Dy-Cf	-31.3	Dy-Pa	-15.3
Nd-Es	-23.4	Ho-Nd	-10.59	U-Es	-13.8	Nd-U	-9.6	Ho-Es	-34.0	Ho-U	-20.2
Pm-Fm	-22.3	Er-Pm	-11.92	Np-Fm	-12.2	Pm-Np	-10.1	Er-Fm	-34.2	Er-Np	-22.0
Sm-Md	-21.1	Tm-Sm	-12.34	Pu-Md	-12.3	Sm-Pu	-8.8	Tm-Md	-33.4	Tm-Pu	-21.1

and actinide single charged ions [40] when changing from an  $f^{n+1} s^0$  into  $f^n s^1$  configuration with an increase in the atomic number of an element (see Tables 9 and 10). It follows from Tables 9 and 10 that an  $f^n s^1$  configuration is more preferable than  $f^{n+1} s^0$  for single charged ions of all lanthanides and actinides with the exception of mendelevium. Since a one unpaired s-electron configuration characterizes high reaction ability of an atom the obtaining of a monovalent state of all lanthanides and most actinides (except for mendelevium and, possibly, fermium) in condensed media is hard to expect. However, apart from the problem of the possibility of existence of monovalent lanthanides and actinides in condensed media the  $f^{n+1} s^0 \rightarrow f^n s^1$  transition energy characterizes the energetics of an f-level of a single charged atom.

The energy differences ( $\Delta E, 10^3 \text{ cm}^{-1}$ ) of lanthanide and actinide single charged ions in configurations  $f^{n+1} s^0$  and  $f^n s^1$  are given in Table 11. As seen from Table 11, the excitation energy differences for respective ions of the first half of lanthanides and the second half of actinides maintain a higher constancy than in the case of elements of the second halves of both groups.

Thus, irrespective the charge of an atom the energy of f-electrons similarly change with an increase in the atomic number for elements of the first half of lanthanides and the second half of actinides. So the studies on regularities of stability change of lower oxidation states of An and Ln with an increase in the atomic number of an element made it possible to solve the problem of "pair analogy" between actinides and lanthanides, however, differently from what SEABORG had predicted [1], believing the elements of the second halves of actinides and lanthanides to be the closest analogues.

#### Ionic Radii of Actinides in the Lower Oxidation States

Because chemical properties of an element in a certain valence state depend on its ionic radius we provided calculations of the ionic radii of actinides in the lower oxidation states [41]. These calculations were based on the ionic radius value of  $\text{Ln}^{3+}$ ,  $\text{An}^{3+}$ , and limited and insufficiently reliable data on the ionic radii of  $\text{Am}^{2+}$  [10] and  $\text{No}^{2+}$  [42, 43]. In this connection it seemed advantageous to carry out calculations of ionic radii of actinides in the lower oxidation states using most reliable data of work [44].

Quantum chemical methods are known to enable calculation of the distance from a nucleus to the part of an ion where the maximum electron density is realized ( $R_{\text{max}}$ ). SLATER established [45] that the value of  $R_{\text{max}}$  for single

charged ions is related to the ionic radius of an element by a simple equation:

$$R = Cn \cdot R_{\max} \quad (11)$$

It may be assumed that the Cn value remains constant for f-elements within one series and in the same oxidation state. To prove this statement we used the ionic radii values of lanthanides in the oxidation state 3+ (coordination

Table 12. Cn coefficient values for Ln<sup>3+</sup>

Element	Ionic radius Å	R <sub>max</sub> Å	Cn
Ce	1.01	0.82	1.23
Pr	0.99	0.81	1.22
Nd	0.98	0.79	1.24
Pm	0.97	0.78	1.25
Sm	0.96	0.77	1.25
Eu	0.95	0.76	1.25
Gd	0.94	0.74	1.27
Tb	0.92	0.73	1.26
Dy	0.91	0.72	1.26
Ho	0.90	0.71	1.27
Er	0.89	0.70	1.27
Tm	0.88	0.69	1.27
Yb	0.87	0.68	1.28

Table 13. Cn coefficient values for Ln<sup>2+</sup>

Element	Ionic radius (Å)	R <sub>max</sub> (Å)	Cn
Eu	1.17	0.76	1.54
Dy	1.07	0.72	1.49
Tm	1.03	0.69	1.49
Yb	1.02	0.68	1.50

Table 14. Ionic radii values of An<sup>3+</sup>

An	Ionic radius of An <sup>3+</sup> (Å)		R <sub>max</sub> (Å)	Cn
	from work [44]	calculated values		
Pu	1.00	—	0.84	1.190
Am	0.975	—	0.83	1.175
Cm	0.97	—	0.82	1.183
Bk	0.96	—	0.81	1.185
Cf	0.95	—	0.80	1.187
Es	—	0.94	0.79	
Fm	—	0.94 (0.93)	0.79	
Md	—	0.92	0.78	
No	—	0.91	0.77	

Table 15. Calculated values of ionic radii of An<sup>2+</sup> (coordination number 6), Cn = 1.34

An <sup>2+</sup>	R <sub>max</sub> Å	Ionic radius (Å)
Pu	0.89	1.19
Am	0.88	1.18
Cm	0.87	1.16
Bk	0.86	1.15
Cf	0.80	1.07
Es	0.79	1.06
Fm	0.79	1.06
Md	0.78	1.045
No	0.77	1.03

number = 6) [44] and HARTREE-FOCK R<sub>max</sub> [46]. The data obtained through calculations are given in Table 12. As it is clear from Table 12 the Cn value remains constant for all lanthanide elements in the trivalent state.

Similar calculations were also made for Ln<sup>2+</sup> using relatively limited data on the Ln<sup>2+</sup> ionic radii (corresponding to the same coordination number 6) [44] and the R<sub>max</sub> values for Ln<sup>2+</sup> [46]. In this case the Cn constancy is also observed (see Table 13).

The constancy of Cn values obtained for lanthanides gives ground for calculating ionic radii of actinides in various oxidation states. Firstly, we made this calculation only for trivalent actinides using the known ionic radii values (*c. n.* = 6) [44], and R<sub>max</sub> values [46] (see Table 14). As can be seen from Table 14, the Cn coefficient remains constant for all elements from plutonium to californium. With the use of this coefficient, we calculated ionic radii of An<sup>3+</sup> from Es to No. Unfortunately, the data on An<sup>2+</sup> ionic radii are limited to those of americium. Am<sup>2+</sup> ionic radius (*c. n.* = 6) is equivalent to 1.18 Å [44]. Using this value and R<sub>max</sub> = 0.88 Å we obtained Cn = 1.34. Based on the latter we calculated ionic radii of An<sup>2+</sup> (see Table 15). The obtained value of nobelium ionic radius coincides with the authors of [42, 43] idea that nobelium holds an intermediate position between calcium and strontium in regard to the ionic radius.

PAULING's equation can be used to calculate the ionic radii of actinide single charged ions [47]:

$$R^{Z+1} = R^{1+} \cdot Z^{-\frac{2}{n-1}} \quad (12)$$

where R – ionic radius, Z – ion charge, n – BORN's repulsion coefficient (*n* = 9). Using the No<sup>2+</sup> ionic radius, isoelectronic with Md<sup>+</sup>, it is possible through equation 12 to calculate the Md<sup>1+</sup> ionic radius, which is equivalent to 1.22 Å. Besides, the Fm<sup>1+</sup> ionic radius can also be calculated through equation 12 and using the No<sup>3+</sup> ionic radius, since No<sup>3+</sup> as well as Fm<sup>1+</sup> have a 5f<sup>13</sup> electron configuration. It appeared that R(Fm<sup>1+</sup>) = 1.20 Å. Using R<sub>max</sub> for Fm<sup>1+</sup> [46], equivalent to 0.84, it is possible to determine Cn = 1.43. Because R<sub>max</sub> for Md<sup>+</sup> equals 0.83, R(Md<sup>1+</sup>) = 1.19 Å.

Thus, using the No<sup>2+</sup> and No<sup>3+</sup> ionic radii for the above-mentioned calculations we obtained well coinciding Md<sup>1+</sup> ionic radius values which, in turn, proves the accordance between the ionic radii of di- and trivalent actinides. The used calculation schemes enable, apparently, the determination of ionic radii of other actinides in the 1+ oxidation state and an f<sup>n+1</sup>s<sup>0</sup> electron configuration, however, it makes sense only if these elements can, in general, exist in the monovalent state in condensed media.

### Monovalent Mendelevium and its Physico-Chemical Properties

Based on the studies on cocrystallization of Md with alkaline metal salts it was established [48, 49] that mendelevium can exist in the 1+ oxidation state in aqua-

ethanolic solutions. The existence of monovalent mendelevium, discovered in this work and proved by further investigations thereafter [50–52], coincides with the theoretical calculations by VANDER SLUIS and NUGENT [40]. According to these Md(I) in the main free ion state has an  $f^{n+1}s^0$  configuration, and its transition into the first excited state ( $f^n s^1$ ) requires an excitation energy equivalent to  $2.7 \cdot 10^3 \text{ cm}^{-1}$ . Unlike mendelevium, for all actinides with a lower atomic number an  $f^n s^1$  configuration is the main state, and a transition from it into an  $f^{n+1}s^0$  state requires excitation energy equivalent to  $5.6 \times 10^3 \text{ cm}^{-1}$  for fermium and about  $11.5 \times 10^3 \text{ cm}^{-1}$  for einsteinium, californium and berkelium (see Table 10). That is why the 1+ oxidation state in an  $f^{n+1}s^0$  configuration is expected to be realized much harder for actinides with an atomic number lower than that of mendelevium.

In order to study the possibility of existence of Md(I) the cocrystallization technique is most frequently used. However, it is impossible to formulate an explicit conclusion about the oxidation state of an element based purely on the fact of its cocrystallization. It was established, for instance, that Md cocrystallizes with samarium dichloride. From this fact a conclusion was drawn that at the  $\text{Sm}^{2+}$  potential mendelevium is present in the divalent state [53]. And the fact that cesium also cocrystallized with samarium dichloride in the same experiments was ignored. If the precipitation of RbCl is provided along with the crystallization of  $\text{SmCl}_2$  the coefficient of cocrystallization of Md with RbCl turns out about tenfold higher than that of  $\text{Fm}^{2+}$  [53]. Thus analyzing the results of the cocrystallization of Md with  $\text{SmCl}_2$  and RbCl we come to a completely opposite conclusion that at the  $\text{Sm}^{2+}$  potential Md reduces to the 1+ oxidation state.

In the same work [53] data on the cocrystallization of Md with samarium difluoride are given. Based on these data the authors also drew the conclusion about the nonobservance of  $\text{Md}^{1+}$ . Deriving from the assumption that  $\text{Md}^{2+}$  cocrystallizes with  $\text{SmF}_2$  it follows, according to the isomorphic cocrystallization theory that the Md cocrystallization coefficient should not depend on the  $\text{Sm}^{2+}$  concentration in the solution:

$$\text{SmF}_{2(\text{S})} + \text{MdF}_{2(\text{L})} \rightleftharpoons \text{MdF}_{2(\text{S})} + \text{SmF}_{2(\text{L})}$$

$$K = \frac{\text{MdF}_{2(\text{S})} \cdot [\text{Sm}^{2+}] \cdot [\text{F}^-]^2 \cdot (\gamma_{\pm \text{SmF}_2})^3}{\text{SmF}_{2(\text{S})} \cdot [\text{Md}^{2+}] \cdot [\text{F}^-]^2 \cdot (\gamma_{\pm \text{MdF}_2})^3} \quad (13)$$

Because the cocrystallization coefficient equals:

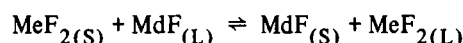
$$D = \frac{\text{MdF}_{2(\text{S})} \cdot [\text{Sm}^{2+}]}{\text{SmF}_{2(\text{S})} \cdot [\text{Md}^{2+}]} \quad (14)$$

it follows that:

$$D = K \frac{(\gamma_{\pm \text{MdF}_2})^3}{(\gamma_{\pm \text{SmF}_2})^3} \quad (15)$$

Since the ratio of activity coefficients of components in the region of diluted solutions is close to one,  $D = K$ ,

the  $\text{Md}^{2+}$  cocrystallization coefficient is a constant value which does not depend on the  $\text{Sm}^{2+}$  concentration in the solution. Actually, the coefficient of cocrystallization of Md with  $\text{SmF}_2$  and  $\text{YbF}_2$  grows with an increase in the  $\text{Me}^{2+}$  concentration [52], which contradicts the conditions of isomorphic cocrystallization of  $\text{Md}^{2+}$  with  $\text{MeF}_2$ . However, this dependence caters to the formation of anomalous mixed crystals  $\text{MeF}_2 - \text{MeF}$ . Deriving from a heterogeneous reaction



we obtain:

$$D = K \cdot \frac{(\gamma_{\pm \text{MdF}})^2}{(\gamma_{\pm \text{MeF}_2})^3} \cdot \frac{1}{[\text{F}^-]} \quad (16)$$

Because  $AP_{\text{MeF}_2} = [\text{Me}^{2+}] \cdot [\text{F}^-]^2 \cdot (\gamma_{\pm \text{MeF}_2})^3$

$$D = K' \cdot \frac{(\gamma_{\pm \text{MdF}})^2}{(\gamma_{\pm \text{MeF}_2})^{3/2}} \cdot \sqrt{[\text{Me}^{2+}]} \quad (17)$$

Figure 3 shows the dependence of the coefficient of cocrystallization of Md with  $\text{SmF}_2$  and  $\text{YbF}_2$ , and that of  $\text{Ag}^{1+}$  with  $\text{SrF}_2$  on the  $\text{Me}^{2+}$  concentration. As follows from Figure 3, a satisfactory correspondence of experimental data with the cocrystallization coefficient change regularities (expressed by equation 17) is observed for all the three systems. It proves that monovalent mendelevium cocrystallizes with  $\text{SmF}_2$  and  $\text{YbF}_2$ .

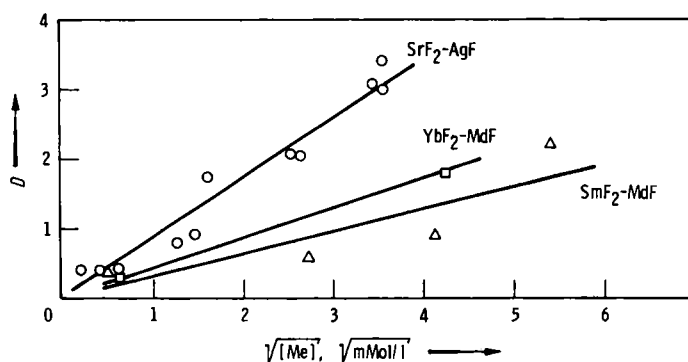
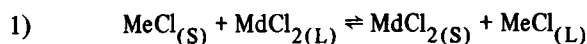
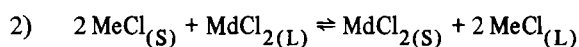


Fig. 3. The dependence of the coefficient of cocrystallization ( $D$ ) of  $\text{Ag}^+$  and  $\text{Md}^+$  with  $\text{MeF}_2$  on the  $\text{Me}^{2+}$  concentration

Because the  $\text{Md}^{1+}$  ionic radius equivalent to 1.20 Å, lies within the range of those of potassium (1.37 Å) and sodium (1.02 Å) [44], the cocrystallization of Md with NaCl and KCl in aqua-ethanolic solutions was studied [57]. It appeared that trivalent Md, Fm and Es are not, practically, captured by the solid phase of potassium and sodium halogenides. HULET believes that Md reduces to the divalent state in the presence of divalent europium [4], however, unlike  $\text{Eu}^{2+}$ ,  $\text{Sr}^{2+}$  and  $\text{Yb}^{2+}$ , Md acquires an ability to cocrystallize with NaCl and KCl. If it is assumed that Md cocrystallizes with NaCl and KCl in the divalent state then its distribution between the phases should be accounted for by one of the exchange reactions:



This process is accompanied by the intrusion of an anion into the lattice interstitial areas and by the formation of Frenkel defects.



which is related to the formation of Schottky defects in the cation part of the lattice.

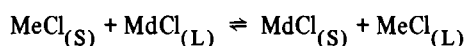
Here, value  $D$  is expressed respectively by the following equations:

$$D = K_1 \cdot \frac{(\gamma_{\pm \text{MdCl}_2})^3}{(\gamma_{\pm \text{MeCl}})^2} \cdot [\text{Cl}^-] \quad (18)$$

$$D = K_2 \cdot \frac{(\gamma_{\pm \text{MdCl}_2})^3}{(\gamma_{\pm \text{MeCl}})^4} \cdot \frac{1}{[\text{Me}^+]} \quad (19)$$

Because  $AP_{\text{MeCl}} = [\text{Me}^+] \cdot [\text{Cl}^-] \cdot (\gamma_{\pm \text{MeCl}})^2$ , equation 18 is identical to equation 19. Therefore, despite the mechanism of the anomalous mixed crystal formation the  $\text{An}^{2+}$  cocrystallization coefficient is described by one and the same equation 18.

On the contrary, if Md cocrystallizes with NaCl and KCl in the monovalent state its cocrystallization will be accounted for by the reaction:



and the cocrystallization coefficient will be as in equation 20:

$$D = K \cdot \frac{(\gamma_{\pm \text{MdCl}})^2}{(\gamma_{\pm \text{MeCl}})^2} \quad (20)$$

As shown in work [54] the activity coefficients of KCl and NaCl in solutions of equal ionic strength are, practically, the same within the ionic strength change up to 2–3. Since the  $\text{Md}^{1+}$  ionic radius lies within the range of those of  $\text{K}^+$  and  $\text{Na}^+$  it follows that  $\gamma_{\pm \text{NaCl}} \approx \gamma_{\pm \text{MdCl}} \approx \gamma_{\pm \text{KCl}}$ , so the equation becomes simpler:

$$D = K = \text{const.}$$

Therefore, if monovalent mendelevium cocrystallizes with NaCl and KCl its cocrystallization coefficient does not depend on the chloride-ion concentration. Thus, the determination of the dependence of the coefficient of cocrystallization of reduced forms of actinides with KCl and NaCl on the chloride-ion concentration enables to explicitly distinguish  $\text{An}^{2+}$  from  $\text{An}^{1+}$ .

In work [51] data are given on cocrystallization of Md with NaCl and KCl in aqua-ethanolic solutions in the presence of  $\text{Eu}^{2+}$  as a reducer.

In work [55] the cocrystallization of Fm with KCl in the same conditions, but with  $\text{Sm}^{2+}$  as a reducer, was studied. Fig. 4 shows the influence of the chloride-ion concentration on the value of the coefficient of cocrystallization of Md and Fm with MeCl. As seen from Fig. 4, the coefficient of cocrystallization of Md with NaCl and KCl does not depend on the chloride-ion concentration

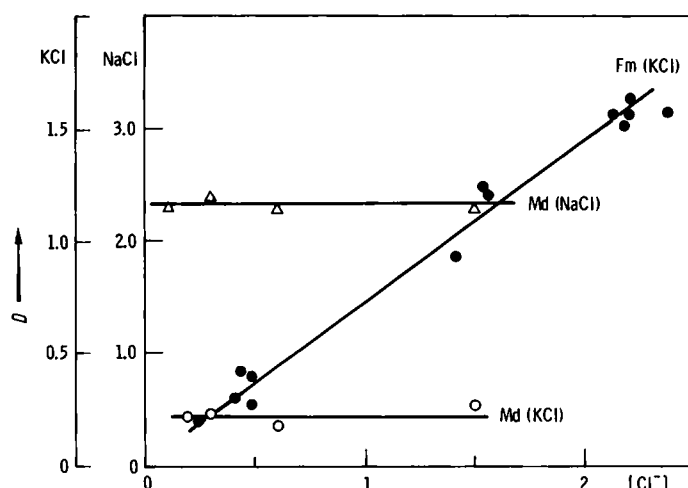


Fig. 4. The influence of the change in the chloride-ion concentration on the values of the coefficients of cocrystallization of Md and Fm with MeCl

while the  $\text{Fm}^{2+}$  cocrystallization coefficient linearly grows with an increase in the chloride-ion concentration. So a conclusion follows that in the presence of  $\text{Eu}^{2+}$  mendelevium reduces to the oxidation state 1+ and isomorphically cocrystallizes with alkaline metal halogenides. Unlike Md, Fm in the presence of  $\text{Sm}^{2+}$  reduces only to the divalent state and its cocrystallization with KCl is accounted for by the formation of anomalous mixed crystals.

We can, based on the data of Fig. 4, make another important conclusion. Because the lowering of the cocrystallization coefficient with an increase in the chloride-ion concentration is not observed it follows that neither  $\text{Md}^{1+}$  nor  $\text{Fm}^{2+}$  form stable chloride complexes.

Based on the values of the coefficient of cocrystallization of mendelevium with NaCl and KCl, respectively equivalent to  $2.2 \pm 0.4$  and  $0.22 \pm 0.03$ , we can calculate the ionic radius of  $\text{Md}^{1+}$  and the solubility product of MdCl. As proved by URUSOV [56–57], the cocrystallization coefficient ( $D$ ) is related to the solubility product (SP) of macrocomponent (1) and microcomponent (2) and to their interatomic distances ( $R$ ) in the following way:

$$\lg D = \lg \frac{\text{SP}_1}{\text{SP}_2} - \frac{(t-T)a}{2.303 R_G t T} \left( \frac{R_1 - R_2}{R_1} \right)^2 \quad (21)$$

where  $R_G$  – gas constant,  $t$  – correlation factor, equivalent to 2800°K,  $T$  – absolute temperature,  $a$  – parameter whose value depends on the crystallo-chemical characteristics of solid solution. For alkaline metal halogenides  $a = 1510$  KJ/mole. If macrocomponents NaCl and KCl are indicated as by the respective I and II indexes we could put down the following:

$$\lg D_{\text{Md, NaCl}} = \lg \frac{\text{SP}_1^{\text{I}}}{\text{SP}_2} - \frac{(t-T)a}{2.303 R_G t T} \left( \frac{R_1^{\text{I}} - R_2}{R_1^{\text{I}}} \right)^2 \quad (22)$$

$$\lg D_{\text{Md, KCl}} = \lg \frac{\text{SP}_1^{\text{II}}}{\text{SP}_2} - \frac{(t-T)a}{2.303 R_G t T} \left( \frac{R_1^{\text{II}} - R_2}{R_1^{\text{II}}} \right)^2 \quad (23)$$

Subtracting equation 23 from equation 22 we obtain:

$$\lg \frac{D_{\text{Md,NaCl}}}{D_{\text{Md,KCl}}} = \lg \frac{SP_1^I}{SP_1^{II}} - \frac{(t-T)a}{2.303 R_G t T} \left[ \left( \frac{R_1^I - R_2}{R_1^I} \right)^2 - \left( \frac{R_1^{II} - R_2}{R_1^{II}} \right)^2 \right]$$

As follows from work [58], the  $SP_1^I/SP_1^{II}$  ratio is equivalent to 9.4. Given the  $K^+$ ,  $Na^+$ , and  $Cl^-$  ionic radii, respectively equivalent to 1.37 Å, 1.02 Å, and 1.81 Å [44], it becomes easy to calculate interatomic distances  $R_1^I$  and  $R_1^{II}$ . As calculated through equation (24),  $R_2$  (MdCl) = 2.995 Å and, therefore, the  $Md^{1+}$  ionic radius at the coordination number = 6 equals 1.19 Å. This well coincides with the theoretically calculated value (see p. ).

If  $R_2$ (MdCl) is known it is possible to calculate through equation (21) the solubility product of MdCl in an aqua-ethanolic solution of the same composition as when the NaCl and KCl solubility products were determined. The results obtained are given in Table 16. As seen from Table 16 the MdCl solubility product value, found with the use of  $SP_{NaCl}$  and  $SP_{KCl}$ , well coincides with and is close to the KCl solubility product.

Table 16. Solubility products of NaCl, KCl and MdCl in 89.6% ethanol

NaCl	Solubility product	
	KCl	MdCl
$5.076 \cdot 10^{-3}$	$5.447 \cdot 10^{-4}$	Calculated according to $SP(NaCl)$ $3.35 \cdot 10^{-4}$ Calculated according to $SP(KCl)$ $3.75 \cdot 10^{-4}$

Thus, resulting from the studies on the cocrystallization of Md with NaCl and KCl, it was proved that Md reduces to the monovalent state in the presence of  $Eu^{2+}$ , and that MdCl, by its properties, is close to sodium and potassium chlorides [59]. These data are in a good accordance with the results of the  $No^{2+}$  properties studied. Works [42–43] proved that in a number of compounds divalent nobelium shows likeness with respective calcium and strontium compounds.

## Summary

Summing up the results of the experimental studies on the lower oxidation states of actinides it should be noted that only mendelevium has been obtained in the monovalent state, while most actinides have been obtained in the oxidation state 2+. All actinides from Cf to No can exist in the divalent state in aqua-ethanolic and water solutions. Other  $An^{2+}$  are unstable in water and ethanolic solutions. The existence of  $Bk^{2+}$ ,  $Pu^{2+}$ , and  $Cm^{2+}$  was established in melted salts. All elements from Cf to No in the 2+ oxidation state are analogous to  $Eu^{2+}$ ,  $Yb^{2+}$ , and  $Sm^{2+}$  and to

alkaline-earth elements. The  $An^{2+}$  stability for the second half of actinides grows with an increase in the atomic number of an element. In the series from Cf to No the oxidation potential  $E_{Me^{3+}/Me^{2+}}^0$  increases with an increase in the atomic number of an element similarly with a growing oxidation potential in the Pr → Eu direction, and in an opposite manner relative to the oxidation potential of elements from Dy to Tm. Likeness between elements of the first half of lanthanides and those of the second half of actinides is shown not only in the oxidation state 2+ but in other anomalous oxidation states as well. The discovered likeness represents similar decreasing of f-electron energy for the first half of lanthanides and the second half of actinides with an increase in the atomic number of an element.

As for monovalent mendelevium, it is analogous, by its properties, to alkaline metal ions. The MdCl solubility product in aqua-ethanolic solutions is close to that of KCl. The low f-electron energy accounts for the likeness between divalent far actinides and the alkaline-metal ions.

On the contrary, it is hard to expect a similarity between alkaline-earth element ions and  $Cm^{2+}$ . Curium atom in the main state is known to have an  $f^7 ds^2$  configuration, so, obviously,  $Cm^{2+}$  must have an  $f^7 d$  configuration, which is analogous to gadolinium. It was recently established that Gd and Tb form cluster compounds of the  $LnCl$  and  $Ln_2Cl_3$  types, isostructural with corresponding compounds of zirconium in the lower oxidation states [60–61]. Cm and, possibly, Pu and Bk, can be expected to show ability to form analogous compounds. If so they will turn out to be similar to d-elements. Studies provided in this direction would certainly open up a new direction in the chemistry of actinides in the lower oxidation states.

## References

- SEABORG, G. T.: The transuranium elements N.N.E.S. 1943, vol. 14B, p. 261; Nucleonics 5, 16 (1949).
- MIKHEEV, N. B.: J. Inorg. Nucl. Chem. Suppl. 1976, p. 117.
- MALY, J., SIKKELAND, T., SILVA, R., GHIORSO, A.: Sciences 160, 1114 (1968).
- HULET, E. K., LOUGHEED, R. W., BRADY, J. D. et al.: Sciences 158, 486 (1967).
- BOBRIK, V. M.: Radiokhimiya 19(5), 606 (1977) (in Russian).
- MALY, J.: Inorg. Nucl. Chem. Lett. 3, 373 (1967).
- MALY, J.: J. Inorg. Nucl. Chem. 31, 1007 (1969).
- BOUSSIÈRES, G., LEGOUX, Y.: Bull. Soc. Chim. France 1965, N° 2, p. 386.
- DAVID, F., BOUSSIÈRES, G.: Inorg. Nucl. Chem. Lett. 4, 153 (1968).
- BAYBARZ, R. D., ASPREY, L. B., STROUSE, C. E., FUKUSHIMA, E.: J. Inorg. Nucl. Chem. 34, 3427 (1972).
- BAYBARZ, R. D.: J. Inorg. Nucl. Chem. 35, 483 (1973).
- SEABORG, G. T.: Ann. Rev. Nucl. Sci. 18, 53 (1968).
- MIKHEEV, N. B., SPITSYN, V. I., KAMENSKAYA, A. N. et al.: Radiokhimiya 14(3), 486 (1972) (in Russian).
- MIKHEEV, N. B., SPITSYN, V. I., CVOSDEV, B. A., KAMENSKAYA, A. N. et al.: Dokl. Akad. Nauk. SSSR 201, 1393 (1971) (in Russian).
- MIKHEEV, N. B., KAMENSKAYA, A. N., RUMER, I. A., SPITSYN, V. I., DIATCHKOVA, R. A., ROZENKEVITCH, N. A.: Radiochem. Radioanal. Lett. 9, 247 (1972).
- MIKHEEV, N. B., KAMENSKAYA, A. N., SPITSYN, V. I. et al.: Inorg. Nucl. Chem. Lett. 8, 929 (1972).

17. MIKHEEV, N. B., SPITSYN, V. I., KAMENSKAYA, A. N. *et al.*: *Inorg. Nucl. Chem. Lett.* **8**, 869 (1972).
18. HAHN, O.: *Applied radiochemistry*, Russian edition Goskhimizdat, 1947, p. 276.
19. DÖLL, W., KLEMM, W.: *Z. anorg. allg. Chem.* **241**, 239 (1939).
20. NUGENT, L. Y., BAYBARZ, R. D., BURNETT, S. L.: *J. Phys. Chem.* **73**, 1177 (1969).
21. MIKHEEV, N. B., DYATCHKOVA, R. A., KAMENSKAYA, A. N. *et al.*: *Radiokhimiya* **14** (3), 471 (1972) (in Russian).
22. MIKHEEV, N. B., KAMENSKAYA, A. N., DYATCHKOVA, R. A. *et al.*: *Inorg. Nucl. Chem. Lett.* **8**, 523 (1972).
23. MERKULOVA, M. S.: *Zh. Neorg. Khim.* **3**, 25 (1958) (in Russian).
24. MIKHEEV, N. B., SPITSYN, V. I., KAMENSKAYA, A. N., RUMER, I. A. *et al.*: *Inorg. Nucl. Chem. Lett.* **13**, 651 (1977).
25. MIKHEEV, N. B., RUMER, I. A.: *Radiokhimiya* **14** (3), 492 (1972).
26. FRIEDMAN, H. A., STOKELY, J. R., BAYBARZ, R. D.: *Inorg. Nucl. Chem. Lett.* **8**, 433 (1972).
27. MORSS, L. R., MCCUE, M. C.: *Inorg. Chem.* **14**(7), 1624 (1975).
28. MIKHEEV, N. B., DYATCHKOVA, R. A., AUERMAN, L. N., RUMER, I. A.: *Radiokhimiya* **24**(1), 112 (1982). (In Russian).
29. JOHNSON, E. K., MACKENZIE, J. R.: *J. Electrochem. Soc., Electrochemical Science* **116**(12), 1697 (1969).
30. MIKHEEV, N. B., AUERMAN, L. N., RUMER, I. A., SPITSYN, V. I., DYATCHKOVA, R. A.: *Izv. Akad. Nauk SSSR*, 1982, N° 4. (In Russian).
31. DYATCHKOVA, R. A., AUERMAN, L. N., MIKHEEV, N. B., SPITSYN, V. I.: *Radiokhimiya* **22**(3), 316 (1980). (In Russian).
32. SPITSYN, V. I., MIKHEEV, N. B., AUERMAN, L. N., RUMER, I. A., DYATCHKOVA, R. A.: *Dokl. Akad. Nauk SSSR* **261**(5), 1154 (1981).
33. MIKHEEV, N. B., AUERMAN, L. N., RUMER, I. A., DYATCHKOVA, R. A.: *Radiokhimiya* **25**(1), 65 (1983). (In Russian).
34. MIKHEEV, N. B., AUERMAN, L. N., RUMER, I. A.: Reduction of gadolinium and terbium up to the bivalent state in molten salts. *Zh. Neorg. Khim.*, in press, 1982, in press. (In Russian).
35. MIKHEEV, N. B., KORSHUNOV, B. G., AUERMAN, L. N., RUMER, I. A., GALUSHKO, A. I.: *Radiokhimiya* **23**(4), 624 (1981). (In Russian).
36. JOHNSON, K. W. R., LEARY, J. A.: *J. Inorg. Nucl. Chem.* **26**(1), 103 (1964).
37. MULLINS, L. J., BEAUMONT, A. J., LEARY, J. A.: *J. Inorg. Nucl. Chem.* **30**(1), 147 (1968).
38. NUGENT, L. J., BAYBARZ, R. D., BURNETT, J. L., RYAN, J. L.: *J. Phys. Chem.* **77**, 1528 (1973).
39. SPITSYN, V. I., IONOVA, G. V., MIKHEEV, N. B.: *Radiokhimiya* **18**(4), 550 (1976). (In Russian).
40. VANDER SLUIS, K. L., NUGENT, L. J.: *J. Opt. Soc. Am.* **64**, 687 (1974).
41. SPITSYN, V. I., IONOVA, G. V., MIKHEEV, N. B.: *Radiokhimiya* **20**(1), 112 (1978). (In Russian).
42. MCDOWELL, W. J., KELLER, O. L., DITTNER, P. E., TARRANT, J. R., CASE, G. N.: *J. Inorg. Nucl. Chem.* **38**(6), 1207 (1976).
43. SILVA, R. J., MCDOWELL, W. J., KELLER, O. L., TARRANT, J. R.: *Inorg. Chem.* **13**(9), 2233 (1974).
44. SHANNON, R. D.: *Acta Crystallogr. A* **32**, 751 (1976).
45. SLATER: *J. Phys. Rev.* **36**(1), 57 (1930).
46. FRAGA, S., KARPOWSKI, J.: *Atomic Data and Nucl. Data Table*, v. 12, p. 467, Technical Report Tc-AS-11-73, 1973.
47. PALING, L.: *The Nature of the Chemical Bond*, Ed. Third, Oxford University Press, 1960.
48. MIKHEEV, N. B., SPITSYN, V. I., KAMENSKAYA, A. N., GVOSDEV, B. A., RUMER, I. A., AUERMAN, L. N., ROZENKEVITCH, N. A.: *Dokl. Akad. Nauk SSSR* **208**(5), 1146 (1973). (In Russian).
49. MIKHEEV, N. B., SPITSYN, V. I., KAMENSKAYA, A. N., GVOZDEV, B. A., RUMER, I. A., ROZENKEVITCH, N. A., AUERMAN, L. N.: *J. Inorg. Nucl. Chem. Suppl.* **1976**, p. 185.
50. CARNALL, W. T., COHEN, D., BERNES, R., SJOBLUM, R. S., WAGNER, F., JR. S. FRIED: ANL-8096, July 1972 through June 1973, Contract W-31-109-Eng.-38.
51. MIKHEEV, N. B., SPITSYN, V. I., KAMENSKAYA, A. N., MIKULSKI, J., PETRYNA, T., KONOVALOVA, N. A.: *New* **43**(1-2), 85 (1980).
52. MIKHEEV, N. B., KAMENSKAYA, A. N., SPITSYN, V. I., MIKULSKI, J., PETRYNA, T., KONOVALOVA, N. A.: New data on physico-chemical properties of mendelevium, *Radiokhimiya*, in press, 1981. (In Russian).
53. HULET, E. K., LOUGHEED, R. W., BAISDEN, P. A., LANDRUM, J. H., WILD, J. F.: *J. Inorg. Nucl. Chem.* **41**(12), 1743 (1979).
54. KIRGINTSEV, A. N.: *Otcherki o termodinamike vodno-solevykh system*, Novosibirsk Nauka, 1976. (In Russian).
55. MIKHEEV, N. B., KAMENSKAYA, A. N., RUMER, I. A., KONOVALOVA, N. A., KULUKHIN, S. A.: Cocrystallization of fermium(II) with potassium chloride in aqua-ethanolic solutions, *Radiokhimiya*, in press, 1981. (In Russian).
56. URUSOV, V. S.: *Geokhimiya* **1980**, N° 5, s. 627. (In Russian).
57. URUSOV, V. S.: *Teoriya isomorfnoy smesimosti*, M., Nauka, 1977, s. 63. (In Russian).
58. FERNER, G. W., MELLON, M. G.: *Ind. Eng. Chem., Anal. Ed.* **6**(5), 345 (1934).
59. MIKHEEV, N. B., KAMENSKAYA, A. N., BERDONOSOV, S. S., KLIMOV, S. I.: *Radiokhimiya* **23**(6), 793 (1981).
60. MATTAUSCH, HJ., SIMON, A., HOLZER, N., EGER, R.: *Z. Anorg. Allg. Chem.* **466**, 7 (1980).
61. SIMON, A., HOLZER, N., MATTANSCH, HJ.: *Z. Anorg. Allg. Chem.* **456**, 207 (1979).

## Valence Stabilities, Size Effects and Actinide Storage Considerations

By R. A. PENNEMAN and P. G. ELLER, Los Alamos National Laboratory, Los Alamos, NM 87545 U.S.A.

(Received October 5, 1982)

*Actinides / Waste storage Americium, Curium, Plutonium, Monazite, Thorite, Huttonite, Oxyfluoride, Dioxide*

### Abstract

Actinide redox properties have important implications for nuclear waste form selection. Valence changes induced by chemical and self-irradiation effects can alter site preferences significantly, and thus could deleteriously influence actinide retentivity in waste forms unless proper provision is made. Bond strength formalism can provide a useful basis for assessing the fit of actinide cations in various host sites. Structural effects in some actinide perovskites are also examined.

Two optimal crystalline systems, which should provide both long-term chemical and radiological stability for either the tri- or tetravalent actinides, are considered. We propose  $\text{ThO}_2$ -MoF and  $\text{LnPO}_4$ - $\text{MSiO}_4$  as systems which should have excellent accommodation for both trivalent and tetravalent actinides, especially Pu, Am and Cm, and be extremely resistant to metamictization and leaching as well.

### Introduction

There is sparse information regarding the valence stabilities of the transuranium elements Np, Pu, Am and Cm in solids important to nuclear waste storage. Indeed, during much of their brief (recent) existence of *ca.* 40 years, valence stabilities and specific occurrence in solids were determined largely incidental to other studies, often in micro samples prepared for X-ray confirmation of chemical constitution. We shall approach the solution to this problem from the point of view of aqueous chemistry, complexation effects and crystal chemistry considerations. We believe that a much stronger and more quantitative case than that based simply on ion sizes can be made on which to base predictions of long term storage stability of actinides. Specifically, it is critical to deal successfully with the enormous range of chemical stabilities of the tri- and tetravalent aquo actinide ions from uranium through curium, which react with water to discharge hydrogen at the uranium end and to discharge oxygen at the curium end [i.e.,  $\text{U(III)} \rightarrow \text{U(IV)}$ ;  $\text{Cm(IV)} \rightarrow \text{Cm(III)}$ ].

Actinide ions are Chatt-Ahrlund Class A cations, and strongly attract Class A anions such as  $\text{F}^-$  and  $\text{O}^{2-}$ . There is no doubt that the actinide(III) and (IV) ions can be incorporated into structures providing cavities of the proper (large) size, even in those furnishing oxide coordination as low as six (although the preferred coordination is certainly eight or greater). However, it is likely that  $\alpha$  radiation and ejected electrons will affect some actinide valences, which, as noted, have widely differing stabilities. To cite a rather extreme example, Am(III) is converted reversibly to Am(II), when host  $\text{CaF}_2$  is held at low temperatures [1]. This occurs even though Mössbauer studies

show that the Np daughters of americium are generally in an oxidation state *higher* than that of the americium parent [2]. Lattice disruption can result because of actinide valence changes, e.g. reduction (IV $\rightarrow$ III) can cause M–O distances to increase by  $\sim 0.15 \text{ \AA}$  [3, 4]. This could well add to the effects of nuclear recoils, known to cause metamictization in some structures.

In particular, we wish to point out the contrast between the stabilities of Th(IV) and U(IV) as observed in natural minerals and the low chemical stabilities of Am(IV) and Cm(IV), which can produce different consequences when these heavier actinides are placed in similar storage media.

To approach a solution to the problem, we shall draw on the large body of quantitative data concerning stabilities of the actinide aquo ions. We shall also use these data and the newer data which provide a measure of the increased stability of the tetravalent state over the trivalent state, as one goes from the aquated ions to those ions with oxygen coordination in solids. The M(IV) and M(III) ions are coordinated with oxygen in aqueous solution as well as in all proposed waste forms (glass, synthetic minerals, etc.). We believe that *oxygen coordination is the common key* and that it is legitimate to draw parallels which allow prediction of chemical and radiation stabilities in oxo-coordinated solids. The thrust of our argument for long term actinide valence stability in storage media is summarized as follows:

- 1) For long term valence stability, the actinide must be inserted initially into the host in the valence state which is best accommodated by size and coordination in the host lattice, and
- 2) the initial actinide valence state selected should be the one most stable to oxidation or reduction in a radiation field. We suggest that this choice can be based in part on the empirical observation that there is an approximate one-volt stabilization of the tetravalent ion in solid oxygen-coordinating hosts compared to the M(IV)/M(III) potentials in aqueous solutions. \*

While the obvious break in aqueous stabilities of the tetravalent over the trivalent states comes for elements past plutonium, the chemical stability of the penta- and hexavalent states in certain solids cannot be disregarded.

Actinides of major significance which are present in TRU (transuranium) wastes are given in Table 1. Many

\* Throughout this paper we will use M for actinide instead of An to avoid confusing An with Am (the symbol for americium).

Table 1. Half lives of isotopes important in transuranic waste

	$t_{1/2}$ (y)
$^{237}\text{Np}$	$2.2 \times 10^6$
$^{239}\text{Pu}$	$2.4 \times 10^4$
$^{240}\text{Pu}$	$6.8 \times 10^3$
$^{241}\text{Am}$	$4.3 \times 10^2$
$^{243}\text{Am}$	$8.0 \times 10^3$
$^{242}\text{Cm}$	0.45
$^{244}\text{Cm}$	18

are long-lived isotopes which constitute the major long term alpha radiation hazard that must be contained if no further separation is envisioned. Of particular significance are  $^{241}\text{Am}$  and  $^{243}\text{Am}$  which lead the hazard index in typical TRU wastes, for times from  $\sim 500$  years to about 50,000 years [5].

### General considerations

At the high temperatures encountered in preparations of most proposed storage media, two conditions need to be controlled:

- 1) Strongly reducing environments are to be avoided since reduced species such as Am(II) or highly volatile Am metal could be formed. The latter might distill out in high temperature waste processing.
- 2) From the chemical viewpoint, actinide valences higher than four should be avoided since the actinides could leach as acid soluble, monomeric aquo cations. Further, since actinide oxides are increasingly acidic as valence increases, an excess of strongly basic oxides and high oxygen fugacity which would stabilize high valences should be avoided. It underlines these arguments to point out that whereas americium is tetravalent in  $\text{BaAmO}_3$ , excess BaO and oxygen lead to the hexavalent state and formation of  $\text{Ba}_3\text{AmO}_6$ . Furthermore, the general stability of the (V) state in solid fluorides and oxides is often overlooked; indeed  $\text{Li}_3\text{AmO}_4$  [containing Am(V)] is stable to  $\sim 1000^\circ\text{C}$ , a much higher temperature than displayed by alkali metal Am(VI) compounds whose thermal stability extends only to 500–600 $^\circ\text{C}$  [6].

We conclude that for greatest long term stability the trivalent or tetravalent states should be chosen. Restricting our discussion to these two valences, we now consider the relative stabilities of the tri- and tetravalent states of the actinide elements, focusing on Pu, Am and Cm.

### Chemical redox properties in aqueous solution and in solid oxide-coordinating hosts

In Table 2 we show the redox potentials of the actinide aquo ions. There is a striking trend in the potentials of the M(IV)/M(III) aquo couples, with greatly increasing difficulty in oxidizing M(III) to M(IV) apparent in the higher actinides. Indeed, the Am(IV) and Cm(IV) ions are such powerful oxidizing agents that they are unknown as simple aquo

Table 2. Redox properties of actinides in aqueous media

Two conditions limit stabilities in water:				
1) Oxidation of water to $\text{H}_2\text{O}_2$ or $\text{O}_2$				
2) Reduction of water to $\text{H}_2$				
			Acid potential (volts)*	Comments
S t a b i l i t y o f I V V a l e n c e	U	IV/III	-0.63	U(III) strongly reducing – can reduce water.
	Np	IV/III	+0.16	Np(III) easily oxidized to IV.
	Pu	IV/III	+0.98	Both valences are stable.
	Am	IV/III	$\sim +2.4$	Am(IV) can oxidize water and disproportionate; Am(IV) is unknown as aqueous ion, but is stable in $\text{F}^-$ , $\text{PO}_4^{3-}$ and phosphotungstate.
	Cm	IV/III	$\sim +3$	Cm(IV) readily oxidizes water; Cm(IV) is metastable in aqueous $\text{F}^-$ , $\text{PO}_4^{3-}$ and in heteropoly anions.

\* IUPAC convention.

ions. A solid line is drawn between Pu and Am to emphasize the limit of aqueous stability of aquo-complexed (IV)'s. A dotted line is drawn between Am and Cm to indicate that Am(IV) can be sufficiently stabilized by strong complexation, both in solution and in oxygen-coordinating hosts, to display stability towards chemical reduction by water. From the estimate of the Am(IV)/(III) redox potential couple, a value of  $\sim 1$  volt stabilization would be necessary ( $\sim 10^{16}$  reduction in Am(IV) activity) to bring Am(IV) within the bounds of aqueous stability (approximately that of the cerium(IV)/(III) couple). Although such stabilization has been demonstrated with americium, the much greater stabilization needed for curium has not yet been achieved, and reduction of Cm(IV) by water (that is, reduction of Cm(IV) to Cm(III) faster than can be accounted for by self-radiolysis alone) has been observed in all cases involving contact with aqueous solutions.

In Table 3 we show the preparation of Am(IV) in various oxide and fluoride coordinated solids. In the 8-coordinated oxygen site provided by phosphotungstate ion, the Am(IV)/(III) redox potential has been found to be  $\sim +1.5$  volts [7]. This corresponds to an estimated overall

Table 3. Preparation of stable Am(IV) in fluoride and oxide-coordinating hosts

$\text{Am}(\text{OH})_3 + \text{NaOCl}$	$\xrightarrow[90^\circ\text{C}]{\text{slurry}}$	$\text{Am}(\text{OH})_4$	[Ref. 9]
$\text{Am}(\text{OH})_4 + \text{NH}_4\text{F}$	$\xrightarrow[\text{R. T.}]{\text{slurry}}$	$(\text{NH}_4)_4\text{AmF}_8$	[Ref. 10]
$\text{Am}(\text{OH})_4 + \text{SiO}_2 \cdot \text{aq}$	$\xrightarrow[7 \text{ days}]{230^\circ\text{C}}$	$\text{AmSiO}_4$ (zircon type)	[Ref. 11]
Am(IV)/(III) (in $\text{P}_2\text{W}_{17}\text{O}_{61}$ ) <sup>-n</sup>	$E = +1.52 \text{ v}$		[Ref. 7]
	(vs. $\sim +2.4$ in aq. soln.)		

stabilization of the (IV) state by  $\sim 1$  volt compared to the aquo species. In the analogous Pu(IV)/Pu(III) and Ce(IV)/Ce(III) cases the simple aquo (IV)/(III) couples are directly measurable, and it is known in those cases that phosphotungstate complexation produces a net stabilization of  $\sim -0.9$  volts for their tetravalent states over the trivalent [8].

With curium(IV)/(III), one volt stabilization is clearly not sufficient as shown by the work of KOSYAKOV *et al.* [7]. Indeed, curium in the tetravalent state is known only in a few cases, e.g., in the tetrafluoride and in the fluorite-type compound  $\text{CmO}_2$ . Even in this generally stable type of lattice, curium(IV) is both radiation sensitive and heat sensitive, losing oxygen at moderate temperatures ( $> 300^\circ\text{C}$ ), to yield Cm(III) in the “ $\text{CmO}_2$ ” host [6]. (We will discuss later the consequences of this behavior and its probable basis.) In Table 4 we show the lower stability of  $\text{CmO}_2$  vs.  $\text{AmO}_2$ , in *parallel* to the trend in stabilities of their tetravalent states in aqueous media shown in Table 2.

Table 4. Radiation and thermal stability of curium (IV) oxide,  $\text{CmO}_2$

$^{244}\text{Cm}_2\text{O}_3$	$(t_{1/2} = 18 \text{ y}, \alpha)$	$\xrightarrow{\text{O}_2}$	$\text{CmO}_{2-x}$
$^{248}\text{Cm}_2\text{O}_3$	$(t_{1/2} = 5 \times 10^5 \text{ y}, \alpha)$	$\xrightarrow{\text{O}_2}$	$\text{CmO}_2$
$^{248}\text{CmO}_2$		$\xrightarrow{\text{ca. } 300^\circ\text{C}}$	Oxygen loss

Note:  $\text{AmO}_2$  is stable to  $\sim 1000^\circ\text{C}$  for both  $^{241}\text{Am}$  and  $^{243}\text{Am}$ .

### Self-irradiation effects

The profound influence which self-radiation effects can have not only on macroscopic properties (e. g. swelling and microfracturing) but also on microscopic properties (e. g. crystalline order and valence states) is well known. In this discussion we are chiefly concerned with actinide valence stability in TRU waste forms. The main effects derive from ionized nuclei and free electrons, which are produced by  $\alpha$ -particles and recoil nuclei. A few examples will suffice to show that such effects can be quite large. Perhaps the most directly relevant example is that the stoichiometric fluorite-like curium dioxide has been prepared only with the  $5 \times 10^5$  y isotope  $^{248}\text{Cm}$ . With the shorter lived isotopes  $^{244}\text{Cm}$  (18 y) and  $^{242}\text{Cm}$  (0.45 y) oxygen deficient “dioxides” are found. One can reasonably expect Cm(IV) diluted in oxide waste forms to show a similar tendency to undergo radiation-induced reduction and become trivalent. On the long time scale required for TRU waste storage, Am(IV) would also be expected to undergo some degree of radiation-induced reduction to the trivalent state.

It is pertinent to point out that the eight equivalent M–O bond lengths comprising the metal coordination in the  $\text{MO}_2$  lattices should *each* increase by *ca.* 0.15 Å on reduction from M(IV) to M(III) (see below). Clearly, if a significant proportion of the cations are reduced in a

lattice designed to accommodate M(IV) cations, the original structure would be severely stressed and probably could not be maintained. However, if the reduction is limited to a small percentage of the cations, or if oxygen loss is permitted (e.g.,  $\text{MO}_2 \rightarrow \text{MO}_{2-x}$ ), compounds of high lattice stabilities could allow M(III) incorporation without drastic structural alteration. The  $\text{MO}_2$  lattice type is especially forgiving in this regard, as we shall point out.

### Bond length-bond strength considerations

ZACHARIASEN’s bond length-bond strength formalism is expressed as

$$D(s) = D(1) - B \ln(s)$$

where  $D(s)$  is the bond length for a bond of strength ( $s$ ) [3].  $D(1)$  and  $B$  are empirical parameters obtained by analysis of many well-determined crystal structures. For structures in which actinide-oxygen bonds predominate, this approach usually works quite well [3, 12]. However, the actinide ions are larger than d-block elements and good agreement is frequently *not* obtained on comparing the known actinide valence with the sum of the “computed” bond strengths based on the bond distances to sites for d-block elements which they replace in the pure host.

In many of the structures dominated by elements other than actinides, but proposed as host lattices, we know the coordination number and bond distances to structural elements such as Zr, Ti, and Ca. For such cases, we have simply taken the distances observed in the host lattice and calculated actinide valence sums, as if the actinide could be substituted without structural change. Obviously, this approach will give a ridiculous valence sum if the actinide is substituted for a much smaller or much larger cation. Nonetheless, some interesting observations can be drawn from such a tabulation as given in Table 5.

- 1) The valence sums suggests that in the  $\text{CaO}_8$  site of zirconolite, the Am(III) distances are satisfied and that Am(III) would fit nicely, and better than Am(IV). Neither Am(III) nor Am(IV) should be accommodated very well in the Zr(IV) site (without lattice distortion or expansion).
- 2) In perovskite, the  $\text{CaO}_{12}$  site is clearly too large for either Am valence. (We address the fit of Pu(IV) in the M(IV) site later in the text).
- 3) Not surprisingly, Am(III) should fit nicely in the monazite lattice. We find the fit of Am(IV) to be poorer, though Th(IV) and U(IV) are known to occur in appreciable amounts in monazites likely as coupled substituents with divalent cations.
- 4) The fit of Th(IV) in tetragonal thorite is apparently better than in the rarer huttonite (monazite-type) form.
- 5) Am(IV) is smaller than Th(IV). The addition of  $\text{AmO}_2$  to  $\text{ThO}_2$  results in a continuous solid solution, with decreasing d spacings ending with the smaller end member,  $\text{AmO}_2$ .

Table 5. Bond length-bond strength calculations for selected structures pertinent to waste forms

Host and coordination site	Observed metal-ligand distance (Å) in host	Actinide	Computed $\Sigma_s$	Ref.
zirconolite eight coordinate Ca site	2.37 – 2.60	Am(III)	2.9	[20]
zirconolite eight coordinate Ca site	2.37 – 2.60	Am(IV)	2.5	[20]
zirconolite seven coordinate Zr site	1.99 – 2.45	Am(III)	6.3	[20]
zirconolite seven coordinate Zr site	1.99 – 2.45	Am(IV)	5.5	[20]
perovskite (CaTiO <sub>3</sub> ) 12 coordinate Ca site	2.85	Am(III)	1.6	[21]
perovskite (CaTiO <sub>3</sub> ) 12 coordinate Ca site	2.85	Am(IV)	1.4	[21]
monazite (monoclinic LaPO <sub>4</sub> ) nine coordinate La site	2.45 – 2.78	Am(III)	3.1	[17]
thorite (tetragonal ThSiO <sub>4</sub> ) eight coordinate Th site	2.37 – 2.47	Th(IV)	4.1	[18]
huttonite (monoclinic ThSiO <sub>4</sub> ) nine coordinate Th site	2.40 – 2.81	Th(IV)	3.7	[18]
ThO <sub>2</sub> cubic eight coordinate site	2.42	Th(IV)	4.0	[3]
AmO <sub>2</sub> cubic eight coordinate site	2.33	Am(IV)	4.0	[3]

‡

### Ion sizes and structural effects in actinide perovskites

At the beginning of this part of the discussion it is useful to recall that actinide ions are much larger than some of the d-block ions whose compounds have been mentioned as storage media hosts. For example, in comparable compounds the thorium-oxygen bond length in eight coordination is 0.24 Å longer than the zirconium-oxygen bond length (see Fig. 1). Compared with the 4f lanthanides, the earlier members of the 5f actinides are larger, with approximate size parity being obtained by moving the lanthanides three elements to the right in the periodic chart so that lanthanum is compared with uranium and praseodymium with plutonium (Fig. 2).

From ZACHARIASEN's formula [3] we find that in cubic coordination the Pr(IV)–O<sub>8</sub> distances should be

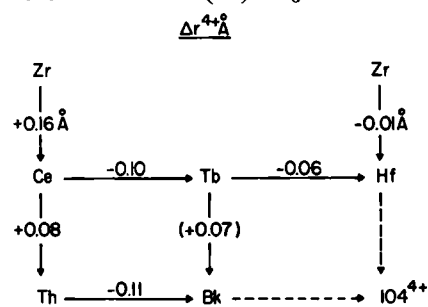


Fig. 1. Trends in differences of M–O<sub>8</sub> distances for some tetravalent elements. [Size data from Ref. 3.]

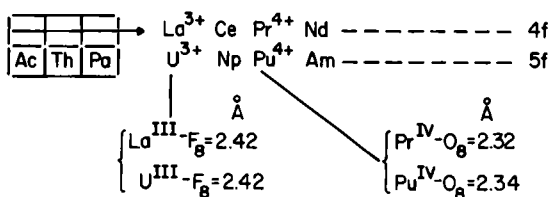


Fig. 2. Approximation of actinide-lanthanide ion-size equality. For approximate size equivalence, 4f/5f, slide 4f series about three elements to right. [Size data from Ref. 3.]

2.32 Å and the Pu(IV)-O<sub>8</sub> distance should be 2.34 Å. For ideal six coordination, the bonds will be shorter since the bond strengths are greater. Thus,

$$\text{Pr(IV)-O}_6 = 2.23 \text{ \AA} \quad \text{Pu(IV)-O}_6 = 2.24 \text{ \AA}.$$

In classic perovskites, the M(IV)-O<sub>6</sub> distance is exactly one-half the edge of the cubic cell since the M-O bond vectors of the octahedra lie along it (Fig. 3). For BaPrO<sub>3</sub> the edge of the putative cubic cell is 4.354 Å giving a Pr-O distance of 2.177 Å. Similarly, the edge of the BaPuO<sub>3</sub> cell is given as *a* = 4.36 [6], yielding a Pu-O distance of 2.18 Å. From our estimates of the preferred Pr(IV)-O<sub>6</sub> and Pu(IV)-O<sub>6</sub> distances, it is clear that both Pr(IV) and Pu(IV) are too large to fit into the classic cubic perovskite structure, given these cell dimensions.

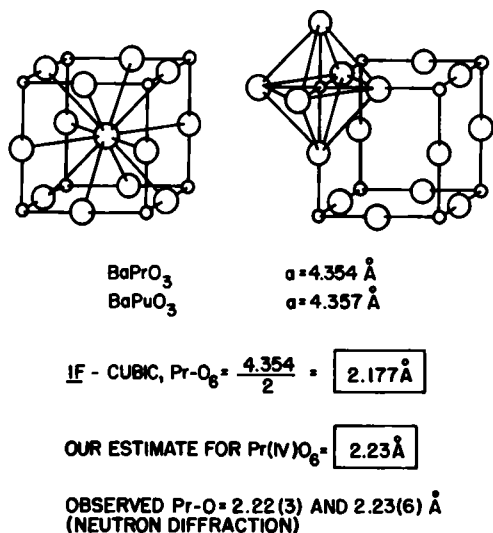


Fig. 3. The perovskite structure. In BaPrO<sub>3</sub> the PrO<sub>6</sub> octahedra are rotated and tilted away from the cell edges [13].

A solution to this difficulty is furnished by a recent, accurate structure determination for the praseodymium case [13].

The neutron diffraction study showed that the symmetry of BaPrO<sub>3</sub> is lower than cubic, and that the Pr-O vectors are *not constrained* to lie along the cell edge but are rotated and tilted off the cell edges allowing for longer Pr-O bonds. JACOBSON *et al.* [13] found values of 2.23 and 2.22 Å for the Pr-O distances - *nearly identical* with the values we obtained from ZACHARIASEN's formula.

We conclude that the so-called cubic constants for BaPuO<sub>3</sub> are incorrect, and that the true lengths of the Pu-O<sub>6</sub> bonds will be found to be nearer to 2.24 Å. (See Fig. 3.)

There is a further problem with the perovskites. In this structure type the large tetravalent actinides are coordinated to only six oxygens; the actinides are simply too large to be completely "enclosed" in six oxygen coordination (i.e. coordinatively unsaturated) and hence are vulnerable to oxide addition and oxidation. Atmospheric oxygen, together with an additional basic oxide such as BaO, yields hexavalent actinides (e.g., BaAmO<sub>3</sub> → Ba<sub>3</sub>AmO<sub>6</sub>) [6]. We conclude that oxygen coordinations as low as six are not likely to retain tetravalent actinides as well as structures furnishing higher coordination values.

### Alternative storage media for tri- and tetravalent actinides

We now wish to propose two systems which we believe offer many advantages as hosts for TRU waste disposal. The first comprises a mixed ThO<sub>2</sub>-MOF matrix; the second is a mixed orthosilicate-phosphate matrix which should be particularly good for stabilizing Pu(IV).

#### A. The ThO<sub>2</sub> - MOF matrix

It is worthwhile to recall that in the Oklo natural uranium reactors, urania (UO<sub>2</sub>) was found to retain the trivalent rare earth fission products for two billion years [14]. Since thoria (ThO<sub>2</sub>) is stable to oxidation in circumstances in which urania is not, we believe that thoria would be an even more stable host for trivalent actinides than urania.

Considerable information is available on radiation-stability of thoria-like phases. The behavior of Cm(IV)/Cm(III) in the dioxide under self irradiation can be explained by the application of ZACHARIASEN's formula. We estimate that the M(III)-O<sub>6</sub> bond distance should be nearly the same as the M(IV)-O<sub>8</sub> bond distance. For example, with oxygen vacancies we estimate the La-O<sub>6</sub> bond length should be 2.43 Å, which is nearly identical to the observed Th-O<sub>8</sub> bond length of 2.42 Å in ThO<sub>2</sub> [3]. Clearly both trivalent and tetravalent lanthanide and actinide ions should be well accommodated in the MO<sub>2</sub> lattice (MO<sub>2</sub> and M<sub>2</sub>O<sub>3</sub> in ThO<sub>2</sub>). The reduction of Cm(IV) to Cm(III) in CmO<sub>2</sub> by radiation or heat is accompanied by an increase in the number of oxygen vacancies to achieve charge compensation. Such lattices are known to be very resistant to metamictization; for example, F. CLINARD at the Los Alamos National Laboratory [15] reports swelling of <sup>238</sup>PuO<sub>2</sub> but retention of crystallinity at an alpha dose of 10<sup>26</sup> α/m<sup>3</sup>.

The above observations underscore the great stability of the MO<sub>2</sub>-MO<sub>2-x</sub> structure and provide a basis for predicting the accommodation of trivalent actinide oxides. We believe that it would be advantageous to use the extremely stable ThO<sub>2</sub> structure type as a host to retain both tri- and tetravalent actinides but to *avoid* oxygen defi-

ciencies for insertion of trivalent actinides. This line of reasoning led us to suggest a *yet untried storage medium* – the structurally similar pair MOF–ThO<sub>2</sub>. In this system, the oxygen vacancies are not needed for charge balance; rather, the vacancies are occupied by singly charged F<sup>−</sup> ions. Such a mixture should be able to host both trivalent and tetravalent actinides. The actinides which are normally trivalent must be added as their oxyfluorides, e.g., CmOF, while ions (like Pu) which are expected to remain tetravalent would be added as MO<sub>2</sub>. The MOF–ThO<sub>2</sub> mixture should be radiation (metamictization) resistant, and highly resistant to leaching. Miscibility of LaOF and ThO<sub>2</sub> has recently been demonstrated in our laboratory.

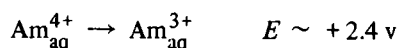
#### B. The Huttonite-Monazite (MSiO<sub>4</sub>–LnPO<sub>4</sub>) Matrix

ABRAHAM, BOATNER *et al.* [16] at Oak Ridge have prepared a series of rare earth orthophosphates LnPO<sub>4</sub> (monazites) by dissolving the lanthanide sesquioxides in molten lead pyrophosphate. In an elegant experiment using ESR measurements they were able to establish unequivocally the presence of highly unusual *trivalent lead* as a substituent in some of the trivalent lanthanide sites.

Some specimens of natural monazite have been reported to contain a significant percentage of thorium and uranium, presumably as tetravalent ions [17]. We have collected in Table 6 the measured gaseous ionization potentials for lead and uranium. Clearly, the lattice energy established by the LnPO<sub>4</sub> host is sufficient to stabilize trivalent lead, which in the gas phase, is about 17 e volts less stable than divalent lead. Note that this is also the difference between U(III)(g) and U(IV)(g), and indicates that U(IV) should be greatly stabilized over U(III) – again in the general stabilization direction which favours U(IV) over U(III).

In addition to redox potentials, a further consideration is that M(III) must fit into the LnPO<sub>4</sub> lattice; the size of Pb(III) (estimated from known Pb(II) and Pb(IV) sizes) is very close to that of Ln(III).

The OAK RIDGE workers doped 1% *trivalent* americium into their synthetic monazite using americium sesquioxide; the americium *remained trivalent*, in accord with the Am(IV)/(III) potential. A clue toward predicting the behavior of uranium, plutonium and americium in solid oxide matrices such as monazite can be derived from their behavior as oxygen coordinated aquo ions.



In the uranium case, the tetravalent aquo ion is already preferred over the trivalent ion and, therefore, the tetravalent state should be even more stable in oxide coordi-

nated solids. It still might be possible, by providing a powerful reducing agent such as europium metal or U metal, to get U<sup>3+</sup> in monazite. However, we note that pure U(III) compounds with only oxygen coordination are rare.

From the viewpoint of radiation stability, we have the report that huttonite (monoclinic, monazite-like ThSiO<sub>4</sub>) is far more resistant to metamictization than is thorite (ThSiO<sub>4</sub> in the often metamict, tetragonal zircon form) [18]. We noted previously that, in spite of the high oxidizing power of Am(IV), the orthosilicate AmSiO<sub>4</sub> can be prepared hydrothermally at 230°C. Since AmSiO<sub>4</sub> involves a tetravalent cation and a tetrahedral anion, an obvious extension is suggested: AmSiO<sub>4</sub> insertion in the LnPO<sub>4</sub> lattice. It is true that AmSiO<sub>4</sub> prepared as above is in the tetragonal ZrSiO<sub>4</sub> form. However, SiO<sub>4</sub><sup>4−</sup> should substitute nicely for the similarly-sized and shaped PO<sub>4</sub><sup>3−</sup> tetrahedron, and thus AmSiO<sub>4</sub> should fit nicely into the LnPO<sub>4</sub> matrix. In essence, this could stabilize AmSiO<sub>4</sub> in the radiation-resistant monoclinic huttonite lattice type. We note that MCCARTHY, *et al.* originally suggested MSiO<sub>4</sub> in LnPO<sub>4</sub> hosts [19].

Comparing the different stabilities of Am(IV) and Cm(IV), it is clear that Cm(IV) is less likely to show long term stability in a radiation field than Am(IV), whose stability we believe is borderline. Thus, we conclude that certainly curium (and perhaps americium) should best be inserted in their trivalent states. In the case of plutonium, PuSiO<sub>4</sub> in LnPO<sub>4</sub> should have extraordinary stability, given that the stabilization of Pu(IV) over Pu(III) should bring the Pu(IV)/(III) potential nearly to zero.

#### Conclusion

In this paper we have attempted to show that actinide redox properties have important implications for waste form selection. Valence changes induced by chemical and self-irradiation effects can alter site preferences significantly, and thus could deleteriously influence actinide retentivity in waste forms unless proper provision is made. A basis for selection of actinide valences is given. ZACHARIASEN's bond-length–bond-strength formalism provides a useful means for assessing the fit of actinide cations in various host sites. Structural effects in some actinide perovskites are also examined.

Two optimal crystalline systems, which should provide both long-term chemical and radiological stability for either the tri- or tetravalent actinides, are considered. We propose ThO<sub>2</sub>–MOF as a new system which not only should have excellent accommodation for *both* trivalent and tetravalent actinides but also be extremely resistant to metamictization and leaching. The LnPO<sub>4</sub>–MSiO<sub>4</sub> system is especially appealing for PuSiO<sub>4</sub>.

#### References

1. EDELSTEIN, N., EASLEY, W., MCLAUGHLIN, R.: *J. Chem. Phys.* **44** (1966) 3130.
2. FRIEDT, J. M., POINSOT, R., REBIZANT, J., MÜLLER, W.: *J. Phys. Chem. Solids* **40** (1979) 279–287.

3. ZACHARIASEN, W. H.: *J. Less-Common Met.* **62** (1978) 17.
4. PENNEMAN, R. A., HAIRE, R. G., LLOYD, M. H., in: *Actinide Separations*, ACS Symposium Series 117, J. D. NAVRATIL and W. W. SCHULZ, eds., American Chemical Society, Washington, D. C., 1980, Ch. 39, pp. 571–581.
5. TELEPLAN, A. B.: *Handling of Spent Nuclear Fuel and Final Storage of Vitrified High Level Reprocessing Waste*, Kaernbraenslesaeakerhet, Stockholm, Sweden, (1978) Dep. NTIS PC A07/MF A01; Report No. INIS-mf-4460.
6. KELLER, C.: *Chemistry of the Transuranium Elements*, Verlag Chemie GmbH, Weinheim, Germany, 1971.
7. KOSYAKOV, V. N., TIMOFEEV, G. A., ERIN, E. A., ANDREEV, V. I., KOPYTOV, V. V., SIMAKIN, G. A.: *Radiokhimiya* **19** (1977) 511–517. [Sov. Radiochem. (Engl. Transl.) **19** (1977) 418–423].
8. SAPRYKIN, A. S., SHILOV, V. P., SPITSYN, V. I., KROT, N. N.: *Dokl. Akad. Nauk SSSR* **226** (1976) 853–856. [Engl. Transl.] **226** (1976) 114–116].
9. PENNEMAN, R. A., COLEMAN, J. S., KEENAN, T. K.: *J. Inorg. Nucl. Chem.* **17** (1961) 138–145.
10. ASPREY, L. B., PENNEMAN, R. A.: *Inorg. Chem.* **1** (1961) 134–136.
11. KELLER, C.: *Nukleonik* **5** (2) (1963) 41–48.
12. ZACHARIASEN, W. H., PENNEMAN, R. A.: *J. Less-Common Met.* **69** (1980) 369–377.
13. JACOBSON, A. J., TOFIELD, B. C., FENDER, B. E. F.: *Acta Crystallogr.* **B28** (1972) 956.
14. COWAN, G. A.: IAEA Symposium, Paris, Dec. 19–21, 1977.
15. CLINARD, F. W., JR., HOBBS, L. W., LAND, C. C., PETERSON, D. E., ROHR, D. L., ROOF, R. B.: *J. Nucl. Mater.* **105** (1982) 248–256.
16. ABRAHAM, M. M., BOATNER, L. A., BEALL, G. W., FINCH, C. B., FLORAN, R. J., HURAY, P. G., RAPPAPAZ, M.: Proc., CONF-8005107, L. A. BOATNER and G. C. BATTLE, JR., eds., Department of Energy, April 1981, pp. 144–169.
17. BEALL, G. W., BOATNER, L. A., MULLICA, D. F., MILLIGAN, W. O.: *J. Inorg. Nucl. Chem.* **43** (1981) 101.
18. TAYLOR, M., EWING, R. C.: *Acta Crystallogr.* **B34** (1978) 1074.
19. MCCARTHY, G. J., WHITE, W. B., PFOERTSCH, D. E.: *Mater. Res. Bull.* **13** (1978) 1239–1245.
20. ROSSELL, H. J.: *Nature* **283** (1980) 282.
21. WYCKOFF, R. W. G.: *Crystal Structures*, 2nd Ed., Interscience Publishers, 1966, p. 400.



## The Behavior of Actinides in the Environments

By R. L. WATTERS<sup>1</sup>, T. E. HAKONSON<sup>2</sup>, and L. J. LANE<sup>2</sup>,

<sup>1</sup>Department of Energy, Office of Health and Environmental Research, Washington, DC 20545

<sup>2</sup>Environmental Sciences Group, Los Alamos National Laboratory, Los Alamos, NM 87545

(Received April 5, 1982)

*Actinides/Plutonium/Ecosystems/Environmental transport/Food-webs*

### Summary

A review of actinide behavior in the environment is presented with emphasis on chemical, physical, and biological factors that influence actinide mobility in ecosystems. Available data from terrestrial and fresh water ecosystems suggest that physical processes which result in the transport of soils and sediments dominate in the translational movement of plutonium and, as well, dominate in the transport of this element through lower trophic levels. Exceptions to that statement occur in arctic ecosystems and in deep oceans. Regardless of mode of transport, plutonium levels in higher trophic levels including man are very low indicating the low solubility of this element in the environment. Very few data on the behavior of the other actinides in the environment are currently available although theoretical considerations and limited laboratory experiments suggest that many of the actinides are more mobile than plutonium.

### Introduction

In the actinide series, the elements of greatest interest as environmental contaminants are uranium, neptunium, plutonium, americium, and curium because the presence of these elements at relatively high concentrations in ecosystems would represent potential health problems. The purpose of this paper is to review current knowledge on the distribution and transport of those elements in terrestrial and aquatic environments under a variety of site and

source conditions. Based on available data, none of the actinides discussed herein are currently present, in an available form in the general environment, at concentrations considered to be a health hazard. Among those elements, only uranium occurs naturally in any significant quantity. The natural isotopes of uranium are so long-lived that their specific activity is very low; thus chemical toxicity involving kidney damage takes precedent over radiotoxicity in considerations of health [1]. However, the isotopes <sup>232</sup>U and <sup>233</sup>U, which have higher specific activities, can be produced in the thorium breeder cycle and could represent a potential environmental health problem [2].

With current reactor technology, the isotopes of neptunium, plutonium, americium, and curium are formed during neutron bombardment of uranium through a complicated series of neutron capture and radioactive decay reactions (Fig. 1, [3]). The importance of those elements as environmental contaminants depends upon factors related to their production, half life, chemistry, mode of dispersion, and biological availability. The transuranic nuclides which may be of interest as environmental contaminants are listed in Table 1.

*Neptunium 237*, by nature of its long half-life, is the only isotope of neptunium that could be considered a possible long-term hazard in the environment. Until recently, very little consideration was given to <sup>237</sup>Np as a radiological problem because of its low production and relatively low

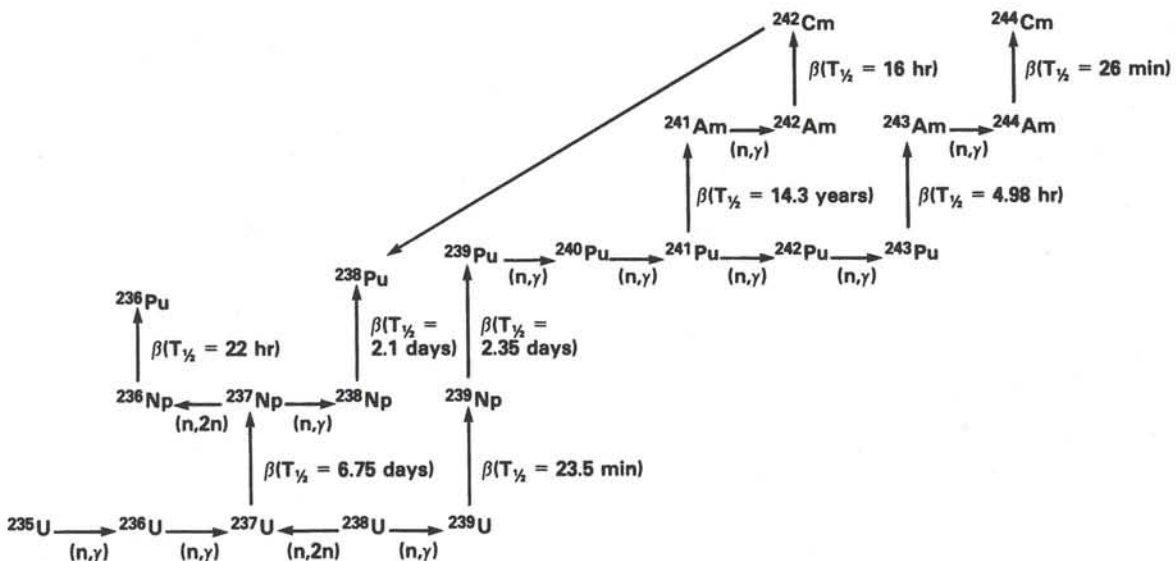


Fig. 1. Formation schemes for important actinides (ref. [3]).

Table 1. Nuclear properties of long lived transuranic elements

Element	Isotope	Emission	Half life
Neptunium	<sup>237</sup> Np	α	2.1 × 10 <sup>6</sup> y.
Plutonium	<sup>238</sup> Pu	α	86.4 y.
	<sup>239</sup> Pu	α	24,400 y.
	<sup>240</sup> Pu	α	6580 y.
	<sup>241</sup> Pu	β	13.2 y.
Americium	<sup>241</sup> Am	α	458 y.
Curium	<sup>244</sup> Cm	α	17.6 y.

specific activity. However, recent data indicate that neptunium is the most mobile of the subject group of transuranic elements in ecosystems and mammalian organisms [4, 5]. This reported mobility could be a compensating factor for the low production and low specific activity of <sup>237</sup>Np when considering the potential radiological consequences of release to the environment.

*Plutonium* has been produced in greater quantity than any other transuranic element. Plutonium has also been the subject of the most biological and ecological research because atmospheric weapons testing, routine waste disposal and various accidents have made it more prevalent than the other subject elements in the environment. The four isotopes of plutonium (Table 1) that are of most concern as environmental contaminants are <sup>238</sup>Pu, <sup>239</sup>Pu, <sup>240</sup>Pu and <sup>241</sup>Pu. Plutonium chemistry is complicated because this element can form relatively stable compounds in several oxidation states under various environmental and biological conditions.

*Americium* 241, with a half-life of over 450 years is the second most prevalent transuranic element in the environment and results primarily from nuclear weapons testing. The complete decay of <sup>241</sup>Pu from present worldwide fallout should produce an amount of <sup>241</sup>Am about equivalent to <sup>239,240</sup>Pu. Under environmental conditions, the chemistry of americium is relatively simple with only the Am(III) oxidation state being of importance in the environment [6].

*Curium* is the least important of the transuranic elements as a global environmental contaminant because very little of its longer lived isotope, <sup>244</sup>Cm, has been released to the environment through weapons testing. However, this element is significant in power reactor wastes [7]. With a half life of 18 years, <sup>244</sup>Cm can persist in the environment for several human generations. As with americium, only one oxidation state, Cm(III), is important under environmental conditions [6].

All of the transuranic elements are considered to be boneseekers, when inhaled or ingested, with about equal distribution between the skeleton and the liver [8]. In experimental animals receiving large radiological doses of transuranic elements, the principal cause of death has been from bone cancer [9, 10].

## Sources and distribution in the environment

Only uranium among the actinides of interest occurs naturally in the environment in easily measurable concentrations. It is essentially ubiquitous and concentrations in soil range from 1 to 10 μg/g [11]. Uranium concentrations in soil tend to reflect the base materials from which they are derived although there is a tendency for the uranium content of organic rich horizons to be greater than other horizons in a soil profile [12]. Concentrations in seawater are reported in the range of 0.3 to 6 μg/l [13] with an average concentration of 3 μg/l [14]. Continental surface waters range from 0.1 μg/l to 500 μg/l depending on the amount and solubility of the uranium in the parent watershed or aquifer. Concentrations of uranium in deep ocean sediments range from 0.4 to 3.0 μg/g and vary inversely with the calcium carbonate content of the sediment [15].

Extremely small amounts of the transuranic elements, principally <sup>239</sup>Pu, are formed naturally by neutron capture in uranium ores [16, 17, 18]. The ratio of <sup>239</sup>Pu relative to uranium under those circumstances is 3 × 10<sup>-12</sup>. Even higher occurrence ratios have been found in volcanic rock [19]; however, the major sources of plutonium in the environment are due to human activities.

The ubiquitous distribution of man-made plutonium is due to the detonation of nuclear weapons in the atmosphere. In particular, the testing of thermonuclear devices, which began in 1952, produced the greatest amount of airborne plutonium. The large energy releases in these explosions injected nuclear debris into the stratosphere where it remained long enough to be distributed globally. An estimated 360,000 curies (Ci) of the isotopes <sup>239,240</sup>Pu, and after complete decay an almost equal number of curies of <sup>241</sup>Am, and smaller amounts of other transuranic elements entered terrestrial and aquatic environments by this route (Table 2, [7]). Most of those radionuclide inventories have deposited in the northern hemisphere due to the tests conducted by the United States and the Soviet Union. Environmental concentrations of fallout radionuclides, including plutonium, are highest at mid-latitudes with attenuated concentrations occurring at higher and lower latitudes as shown in Table 3 [20].

About 16 kCi of <sup>238</sup>Pu were dispersed in the upper atmosphere of the southern hemisphere in April 1964 when a navigational satellite with its SNAP 9A generator

Table 2. Estimated amounts of transuranium elements that have been injected into the atmosphere [7]

Radionuclide	Total injected kCi
<sup>238</sup> Pu	24 <sup>a</sup>
<sup>239</sup> Pu	154
<sup>240</sup> Pu	209
<sup>241</sup> Pu	9720
<sup>241</sup> Am	336 <sup>b</sup>

<sup>a</sup> Represents 16 kCi from SNAP 9A and 8 curies from weapons tests.

<sup>b</sup> Americium-241 formed on total decay of <sup>241</sup>Pu.

Table 3. Average latitudinal distributions of cumulative Pu-239, 240 and Pu-238 fallout [20]

Hemisphere	Latitude Band	mCi per km <sup>2</sup>		
		Pu-239, 240	Pu-238	
			Weapons	SNAP-9A
Northern	90 – 80	(0.10 ± 0.04) <sup>a</sup>	(0.002 ± 0.001)	(< 0.001)
	80 – 70	0.36 ± 0.05	0.009 ± 0.001	< 0.001
	70 – 60	1.6 ± 1.0	0.038 ± 0.025	0.026 ± 0.015
	60 – 50	1.3 ± 0.2	0.031 ± 0.004	0.013 ± 0.004
	50 – 40	2.2 ± 0.5	0.053 ± 0.011	0.026 ± 0.011
	40 – 30	1.8 ± 0.6	0.042 ± 0.014	0.025 ± 0.015
	30 – 20	0.96 ± 0.07	0.023 ± 0.002	0.011 ± 0.004
	20 – 10	0.24 ± 0.10	0.006 ± 0.002	0.003 ± 0.002
	10 – 0	0.13 ± 0.06	0.003 ± 0.001	< 0.001
Southern	0 – 10	0.30 ± 0.20	0.007 ± 0.005	0.010 ± 0.007
	10 – 20	0.18 ± 0.05	0.004 ± 0.001	0.036 ± 0.021
	20 – 30	0.39 ± 0.16	0.009 ± 0.004	0.070 ± 0.042
	30 – 40	0.40 ± 0.12	0.009 ± 0.003	0.061 ± 0.020
	40 – 50	0.35 ± 0.21	0.008 ± 0.005	0.069 ± 0.038
	50 – 60	(0.20 ± 0.09)	(0.005 ± 0.002)	(0.044 ± 0.023)
	60 – 70	(0.10 ± 0.04)	(0.002 ± 0.001)	(0.022 ± 0.012)
	70 – 80	(0.03 ± 0.01)	(0.001 ± 0.001)	(0.008 ± 0.005)
	80 – 90	(0.01 ± 0.004)	(< 0.001)	(0.004 ± 0.002)

<sup>a</sup> Results in parentheses were derived by extrapolation; error terms are standard deviations.

failed to achieve orbit and vaporized upon reentry. Essentially all of the <sup>238</sup>Pu released by this event has reached the surface of the earth; about 75 percent of this material deposited in the southern hemisphere (Table 3).

Localized sources of plutonium were created by accidents involving aircraft that were carrying nuclear weapons. An explosion during mid-air refueling of a U.S. Air Force B-52 occurred on January 16, 1956, above Palomares, Spain. The high explosives in two unarmed nuclear weapons detonated on impact near Palomares scattering the plutonium into the surrounding area. The plutonium was reduced to acceptable concentrations in soil by decontamination procedures [21]. On January 21, 1968, another B-52 carrying unarmed nuclear weapons crashed and burned on the ice near Thule, Greenland. Most of the plutonium contained in the weapons was recovered, however, an estimated 25 Ci deposited in marine sediments of Bylot Sound and an additional 1 to 5 Ci were dispersed to nearby shore areas [22].

Plutonium 239, 240 and americium 241 are the primary alpha emitters resulting from nuclear explosions, however, under longer irradiation times such as incurred in nuclear reactors, neptunium and curium will also be produced in considerable quantities [23]. Although neptunium and curium are present in irradiated reactor fuel, releases of transuranic elements during chemical separation of plutonium from reactor fuel primarily involve plutonium and americium. Part of the releases from such facilities has been in the form of aerosols from ventilation systems where absolute retention of particles cannot be achieved or where air cleaning equipment has failed [24, 25]. Those airborne releases result mainly in localized contamination in terrestrial ecosystems. Transuranic elements also have

been distributed in localized terrestrial systems through release of liquid wastes in such places as the White Oak Creek flood plain at Oak Ridge, Tennessee [26], and the waste disposal canyons at Los Alamos, New Mexico [27]. Dispersal of transuranic elements into aquatic environments occurs during planned releases of low-level liquid wastes into river [28, 29] or marine waters [30, 31] in accordance with national and international regulations and guidelines.

The distribution of transuranic elements from point sources at nuclear facilities typically produces decreasing concentrations with distance from the source. As a result, much of the readily detectable material is located within the controlled boundaries of nuclear facilities. In those areas and in areas with limited public access, concentrations of those elements in soils and sediment may exceed fallout levels but generally are still low with respect to levels that would constitute a hazard to animals and humans [26, 29, 31, 32, 33, 34, 35]. Controlled areas such as the Nevada Test Site, where plutonium was scattered by high explosives to simulate accident conditions, may be an exception to the latter statement. As much as 200 Ci may still be distributed in relatively small areas after decontamination procedures removed most of the material [36].

A range of concentrations of plutonium in soils, sediments, and water are given in Table 4. An interesting observation from the table is that the concentrations of plutonium in water are quite low compared to soils and sediments. In fact in several terrestrial ecosystems which have been studied, more than 99 percent of the plutonium inventory is ultimately associated with soil and less than 1% is associated with biota (Table 5). There are unique

Table 4. *Plutonium in soils, sediments and water*

Source and locations	Concentration ( <sup>239,240</sup> Pu) Soils and sediments <sup>a</sup> (pCi/g dry wgt)	Reference
<b>Nuclear weapons testing</b>		
Global Fallout (Soil)	$5 \times 10^{-4} - 2 \times 10^{-2}$	37
Debris (NTS, Soil)	80 - $5 \times 10^4$	38
Bikini Atoll (Soil)	0.5 - 400	39
Lake Michigan (Sediment)	0.09 - 0.40	40
Trinity Site Fallout (Soil)	0.02 - 0.32	35
<b>Chemical processing</b>		
Savannah River, S. C. (Soil)	$6 \times 10^{-3} - 3.7$	24
Hanford, Wash. (Soil)	$4 \times 10^{-3} - 0.7$	41
Rocky Flats, Colo. (Soil)	$4 \times 10^{-3} - 70$	42
Irish Sea (Sediment)	0.3 - 50	30
Los Alamos, NM (Alluvium)	1 - 290	35
<b>Water, (pCi/liter)</b>		
<b>Nuclear weapons testing</b>		
Enewetak Atoll (groundwater)	$2 \times 10^{-4} - 0.7$	43
Lake Michigan	$2 \times 10^{-4} - 3 \times 10^{-4}$	44
Atlantic Ocean	$1 \times 10^{-4}$	45
<b>Chemical processing</b>		
Savannah River, S. C. (freshwater)	$2 \times 10^{-8}$	46
Savannah River, S. C. (treated drinking water)	$1 \times 10^{-4}$	46
Irish Sea	0.05 - 0.5	30
Los Alamos, NM (treated effluent, surface and ground water, Mortandad Canyon)	0.14 - 17	47

<sup>a</sup> pCi =  $10^{-12}$  curie

Table 5. *Inventory ratios for plutonium in soil at terrestrial research sites*

Site	Compartment	Reference
Los Alamos (Mortandad Canyon)	0.997	49
Oak Ridge (White Oak Creek Flood Plain)	0.999	49
Rocky Flats	> 0.99	50
Nevada Test Site	0.997	51
Trinity Site	0.99	35

ecosystems in which plutonium behavior can differ from the norm. For example, fallout plutonium in arctic ecosystems can be retained by dense lichen mats that effectively delay the transfer of plutonium to soil by several years due to an effective weathering half time of plutonium from lichens of about 6 years [22, 48]. Although such circumstances can have short term significance in terms of entry of plutonium into food webs (i.e. lichen-caribou-eskimo), the final repository of fallout plutonium in those ecosystems will also be soil. In aquatic ecosystems, the transuranic elements may vary in distribution between water and sediment depending upon the chemical environment, the volume of water relative to sediment surfaces, and the size and type of sediment material. In relatively shallow water such as Lake Michigan [52], Buzzards Bay [53], the Irish Sea [54], and Trombay Harbor [55] greater than 95% of the Pu is associated with sediments. In the open ocean, a smaller proportion of the plutonium may be

in sediments because of the long settling time of particulate matter or slow diffusion of soluble forms to great depths [45]. Data for americium are limited but indicate a distribution between water and sediment that is similar to plutonium [54]. A similar inference can be made for curium; however, neither curium nor neptunium have been measured in aquatic environments in sufficient amounts to provide reliable inventories.

#### Transport and fate in the environment

In general the actinide elements show a strong association with soils and sediments. That degree of association influences the concentrations that are available for abiotic and biotic transport processes. In most cases the mobile or soluble fraction is small relative to the amount adsorbed on solid matter, however, solubility is highly dependent

upon the chemistry of the element and upon the chemical environment to which the element is exposed.

One of the most important aspects of chemical behavior of the actinide elements is the stability of the various oxidation states in the ranges of oxidation-reduction potentials (Eh from 0.6 V to -0.2 V) and pH [4-9] found in most environments [56]. The actinide elements display similar behavior when they are in the same oxidation state, but, chemical characteristics can be markedly different if oxidation states are changed [26]. Those changes in chemistry are very important for plutonium, neptunium and uranium because they display multiple oxidation states in aqueous solutions within the natural range of conditions. The oxidation states for those elements in the environment may be U(IV), U(VI), Np(IV), Np(V), Pu(III), Pu(IV), Pu(V) and Pu(VI). The stability of their oxidation states varies considerably as demonstrated by the Eh-pH diagrams for uranium (Fig. 2) [57] and plutonium (Fig. 3) [58]. Uranium is capable of maintaining the more soluble uranyl (+6) species at lower Eh values within the natural pH range than is plutonium in maintaining the plutonyl species (+6). However, over a fairly large Eh-pH region  $\text{PuO}_2^+$  (+5) appears to be stable. The higher oxidation state for neptunium,  $\text{NpO}_2^+$ , is intermediate in stability to those of uranium and plutonium and reduction to Np(IV) begins at an Eh of about 0.3 V at pH 6 [59] which means that Np(V) can exist over much of the normal environmental range of Eh and pH.

Stability field diagrams are useful for establishing the boundary parameters for the existence of chemical species in the environment but they are limited in predictive capability because they can only be valid for the conditions under which they were measured. The presence of complexing ligands and competing reactions in environmental media may modify the predicted oxidation state of actinides in soils and natural waters. However, americium and curium appear to remain in the (+3) oxidation state over the normal range of environmental conditions.

Measurements in the Irish Sea [60], Lake Michigan [61], North Pacific [62] and a Marshall Islands lagoon [63] show that 50 to 90 percent of the dissolved plutonium in oligotrophic water (low in plant nutrients, high in oxygen), with pH greater than 7, exists as an oxidized form. The lower percentage is typical of measurements made at the surface and at intermediate depths in the open ocean. The higher percentages were measured in Lake Michigan, the Irish Sea near Windscale, near the deep ocean bottom, and in lagoon water where interactions with sediment are more likely. NELSON and ORLANDINI [64] adapted a method developed by INOUE and TOCHIYAMA [65] for determining the presence of Np(V) to measure Pu(V) at environmental concentrations; they demonstrated that the oxidized form in several natural waters was in fact  $\text{PuO}_2^+$ . BONDIETTI, using a different procedure, produced confirmatory evidence for the existence of Pu(V) in a pond at Oak Ridge [66]. Calculations based on the data in Table 4 suggest that Pu(V) is present in aqueous environments at concentrations of  $10^{-13}$  to  $10^{-17}$  M.

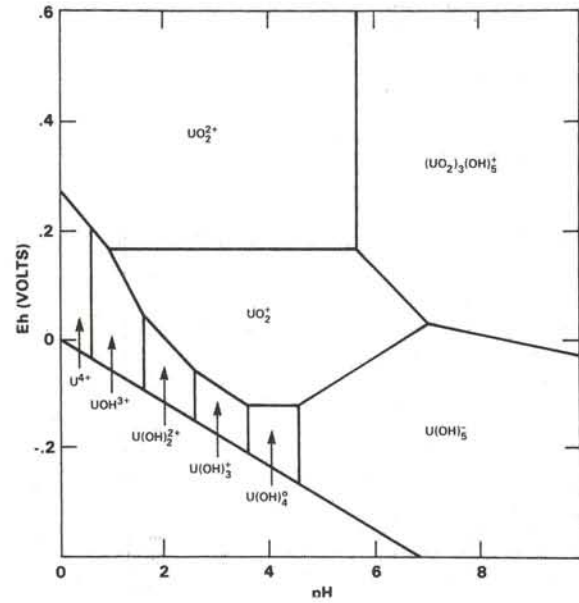


Fig. 2. Eh-pH diagram for uranium oxidation states at an equilibrium temperature of 25°C and total uranium concentration of  $10^{-6}$  M (ref. [57]).

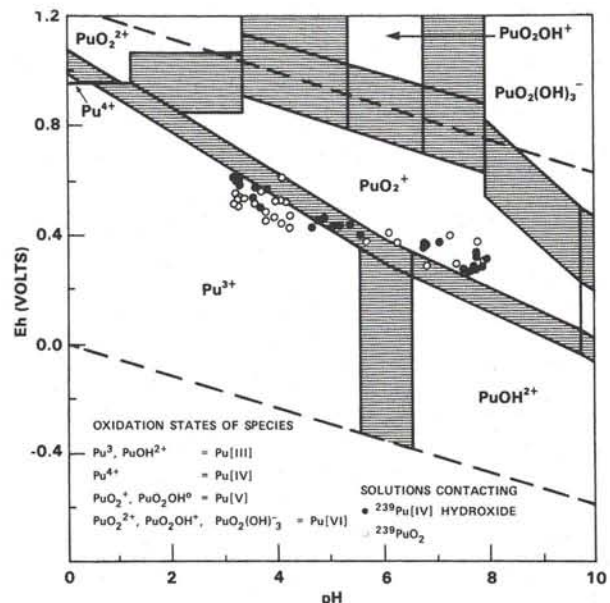


Fig. 3. Equilibrium diagram of Eh-pH at 25°C showing stability fields of different aqueous Pu species. Dashed lines represent one atmosphere  $\text{O}_2$  (upper) and one atmosphere  $\text{H}_2$  (lower). Shaded areas represent regions of known uncertainty. Data points represent Eh values measured at given pH for Pu(IV) hydroxide and  $\text{PuO}_2$  (crystalline) in control with 0.0015 M  $\text{CaCl}_2$  (ref. [58]).

Actinide concentrations often will be increased in water due to the presence of ligands that produce soluble complexes. Those complexes may compete with redox and hydrolysis reactions that result in sorption of the actinide to soil and/or sediment. It is clear that carbonate complexes of  $\text{UO}_2^{2+}$  enhance uranium solubility. The formation of soluble complexes likely accounts for higher plutonium concentrations in some lake water compared with water from oligotrophic lakes (Table 6) [67]. Higher concentrations in natural waters may be due to ligands such as sulfate ion or functional groups associated with dissolved

Table 6. Comparison of plutonium concentrations and chemical variables in freshwater lakes [67, 68, 69]

Lake	pH	DOC	SO <sub>4</sub> <sup>2-</sup> μg/l	Pu ML <sup>-1</sup> × 10 <sup>17</sup>
Lake Michigan	8.2	Oligotrophic	16	2.1
Last Mountain (Saskatchewan)	8.4	Oligotrophic	1300	4.5
Little Manito (Saskatchewan)	8.0		10 <sup>5</sup>	47
Banks (Georgia)	3.9			20
Okefenokee (Florida)	5.0	35 ppm		15.4
Mono Lake	>9.0	high		130

organic carbon (DOC). The enhanced solubility of Pu, which has been observed in certain waters, seems to be best correlated with DOC. NELSON *et al.* [68], in a summary of available field data, showed an inverse relationship between the sediment to water distribution ratio,  $K_d$ , and the concentration of DOC. Further experiments, in which the amount of natural DOC was varied in the water, confirmed the inverse dependency of  $K_d$  on DOC and demonstrated that the binding capacity for plutonium may vary between sources of DOC. Measurements at Mono Lake (California), which has a pH > 9 and is high in carbonate ion, has an elevated plutonium concentration in water, however, the oxidation state of this material has not yet been determined [69]. The conditions in the lake appear to be appropriate for the presence of PuO<sub>2</sub><sup>2+</sup> as a soluble carbonate complex.

The sorption of actinides on sediments and soils represents one of the most important processes related to environmental mobility. The stability with which actinides are bound to sediment and soil particles determines their concentration in natural waters, the relative importance of leaching and erosional processes in their movement in watersheds, and the ease with which they can transfer to plants through root uptake. Sorption processes are complex in environmental media and may include various chemical reactions such as ion exchange reactions on soils and organic matter, surface adsorption mechanisms, oxidation reduction reactions and coprecipitation phenomena. In a series of experiments using pond sediments contaminated with <sup>238</sup>Pu, EDINGTON *et al.* [70] demonstrated that the sorption-desorption of <sup>238</sup>Pu in contact with Lake Michigan water was an equilibrium process.

Sorption of actinides with soils and sediments is significantly affected by the oxidation state as shown by studies with clay (Table 7) [26] and ocean sediments (Table 8). In the absence of stabilizing ligands, actinides in the lower oxidation states are more readily removed from aqueous solutions than those in the higher oxidation states because of their high ionic charge and tendency to hydrolyze to sparingly soluble forms.

The mobile forms in soils and sediments, where both organic matter and microbial activity produce a low oxidation-reduction potential, are likely to be the (III) and

Table 7. Sorption of actinides to Miami silt loam clay [26]

Actinide	% Sorbed <sup>a</sup>	$K_d$ <sup>b</sup>
<sup>237</sup> Pu (IV)	99.9	300 000
<sup>233</sup> U (VI)	95.6	4400
<sup>237</sup> Np (V)	61.8	320

<sup>a</sup> At pH 6.5 and in 5 mM Ca(NO<sub>3</sub>)<sub>2</sub> solutions

<sup>b</sup>  $K_d = \frac{\text{conc. on sorbent}}{\text{conc. in solution}}$ , units ml/g

Table 8. Distribution coefficients ( $K_d$ ) for Pu (III and IV) and Pu (V and VI) in windscale suspended sediments [60]

Sample station	Pu (III + IV)	Pu (V + VI)
1	3.4 × 10 <sup>5</sup>	8 × 10 <sup>3</sup>
2	2 × 10 <sup>6</sup>	1.4 × 10 <sup>4</sup>
3	1 × 10 <sup>6</sup>	9 × 10 <sup>3</sup>
4	6 × 10 <sup>6</sup>	6 × 10 <sup>3</sup>
5 surface	1.7 × 10 <sup>6</sup>	1.4 × 10 <sup>4</sup>
5 bottom	3 × 10 <sup>6</sup>	2.8 × 10 <sup>4</sup>
6	5.4 × 10 <sup>6</sup>	—
7	5 × 10 <sup>5</sup>	2.5 × 10 <sup>4</sup>

(IV) states. NELSON and LOVETT [60, 71] determined that the plutonium adsorbed on sediments in the Irish Sea near Windscale was in the reduced state and that most of the Pu in interstitial water was also in the reduced state DAHLMAN *et al.* [26] in experiments with fulvic acid extracted from soil demonstrated the reduction of Pu(VI) and the stabilization of soluble species of Pu(IV). WILDUNG and GARLAND [72] provided evidence that soil microflora produce soluble complexes with reduced plutonium through direct metabolic processes or indirectly by combination with microbial metabolites which may be present in soil.

### Physical transport processes

The importance of wind and water as transport mechanisms for actinides results from the fact that soil is a major repository of these elements in terrestrial ecosystems and that these elements are strongly sorbed to soils [73]. Consequently, processes which transport soil have a direct impact on transport of soil-associated contaminants. Past studies have suggested a strong relationship between contaminant concentration and soil particle size for agricultural chemicals [74, 75] and for plutonium [76, 77, 78]. Because specific surface area (m<sup>2</sup> per g of soil) increases markedly with decreasing particle size [79] and because different chemical associations are influenced by particle size [80], much higher contaminant concentrations are usually associated with particles in the silt-clay size range than with larger particles. Wind and water driven erosional processes result in particle sorting [81, 82]. The combination of particle sorting by erosional processes and the differential association of contaminants by sediment particle size produce complex relationships for contaminant transport in terrestrial ecosystems. The physics of sand trans-

port by wind is described in detail by BAGNOLD [81] and climatic factors affecting wind erosional processes, especially in arid and semiarid areas, are described by MARSHALL [83]. Prediction of actinide transport by physical processes is not a well developed technology at the present time because of the highly variable nature of the driving force and a lack of understanding of the relationships that govern these processes. Studies of plutonium transport by wind in arid and semi-arid regions are reported elsewhere [84, 85, 86]. Recent advances in the ability to predict plutonium transport by hydrologic processes will be discussed further to illustrate relationships that govern physical transport of actinides.

Hydrologic transport processes of particular importance in the physical transport of soil-associated actinides include soil detachment by raindrop splash [87, 88, 89] and soil detachment and transport by overland flow [90, 91, 92]. Soil particles detached by raindrop impact are important because they can be deposited on vegetation surfaces and thus provide a pathway for movement of soil-associated actinides to plants (see section on transport to vegetation). Sediment transported by overland flow is important because it can redistribute contaminants and also deliver them to stream channels for subsequent transport to downstream areas.

The combined phases of runoff, erosion, sediment transport, and deposition on upland areas and in stream channels usually result in enrichment of smaller sediment particles and organic matter in the transported sediment [82] and enrichment in concentration of sediment associated contaminants [74, 75, 93]. This enrichment, which results from particle sorting and differential association of contaminants by particle size, is often expressed as an enrichment ratio: the concentration of contaminant in the transported sediment divided by its concentration in the residual or uneroded soil. Enrichment ratios tend to increase as the amount or rate of soil erosion (or runoff velocity) decreases [74] and have been related by regression analysis to sediment concentration, sediment discharge rate, and sediment yield [74, 75]. By analyzing sediment transport rates by particle size classes in alluvial channels, LANE and HAKONSON [93] derived the following analytic expression for enrichment ratio in alluvial channels:

$$ER = \frac{\sum C_s(d_i) Q_s(d_i)}{C_s \sum Q_s(d_i)} \quad (1)$$

where:

- ER = alluvial channel enrichment ratio,
- $C_s(d_i)$  = Concentration of contaminant in sediment particles of size class  $i$ , with representative diameter  $d_i$  in millimeters.
- $Q_s(d_i)$  = Sediment transport (mass/time) for particles in size class  $i$ , with representative diameter  $d_i$  in millimeters.
- $C_s$  = Mean concentration of contaminant over all particle size classes.

Thus enrichment ratio was shown to be a variable and to

be a function of contaminant concentrations in the soil by particle size classes, the particle size distribution, and the sediment discharge rates by particle size classes. Equation 1 supports the empirical observation that enrichment ratio increases with decreasing sediment discharge rates. For example, at very low sediment discharge rates (those associated with low runoff velocities) the bedload (coarse sediment particles) discharge rate is low and most of the transported sediment is in the smaller particle size classes. Under those conditions, ER in Equation 1 would approach the ratio of concentrations in the finest size classes ( $C_s(d_i)$ ) to the mean concentration over all size classes ( $C_s$ ). At high sediment discharge rates (those associated with high runoff velocities) more of the bed sediments are in transport. In the limit, if all of the bed sediments were in transport in the same proportion as they exist in the bed material, ER in Equation 1 would be unity.

Field measurements of enrichment ratios for several elements at several locations in the United States are listed in Table 9. The first four entries in Table 9 represent enrichment ratios for soil nutrients in runoff from small agricultural areas; mean values vary from 2.6 to 7.1. The next two entries in Table 9 represent enrichment of fallout plutonium in runoff from small agricultural watersheds; values range from about 1 to 4. The last two entries in Table 9 represent enrichment of plutonium in runoff in stream channels representing larger watersheds. Enrichment ratios observed at Los Alamos ranged from 1.4 to 13.3 with a mean of 5.5. Based on Equation 1, predicted enrichment ratios for Los Alamos stream channels ranged from 2.9 to 7.0 with a mean of 5.2. The rather close agreement between observed and predicted enrichment ratios suggests that particle sorting alone can account for the enrichment ratios observed at Los Alamos. Although other factors undoubtedly influence the observed enrichment ratios, recent analyses [75, 79, 93] suggest that particle sorting alone can produce enrichment ratios on the same order as those that are observed under field conditions. In spite of wide differences in watershed size, hydrologic regime, and chemical characteristics inherent in the data in Table 9, enrichment ratios resulting from sediment transport are quite similar for several sediment associated contaminants. Although transport processes undoubtedly differ between locations and contaminants, we suggest that particle sorting is one of the important factors involved in transport of sediment associated contaminants.

### Transport of biota

The importance of actinides as environmental contaminants depends on whether these materials enter biological pathways, and if so, do these pathways lead to man. Considerable insight has been obtained on the behavior of plutonium and to a lesser extent, americium in terrestrial ecosystems. The postulated behavior of the other actinides in the terrestrial environment is weakly supported by a few laboratory studies and by essentially, no field studies.

Table 9. *Approximate enrichment ratios for nutrients and plutonium associated with sediment at various locations in the United States*

Land use and location	Approximate enrichment ratios		Comments	References
	mean	range		
Cropland, USA <sup>a</sup>	4.5	2.5 – 7.4	Nitrogen	75
	3.6	2.6 – 6.0	Phosphorus	75
Rangeland, USA <sup>a</sup>	2.6	1.1 – 6.7	Nitrogen	75
	7.1	2.7 – 17	Phosphorus	75
Cropland, USA <sup>b</sup>	1.6	1.1 – 2.5	Fallout Plutonium	94
Pasture, USA <sup>b</sup>	2.3	0.8 – 4.0	Fallout Plutonium	94
Mixed Cropland, USA <sup>c</sup>	2.5	1.2 – 4.0	Fallout Plutonium, Transport in Perennial River	95
Semiarid, USA <sup>d</sup>	5.5	1.4 – 13.3	Waste Effluent Plutonium, Transport in Ephemeral Streams	93, 96

<sup>a</sup> Small agricultural watersheds (5.2–18 ha) at Chickasha, Oklahoma

<sup>b</sup> Small agricultural watersheds (2.6–2.9 ha) near Lebanon, Ohio

<sup>c</sup> Great Miami River (Drainage area = 1401 km<sup>2</sup>) at Sidney, Ohio

<sup>d</sup> Los Alamos Watersheds (176–15,000 ha) near Los Alamos, New Mexico

By nature of the wide diversity of conditions under which plutonium studies have been conducted in terrestrial ecosystems, we are in a position to evaluate the behavior of this element under a wide spectrum of study site and plutonium source conditions. Climatic conditions ranging from arid to humid and involving plutonium from weapons fallout, industrial waste effluents and accidental spills have been investigated [73].

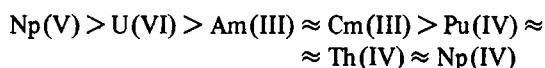
#### Transport to vegetation

The two processes controlling actinide content of terrestrial plants are:

- physiological availability to plant roots with subsequent translocation to plant parts, and
- the deposition of particles on foliage surfaces with or without subsequent absorption into plant tissues.

The physiological availability of plutonium, americium and to a lesser degree, curium, and neptunium have been studied under a variety of controlled laboratory conditions [97, 98, 99, 100].

Based upon theoretical considerations the postulated availability of the actinides to plants [6, 101] is as follows:



Pot culture studies tend to support that order of plant availability of the actinides to plants [6, 101] is as follows: tation in plant over that in soil [97]. The concentration ratio as applied to the actinides has been defined [102] as:

$$\frac{\text{Activity/mass of receptor}}{\text{Activity/mass of donor}}$$

In terrestrial systems the donor compartment is usually considered to be soil. Concentration ratios range from 10<sup>-4</sup> to 10<sup>-8</sup> for plutonium and 10<sup>-1</sup> to 10<sup>-7</sup> for americium.

Limited data for other actinides show concentration ratios of 10<sup>-3</sup> to 10<sup>-4</sup> for curium and 10<sup>-1</sup> to 10<sup>-2</sup> for neptunium.

The physiological availability of any one actinide can be increased or decreased by at least an order of magnitude by soil amendments and indigenous soil factors. For example, the addition of a chelating agent (DPTA) generally increases availability of plutonium and americium to plants, while liming treatment of the soil has been shown to reduce plant availability of americium [97]. The importance of understanding the influence of soil amendments and indigenous soil factors on actinide availability to plants results from the fact that wastes from nuclear industries and fertilizers applied to agricultural lands often contain chemicals (e.g. chelators) that can modify actinide mobility [97].

Reduced plutonium that passes the root membrane migrates to the shoots of plants in the xylem in association with organic ligands [72]. Differences in the gastrointestinal absorption of plutonium deposited in leaves versus stems, suggest that the chemical form of plutonium in these two plant tissues differ [72]. Based on pot culture studies, available data on actinide distributions in various plant parts suggest that concentration patterns are as follows:



Concentration ratios (plant/soil) of plutonium, americium, curium, and neptunium in seed-fruits generally average from 1 to 2 orders of magnitude lower than the ratio for stem-leaves [4, 98, 99]. Thus, in situations where root uptake predominates in actinide movement to agricultural crops, food chain transport of the actinides to humans through ingestion of fruits and seeds will be diminished.

Despite the host of chemical, biological and physical factors which can modify the physiological availability of actinides and subsequent transport within plant tissues [72, 97, 103], field studies in contaminated sites suggest

Table 10. Comparison of plutonium concentration ratios for field and glasshouse conditions [51]

Soil source	Field	Glasshouse
NTS <sup>a</sup> Area 11B	$1.3 \times 10^{-2}$ to $1.6 \times 10^{-1}$	$1.5 \times 10^{-4}$
NTS Area 11C	$4.5 \times 10^{-2}$ to $3.4 \times 10^{-1}$	$1.8 \times 10^{-4}$
NTS Area 13	$7.8 \times 10^{-2}$ to $4.4 \times 10^{-1}$	$1.1 \times 10^{-4}$

<sup>a</sup> NTS (Nevada Test Site)

that contamination of foliage surfaces with particles containing actinides is the dominant transport mechanism in the environment under many conditions of climate for varied sources. Comparative studies of plant uptake of plutonium under both field and laboratory conditions generally yield the relationships shown in Table 10. Studies focused specifically on root uptake of plutonium from soils yield plant-soil concentration ratios which are at least one order of magnitude lower than the ratios observed under comparable conditions at field sites. Those differences in concentration ratios imply that a mechanism exists in the environment for delivering at least 10 times more plutonium to vegetation than transport across root membranes. The higher ratios observed at field sites are generally attributed to the presence of surficial contamination on field site vegetation. That conclusion is supported by the obvious presence of soil on foliage surfaces and by the ability to remove some of the plutonium contamination from vegetation by washing [34, 104].

Plutonium from a reprocessing plant atmospheric effluent serves as the major source of contamination on adjacent vegetation at a site in the humid southeast U.S. [105]. However, in most terrestrial sites contaminated with plutonium, direct fallout sources of plutonium are minimal relative to terrestrial sources such as wind and water re-suspended soil.

Studies in semi-arid regions of New Mexico demonstrated that rain-splash of soil particles with subsequent deposition on foliage surfaces can contribute essentially all of the plutonium measured in field-site vegetation [47]. More importantly, those studies, which employed a labeled-soil particle technique and the scanning electron microscope, have shown that relationships that govern translational movement of plutonium by erosion processes in soil also govern transport of plutonium to foliage surfaces. For example, impacting raindrops caused an enrichment of small soil particles ( $< 105 \mu\text{m}$ ) on foliage surfaces. In general, only the highly transportable silt-clay particles ( $< 53 \mu\text{m}$  diameter), which generally contain higher concentrations of plutonium [106], are retained by plant surfaces. Calculations based on the mass and plutonium content of soil measured on plants demonstrated that the rainsplash mechanism could easily account for the plutonium concentration ratios of  $5 \times 10^{-2}$  that were observed at this field site [34].

The absorption of plutonium through leaf surfaces has been demonstrated [103] but is considered to be a low order process in contaminated field sites particularly with annual or deciduous vegetation species.

Studies on the uptake of plutonium by vegetable crops grown in contaminated field sites show that as much as 50% of the plutonium in crop samples was surficial contamination that could be removed by standard food preparation procedures [34]. Plutonium that cannot be removed from vegetable crop surfaces by washing does not necessarily reflect plutonium incorporated into plant tissues. CATALDO and VAUGHN [103] have shown that sub-micron particles on foliage surfaces are extremely difficult to remove by either simulated wind or rain.

Under large-scale agricultural conditions, a major source of actinides in crops may result from harvesting practices. For example, most of the plutonium in grain grown in a contaminated field site at Savannah River Laboratory was attributed to cross-contamination with dust generated during mechanical threshing [24].

#### Transport to animals

The transport of actinides to animals is governed by the same processes that control the transport of these elements to plants. That is, the actinides can be incorporated into animal tissues and/or they can be deposited on tissues exposed directly to the environment (i.e. lung, pelt-skin, and gastro-intestinal tract).

Based upon theoretical considerations and the assumption of similar conditions in the gut, actinide absorption from the gut [67] should follow:



Laboratory experiments on the physiological availability of actinides to animals generally follow the pattern listed above; plutonium is least available to animals, americium and curium are intermediate in availability, and neptunium is most available [10]. However, many factors influence gut availability of the actinides such that rankings of availability are not rigid [67]. For example, Pu(IV), which is complexed by microbial and/or plant tissues, may be more available for gut absorption than uncomplexed plutonium [107, 108] while P(VI) added to the gut containing food residues is reduced to P(IV) and thus becomes less available for gut absorption [109]. The current ICRP [8] recommendation for gut absorption of plutonium by man is  $1 \times 10^{-4}$ .

The concentrations of plutonium in animals collected from field sites indicates that gut availability of this element in the environment is low as shown by the low concentrations in internal organs and tissues. In addition, highest concentrations of plutonium are invariably measured in tissues exposed to contamination with soil particles. Plutonium in the pelt, gastro-intestinal tract and to a lower degree, lungs accounts for nearly all of the animal's body burden [35, 50, 110].

Various assessments of the critical pathways of plutonium movement into man suggest that inhalation is the dominant pathway contributing to internal tissue dose [26, 111]. While ingestion contributes as much as 10 times

more plutonium to man than inhalation, the low gut absorption (based on ICRP [8]) reduces the significance of the ingestion pathway in contributing to internal dose. However, the recommended gut absorption factor of  $1 \times 10^{-4}$  [8] is based on laboratory studies with rats that were fed plutonium. In light of recent concerns [112], a closer examination of gut absorption values for plutonium and other actinides, under environmental conditions is needed.

The high mobility of large herbivores coupled with natural elimination processes provides a mechanism for actinide transport across the landscape. Studies in nuclear fallout areas at Nevada Test Site [113] and in a nuclear spill area at Rocky Flats, Colorado [104] show that large herbivores (deer and cattle) ingest substantial quantities of plutonium-contaminated soil (i.e. several hundred grams per day for range cattle). Although the amount of plutonium transported across the landscape by this mechanism is considered to be small in areas where the extent of contamination is large (i.e. fallout areas) relative to the home range of the animal, there are circumstances where this transport mechanism becomes important. For example, in a nuclear waste burial site at Hanford Washington, jack rabbits (*Lepus californicus*) which gained access to buried waste, ingested radioactive salts and subsequently excreted the salts on the surface of the site and surrounding area [114].

Studies on pocket gophers (*Thomomys bottae*) inhabiting a low-level waste site at Los Alamos, New Mexico [115], show that the burrowing activities of this animal can greatly perturb cover profiles placed over low-level radioactive waste disposal trenches. Over a one year period, gophers excavated about 11 metric tons of soil per hectare from within the trench cover and created about 3000 m of tunnel system in the cover profile. Animal burrowing activities can alter actinide distributions within the soil profile, as has been shown for pocket gophers in contaminated sites at Rocky Flats, Colorado [116] and for other small mammals at the Radioactive Waste Management Complex at Idaho National Engineering Laboratory [117].

Burrowing activities by animals can have a significant effect on the structure and output of dose assessment models for the actinides. For example, at low-level waste sites, that use shallow-land burial methods, radionuclides brought to the surface along with soil casts become subject to physical transport processes as well as to physiological processes associated with root uptake. As discussed previously, physical processes transfer at least 10 times more plutonium to vegetation than do physiological processes.

Studies with honeybees at Los Alamos [118] demonstrated that small amounts of plutonium present in treated liquid wastes used by bees appear in honey. Considering that most of the plutonium in the effluent is associated with particles (< 30% is associated with the fraction <  $0.05 \mu\text{m}$  [119]), honeybees may be capable of transporting actinides that are both in solution and in association with particles in a liquid source to the honey.

Based upon the analysis of available concentration ratios for the actinides, both chemical and physical processes contribute to the contamination of biological components of ecosystems. Physical processes that cause soil to be transported to plants and animals dominate in the transport of plutonium and perhaps to a lesser degree, americium through food webs. Although the plutonium and americium passing through an animal may be largely associated with particles, the relative importance of this source of actinide compared to that incorporated into food-stuffs in contributing to internal tissue burdens is unknown. However, it is a fact, in the case of plutonium, that physical processes can deliver at least 10 times more plutonium to plants than root uptake. That fact would suggest the need to determine the relative importance of plutonium deposited on plants versus that incorporated into plants as a source of contamination to plant consumers.

The general lack of data on curium, neptunium, uranium and thorium in terrestrial ecosystem components precludes any conclusions on food web transport. All available data from laboratory studies indicate that those elements are more mobile than plutonium.

Recent field studies at Oak Ridge [120, 121] show that the availability of actinides to plants and animals in two terrestrial study sites was:

$$U > Cm \geq Am > Th \approx Pu$$

Uranium was about 10 times more available to plants and animals than plutonium and thorium. Further field studies are needed to place bounds on the degree of transport of those elements to biota.

## Aquatic

### Distribution and transport

Assessing the transport of actinides to aquatic biota by the conventional concentration ratio, as defined previously [102], presents a dilemma in that it is not always clear which aquatic component serves as the donor of the actinides to receptor components. Concentration ratios for aquatic systems are usually based on water as the donor compartment. Thus, CR's reported for plutonium suggest that aquatic organisms highly concentrate this element.

As an example of the problem, a comparison of concentration ratios based on water versus those based on sediment as the donor compartment is given in Table 2 for several biotic components of Lake Michigan [122].

Regardless of how the ratio is calculated, it is clear that plutonium is attenuated as it passes through successively higher trophic levels. Based upon observations in both freshwater and marine environments, it appears that concentration ratios decrease about one order of magnitude at each succeeding trophic level. There is strong evidence

Table 11. Comparison of plutonium concentration ratios for biological components of Lake Michigan using water versus sediment as the donor compartments (Adapted from ref. [122])

Compartment	Donor compartment	
	Water <sup>a</sup>	Sediment
Mixed plankton	6300	$5 \times 10^{-2}$
Benthic invertebrates	1300	$1 \times 10^{-2}$
Zooplankton	250	$2 \times 10^{-3}$
Benthic fish	250	$2 \times 10^{-3}$
Planktivorous fish	60	$5 \times 10^{-4}$
Piscivorous fish	0.5	$3 \times 10^{-6}$
Water	1	$8 \times 10^{-6}$
Sediment	130000	1

<sup>a</sup> concentration ratio =  $\frac{\text{pCi Pu/g receptor}}{\text{pCi Pu/g donor}}$ ; data in table based on wet weights.

that physical processes (i.e. surface attachment and/or ingestion of suspended particles and/or sediments) play an important role in contaminating aquatic biota with plutonium [112]. Organisms living in close association with bottom sediments generally have the highest plutonium concentration ratios (Table 11).

The small amount of data on americium in aquatic biota do not provide a sufficient basis for comparison with corresponding plutonium data. Some studies suggest that americium is more available than plutonium in the aquatic environs [123, 124] while other studies show no such patterns [125, 126]. Field data on the other actinides appear to be completely lacking.

### Summary and conclusions

The chemical characteristics of the actinide elements cause them to be sorbed to soils and sediments to a large extent. The stability of the sorption largely controls how mobile these elements will be in food chain processes such as root uptake in plants, gill transfer in fish, or ingestion via food or water.

Although plutonium and americium are tightly bound to soils and sediments in the environment, a very small fraction of these elements is soluble and enters biological tissues. The limited time-span (< 40 years) over which we have observed actinide behavior in the environment seriously limits our ability to forecast their behavior over the centuries and millenia during which many of these elements will be present in the environment. However, preliminary observations on naturally occurring analog elements indicate that actinide solubility will likely not change appreciably with time.

Present data demonstrate that soils and sediments serve as the major repository of plutonium in freshwater and terrestrial ecosystems and that processes which redistribute soils and sediment can also cause major changes in the environmental distribution of this element. Although data-bases for the other actinides are small, physical processes will also provide a potentially important transport mechanism for these elements.

It is clear that there is a need to determine the relative importance of actinides associated with soil and sediment as a source of contamination to biota. Available data on actinides in terrestrial and fresh water ecosystems point to the potential importance of soil and sediment movement through food webs.

Because physical transport processes operate at the soil-air or sediment-water interface, changes in the distribution of plutonium within the soil-sediment profile will alter the importance of this transport pathway. Present distributions of plutonium in soil profiles from sites contaminated up to 35 years ago [35, 50] indicate that with time plutonium is depleted from the soil surface either from losses with eroding soil or from transport into the soil profile. Whether those changes in plutonium distribution will change the relative importance of, what at present, are low order chemical processes is unknown. In many aquatic systems, plutonium migration into the sediments through sedimentation and/or chemical processes may isolate the plutonium from the biosphere. In terrestrial systems, losses of plutonium into the soil profile may create conditions more favorable for root uptake.

Any phenomena which retain actinides in contact with the biosphere for extended times such as has been observed in arctic ecosystems will increase risks due to exposure to these elements. The interception properties of vegetation cover, action by organisms living in the soil, and processes which resuspend sediments in aquatic ecosystems all contribute to maintaining actinides within the biosphere.

With few exceptions, all present sources of actinides in terrestrial and aquatic ecosystems have resulted in very low transfer of these elements into food webs regardless of the transport process. Doses to humans resulting from ingestion of food-stuffs contaminated with the actinides have been uniformly low – much below doses incurred by humans from natural sources.

### Acknowledgements

This work was funded by the Department of Energy under contract W-7405-ENG-36 with Los Alamos National Laboratory. We gratefully acknowledge the assistance of E. MONTOYA in manuscript preparation.

### References

1. SPOOR, N. L., HURSH, J. B.: Protection Criteria. In: *Handbook of Experimental Pharmacology XXXVI, Uranium, Plutonium, Transplutonic Elements* (H. C. HODGE, J. N. STAN NARD, J. B. HURSH, eds.) Springer-Verlag, New York 1973.
2. TILL, J. E.: Assessment of the Radiological Impact of  $^{232}\text{U}$  and Daughters in Recycled HTGR Fuel. ORNL-TM-5049. Oak Ridge National Laboratory, Oak Ridge, Tennessee (1976).
3. ERDMAN, C. A., REYNOLDS, A. B.: Radionuclide Behavior During Normal Operation of Liquid-Metal-Coolant Fast Breeder Reactors. Part I: Production, Nucl. Safety 16, 43 (1975).
4. SCHRECKHISE, R. G.: Comparative Uptake and Distribution of Plutonium, Americium, Curium and Neptunium in Four Plant Species, Health Phys. 38, 817 (1980).

5. SULLIVAN, M. F.: Absorption of Actinide Elements from the Gastrointestinal Tract of Rats, Guinea Pigs and Dogs. *Health Phys.* **38**, 159 (1980).
6. BONDIETTI, E. A., SWEETON, S. H., FOX, H.: Transuranic Speciation in the Environment. In: *Transuranics in Natural Environments* (M. G. WHITE and P. B. DUNAWAY, eds.), NVO-178. U.S. Energy Research and Development Administration. NTIS, Springfield, VA. 1977.
7. PERKINS, R. W., THOMAS, C. W.: Worldwide Fallout. In: *Transuranic Elements in the Environment* (W. C. HANSON, ed.) DOE/TIC 22800. U.S. Department of Energy, NTIS, Springfield, VA. 1980.
8. I.C.R.P. Publication 30, Part I: Limits for Intakes of Radionuclides by Workers. A report to Committee 2 of the International Commission on Radiological Protection. *Annals of the ICRP* **2** (3/4), Pergamon Press, 1979, p. 105.
9. VAUGHAN, J., BLEANEY, B., TAYLOR, D. M.: Distribution, Excretion and Effects of Plutonium as a Bone-Seeker. In: *Handbook of Experimental Pharmacology XXXVI Uranium, Plutonium, Transplutonic Elements*. (H. C. HODGE, J. N. STANNARD, and J. B. HURSH, eds.) Springer-Verlag, New York 1973.
10. DURBIN, P. W.: Metabolism and Biological Effects of the Transplutonium Elements. In: *Handbook of Experimental Pharmacology XXXVI Uranium, Plutonium, Transplutonic Elements*, p. 739 (H. C. HODGE, J. N. STANNARD, and J. B. HURSH, eds.) Springer-Verlag, New York 1973.
11. KLEMENT, A.: Natural Radionuclides in Foods and Food Source Materials. In: *Radioactive Fallout, Soils, Plants, Foods, Man* (E. B. FOWLER, ed.) Elsevier, New York 1965, p. 113.
12. VINOGRADOV, A. P.: The Geochemistry of Rare and Dispersed Chemical Elements in Soils. Consultants Bureau, Inc., New York 1959.
13. ADAMS, J. A. S., OSMOND, J. K., ROGERS, J. J. W.: The Geochemistry of Thorium and Uranium. In: *Physics and Chemistry of the Earth* (L. H. AHRENS, ed.) Pergamon Press, New York 1959.
14. GOLDBERG, E. D., BROECKER, W. S., GROSS, M. G., TUREKIAN, K. K.: Marine Chemistry. In: *Radioactivity in the Marine Environment*. National Academy of Sciences, Washington, D.C., 1971.
15. IAEA Working Group: Chapter I, Concentrations of Radionuclides in Aquatic Environments and the Resultant Radiation Dose Rates Received by Aquatic Organisms. In: *Effects of Ionizing Radiation on Aquatic Organisms and Ecosystems*. STI/DOC/10/172. IAEA, Vienna 1976.
16. LEVINE, C. A., SEABORG, G. T.: The Occurrence of Plutonium in Nature. *J. Am. Chem. Soc.* **70**, 3278 (1951).
17. PEPPARD, D. F., STUDIER, M. H., GERGEL, M. V., MASON, G. W., SULLIVAN, J. C., MECH, J. F.: Isolation of Microgram Quantities of Naturally-Occurring Plutonium and Examination of the Isotopic Composition. *J. Am. Chem. Soc.* **70**, 2529 (1951).
18. MYERS, W. A., LINDER, M.: Precise Determination of the Natural Abundance of  $^{237}\text{Np}$  and  $^{239}\text{Pu}$  in Katanga Pitchblende. *J. Inorg. Nucl. Chem.* **33**, 323 (1971).
19. MEIER, H., BOSCHE, D., ZEITLER, G., ALBRECHT, W., HECKER, W., MENGE, P., UNGER, E., ZIMMERHACLE, E.: Anomalies in the Natural Occurrence of  $^{239}\text{Pu}$ . *Radiochim. Acta* **21**, 110 (1974).
20. HARLEY, E. P., KREY, P. W., VOLCHOK, H. L.: Global Inventory and Distribution of Fallout Plutonium. *Nature* **241**, 444 (1973).
21. FACER, G.: Transuranics from Nuclear Weapons Operations. In: *Transuranic Elements in the Environment* (W. C. HANSON, ed.) DOE/TIC 22800. U.S. Department of Energy, NTIS, Springfield, VA. 1980.
22. HANSON, W. C.: Transuranic Elements in Arctic Tundra Ecosystems. In: *Transuranic Elements in the Environment* (W. C. HANSON, ed.) DOE/TIC 22800. U.S. Department of Energy, NTIS, Springfield, VA. 1980.
23. KREITER, M. R., MENDEL, J. E., MCKEE, R. W.: Transuranic Waste from the Commercial Light-Water-Reactor Cycle. In: *Transuranic Elements in the Environment* (W. C. HANSON, ed.) DOE/TIC-22800. U. S. Department of Energy, NTIS, Springfield, VA. 1980.
24. MCLEOD, K. W., ADRIANO, D. C., BONI, A. L., COREY, J. C., HORTON, J. H., PAINE, D., PINDER, J. E.: Influence of a Nuclear Fuel Chemical Separations Facility on the Plutonium Contents of a Wheat Crop. *J. Environ. Qual.* **9**, 306 (1980).
25. ADRIANO, D. C., COREY, J. C., DAHLMAN, R. C.: Plutonium Contents of Field Crops in the Southeastern United States. In: *Transuranic Elements in the Environment* (W. C. HANSON, ed.) DOE/TIC 22800. U.S. Department of Energy, NTIS, Springfield, VA. 1980.
26. DAHLMAN, R. C., BONDIETTI, E. A., EYMAN, L. D.: Biological Pathways and Chemical Behavior of Plutonium and Other Actinides in the Environment. In: *ACS Symposium Series, No. 35. Actinides in the Environment* (A. M. FRIEDMAN, ed.), 1976.
27. HAKONSON, T. E., NYHAN, J. W., PURTYMAN, W. D.: Accumulation and Transport of Soil Plutonium in Liquid Waste Discharge Areas at Los Alamos. In: *Transuranium Nuclides in the Environment*, S.T.I./PUB/410. IAEA, Vienna 1976.
28. BARTELT, G. E., WAYMAN, C. W., GROVES, S. E., ALBERTS, J. J.:  $^{238}\text{Pu}$  and  $^{239,240}\text{Pu}$  Distribution in Fish and Invertebrates from the Great Miami River, Ohio. In: *Transuranics in Natural Environments*, NVO-178. (M. G. WHITE and P. B. DUNAWAY, eds.) U.S. Department of Energy, NTIS, Springfield VA. 1977.
29. SCHUTTELKOPF, H.: Environmental Surveillance for Plutonium at the Karlsruhe Nuclear Research Center from 1973 to 1975. In: *Transuranium Nuclides in the Environment*, STI/PUB/410. Vienna 1976.
30. HETHERINGTON, J. A., JEFFRIES, D. E., MITCHELL, N. T., PENTREATH, R. J., WOODHEAD, D. S.: Environmental and Public Health Consequences of the Controlled Disposal of Transuranium Elements to the Marine Environment. In: *Transuranium Nuclides in the Environment*, STI/PUB/410. Vienna 1976.
31. HAYES, D. W., LEROY, J. W., CROSS, F. A.: Plutonium in Atlantic Coastal Estuaries in the Southeastern United States of America. In: *Transuranium Nuclides in the Environment*, STI/PUB/410. Vienna 1976.
32. WHICKER, F. W.: Ecological Effects of Transuranics in the Terrestrial Environment. In: *Transuranic Elements in the Environment* (W. C. HANSON, ed.) DOE/TIC 22800. U.S. Department of Energy, NTIS, Springfield, VA. 1980.
33. MILHAM, R. C., SCHUBERT, J. F., WATTS, J. R., BONI, A. L., COREY, J. C.: Measured Plutonium Resuspension and Resulting Dose from Agricultural Operation of an Old Field at the Savannah River Plant in the Southeastern United States of America. In: *Transuranium Nuclides in the Environment*, STI/PUB/410. Vienna 1976.
34. WHITE, G. C., HAKONSON, T. E., AHLQUIST, A. J.: Factors Affecting Radionuclide Availability to Vegetables Grown at Los Alamos. *J. Environ. Qual.* **10**, 294 (1981).
35. HAKONSON, T. E., NYHAN, J. W.: Ecological Relationships of Plutonium in Southwest Ecosystems. In: *Transuranic Elements in the Environment* (W. C. HANSON, ed.) DOE/TIC-22800. U.S. Department of Energy, NTIS, Springfield, VA. 1980.
36. GILBERT, R. O., EBERHARDT, L. L., FOWLER, E. B., ROMNEY, E. M., ESSINGTON, E. H., KINNEAR, J. E.: Statistical Analysis of  $^{239,240}\text{Pu}$  and  $^{241}\text{Am}$  Contamination of Soil and Vegetation on NAEG Study Sites. In: *The Radioecology of Plutonium and Other Transuranics in Desert Environments*, NVO-153 (M. G. WHITE and P. B. DUNAWAY, eds.) U.S. Department of Energy, NTIS, Springfield, VA. 1975.
37. HARDY, E. P.: Depth Distribution of Global Fallout  $^{90}\text{Sr}$ ,  $^{137}\text{Cs}$  and  $^{239,240}\text{Pu}$  in Sandy Loam Soil. In: *Fallout Program Quarterly Summary Report*, HASL-286, U.S. Atomic Energy Commission, NTIS, Springfield, VA. 1974.
38. ROMNEY, E. M., WALLACE, A., GILBERT, R. O., KINNEAR, J. E.:  $^{239,240}\text{Pu}$  and  $^{241}\text{Am}$  Contamination of Vegetation in Aged Fallout Areas. In: *Transuranium Nuclides in the Environment*, STI/PUB/410, Vienna 1976.
39. NEVISSI, A., SCHELL, W. R., NELSON, V. A.: Plutonium and Americium in Soils of Bikini Atoll. In: *Transuranium Nuclides in the Environment*, STI/PUB/410, Vienna 1976.
40. EDGINGTON, D. N., WAHLGREN, M. A., MARSHALL, J. S.: The Behavior of Plutonium in Aquatic Ecosystems: A Summary of Studies of the Great Lakes. In: *Environmental Toxicity of Aquatic Radionuclides: Models and Mechanisms* M. W. MILLER and J. N. STANNARD, eds.) Ann. Arbor

- Science Publishers, Ann Arbor, Michigan 1976.
41. CORLEY, J. P., ROBERTSON, D. M., BRAUER, F. P.: Plutonium in Surface Soil in the Hanford Plant Environs. In: *Proceedings of Environmental Plutonium Symposium*, LA-4756, Los Alamos Scientific Laboratory, NTIS, Springfield, VA. 1971.
  42. KREY, P. W., HARDY, E. P.: Plutonium in Soil Around Rocky Flats Plant. In: *Fallout Program Quarterly Summary Report*, HASL-235, U.S. Atomic Energy Commission, 1970.
  43. NOSHKIN, V. E., WONG, K. M., MARCH, K., EAGLE, R., HOLLADAY, G., BUDDEMEIER, R. W.: Plutonium Radionuclides in the Groundwaters of Enewetak Atoll. In: *Transuranium Nuclides in the Environment*, STI/PUB/410 IAEA, Vienna 1976.
  44. WAHLGREN, M. A., ALBERTS, J. J., NELSON, D. M., ORLANDINI, K. A.: Study of the Behavior of Transuranics and Possible Chemical Homologues in Lake Michigan Water and Biota. *Ibid.*
  45. BOWEN, V. T., WONG, K. M., NOSHKIN, V. E.:  $^{239}\text{Pu}$  In and Over the Atlantic Ocean. *J. Mar. Res.* 29(1), (1971).
  46. COREY, J. C., BONI, A. L.: Removal of Pu from Drinking Water by Community Water Treatment Facilities. In: *Transuranium Nuclides in the Environment*. STI/PUB410. IAEA, Vienna 1976.
  47. ANONYMOUS: Environmental Surveillance at Los Alamos During 1980. Los Alamos National Laboratory Report, LA-8810-ENV, UC-41 (1981).
  48. HOLM, E., PERSSON, R. B. R.: Fallout Plutonium in Swedish Reindeer Lichens. *Health Phys.* 29, 43 (1975).
  49. DAHLMAN, R. C., GARTEN, C. T., HAKONSON, T. E.: Comparative Distribution of Plutonium in Contaminated Ecosystems at Oak Ridge, Tennessee, and Los Alamos, New Mexico. In: *Transuranic Elements in the Environment*. (W. C. HANSON, ed.) DOE/TIC-22800. U.S. Department of Energy, NTIS, Springfield, VA. 1980.
  50. LITTLE, C. A.: Plutonium in a Grassland Ecosystem. In: *Transuranic Elements in the Environment* (W. C. HANSON, ed.) DOE/TIC-22800. U.S. Department of Energy, NTIS, Springfield, VA. 1980.
  51. ROMNEY, E. M., WALLACE, A.: Plutonium Contamination of Vegetation in Dusty Field Environments. In: *Transuranics in Natural Environments*. NVO-178 (M. G. WHITE and P. B. DUNAWAY, eds.) U.S. Department of Energy, NTIS, Springfield, VA. 1977.
  52. EDGINGTON, D. N., ROBBINS, J. A.: The Behavior of Plutonium and Other Long-Lived Radionuclides in Lake Michigan, II: Patterns in Sediments. In: *Impacts of Nuclear Releases into the Aquatic Environment*. STI/PUB/406. IAEA, Vienna 1976.
  53. LIVINGSTON, H. L., BOWEN, V. T.: Americium in the Marine Environment-Relationships to Plutonium. In: *Environmental Toxicity of Aquatic Radionuclides: Models and Mechanisms* (M. W. MILLER and J. N. STANNARD, eds.) Ann Arbor Science Publishers, Ann Arbor, Michigan 1976.
  54. HETHERINGTON, J. A.: The Uptake of Plutonium Nuclides in Marine Sediments. *Marine Science Commun.* 4 (3), 239 (1978).
  55. PILLAI, K. C., MATHEW, E.: Plutonium in the Aquatic Environment, Its Behavior, Distribution, and Significance. In: *Transuranium Nuclides in the Environment*. STI/PUB/410. IAEA, Vienna 1976.
  56. BAAS BECKING, L. G. M., KAPLEN, I. R., MOORE, D.: Limits of the Natural Environment in Terms of pH and Oxidation-Reduction Potentials. *J. Geol.* 68, 243 (1960).
  57. LANGMUIR, D.: Uranium Solution-Mineral Equilibria at Low Temperatures with Applications to Sedimentary Ore Deposits. *Geochem. Cosmochem. Acta* 42, 547 (1978).
  58. RAI, D., SERNE, R. J., SWANSON, J. L.: Solution Species of  $^{239}\text{Pu}$ (V) in the Environment. In: *Waste Isolation Safety Assessment Program, Task 4, Second Information Meeting*, PNL-SA-7352. (R. J. SERNE, ed.) Vol. I. U.S. Department of Energy, 1978.
  59. BONDIETTI, E. A.: Environmental Chemistry of Np: Valence Stability and Soil Reactions. In: *Agron. Abs.*, Amer. Soc. of Agron., Madison, Wisc. 1976.
  60. NELSON, D. M., LOVETT, M. B.: Oxidation State of the Plutonium in the Irish Sea. *Nature* 276, 599 (1978).
  61. WAHLGREN, M. A., ALBERTS, J. J., NELSON, D. M., ORLANDINI, K. A., KUCERA, E. T.: Study of the Occurrence of Multiple Oxidation States of Plutonium in Natural Water Systems. Radiological and Environmental Research Division Annual Report, ANL-77-65, Part III, 1977.
  62. NELSON, D. M., METTA, D. N., LARSEN, R. P.: Oxidation State Distribution of Plutonium in Marine Waters. Radiological and Environmental Research Division Annual Report, ANL-80-115, Part III. Argonne National Laboratory, 1981.
  63. NOSHKIN, V., EAGLE, R., WONG, K., JOKELA, T. A.: Transuranic Concentrations in Pelagic Fish from the Marshall Islands. In: *Impacts of Radionuclide Releases into the Marine Environment*. STI/PUB565, IAEA, Vienna 1981.
  64. NELSON, D. M., ORLANDINI, K. A.: Measurement of Pu(V) in Natural Waters. Radiological and Environmental Research Division Annual Report, ANL-79-65, Part III. Argonne National Laboratory, 1980.
  65. INOUE, Y., TOCHIYAMA, O.: Determination of the Oxidation States of Neptunium at Tracer Concentrations by Adsorption on Silica Gel and Barium Sulfate. *J. Inorg. Nucl. Chem.* 39, 1443 (1977).
  66. BONDIETTI, E. A., TRABALKA, J. K.: Evidence for Plutonium(V) in an Alkaline Freshwater Pond. *Radiochem. Radioanal. Chem. Lett.* 42, 169 (1980).
  67. WATTERS, R. L., EDGINGTON, D. N., HAKONSON, T. E., HANSON, W. C., SMITH, M. H., WHICKER, F. W., WILDUNG, R. E.: Synthesis of the Research Literature. In: *Transuranic Elements in the Environment*, DOE/TIC 22800 (W. C. HANSON, ed.) U.S. Department of Energy, NTIS, Springfield, VA. 1980.
  68. NELSON, D. M., KARTTUNEN, J. O., ORLANDINI, K. A., LARSEN, R. P.: Influence of Dissolved Organic Carbon on the Sorption of Plutonium to Natural Sediments. Radiological and Environmental Research Division Annual Report, ANL-80-115, Part III. Argonne National Laboratory. Argonne, Illinois, 1981.
  69. SIMPSON, H. J., TRIER, R. M., OLSEN, C. R., HAMMOND, D. E., EGE, A., MILLER, L., MELACK, J. M.: Fallout Plutonium in an Alkaline, Saline Lake. *Science* 207, 1071 (1980).
  70. EDGINGTON, D. N., KARTTUNEN, J. O., NELSON, D. M., LARSEN, R. P.: Plutonium Concentrations in Natural Waters - Its Relation to Sediment Adsorption and Desorption. Radiological and Environmental Research Division Annual Report, ANL-79-65, Part III. Argonne National Laboratory, NTIS, Springfield, VA. 1979.
  71. NELSON, D. M., LOVETT, M. B.: Measurement of the Oxidation State and Concentration of Plutonium in Interstitial Waters of the Irish Sea. In: *Impacts of Radionuclide Released into the Marine Environment*. STI/PUB/5651 IAEA, Vienna 1981.
  72. WILDUNG, R. E., GARLAND, T. R.: The Relationship of Microbial Processes to the Fate and Behavior of Transuranic Elements in Soils, Plants, and Animals. In: *Transuranic Elements in the Environment*, DOE/TIC 22800 (W. R. HANSEN, ed.) U.S. Department of Energy, NTIS, Springfield, VA. 1980.
  73. HANSON, W. C.: Ecological Considerations of the Behavior of Plutonium in the Environment. *Health Phys.* 28, 529-537 (1975).
  74. MASSEY, H. F., JACKSON, M. L.: Selective Erosion of Soil Fertility Constituents. *Proc. SSSA* 16, 353-356 (1952).
  75. MENZEL, R. G.: Enrichment Ratios for Water Quality Modeling. In: *CREAMS' A Field Scale Model for Chemicals, Runoff, and Erosion from Agricultural Management Systems* (W. G. KNISEL, ed.) U.S.D.A., Conservation Research Report No. 26., III, 12, 486-492 (1980).
  76. HAKONSON, T. E.: Environmental Pathways of Plutonium into Terrestrial Plants and Animals. *Health Phys.* 29, 583 (1975).
  77. WHICKER, F. W., LITTLE, C. A., WINDSOR, T. F.: Plutonium Behavior in the Terrestrial Environs of the Rocky Flats Installation. In: *Environmental Surveillance Around Nuclear Installations* (proc. Symp. Warsaw, 1973) 2. IAEA, Vienna 89 (1974).
  78. NYHAN, J. W., MIERA, F. R., JR., PETERS, R. J.: Distribution of Plutonium in Soil Particle Size Fractions of Liquid Effluent-Receiving Areas at Los Alamos. *Jour. Environ. Qual.*

- 5, 50–56 (1976).
79. FOSTER, G. R., LANE, L. J., NOWLIN, J. D., LAFLEN, J. M., YOUNG, R. A.: Estimating Erosion and Sediment Yield on Field-Sized Areas. *Trans. ASAE* **24**, 1253–1262 (1981).
  80. SHEN, H. W.: Review of Major Problems in Sedimentation, 1975–1978. In: *Proc. 17th General Assembly, Inter. Union of Geodesy and Geophysics*, Canberra, Australia, p. 1210–1220. 1979.
  81. BAGNOLD, R. A.: *The Physics of Blown Sand and Desert Dunes*, Methuen, London, p. 265, 1941.
  82. GRAF, W. H.: *Hydraulics of Sediment Transport*, McGraw-Hill Book Co., New York, p. 513, 1971.
  83. MARSHALL, J. K.: In: *The Environmental, Economic, and Social Significance of Drought* (J. V. LOVETT, ed.) Angus and Robertson, London 1973.
  84. GALLEGOS, A. F.: Preliminary Model of Plutonium Transport by Wind at Trinity Site. In: *Selected Environmental Plutonium Research Reports of the NAEG*, NVO-192. (M. G. WHITE and P. B. DUNAWAY, eds.), U.S. Department of Energy, NTIS 1978.
  85. SEHMEL, G. A.: Transuranic and Tracer Simulant Resuspension. In: *Transuranic Elements in the Environment* (W. C. HANSON, ed.) DOE/TIC 22800, U.S. Department of Energy, NTIS 1980.
  86. ANSPAUGH, L. R., SHINN, J. H., WILSON, D. W.: Evaluation of the Resuspension Pathway Toward Protective Guidelines for Soil Contamination with Radioactivity. In: *Population Dose Evaluation and Standards for Man and His Environment*, STI/PUB/375, Vienna 1974, p. 513–524.
  87. ELLISON, W. D.: Some Effects of Raindrops and Surface Flow on Soil Erosion and Infiltration. *Trans. AGU*, **26**, 415–429 (1945).
  88. MUTCHLER, C. K., YOUNG, R. A.: Soil Detachment by Raindrops. In: *Present and Prospective Technology for Predicting Sediment Yields and Sources*, USDA, Agric. Res. Serv., Wash., D.C., ARS-S-40, p. 285 (1975).
  89. MARTINEZ-MENEZ, M. R.: *Erosion Modeling for Upland Areas*, Ph. D. Diss. Univ. of Ariz., Tucson, Ariz., p. 145, 1979.
  90. MEYER, L. D., WISCHMEIER, W. H.: Mathematical Simulation of the Process of Soil Erosion by Water. *Trans. ASAE* **12**, 6, 754–758 (1966).
  91. FOSTER, G. R., MEYER, L. D.: A Closed-Form Soil Erosion Equation for Upland Areas. In: *Sedimentation: Symposium to Honor Professor H. A. Einstein* (H. W. SHEN, ed.) Fort Collins, Colo. p. 121–129, 1972.
  92. WISCHMEIER, W. H., SMITH, D. D.: *Predicting Rainfall Erosion Losses – A Guide to Conservation Planning*. USDA, Agriculture Handbook No. 537, p. 58, 1978.
  93. LANE, L. J., HAKONSON, T. E.: Influence of Particle Sorting in Transport of Sediment Associated Contaminants. In: *Proc. Waste Management '82 Symp.*, Tucson, Ariz. p. 12, 1982.
  94. MULLER, R. N., SPRUGEL, D. G., KOHN, B.: Erosional Transport and Deposition of Plutonium and Cesium in Two Small Midwestern Watersheds. *Jour. Environ. Qual.* **7**, 171–174 (1978).
  95. SPRUGEL, D. G., BARTELT, G. E.: Erosional Removal of Fallout Plutonium from a Large Midwestern Watershed. *Jour. Environ. Qual.* **7**, 3, 175–177 (1978).
  96. PURTYMUN, W. D.: Appendix A – Geohydrology of Acid – Pueblo and DP-Los Alamos Canyons. In: *Formerly Utilized MED/AEC Sites Remedial Action Programs* (A. STOKER, et al.) Los Alamos Nat. Lab., Los Alamos, NM, LA-8890-ENV, 1981.
  97. ADRIANO, D. C., WALLACE, A., ROMNEY, E. M.: Uptake of Transuranic Nuclides from Soil by Plants Grown Under Controlled Environmental Conditions. In: *Transuranic Elements in the Environment* (W. C. HANSON, ed.) DOE/TIC-22800, U.S. Department of Energy, NTIS 1980.
  98. PRICE, K. R.: A Review of Transuranic Elements in Soils, Plants, and Animals. *J. Environ. Qual.* **2**, 62–66 (1973).
  99. SCHULZ, R. K.: Root Uptake of Transuranic Elements. In: *Transuranics in Natural Environments* (M. G. WHITE and P. B. DUNAWAY, eds.) NVO-178, Energy Research and Development Administration, NTIS, 1977.
  100. FRANCIS, C. W.: Plutonium Mobility in Soil and Uptake in Plants. *J. Environ. Qual.* **2**, 67–70 (1973).
  101. BONDIETTI, E. A., TRABALKA, J. R., GARTEN, C. T., KILLOUGH, J. J.: Biogeochemistry of Actinides: A Nuclear Fuel Cycle Perspective. In: *Radioactive Waste in Geologic Storage* (S. FRIED, ed.) ASC Symposium Series 100, American Chemical Society, Washington, D. C. 1979.
  102. *Energy Research and Development Administration: Workshop on Environmental Research for Transuranic Elements*. ERDA 76/134, NTIS, Springfield VA. 1976, p. 62.
  103. CATALDO, D. A., VAUGHN, B. E.: Interaction of Airborne Plutonium with Plant Foliage. In: *Transuranic Elements in the Environment* (W. C. HANSON, ed.) DOE/TIC-22800, U.S. Department of Energy, NTIS, 1980.
  104. ARTHUR, W. J., III, ALLREDGE, A. W.: Soil Ingestion by Mule Deer in Northcentral Colorado. *J. Range Manage.* **32**, 67–71 (1979).
  105. ADRIANO, D. C., COREY, J. C., DAHLMAN, R. C.: Plutonium Contents of Field Crops in the Southeastern United States. In: *Transuranic Elements in the Environment* (W. C. HANSON, ed.) DOE/TIC-22800, U.S. Department of Energy, NTIS, 1980.
  106. NYLHAN, J. W., MIERA, F. R., JR., PETERS, R. J.: Distribution of Plutonium in Soil Particle Size Fractions in Liquid Effluent-Receiving Areas at Los Alamos. *J. Environ. Qual.* **5**, 50–56 (1976).
  107. SULLIVAN, M. F., GARLAND, T. R.: Gastrointestinal Absorption of Alfalfa-Bound Plutonium-238 by Rats and Guinea Pigs. Pacific Northwest Laboratory Report, BNWL-2100 (Pt. I) NTIS, 1977.
  108. BALLOU, J. E., PRICE, K. R., GIES, R. A., DOCTOR, P. G.: The Influence of DTPA on the Biological Availability of Transuranics. *Health Phys.* **34**, 445–450 (1978).
  109. SULLIVAN, M. F., RYAN, J. L., GORHAM, L. L., MCFADDEN, K. M.: The Influence of Oxidation State on Maximum Permissible Concentration in Drinking Water. *Radiation Res.* (1979).
  110. BRADLEY, W. G., MOOR, K. S., NAEGLE, S. R.: Plutonium and Other Transuranics in Small Vertebrates: A Review. In: *Transuranics in the Natural Environment* (M. G. WHITE and P. B. DUNAWAY, eds.) NVO-178. U. S. Energy Research and Development Administration. NTIS, 1977.
  111. MARTIN, W. E., BLOOM, S. G.: Nevada Applied Ecology Group Model for Estimating Plutonium Transport and Dose to Man. In: *Transuranic Elements in the Environment* (W. C. HANSON, ed.) DOE/TIC-22800. U. S. Department of Energy, NTIS, 1980.
  112. EYMAN, L. D., TRABALKA, J. R.: Patterns of Transuranic Uptake by Aquatic Organisms: Consequences and Implications. In: *Transuranic Elements in the Environment* (W. C. HANSON, ed.) DOE/TIC-22800. U.S. Department of Energy NTIS, 1980.
  113. SMITH, D. D.: Review of Grazing Studies on Plutonium-Contaminated Rangelands. In: *Transuranics in Natural Environments* (M. G. WHITE and P. B. DUNAWAY, eds.) NVO-178 Energy Research and Development Administration NTIS, 1977.
  114. O'FARRELL, T. P., GILBERT, R. O.: Transport of Radioactive Materials by Jackrabbits on the Hanford Reservation. *Health Phys.* **29**, 9–15 (1975).
  115. HAKONSON, T. E., MARTINEZ, J. L.: Disturbance of a Low-Level Waste Site Cover by Pocket Gophers. *Health Phys.* **42** (6), 868–872 (1981).
  116. WINSOR, T. F., WHICKER, F. W.: Effects of Pocket Gopher Activity on Soil Plutonium Distribution at Rocky Flats, Colorado. *Health Phys.* **39**, 257–262 (1980).
  117. ARTHUR, W. J., MARKHAM, O. D.: Small Mammal Soil Burrowing as a Radionuclide Transport Vector at a Radioactive Waste Disposal Area in Southeastern Idaho. *J. Environ. Qual.* **12** (1), 117–122.
  118. HAKONSON, T. E., BOSTICK, K. V.: The Availability of Environmental Radioactivity to Honey Bee Colonies at Los Alamos. *J. Environ. Qual.* **5**, 307–310 (1976).
  119. POLZER, W. L., FOWLER, E. B., ESSINGTON, E.: Characteristics of Wastes and Soils Which Affect Transport of Radionuclides Through the Soil and Their Relationship to Waste Management. NUREG/CR-0842, LA-UR-79-1025, 1979, p. 71.
  120. GARTEN, JR., C. T., BONDIETTI, E. A., WALKER, R. L.:

- Comparative Uptake of Uranium, Thorium, and Plutonium by Biota Inhabiting a Contaminated Tennessee Flood Plain. *J. Environ. Qual.* **10**: 207–210 (1981).
121. GARTEN, JR. C. T.: Comparative Uptake of Actinides by Plants and Rats from a Radioactive Pond. *J. Environ. Qual.* **10**: 487–491 (1981).
122. WAHLGREN, M. A., MARSHALL, J. S.: Distribution Studies of Plutonium in the Great Lakes. In: *Proc. 2nd International Conference on Nuclear Methods in Environmental Research*. CONF-740701, NTIS, 1974.
123. PENTREATH, R. J., LOVETT, M. B.: Occurrence of Plutonium and Americium in Plaice from the North-Eastern Irish Sea. *Nature* **262**, 814–816 (1976).
124. BEASLEY, T. M., FOWLER, S. W.: Plutonium Isotope Ratios in Polychaete Worms. *Nature* **262**, 813–814 (1976).
125. BOWEN, V. T.: Transuranic Elements in Marine Environments. HASL-291, Health and Safety Laboratory, Energy Research and Development Administration, NTIS, 1975.
126. LIVINGSTON, H. L., BOWEN, V. T.: Americium in the Marine Environment. Relationships to Plutonium. In: *Environmental Toxicity of Aquatic Radionuclides: Models and Mechanism* (M. W. MILLER and J. N. STANNARD, eds.) Ann Arbor Science Publishers, Ann Arbor, Michigan, 1976, p. 197–130.

